UNIVERSITÀ DEGLI STUDI DI TRIESTE

UNIVERSITÀ DEGLI STUDI DI UDINE
hic sunt futura

UNIVERSITÀ DEGLI STUDI DI TRIESTE
UNIVERSITÀ DEGLI STUDI DI UDINE

XXXVI CICLO DEL DOTTORATO DI RICERCA IN AMBIENTE E VITA

EXPLORING THE BEHAVIOUR OF GRAPHENE-RELATED MATERIALS IN AQUEOUS ENVIRONMENTS: FROM STANDARD PROTOCOLS TO ENVIRONMENTAL IMPLICATIONS IN FRESHWATER SYSTEMS

Settore scientifico-disciplinare: **BIO/01**

DOTTORANDO / A
GIADA CAORSI

COORDINATORE
PROF. GIORGIO ALBERTI

SUPERVISORE DI TESI
PROF. MAURO TRETIACH

CO-SUPERVISORE DI TESI
PhD. FABIO CANDOTTO CARNIEL

ANNO ACCADEMICO 2022/2023

Table of contents

Riassunto della tesi

Grazie alle loro peculiari proprietà chimico-fisiche, i materiali grafenici (GRMs) vengono impiegati in molti campi innovativi. Il crescente sviluppo di prodotti contenenti GRMs e la loro sempre più ampia disponibilità potrebbero comportare un rilascio involontario di GRMs con conseguenze ancora sconosciute per l'ambiente. Secondo il regolamento REACH, tutte le nuove sostanze prodotte nell'Unione Europea devono essere sottoposte a una serie di saggi ecotossicologici sviluppati dall'OECD per valutarne il rischio ambientale. È importante precisare che le linee guida (TGs) suggerite per valutare il rischio per gli ambienti di acqua dolce, ovvero le TG 201, 202 e 203, sono state sviluppate per sostanze solubili in acqua e richiedono che venga rispettato un criterio di applicabilità che prevede che la concentrazione delle sostanze testate non cambi più del ± 20% durante il test. Tuttavia, i GRMs dispersi in mezzi acquosi tendono ad aggregare e sedimentare, alterando la loro concentrazione e biodisponibilità nel tempo. Pertanto, lo scopo del mio progetto di dottorato è stato valutare il comportamento dei GRMs sia in mezzi sintetici che naturali, prestando attenzione anche all'ecotossicità algale.

A tal fine, sono stati condotti diversi esperimenti per verificare l'applicabilità del "Test 201: Inibizione della crescita di alghe e cianobatteri d'acqua dolce" per few-layers graphene (FLG), grafene ossido (GO) e grafene ossido ridotto (rGO), concentrandosi sui possibili fattori che influenzano la stabilità delle dispersioni di GRMs (GDS): (*i*) composizione delle particelle e (*ii*) concentrazione, (*iii*) turbolenza, (*iv*) composizione del mezzo e (*v*) presenza delle alghe, *Raphidocelis subcapitata*, la specie algale più comunemente utilizzata per questa TG.

In primo luogo, è stato sviluppato un approccio metodologico idoneo a valutare gli endpoints della TG 201, che prevede l'utilizzo di tecniche di citofluorimetria (FCM), Turbiscan e camere di sedimentazione Utermöhl (USC). I risultati hanno evidenziato una forte aggregazione e sedimentazione, e la GDS dipendeva principalmente dalla natura chimico-fisica dei GRMs: l'FLG aveva la più rapida aggregazione e sedimentazione, mentre il GO era il più stabile. Purtroppo, nessuna delle modifiche testate ha permesso di soddisfare il requisito di stabilità della TG 201. Tuttavia, è stato possibile determinare un tempo di inizio ritardato del test oltre il quale le dispersioni di GRMs non subiscono ulteriori cambi significativi a causa dei fenomeni di aggregazione e sedimentazione. Inoltre, la ricaratterizzazione dei GRMs ha mostrato una diminuzione delle dimensioni dei flakes rimasti in dispersione, un fattore importante che influisce sia sulla biodisponibilità che sul potenziale destino ambientale.

A causa della natura instabile dei GRMs nei mezzi acquosi, è stata anche indagata la loro sorte in ambienti d'acqua dolce. Innanzitutto, valutando il loro comportamento in diverse acque minerali commerciali, per testare l'effetto del contenuto ionico sulla GDS, e successivamente in acque dolci

raccolte da corpi idrici del Friuli Venezia Giulia, selezionate per le loro diverse caratteristiche, al fine di testare l'effetto di condizioni simil-ambientali sulla GDS. Sono stati osservati forti fenomeni di aggregazione e sedimentazione, anche superiori a quanto riscontrato in un mezzo comunemente utilizzato (*i.e*. il mezzo standard della TG 201) e in acqua deionizzata, probabilmente a causa dell'alto contenuto di sali, argille e materia organica naturale (NOM) nelle acque. Inoltre, le alghe esposte al GO in campioni d'acqua dolce hanno mostrato una elevata inibizione della crescita, probabilmente a causa all'interazione del GO con inquinanti ambientali, che andrebbe ulteriormente investigata.

Nel complesso, questi dati contribuiscono a prevedere non solo il comportamento dei GRMs durante i saggi ecotossicologici, un fattore importante per una corretta interpretazione dei risultati della TG 201, ma anche il comportamento e il destino dei GRMs in ambienti d'acqua dolce.

Thesis abstract

Thanks to their unique physicochemical properties, graphene-related materials (GRMs) are used in many innovative fields. The increasing development of GRMs-containing products and resulting widespread availability could lead to unintended GRMs release with unknown consequences for the environment. According to the Registration, Evaluation, Authorisation and Restriction of Chemicals (REACH) regulation, all new substances manufactured in the European Union must undergo a battery of ecotoxicological bioassays from the Organisation for Economic Co-operation and Development (OECD) to assess their risk to human health and environment, *i.e.* the OECD Test Guidelines (TG). Importantly, the TGs recommended to assess the risk for freshwater environments, *i.e.* TGs 201, 202, and 203, were developed for water-soluble substances and include an applicability criterion requiring that the concentration of tested substances does not change more than ± 20 % during the testing period. However, GRMs dispersed in aqueous media tend to aggregate and settle, changing their concentration and bioavailability over time. Therefore, the aim of my PhD project was to assess the behaviour of GRMs in both synthetic and natural media, posing a focus also to algal ecotoxicity.

To this end, several laboratory experiments were conducted to verify the applicability of the "OECD TG 201: Freshwater algae and cyanobacteria growth inhibition test" to few-layers graphene (FLG), graphene oxide (GO), and reduced GO (rGO), focusing on the possible factors affecting the GRMs dispersion stability (GDS): (*i*) particles composition and (*ii*) concentration, (*iii*) turbulence, (*iv*) medium composition, and (*v*) the presence of the algae, *Raphidocelis subcapitata*, the most commonly used green alga of this TG.

First, a suitable methodological approach was developed to assess the TG 201 test endpoints, which involves the utilization of flow cytometry (FCM), Turbiscan, and Utermöhl sedimentation chambers (USC). The results reported high aggregation and sedimentation of GRMs, and the GDS mainly depended on the GRMs physicochemical nature: FLG had the fastest aggregation and sedimentation, while GO was the most stable. Unfortunately, none of the tested modifications to exposure conditions ensured the fulfilment of the TG 201 stability requirement. However, it was possible to determine a delayed starting time of the test after which GRMs dispersions do not change significantly due to aggregation and sedimentation phenomena. Furthermore, the GRMs re-characterization showed a decrease in dimensions of flakes remaining in dispersion, an important factor influencing both the bioavailability and the potential environmental fate.

Due to the unstable nature of GRMs in aqueous media, their fate in freshwater environments was also investigated. First, by evaluating their behaviour in different commercial mineral waters to test the effect of the ionic content on the GDS, and then in real fresh waters collected from water bodies

of Friuli Venezia Giulia. Waters were collected from different sites, selected for their different environmental characteristics, to test the effect of environmental-like conditions on the GDS. Strong aggregation and sedimentation were observed, even greaater than in common test medium (*i.e*. TG 201 medium) and deionized water, likely due to the high content of salts, clay, and NOM in the waters. Furthermore, algae exposed to GO in fresh waters samples exhibited significant growth inhibition, possibly as a result of interactions of GO with environmental pollutants, that should be further investigated.

These data help predicting not only the behaviour of GRMs during ecotoxicological testing, an important factor for a reliable interpretation of TG 201 results, but also the behaviour and fate of GRMs in real freshwater environments.

General introduction

Graphene and GRMs: background and beyond the "wonder material"

The historical background leading to the discovery of graphene dates back to the late 1940s, when it has been first theoretically studied by Wallace [1], McClure [2], and Semenoff [3], laying the foundations for understanding its properties. However, according to Peierls [4], Landau [5], and later Mermin [6], the isolation of strictly two-dimensional crystals should have been thermodynamically impossible. Thus, while graphene monolayers have always been known to be part of the larger 3D structures of graphite, it was believed that standing-alone 2D materials could not exist, and the practical isolation of a single graphene layer remained an elusive goal for several years.

However, as often happens, the seemingly impossible could indeed become reality. The turning point came in 2004, when Andrej Geim and Konstantin Novoselov, for the first time successfully isolated and characterized a single layer of graphene from graphite using the now-famous and astoundingly simple method of mechanical exfoliation with adhesive tape [7]. Later, in 2010, the two researchers from the University of Manchester were awarded the prestigious Nobel Prize in Physics for these "*groundbreaking experiments regarding the two-dimensional material graphene*", which revolutionized the field of nanomaterials science.

Since that moment, graphene has attracted an ever-increasing amount of attention from both research and industrial communities due to its unique physicochemical properties, offering endless possibilities for future innovations and technologies.

Graphene is composed of a single layer of carbon atoms arranged in a two-dimensional honeycomb crystal lattice, held together by a backbone of overlapping sp^2 orbitals. Owing to its particular atomic structure, graphene displays excellent thinness, lightness, with almost zero effective mass, nearly optical transparency, mechanical strength, flexibility, and exceptional electrical and thermal conductivity, earning it the nickname of "wonder material".

All these unique and extraordinary properties make graphene suitable for potential employment in a broad variety of fields, ranging from electronics, photonics, construction, transportation, agriculture, energy generation and storage, sensors, metrology and biomedicine [8–12].

Exploring the world of graphene-related materials (GRMs)

Although the International Union of Pure and Applied Chemistry clearly defines graphene as a single layer of carbon atoms, the term "graphene" is often applied generically to a range of graphene-related materials (GRMs). GRMs encompass a broad family of materials that share their origins and structural features with graphene, but could exhibit differences in terms of defects of the

carbon lattice, redox state due to oxygen functional groups bound to the lattice (*e.g*. hydroxyl and carboxylic), number of layers, lateral dimensions.

Among the numerous members, few have gained particular attention, becoming the most relevant and studied, namely FLG, GO, and rGO [13]. Few-layers graphene (FLG), as the name suggests, consists of three to ten well-defined stacked graphene layers. It combines the electrical and mechanical properties of single-layer graphene with the feasibility of large-scale production, making it an appealing candidate for various applications, including transparent conductive coatings, supercapacitors, and lightweight materials for structural applications [14,15]. Graphene oxide (GO), is a highly oxidized form of chemically modified graphene exposing oxygen-containing functional groups, such as carboxyl, hydroxyl, and epoxy, on its planar surface and edges. The result is an amphiphilic "giant" sheet-like molecule, that renders GO a versatile material suitable for a multitude of applications, from nanocomposites to drug delivery systems [12,16]. Reduced graphene oxide (rGO), on the other hand, is obtained by reducing GO, typically through thermal or chemical methods. This process reduces oxygen content, increases hydrophobicity, introduces holes or defects in the carbon lattice, and partially restores its electrical conductivity. This makes rGO an attractive choice for electronics, sensors, and energy storage as the intrinsic properties derived from its structure can be tuned according to the reduction procedure, as appropriate [17,18].

These are just a few examples of a family of materials in continuous expansion. To put a little bit of order in this realm of GRMs, within the EU Graphene Flagship project, three physicochemical descriptors were defined to provide a clear and consistent classification of GRMs. These are the number of layers of graphene characterizing the material, the average lateral size of its flakes/sheets, and the oxidation degree, quantified by the carbon-to-oxygen (C/O) atomic ratio (Fig. 1). This proposed model framework to characterize GRMs covers the largest set of current graphene materials encountered in practice [19].

Material characterization is a key element also in hazard assessment. Thus, investigating these three fundamental parameters is essential to understand the relationship between physicochemical characteristics and the associated potential environmental risks [16,19]. Indeed, these parameters can affect the interactions between GRMs and organisms, thereby strongly impacting food chains and ecosystems. Consequently, a comprehensive characterization of the tested materials is essential, both for comparison of results among studies and for elucidating the underlying mechanisms of observed ecotoxicological effects.

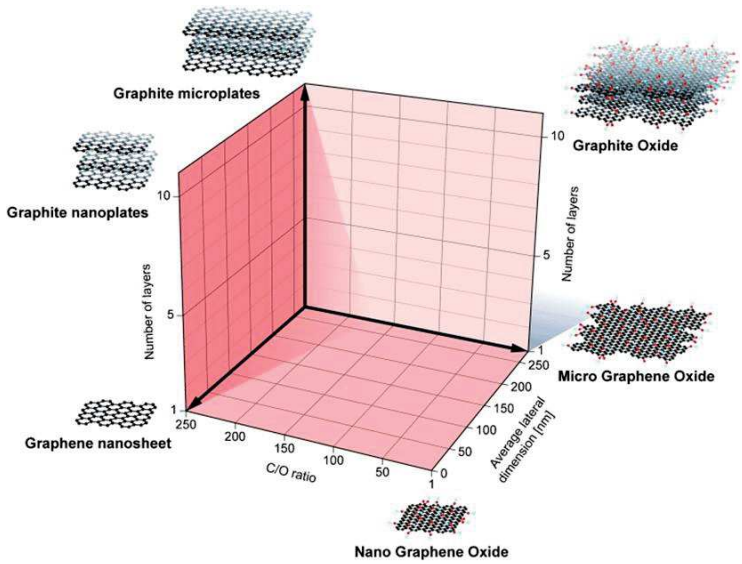

Figure 1. Classification grid for the categorization of different graphene types according to three fundamental GRM properties: number of graphene layers, average lateral dimension, and atomic carbon/oxygen ratio. The different materials drawn at the six corners of the box represent the ideal cases according to the lateral dimensions and the number of layers reported in the literature. The values of the axes are related to the GRMs at nanoscale, but it is feasible to expand the values to microscale [19].

Due to the GRMs aforementioned unique properties, triggering high expectations for the development of new technological applications, they are forecasted to be produced at industrial-scale. Indeed, following the increasing development of new GRMs and their employment in many different applications, also the graphene production has increased continuously over this period. This is expected to continue in the coming years in tandem with the rapid growth in GRM research and development, increased industrial production capacity, and lower manufacturing costs. [20,21]. As a consequence, a steep increase of GRMs production is expected in the next years. The projected production for 2025 (828 t) is 14 times higher than that of 2015 (60 t), whereas the expected 2030 production (3461 t) is 24 times higher than that of 2020 (144 t) (Fig. 2a) [22]. Product category allocations also show a dynamic perspective (Fig. 2b). While for the first nine years with records, GRMs were primarily employed for research and development purposes, later on their usage spans into the realm of commercial products. One of the first applications of GRMs in everyday products emerged in sporting items, including tennis rackets and skis. Applications in batteries and electronics followed in subsequent years [22]. Nowadays, GRMs found their way into an ever-expanding array of applications across various industries and are actually present in a number of products. Just to cite a few, they are now integrated into diverse items such as such as concrete, asphalts, tires, shoe soles, filtering systems, prosthetic application, biosensors, and much more. [23–25].

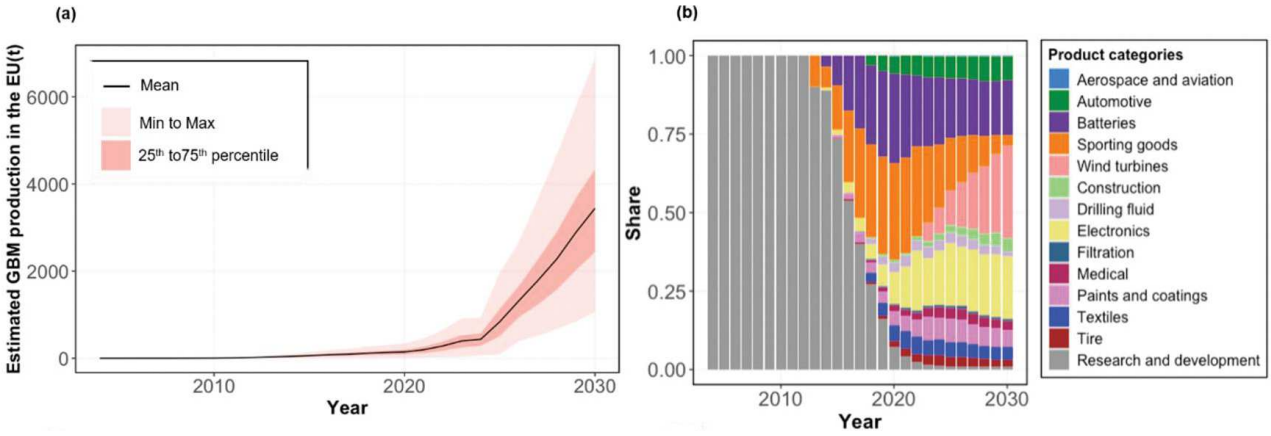

Figure 2. (a) Yearly GRM production. The red line shows the mean yearly GRM production in Europe. The lighter orange colour represents the area between the minimum and maximum estimations for annual production, and the darker orange colour indicates the range between the 25th and 75th percentiles. (b) Trend of allocations to product categories from 2004 to 2030 [22].

GRMs in the environment: ecotoxicological risk assessment

As the importance of GRMs in everyday-life is constantly growing, and GRMs production will rise exponentially in the next few years, this could lead to an uncontrolled release into the environment, raising significant concerns about the unpredictable consequences for the environment [26].

Indeed, even if GRMs-containing products offer undeniable advantages, they inevitably face wear and tear over time, leading to their eventual disposal and the unintended release of GRMs into the environment. Additionally, a deliberate and expected release of GRMs is on the horizon if these materials find applications in open fields as GRMs-composites in pesticides [27,28], plant fertilizers [29–31], improvement agents for soil remediation [32], paints and protective coatings [14].

Thus, attention should be paid on potential environmental risks and mostly on potential adverse outcomes on living organisms, especially toward microorganisms, such as algae, constituting the basis of the trophic chain in freshwater ecosystems [33].

Photoautotrophic organisms play a fundamental role in trophic webs, serving as major source of oxygen and organic matter in both aquatic and terrestrial environments. Consequently, considerable emphasis should be placed on assessing the possible adverse impacts of GRMs on these organisms. In this regard, freshwater cyanobacteria, unicellular green algae, and diatoms have received extensive attention, and have been outlined as target species in standard guidelines, *e.g.* those developed by the Organisation for Economic Co-operation and Development (OECD). These guidelines are required by specific REACH regulations to evaluate the potential effects of chemicals on aquatic ecosystems, forming the basis of the approval process for marketing new substances and materials on the EU market [16].

Thus, as the production and use of GRMs grows, it should be accompanied by an evaluation of the associated safety issues, to exclude possible risks to the environment. This risk assessment is essential for regulatory purposes and sustainable nanotechnological development.

However, when innovative technologies develop rapidly, as in the case of graphene, progress toward suitable governance often lags behind. Despite the major efforts focused on the adaptations of the OECD TGs to nanomaterials (NMs) [34], knowledge gaps on other "difficult to test" NMs such as GRMs still remain [35]. Currently, efforts to adapt existing TG or develop GD focusing in particular on GRMs are being carried out.

In this context, the recently concluded Graphene Flagship represented a 10-year EU project, whose mission was to take graphene from the realm of academic laboratories into European society. To do this, safety assessment is an essential requirement that cannot be dissociated from the development of new technologies. Therefore, a dedicated research program of the Graphene Flagship, the Work Package 4 (WP4), invested considerable efforts in assessing the potential impact of GRMs on human health and the environment, by evaluating the applicability of the OECD guidelines to GRMs, to ensure future safety production, handling, commercialisation, and use of GRMs. A collective effort among selected WP4 partners culminated in a joint review that thoroughly explored this critical matter.

Applicability of OECD TG 201, 202, 203 for the Aquatic Toxicity Testing and Assessment of 2D Graphene material nanoforms to meet regulatory needs

Published on NanoImpact; Vol. 29, on 20th December 2022

M. Connolly[a], G. Moles[a], F. Candotto Carniel[b], M. Tretiach[c], G. Caorsi[c], E.Flahaut[d], B. Soula[d] E. Pinelli[d], L. Gauthier[d], F. Mouchet[d], J.M Navas[a]

[a]INIA-CSIC, Department of Environment and Agronomy, Instituto Nacional de Investigación y Tecnología Agraria y Alimentaria-Consejo Superior de Investigaciones Científicas, Ctra. de La Coruña, km 7, 5, 28040 Madrid, Spain

[b]UNITS, Department of Chemical and Pharmaceutical Sciences, University of Trieste, via L. Giorgieri 1, Trieste I-34127, Italy

[c]UNITS, Department of Life Sciences, University of Trieste, via L. Giorgieri 10, Trieste I-34127, Italy

[d]CNRS CIRIMAT/ECOLAB, Centre National de la Recherche Scientifique, Centre Inter-universitaire de Recherche et d'Ingénierie en Matériaux (CIRIMAT)/Laboratoire Ecologie Fonctionnelle et Environnement,16 Av Edouard Belin, 31400 Toulouse, France

Graphical Abstract

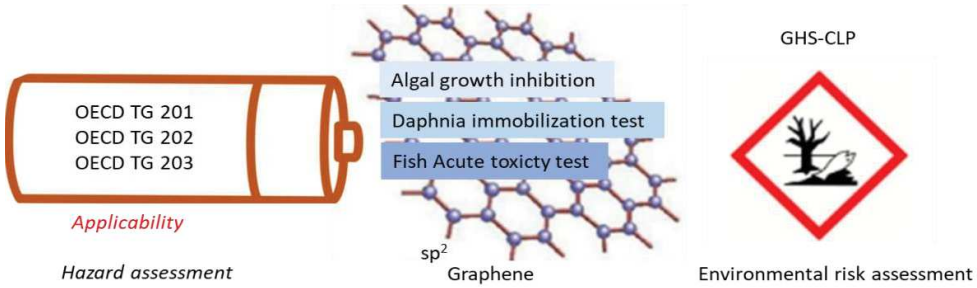

Abstract

Tests using algae and/or cyanobacteria, invertebrates (crustaceans) and fish form the basic elements of an ecotoxicological assessment in a number of regulations, in particular for classification of a substance as hazardous or not to the aquatic environment according to the Globally Harmonised System of Classification and Labelling of Chemicals (GHS-CLP) (GHS 2022) and the REACH regulation (Registration, Evaluation, Authorisation and Restriction of Chemicals, EC 2006). Standardised test guidelines (TGs) of the Organisation for Economic Co-operation and Development (OECD) are available to address the regulatory relevant endpoints of growth inhibition in algae and cyanobacteria (TG 201), acute toxicity to invertebrates (TG 202), and acute toxicity in fish (TG 203). Applying these existing OECD TGs for testing two-dimensional (2D) graphene nanoforms may require more attention, additional considerations and/or adaptations of the protocols, because graphene materials are often problematic to test due to their unique attributes. In this review a critical analysis of all existing studies and approaches to testing used has been performed in order to comment on the current state of the science on testing and the overall ecotoxicity of 2D graphene materials. Focusing on the specific tests and available guidance's, a complete evaluation of aquatic toxicity testing for hazard classification of 2D graphene materials, as well as the use of alternative tests in an integrated approach to testing and assessment, has been made. This information is essential to ensure future assessments generate meaningful data that will fulfil regulatory requirements for the safe use of this "wonder" material.

Keywords

2D graphene nanoforms, acute aquatic toxicity, fish, algae, *Daphnia spp.*

Abbreviations

NM: Nanomaterials
OECD: The Organisation for Economic Co-operation and Development
TGs: Test guidelines
GHS: Globally Harmonised System
CLP: Classification, Labelling and Packaging of substances and mixtures
CAS: Chemical Abstracts Service
EC: European Commission
GD: Guidance document
IATA: Integrated Approaches to Testing and Assessment
WoE: Weight of evidence
CAGR: Compound Annual Growth Rate
C/O ratio: Carbon to Oxygen ratio
GO: Graphene oxide
FLG: Few-layers graphene
rGO: Reduced graphene oxide
FET: Fish embryo acute toxicity
HO: Hoffman
UV-Vis: Ultraviolet-visible (UV-Vis) spectrophotometry
Chl: Chlorophyll
Chl-a: Chlorophyll a
ISO: International Organization for Standardization
ISO/TS: ISO Technical Specification
ISO/TR: ISO Technical Reports
IEC: International Electrotechnical Commission
NAM: New approach methodology
PPAR-α: Peroxisome proliferator-activated receptor alpha
AhR: Aryl hydrocarbon receptor
HO-1: Heme oxygenase-1
iNOS: Inducible nitric oxide synthase
mRNA: Messenger RNA
ID/IG: Ratio of the intensity of D- Raman peak and G- Raman peak
EtOH: Ethanol
ASTM: American Society for Testing and Materials
HA: Humic acid
EPA: Environmental Protection Agency
NOM: Natural organic matter
DOM: Dissolved organic matter
WNT: Working Group of National Co-ordinators of the TGs programme

Glossary

Two-dimensional material/2D material: material, consisting of one or several layers with the atoms in each layer strongly bonded to neighbouring atoms in the same layer, which has one dimension (*i.e.* the thickness) in the nanoscale or smaller and the other two dimensions generally at larger scales.

Graphite: allotropic form of the element carbon, consisting of graphene layers stacked parallel to each other in a three-dimensional, crystalline, long-range order (ISO 2017).

Graphene/single-layer graphene/monolayer graphene: single layer of carbon atoms with each atom bound to three neighbours in a honeycomb structure (ISO 2017). Graphene layers can be classified as a two-dimensional material up to 10 layers thick for electrical measurements, beyond which the electrical properties of the material are not distinct from those for the bulk [also known as graphite] (ISO 2017).

Few-layers graphene (FLG): two-dimensional material consisting of three to ten well-defined stacked graphene layers (ISO 2017).

Graphene oxide (GO): chemically modified graphene prepared by exfoliation and oxidation of graphite, causing extensive oxidative modification of the basal plane. Graphene oxide is a single-layer material with a high oxygen content, typically characterized by C/O atomic ratios of approximately 2.0 depending on the method of synthesis (ISO 2017).

Reduced graphene oxide (rGO): reduced oxygen content form of graphene oxide. It can take the form of several morphological variations such as platelets, fibres and worm-like structures (ISO 2017).

Hummers' method: method for production of graphene oxide from graphite in a sodium nitrate and sulfuric acid solution after the addition of potassium permanganate (Hummers 1958).

Lateral size: lateral dimensions of a 2D material flake. If the flake is approximately circular then this is typically measured using an equivalent circular diameter or if not via x, y measurements along and perpendicular to the longest side (ISO 2017).

Nanoform: term used to distinguish forms of a substance that fulfil the EC Recommendation on the definition of the term 'nanomaterial' but differ with regard to size distribution, shape and other morphological characterisation, including surface treatment and functionalisation and specific surface area of the particles. Variation of one or several of the defined characteristics results in a different nanoform, unless such variation results from a batch-to-batch variability (ECHA, 2022).

1. Introduction

1.1 Regulation and environmental hazard classification of graphene

According to the European Commission Regulation (EU) No 2020/878 chemical manufacturers or importers are obliged under REACH to provide specific information requirements and chemical safety assessments for nanoforms of chemical substances (EC, 2020). This information is also used as criterion for the classification, labelling and packaging of substances as hazardous or not according to Regulation (EC) No 1272/2008 on the classification, labelling and packaging of substances and mixtures (CLP), which aligns with the United Nations globally Harmonised System of Classification and Labelling of Chemicals (GHS) and facilitates the entry and safe use of chemicals in the market place (EC, 2009). As well as information on physical and health hazards,

environmental hazards must be reported and include hazard classification to the aquatic environment and the atmosphere.

Graphene is a nanomaterial according to the recently updated EC definition, and by its implementation into REACH graphene and its specific nanoforms are subject to regulation within the European Union (EC, 2022). Graphene nanoforms can exist with assembly structures of single, bi-, or few layers (3-10), with external dimensions (thicknesses) of <1 nm, lateral sizes ranging from a few nanometres to a few microns and in the form of nanoflakes/nanosheets/nanoplatelets, ribbons, fibres or quantum dots. They are all characterised by the presence of sp^2 hybridized carbon atoms arranged in a honeycomb lattice, but they can have different assembly structures, distinct edge types/defects, surface states (e.g. oxidations/reductions) and functionalisations according to the vast number of production methods and post processings. Graphene materials have received the CAS number 1034343-98-0, EC number 801-282-5. They have been registered under REACH and classified under the aquatic environment hazard class, as harmful to aquatic life with long lasting effects following chronic exposure (CLP-GHS H412) (ECHA, 2022 a, b). However, there is insufficient data to enable aquatic environment hazard classification following acute exposure. There are also distinct EC numbers for different surface treated graphene materials (e.g. graphene oxide: EC 947-768-1 and reduced graphene oxide: EC 922-453-1). Similarly, while the materials are registered under REACH, the data is not sufficient for aquatic environment hazard classification. Remarks have been made that hazard assessment on a case-by-case basis approach is most appropriate, as any available data on the specific tested graphene materials may not necessarily be relevant to all graphene/graphene oxide/reduced nanoforms (ECHA, 2022c). For example, the specific production methods used, post-modifications applied, and post-processing steps introduced to form the final material may contribute significantly to material properties. Furthermore, a single substance may have one or more different nanoforms, based on differences in size distribution, shape, and other morphological characteristics, presence of a surface treatment or functionalisation, and the specific surface area (SSA) of the particles (ECHA, 2022d). Therefore, due to the unique structures and features that nanoforms of graphene materials can have, the extent to which they will fall into a single substance category, and to which grouping or control banding for risk management can be applied, may not be justified (as recently argued in the case of carbon nanotubes (Fadeel and Kostarelos, 2020)).

Current hazard assessments for aquatic toxicity testing include growth inhibition studies with algae and cyanobacteria, short-term toxicity testing on invertebrates and fish lethality tests of short- and long-term. The standardised tests used and heavily relied upon include the OECD TG 201 Algae and Cyanobacteria Growth Inhibition Test (OECD 2011), the OECD TG 202 Daphnia Acute

Immobilization Test (OECD 2004a), and the OECD TG 203 Fish Acute Toxicity Test (OECD 2019c), respectively. Such a test battery can be seen as comprehensive and provides the apical endpoints for hazard classification upon which regulation relies (*e.g.* for CLP hazard classification). While these tests are considered generally applicable for the testing of nanomaterials (NMs) (OECD, 2013a; Ramussen et al. 2016), they have not been assessed for their applicability when testing specifically 2D graphene materials. Adaptations/procedural modifications to these standardised tests may be needed according to the unique characteristics of the material/nanoform being tested. This has been recognised in the NM community with the establishment of the Malta Initiative to advance the development and amendment of the OECD TGs and guidance documents (GDs) to the unique characteristics of NMs. Also, the aim of the recently published GD for aquatic testing of NMs (GD 317) is to identify how existing OECD TGs can be applied to NMs (OECD 2022a, Petersen et al 2021). However, this guidance is not prescriptive for testing of a particular NM type and thus other specific guidance may need to be consulted for testing of certain "difficult to test" materials, for which graphene materials could be considered and for which the OECD GD 23 on Aqueous-Phase Aquatic Toxicity Testing of Difficult Test Chemicals could provide further reference (OECD, 2019a).

Therefore, within this article the applicability of the basic battery of tests for aquatic toxicity assessment (*i.e*. OECD TGs 201, 202, 203) for testing graphene materials was reviewed. All available information on the testing of 2D graphene materials using the test organisms, and specific taxa specified in the single tests, was collected. The following aspects were taken into account *i*) if standardised test guidelines were used or followed, (*ii*) if relevant endpoints were reported, and (*iii*) the specific experimental setups used.

Specific considerations unique to this class of NMs were identified and overall comments on the adequateness of data generated and the extent to which traditional protocols were used have been made. In instances where there are information gaps or inconsistencies in data sets weight of evidence (WoE) approaches to testing and assessment have also been proposed ((Annex XI, Section 1.2 to the REACH Regulation) (EC, 2006) (OECD, 2019b)). Specifically, a WoE refers to "a positive expert opinion that considers available evidence from different independent sources and scientific viewpoints on a particular issue, coming to a considered view of the available, oftentimes conflicting data. It is preferred when every source does not provide sufficient information individually" (OECD 2019b). An example of how such approaches can facilitate classification of NMs according to CLP criteria for acute aquatic toxicity into specific hazard classes has been recently presented by Basei and colleagues (Basei et al. 2021). Tests that can be considered in WoE approaches for acute toxicity in fish include fish embryo acute toxicity tests (TG 236, OECD

2013b) and the recently published *in vitro* fish cell line acute toxicity test (TG 249, OECD 2021a). Taking into consideration such approaches and the potential value of such data, any information that was available from tests performed using embryos and fish cells to assess hazard of graphene materials were also collected and evaluated for their use in a WoE and integrated approach for testing and assessment (IATA).

1.2 Aquatic toxicity of 2D graphene materials

Aquatic environmental exposure to graphene is particularly relevant according to the potential direct uses of graphene materials in environmental settings (*e.g*. in environmental remediation (Karthik et al. 2021), water filtration (Buelke et al. 2018), and as an effective antifreeze (Zhang et al. 2021)), and the potential release at the end of life of graphene enabled consumer products such as electronics. This, together with the demonstrated potential for environmental persistence (Candotto Carniel et al. 2021) and mobility in water bodies of aquatic ecosystems for certain types of graphene materials (*e.g*. GO (Avant et al. 2019, Lanphere et al. 2014) and FLG (Su et al. 2016)), warrants concern for risks to the environment and emphasises the need for regulation to protect such environmental compartments. There is also a high predicted market growth for graphene materials according to the calculated compound annual growth rate (CAGR) of 39 % for the years between 2020 and 2027 (https://www.fortunebusinessinsights.com/graphene-market-102930)).

There are a number of general reviews detailing studies that have assessed ecotoxicological effects and potential environmental risks of graphene based NMs (Guo et al. 2014; Arvidsson et al. 2013; Jastrzebska and Olszyna 2015; Montagner et al. 2017; Fadeel et al. 2018; Evariste et al. 2020). These studies have concluded that there are deficiencies/inconsistencies in the reported toxicity data related to the lack of use of standardized approaches (*e.g*. TGs) when testing and that additional investigations are needed using standardised approaches. Furthermore, specific reviews on the toxicity of graphene material to aquatic organisms highlight knowledge gaps and the need for more studies to make definite conclusions on the toxic potential of graphene materials to aquatic organisms (Malhotra et al. 2020). Reaching definite conclusions is also hindered by the sheer diversity of graphene materials with distinct sizes, features, and forms. Studies have identified concentration dependent adverse effects for particular GO nanoforms to aquatic organisms (Evariste et al. 2020). However, these need further investigation in order to demonstrate a comprehensive understanding of the possible mechanisms dictating the adverse effects observed.

Studies performed using algae have reported half maximal effective concentration (EC_{50}) values and obvious effects of tested graphene materials related to the reduction of light availability for photosynthesis (shading effect), nutrient depletion effects (Zhao et al. 2017) and membrane damaging effects (Malina et al. 2019). Furthermore, distinct algal interactions for different

nanoforms (*e.g*. GO and GO quantum dots (GOQDs)) have been detailed (Yan et al. 2022). In addition, tests performed using the crustacean *Daphnia magna* with GO (single layer, 200-300 nm) report modest acute toxicity with $LC_{50\ 72h}$ of 45.4 mg/L (Lv et al. 2018) and also distinct effects have been reported for different functionalised GO nanoforms in this test species (Yao et al. 2018).

A specific review on the toxicity of graphene materials in fish has identified that graphene materials have the potential to induce developmental, respiratory, neurobehavioral, inflammatory, and metabolic disorders in fish (Dasmahapatra et al. 2019). A reduction in hatching efficiencies of embryos and Parkinson's disease-like effects have also been evidenced following GO exposure to fish embryos (Ren et al. 2016). Also studies performed hint at possible immunomodulatory effects through perturbations of pathways and signalling, specifically the perturbation of the aryl hydrocarbon receptor (AhR) has been demonstrated for graphene quantum dots in zebrafish (Zhang et al. 2017b). While further studies are needed, this may be caused by a direct binding mechanism, as predicted by recent modelling of binding scores for small graphene fragments to rainbow trout receptors (Connolly et al. 2021). Graphene materials cytotoxicity towards fish cell lines has also been evidenced (Kalman et al. 2019, 2022; Lammel and Navas 2014; Srikanth et al. 2017; Lammel et al. 2013) associated with oxidative stress responses. A recent review on the *in vitro* toxicity of graphene materials (Achawi et al. 2021), found over 80 publications reporting on the cytotoxicity of graphene materials with no specific trend or agreement for cytotoxicity for the GOs and FLGs tested. However, graphene quantum dots (GQD) could be classified as highly (EC_{50} ≤30 mg/L) or moderately cytotoxic (EC_{50} ≤100 mg/L), and rGO ranged from weakly (EC_{50} ≥110 mg/L) to highly cytotoxic (EC_{50} ≤30 mg/L). Again, the overall conclusion was that a lack of standardized assessments makes comparisons of studies and results difficult.

Therefore, to this end and in an attempt to evaluate the applicability of the standardised test battery (*i.e*. TG 201, 202 and 203), all existing data was collected relating to 2D graphene material testing and the specific endpoints of growth inhibition in algae/cyanobacteria, immobilisation in *Daphnia spp*., and mortality in fish. All the studies and information collected are presented in tables 1, 2 and 3 respectively. For each test/endpoint, together with available EC_{50} or LC_{50} values, details of the test material specific inherent physicochemical properties, any processing steps for test dispersion preparation, test protocol/conditions, and any observations regarding potential adverse effects besides the specific endpoint under investigation were recorded. A summary of the findings from specific tests is provided under specific subheadings, and comments on any peculiarities witnessed and any aspects of standard test methodologies that have been modified either leading to improvement in assay performance or directly affecting results have been made. Due to the scarce data on fish testing performed using TG 203, studies using fish embryos and fish cell lines were

also collected as they can be seen as alternative approaches to the use of juvenile fish and are presented in Tables 4 and 5, respectively. Standardised tests such as the OECD TG 236 fish embryo acute toxicity (FET) test and the OECD TG 249 fish cell line test can contribute to a hazard evaluation in a WoE approach for fish acute toxicity (Belanger et al. 2022, OECD 2019d).

All of this information provides guidance for the application of standardised tests for aquatic toxicity testing of graphene materials in the future and thus, will improve the quality/reliability of future studies.

2. Results

2.1 Aquatic toxicity test endpoints used in test battery for CLP classification

2.1.1 Freshwater Alga and Cyanobacteria, Growth Inhibition

Dose-dependent inhibitory effects of a test substance on algal/cyanobacterial growth can be monitored using the OECD TG 201 (OECD, 2011). According to this test freshwater algae or cyanobacteria in the exponential growth phase are exposed to the test substance for 72 h and the growth rate is quantified using either cell counts, measurement of cell volume, fluorescence or optical density readings. The concentration causing a 50% growth inhibition is calculated from specific growth rates and reported as an EC_{50} value (usually at the end of the exposure phase: $EC_{50\ 72h}$).

Only thirteen studies were collected assessing the inhibitory effects of graphene materials on algal growth (Table 1). Five of them explicitly followed TG 201, while the others used similar protocols (*e.g.* ISO 8692:2004) or modified OECD TG 201 protocols. The species used were *Raphidocelis subcapitata* (6 studies) (one of the recommended species of OECD TG 201), *Scenedesmus obliquus* (5 studies), *Chlorella pyrenoidosa* (1 study), and *Trebouxia gelatinosa* (1 study), all being freshwater green algae, with the exception of *T. gelatinosa* (aero-terrestrial). The cyanobacterial species, *Microcystis aeruginosa*, was also among the organisms used for testing in one of the studies. Test vessels used included conical flasks, micro-centrifuge tubes, 24 and 96-well plates, microbox micropropagation containers, while agitation was introduced in most cases using either magnetic stirring, orbital mixers or simple hand shaking at specific intervals over the test duration.

The graphene material most frequently tested was GO (7/13 studies). Pristine graphene (G), FLG, graphene nanofibers, rGO alone and composites with specific metal ions, and nanoforms with various functionalisations (e.g. -COOH, $-NH_2$) were also tested. Most studies reported dose-dependent inhibitory effects of graphene materials on algal growth (12/13 studies). $EC_{50\ 72\ h}$ values for GO materials ranged from 0.5 to 66.6 mg/L according to the nanoform tested and species used. Differences in the physiology, cell wall composition and structure (*e.g.* thickness) among the

unicellular algae/cyanobacteria affected the way in which the graphene materials tested interacted with the organisms (Yin et al. 2020, Banchi et al. 2018). The reported $EC_{50\ 72h}$ for rGO was 148 mg/L, according to a single study performed (Du et al. 2016). When rGO materials functionalised with Ag, Co_3O_4 or Pd metal NMs were tested, $EC_{50\ 96h}$ values of between 0.2 to 1 were reported (Yin et al. 2020), however, in these composite materials, toxicity is influenced by the metal NMs loadings and also the release of metal ions. Pristine graphene (G) nanosheets tested had a reported $EC_{50\ 72h}$ of 8 mg/L (Zhang et al. 2018), with an increase in EC_{50} values measured for different functionalised graphene nanosheet nanoforms (e.g. 32 and 84 mg/L, for -COOH and $-NH_2$ functionalised G, respectively) (Zhang et al. 2018). The graphene nanofiber tested (GANF®) and nanofibers produced through superheating (GANFg) and a scaled up production process of GANF® (GATam) had $EC_{50\ 72h}$ values of 3.09, 8.48, and 2.12 mg/L, respectively (Barrick et al. 2019). This influence of production process on effects was also evidenced in the case of different production methods used for GO with EC_{50} values of 0.5, 14 and 10 mg/L according to the distinct production methods used (Hoffman, Hummers, and Tour, respectively) (Malina et al. 2019). Thus, most of the graphene materials tested would be classified as slightly toxic (US.EPA, Toxic Substances Control Act of 1976) or in Category: Acute 3 (U.N, GHS 2022) (EC_{50} values >10-100 mg/L), while the graphene materials tested with EC_{50} >1 and <10 mg/L would fall into Category: Acute 2 in the GHS system (GHS, 2022). Only HO-GO tested in *R. subcapitata* with EC_{50} 0.5 mg/L would be classified in Category: Acute 1 (EC_{50} ≤1 mg/L) according to CLP classification categories (EC 2009). This highlights the distinct effects nanoforms have according to different sizes, oxygen contents, functionalisations, shapes and even the different production processes used. In fact, the latter can leave by-products or impurities in the final material that in some cases, especially if they are in significant amounts, can have adverse effects on the target organisms. If not taken into account, their presence can lead to misinterpretation of the results (Petersen et al. 2014). Unfortunately, the possible role of impurities in the GO and rGO materials tested was not considered in the majority of studies but independent studies show that a myriad of metallic elements can be introduced following different synthesis processes of graphene (An Wong et al. 2014). In some, a complete elemental analysis of samples was carried out (Banchi et al. 2019, Malina et al. 2020) and distinct levels of particular elements, e.g. manganese, were identified according to the different production processes (Malina et al. 2020). Filtrate controls should be used as approaches to determine the possible contribution of byproducts to the toxicity and the purification of the materials using distilled H_2O, both to enhance performance and limit any impurities (Barbolina et al. 2016).

Table 1. Freshwater Alga and Cyanobacteria growth inhibition studies

	Test Material Raw material (supplier) Production method	No. layers Thickness Later size Oxidation level Defect level	Processing step	Test Species	Protocol Medium used Readout	EC_{50} 72 h (mg/L)	Observations	Reference
1.	**FLG** Graphite (Bay Carbon, USA) Ball-milling treatment **GO** GANF® helical-ribbon carbon nanofibres (Grupo Antolin Ingeniería (Burgos, Spain) Oxidation	200-400 nm 5.2% O I_D/I_G=0.49 100 nm 48.8% O	Shaking (30 min) Vacuum-filtration of aqueous suspensions on PTFE membranes Growth in Microbox micropropagation containers	*Trebouxia gelatinosa*	OECD TG 201 (modified to facilitate growth on solid *Trebouxia* Medium) Cell counts, Chl-a content, Chl-a Fluorescence Membrane damage	FLG: > 50 GO: >50	No effects on growth dynamics at concentrations tested (0.01, 1 and 50 mg/L) FLG: down-regulation of HSP70-1 gene expression	Banchi et al. 2019
2.	**GANF®** (Grupo Antolin Ingeniería (Burgos, Spain)) Catalytic vapor deposition **GANFg** (Grupo Antolin Ingeniería (Burgos, Spain)) Superheating of GANF® (1500 °C) **GATam** (Grupo Antolin Ingeniería (Burgos, Spain)) Scaled-up production of GANF®	Fibres 20–80 nm (diam.)	Nanogenotox protocol: EtOh prewetting, Sonication (probe) (16 min) ± BSA 0.05 % Continuous stirring	*Raphidocelis subcapitata*	OECD TG 201 OECD 201 Test media Chl-a Fluorescence Magnetic stirring	GANF®: 3.09 GANFg: 8.48 GATam: 2.12	Stability measurement: UV-Vis spectroscopy After 72h 0-6 % nominal conc. Interferences at conc. >12.5 mg/L BSA improved stability but interfered with algal growth Interference with fluorescence readout	Barrick et al. 2019
3.	**GO** (Sigma Aldrich, USA)	Single layer 2 nm 225.1±105.4 nm 32.2% O I_D/I_G= 1.04	Sonication (bath) (30 + 5 min) ± HA (20 mg/L)(Sigma Aldrich)	*Raphidocelis subcapitata*	96-well plates Absorbance	GO: 66.60 GO+HA: 242.78	Stability measured using UV-Vis spectrophotometry (OECD 2017) After 24 h GO: 60 % nominal conc. and GO+HA: >80 % nominal conc.	Castro et al. 2018
4.	**rGO** (Hengqiu Graphene Technology Co, (Suzhou, China))	Single layer 0.5-0.6 nm 0.2-5 µm	Ultrasonication (150 W) (30 min)	*Scenedesmus obliquus*	OECD TG 201 (modified) HB-4 medium Cell counts, Absorbance	148	Shaking 1h intervals Chlorophyll a (Chl a) and chlorophyll b (Chl b) contents also measured	Du et al. 2016
5	**GO** (Abalonyx AS (Oslo, Norway))		Sonication (probe) (13 min and 45 sec)	*Raphidocelis subcapitata*	TG 201 media		Autofluorescence from GO caused an overestimation of Chl-a concentration	Farkas et al. 2017
6	**GO** Graphite powder (Sigma Aldrich, USA) Hoffman method (Hoffman et al. 1937):		Sonication (bath) (60 min)	*Raphidocelis Subcapitata**	ISO 8692:2012 (modified) 24-well cell culture plate	HO-GO: [0.5*, 9^] HU-GO:	No shaking/mixing Interference with fluorescence readout	Malina et al. 2019

	HO-GO Hummers method (Hummers et al. 1958): HU-GO Tour method (Marcano et al. 2010): TO-GO	C/O=2.60, 27.8% O I_D/I_G= 0.75 C/O=1.95, 33.9% O I_D/I_G= 0.98 C/0=1.72, 36.8% O I_D/I_G=1.16	Sonication (probe) (pulsed 3x, each 5 sec)	*Scenedesmus Elongatus*^	ZBB medium Cell counts, Chl-a Fluorescence	[14*, 27^] TO-GO: [10.1*, 10^]	Nutrient absorption and shading effects	
7.	**GO** Graphite powder (Sigma Aldrich, USA) Improved Hummer's method (Tour method; Marcano et al. 2010)		Sonication (probe) (pulsed: 5 sec on, 5 off) (4 h) Centrifugation (4602 *g* for 6 min) Filtration (0.22 µm pore-size) 3- day pre-incubation step in media and continuous orbital shaking until use	*Raphidocelis subcapitata*	MA-MS media OECD TG 201 media Orbital mixing (80 rpm) and shaking by hand 3 times every 24 h Cell counts, Chl-a Fluorescence	9.71 (MA-MS media) 5.82 (OECD media)	UV-vis spectrophotometry for concentration measurement only possible at high conc. (at 16 and 32 mg/L >90% nominal conc.) Shaking, orbital mixer and by hand shaking Drift in the pH value in MA-MS media Interference with fluorescence readout Cell count decrease due to algae attaching to GO	Markovic et al. 2020
8.	**GO** Graphite powder (Nacional de Grafite, Brazil) Modified hummers	Single layer 3.5 nm 120–200 nm	Sonication (probe) (pulsed) (4 h) Centrifugation and Drying step	*Raphidocelis. subcapitata*	Oligo medium Cell counts	20 (96 h)	UV–Vis spectrophotometry for stability Increase in size of GO flakes from 145 nm to 429 nm	Nogueira et al. 2015
9.	**GNPs** (PlasmaChem GmbH, Germany)	Single layer 1–4 nm 2 µm <7% O	Stirring 24 h Sonication (30 sec) ± LOA (GA or BA) (1-40 mg/L)	*Scenedesmus obliquus*	OECD TG 201 OECD 201 media	Nd (LOEC 0.5)	Shaking by hand 3 times a day Sedimentation experiments Increased stability with LOAs present but this also lead to increased toxicity	Wang et al. 2016
10.	**GNPs** (PlasmaChem GmbH, Germany) **rGO** (XFNANO Materials Tech Co. (China, Nanjing))	Single layer 1-4 nm 2 µm <7% O 8-1.2 nm 0.5-5 µm	Sonication (bath) (30 min)	*Chlorella pyrenoidosa*	OECD TG 201 (modified) OECD 201 Test media	Nd GNPs: NOEC 0.1 rGO: NOEC 1	Shaking by hand 3 times a day	Wang et al. 2021
11.	**GO** Graphite (supplier not specified) Modified hummers	1.34 ± 0.071 nm 3-8 µm 32.9% O	Sonication (bath) (30 min)	*Chlorella vulgaris Scenedesmus*	OECD TG 201 (modified) G-11 media	10 (*Scenedesmus obliquus*)	Shaking by hand 3 times a day Stability measurement: UV–Vis spectrophotometry	Yin et al. 2020

				obliquus *Microcystis aeruginosa* *Chlamydomonas reinhardtii* *Cyclotella sp.*	SE media CSI media Cell counts, Cell area, Chl-a content		Sensitivity ranking: *S. obliquus > C. vulgaris > M. aeruginosa > Cyclotella sp.> C. reinhardtii*	
12.	**rGO** **rGO-Au** **rGO-Ag** **rGO-Pd** **rGO-Fe_3O_4,** **rGO-Co_3O_4** **rGO-SnO_2** (XFNANO Materials Tech Co., Ltd. (China, Nanjing))	Single layer 0.5-5 mm 5-8 layers 2-4 layers 4-8 layers 3-6 layers 2-6 layers 2-4 layers	Sonication (bath) (1 h)	*Chlamydomonas reinhardtii** *Scenedesmus obliquus^*	OECD TG 201 (modified) Simplified SE medium Cell counts, Chl-a content	rGO-Ag: [<0.2*, <0.2] rGO-Co_3O_4: [1*, Nd^] rGO-Pd:1, Nd^] All other materials: [Nd (>1)*, Nd (>1)^]	Shaking every 8 h by hand Stability measurement: UV-Vis spectrophotometer 30%-55% of nominal conc. (96h) Increase in Chl-a content evidenced	Yin et al. 2020
13.	**G** **GO** **G-COOH** **G-NH_2** (XFNANO Materials Tech Co., Ltd. (China, Nanjing))	Single layer 0.8–1.2 nm 0.5–2.0 µm Single layer 0.8–1.2 nm 0.5–5.0 µm 0.8–1.2 nm 0.5–2.0 µm 0.8–1.2 nm 0.5–2.0 µm	Sonication (150 W) (2 h) ±HA 10 mg/L	*Scenedesmus obliquus*	OECD TG 201 BG-11 medium Absorbance, Chl-a content	G: 8 GO: 21 G-COOH: 32 G-NH_2: 84	Shaking 3 times daily by hand HA significantly mitigated the inhibition of cell growth and Chl-a synthesis Shading effect on algal growth and Chl-a synthesis	Zhang et al. 2018

GANF®; graphitized carbon nanofibers, GNPs ; HSP70-1, heat shock protein 70.1, diam,; diameter, PTFE; polytetrafluoroethylene polymer, EtOh; Ethanol, BSA; bovine serum albumin, HA; humic acids, LOA; low-molecular-weight organic acids, GA; gallic acid, BA; benzoic acid, GNPs; graphene nanoplatelets, G; graphene, rGO; reduced graphene oxide, I_D/I_G; the intensity ratio of defect according to D (ID) and G bands (IG), Chl-a; chlorophyll a, W; Watt, NOEC; No observed effect concentration, LOEC; lowest observed effect concentration, Nd; not determined, concn.; concentration, G-COOH; carboxyl-modified graphene, G-NH_2; amine-modified graphene.

Other critical issues that were identified by some of the authors are: *(i)* graphene material hetero-aggregation with algae and precipitation out of the water column (Markovic et al. 2020); *(ii)* shading effects of the test dispersions on growth and/or nutrient depletion due to adsorption to graphene materials (Malina et al. 2019); and *(iii)* interferences with fluorescent readouts at high test material concentrations (Barrick et al. 2019, Malina et al. 2019, Markovic et al. 2020). These three points are discussed herein.

According to the revised studies the graphene materials tend to agglomerate/aggregate and rapidly settle in TG 201 medium and/or the other standard media used. Importantly, this aggregation and precipitation phenomena could affect the applicability of TG 201, since one of the quality criteria of this TG is that the concentration of the tested substance be satisfactorily maintained within 80% of the nominal or measured initial concentration throughout the test. Only a few studies partially addressed this issue using UV-Vis measurements to monitor the stability of graphene dispersions, obtaining contrasting results. Markovic et al. (2020) reported achieving > 90% of GO nominal concentrations throughout the test, whereas Castro et al. (2018) reported an absorbance decrease of c. 40% already after 24 h for another GO. Similarly, Yin et al. (2020) reported a decrease of 45% to 70% of the nominal concentration in dispersions of rGOs composites with metal ions. This data suggests the importance of the chemical composition of graphene materials on their stability in aqueous media, as large differences can be expected according to graphene material C/O ratio, even though this factor is not the only one affecting the stability of graphene dispersions. Indeed, as mentioned in the OECD GD 317 document, the medium ionic composition is another factor that can strongly influence the stability of NM dispersions. Organic acids have been used as natural dispersants to increase the concentration maintenance time of GO dispersions but this also leads to mitigation of toxic effects (EC_{50} 66.60 to 242.78 mg/L) (Castro et al. 2018). The incorporation of bovine serum albumin (BSA) as a dispersant also appeared to interfere with algal growth (Barrick et al. 2019). Therefore, careful consideration towards the use of dispersants is needed along when applying TG 201 to graphene materials.

As graphene materials are often dark coloured and light absorbing, and as algal cells rely on light for photosynthesis, concentration-dependent shading effects are likely to occur in a test system with graphene material dispersions (Malina et al. 2019, Zhang et al. 2018, Zhao et al. 2017)). This shading effect was tested by submerging conical flasks with growing algae in beakers filled with the test material. A significant contribution of shading to the growth inhibition was observed (16.4 %) when testing graphene at concentrations of 50 mg/L (Zhao et al. 2017).

Interferences with readouts (e.g. direct fluorescence measurement of cell density) at concentrations >12.5 mg/L and when using haemocytometers, as it can be difficult to count individual algae if

within graphene material aggregates, can lead to false readings (Markovic et al. 2020). It was also seen that even when using alternative approaches (*e.g*. chlorophyll (chl) extraction) interferences can be evidenced (*e.g*. due to adsorption of the extracted chl to the graphene materials) (Malina et al. 2019, Farkas and Booth 2017).

The depletion of nutrients (*e.g*. metal ions, which are often essential for algal growth) by adsorption to graphene materials is another witnessed phenomenon raising concerns. This can lead to a reduction in nutrient availability and inhibit algal growth. Approaches to characterise/quantify shading effects and assay interferences have been discussed in GD 317 (OECD 2022a) along with efforts that can be made to overcome them, for example the use of specialized exposure vessels to maximise light transmission and reduce potential shading effects and alternative methods of chl measurement. One example of a specialised equipment to maximise illumination is the LEVITATT (LED Vertical Illumination Table for Algal Toxicity Tests) system for vertical illumination for testing coloured substances or nanomaterials (Skjolding et al. 2020). While test setups using double-vial systems to distinguish direct toxic effects and indirect physical effects have also been used (Sørensen et al. 2015). Alternative method for chl measurement that have been described include modified versions of ISO 10260:1992 incorporating an algal filtration step (Farkas and Booth 2017), as well as a locust bean gum separation technique (Hund-Rinke et al. 2022). Such approaches may not be applicable in all cases and thus prior validation studies would be needed. Furthermore, the benefit and assurance of including a second endpoint, as used in many of the studies, is evident.

[…]

2.3 Specific factors to consider when applying standardised OECD tests for testing graphene materials

The possible need for adaptations to standard ecotoxicity tests for testing NMs was first eluded to in early publications (Crane et al. 2008). Progress has now been made in identifying areas in which changes, developments, and standardisations may be needed (Boros and Ostafe 2020; Nesser and Lynch 2019). OECD GD 317 has been published to aid in the application of existing OECD TGs on aquatic (and sediment) toxicity testing to allow more reliable and reproducible data generation for NMs, and it includes a section with advice on specific modifications for specific TGs when testing NMs (OECD 2020). Among the particular TGs mentioned, and for which it has been recognised that additional considerations are needed, are TG 201 and TG 236. In addition, there are also publications dedicated to the specific considerations which may be needed when testing certain

types of NMs (*e.g*. Nanobiomaterials; Amorim et al. 2020), albeit with no specific reference to TG 201, 202, 203 or 236.

In the following section, based on the observations made via this comprehensive review, a number of factors to consider when performing acute aquatic toxicity testing of graphene materials using these TGs have been identified. These specific factors will be detailed under the relevant subheadings concerning test dispersion preparation, the conduct of tests and data analysis and reporting. Specific guidance tailored to the needs of acute aquatic toxicity testing of graphene materials is highlighted in Table 6 and 7 and 8. This specific guidance goes beyond the generic guidance given in GD 317 by drawing on evidence from all the studies performed with 2D graphene materials. This additional information contributes to the generation of a more prescriptive guidance to facilitate the increased use of OECD TGs for testing NMs such as graphene materials in the future.

Table 6 General and specific factors to consider towards a prescriptive guidance for aquatic testing of graphene materials related to stock dispersion preparation

	Recommendation	
Dispersion Preparation	**GD 317**	**Graphene material specific consideration**
Method/Protocol selection	Begin with evaluation of material stability in ultrapure water Use of dispersion method described in OECD TG 318 as a starting point	Dispersion method described in TG 318 may not be suitable. Use of less aggressive approaches (e.g. bath sonication) that may cause less defects and breaks
Use of sonication	Beyond the GD scope but its use should not alter the test material or medium and an optimum sonication time and energy should be considered	Sonication time and energy should be optimised to achieve minimum agglomerate/particle size distribution without altering material properties (e.g. introducing breaks or defects)
Use of dispersants	It is preferred to avoid the addition of stabilizing substances The stability of the stock dispersion should be evaluated if it is to be reused for media renewal during the test	To avoid the need for use of dispersants, freshly prepared stock dispersions can be generated for each renewal

2.3.1 Test stock dispersion preparation

For aquatic toxicity testing, normally aqueous (stock) dispersions of graphene materials are applied to the test systems/vessels of respective tests, by dosing test media to generate the test concentrations required for testing. The majority of the graphene materials tested were supplied/produced in powder form and therefore needed to be dispersed prior to testing. The dispersion method heavily relied upon to prepare aqueous (stock) dispersions of graphene in the studies reviewed was ultrasonication. The protocols used were highly variable, and included the use of different sonication techniques (probe or bath sonication, continuous or pulsed modes) and different time scales (from 10-15 min up to 4-6 h). Use of ultrasonication, and particularly probe sonication, may cause a significant change in material properties. For example, breaks in flakes have been evidenced after probe sonication (Baig et al. 2018) and strikingly different size distribution profiles were evidenced when using bath or probe sonicators to prepare graphene nanoribbon stock dispersions (Mullick Chowdhury et al. 2014) and after short and prolonged sonication times (30 min vs. 2.5 h) (Jiang et al. 2021). In fact, prolonged sonication times were used to achieve dispersions of materials with smaller sizes for comparative testing. These distinct dispersions, produced using prolonged sonication times, have shown different interactions with organisms including enhanced membrane penetration ability (Su et al. 2017), increased cytotoxicity to cells (yeast and lung epithelial cells) (Jiang et al. 2021), and increased fish embryo mortality (Mullick Chowdhury et al. 2014). Aggressive sonication techniques have also been shown to increase defects (detected according to increased ratios of the intensity of D- Raman peak and G- Raman peak (I_D/I_G) of 1.3 to 2.3) (Mullick Chowdhury et al. 2014), and likely also contributes to an increased toxicity as evidenced in the case of graphene nanoribbons, which, due to their form, may prove particularly susceptible to material transformations under such conditions. Besides considerations for sonication type and time, one must consider the power and total ultrasonication energy (kJ) applied. This is rarely reported in studies making comparisons problematic. Occasionally the electrical input and output power were specified, however it is the effective acoustic power that is delivered to the suspension that is critical and that can be measured using calorimetry. An excellent attempt towards a standardisation of ultrasonic dispersion of NMs has been made by Taurozzi and colleagues describing the calorimetric method and detailing the parameters and material characteristics recommended for reporting purposes (Taurozzi et al. 2011). The total power delivered will also determine the dispersion state, with an alteration of chemical structure (exfoliation and destruction of surface groups) being shown to occur at sonication energies of 100 kJ (Dimou et al. 2021). At these high energies there is also an increase in temperature and this must be controlled as it may also influence a change in material form due to heating. Therefore,

careful consideration is needed regarding initial dispersion method selection and a thorough characterisation of the dispersed material, including the characterisation of any potential changes in nanoform caused by the processing, is essential and must be assessed (see section 2.3.3). On one hand, according to GD 317, the method used to disperse NMs should be optimized to achieve the smallest agglomerate size, narrowest distribution and adequate dispersion stability, yet the use of sonication should not alter the test material or medium. Therefore, careful selection of a dispersion method should be made for graphene materials. However, to date, to our knowledge, no standardised protocol specifically for graphene material dispersion has been developed. Dispersion protocols such as those described in TG 318, and advocated for as a starting point in GD 317, use probe sonication, however a less aggressive dispersion technique (*e.g*. bath sonication), may be more appropriate for graphene material dispersion preparation. For example, using probe sonication and the generic nanogenotox dispersion protocol, which has been developed within the EU project NANoREG to facilitate a standard operating procedure (SOP) for NM dispersion (Jensen et al. 2011), graphene material dispersions were prepared with 7056 J of delivered acoustic energy (Barrick et al. 2019). While not characterised in this study, increases in defect ratios (I_D/I_G of 0.07 to 0.2) and fragmentation of FLGs have been evidenced when such energies were applied (Baig et al. 2018). Another approach applied when preparing graphene material stock dispersions was the use of dispersants. For example, again following the SOP of the nanogenotox protocol, bovine serum albumin (BSA) was used as a dispersant (Barrick et al. 2019). While it improved the stability of dispersions, it also led to changes in the interaction between graphene and organisms in *Daphnia* studies (*e.g*. decreased adherence to body and lower toxicity). Also distinct EC_{50} values were observed in fish cell lines depending on the addition of BSA in the stock dispersions (Barrick et al. 2019) (Table 5). The addition/use of dispersants for stock dispersion preparation must be considered in the context of the test design and can be differentiated from their use in working test dispersions (discussed later). Fresh stock dispersions serve to prepare working test dispersions at the start of the test, thus stability of these dispersions over an extended timeframe is only relevant if the same stock dispersions are going to be used for water renewals. Also it is preferred that the use of stabilising agents is avoided (GD 317) and not advocated for (GD 23). In this particular example BSA has been used as a dispersant, and in the context of environmental relevance this material is not representative or found in aquatic environments.

Therefore, regarding the preparation of stock dispersions of graphene materials, some specific factors to consider relate to the dispersion method or protocol selection, the effective acoustic power delivered when using sonication and the need for use of dispersants. Such factors are detailed in Table 6.

Table 7 General and specific factors to consider towards a prescriptive guidance for aquatic testing of graphene materials related to the conduct of tests

	Recommendation	
Test Conduct	**GD 317**	**Graphene material specific consideration**
Exposure concentration/ dosimetry	Should be measured in the highest and lowest test concentration at the start and end of test, and before and after water renewals (if used). Should be maintained at ≥ 80% of the nominal chemical concentration throughout the test. Averaging, time-weighted averaging, or geometric mean approaches can be used if concentrations not maintained at 80%. Considerations needed for contribution of any settled fractions to exposure dose.	Limitation in analytical sensitivity (UV-Vis) in measuring low concentrations (<1 mg/L). More robust analytical techniques required. Low stability under test conditions but such approaches to date have not been used in studies Both overlying and sedimented dose must be considered if performing renewals (e.g. TG 236). In static systems using submerged cells (e.g. TG 249) effective dose during exposures should be considered
Methods for concentration maintenance	Agitation can be used in specific tests (TG 201, 203) but such protocols must be optimised using pre-tests. Semi-static water renewals can be used in specific tests (e.g. TG 203, TG 236) but renewal frequency must be dictated by concentration measurements. Potential settling effects should be considered (e.g. fish embryo testing). Caution embryos not sensitive to drying effects when performing concertation renewals	Agitation protocols need to be developed on a graphene material and test specific basis. Renewals can be applied, but there are limitation in analytical sensitivity (UV-vis can be used for approximations). Water renewals may also be an approach for use in TG 202. Agitation may also be appropriate in other tests (e.g. TG 236 and TG 249), to address uncertainty and inconsistency in exposure levels due to test materials settling and improve dispersion.
Media supplementation /modification	General considerations for performing test media adjustments are provided. Environmental realism issues are beyond the scope of this GD. DOM/NOM can be used on case basis but minimum amount to achieve	Use of standardised media (when described) in tests to ensure comparisons between studies (e.g. TG 201 medium, L-15/ex medium). NOM has a stabilising effect but also reduces the toxicity of the graphene

	stability and controls needed.	material and therefore it is advisable to avoid its use. Include controls and also tests with materials without NOM.
Media interaction	Possible adsorption of media components and depletion of nutrients in test dispersions need specific consideration when testing NMs. No guidance provided	Nutrient depletion effect evidenced caused by the adsorption of Ca^{2+} and Mg^{2+} to graphene materials. Approach using materials pre-conditioned in media proposed to negate effects. Pre-tests should be used to assess media interaction.
Interferences	Shading effects in particular with TG 201 Efforts to reduce or quantify these effects should be made in pre-tests or parallel tests.	Specialised experimental setup should be used to assess and quantify shading effect (see Zhao et al. 2017).
	Measurement interference of the tested NM in the test dispersion on the toxicity endpoint to be measured should be evaluated.	Fluorescence quenching evidenced for graphene materials with TG 249 assay readouts.
	Physical interferences (e.g. hetero-aggregation may cause reduction in algal cell number in TG 201)	Hetero-aggregations evidenced to cause reduction in algal cell number. Pre-tests or parallel tests should be used to assess physical interferences.

2.3.2 Conduct of the test

2.3.2.1 Exposure concentration

According to the OECD standardised TGs, working test dispersions should be analysed to measure exact exposure concentration, as a minimum, at the highest and lowest test concentrations. In a static system measurements should be taken at the beginning and end of the test, whereas in a semi-static system before and after renewals. This is used to verify the initial concentration and to assess if the exposure concentration can be maintained. Concentration measurement and stability assessment, related to the maintenance of 80% of nominal (measured) exposure concentrations are prescribed in TG 201, 202 and 203 as well as TG 236 for embryo testing. Despite this, in the studies collected overall there was a lack of analytical determination of graphene material test exposure concentrations and instead effective values were reported in the majority of studies based on nominal concentrations. While this could be explained by the poor availability of robust/available

analytical techniques and procedures for graphene material quantification, effects based on nominal concentrations can only be relied upon in cases where stability and concentration maintenance are assured. UV-vis has been used by a number of authors for approximate estimations of initial concentrations. However, it has specific limits of quantification ((LOQ) (e.g. 3.21 mg/L for graphene materials (Markovic et al. 2020)). On a number of occasions UV-Vis spectroscopy was used to monitor any alterations in absorbance spectra in test dispersions over the exposure duration and any decreases were expressed as % loses of initial nominal concentrations. Results from these studies, as well as visual observations of precipitates, indicate that often in the tests performed nominal concentrations were not maintained and therefore uncertainties surround actual exposure concentrations in these studies.

The loss/change in the initial nominal concentration is related to the materials physical and chemical characteristics as well as to the molecules/compounds released by the organisms and specific media compositions. The materials tend to spontaneously aggregate/agglomerate because of *i)* their hydrophobicity (as in the case of FLG, graphene and other very reduced graphene materials) or *ii)* because of the presence of functional groups negatively or positively charged (as in the case of GO, rGO, and functionalised materials) that can coordinate ions in the medium and create cross-flakes bonds (drove especially by polyvalent ions). Furthermore, organisms such as algae can release molecules and compounds, such as extracellular polymeric substances (generally polysaccharides), that can agglomerate with the graphene materials causing their precipitation. These substances can be produced as a defence response to toxicants (Andrade et al. 2010) or for other physiological functions. In the case of graphene materials it was observed that these substance can help to slough off the materials from the algae surface (Garacci et al. 2017).

Any losses in the water column concentration, as well as reducing the exposure dose to free swimming test organisms (*e.g.* algae, fish), also may lead to increases in exposure doses of fish cells or test organisms such as fish embryos that reside at the bottom of test systems. In fact, often in these particular test setups and when testing materials susceptible to sedimentation, there is a particular contribution of this sedimented fraction to exposure that can be referred to as a delivered dose. In this field of NM in vitro dosimetry, models and approaches have been proposed and are being developed to estimate this dose (Deloid et al. 2014; Botte et al. 2021). While very few studies report this delivered dose, once methodologies are developed and validated this will become very important information for interpreting NM in vitro testing results. According to TG 249 the exposure concentration of a test substance to fish cell lines is quantified by measuring the concentration in suspension at the start of the test and at the end and a geometric mean is calculated to express the exposure concentration. While such an approach has been standardised for chemicals,

further consideration may be needed when testing NMs to include also consideration for the delivered dose.

Therefore, in the context of NM and graphene material testing, the validity criteria in OECD TGs concerning the maintenance of exposure concentrations becomes increasingly important and even a special consideration of this issue is needed that may be extended to proposing specific suitable methods to achieve this criteria.

Table 8. Inherent and system dependent physicochemical properties for graphene material characterisation and reporting

Physicochemical property	**Graphene material specific reporting**	**Monitoring Approach (Standardised TG and guidance documents available and/or being developed)**
Chemical composition	Elemental composition [*identification based on sp^2 bonded carbon detection*] Oxygen content Raw material Production method Material form (*e.g.* powder, solution)	Raman spectroscopy (tip enhanced) XPS, ICP-MS, TGA, FTIR, XRD
Impurities	**%,** μg L^{-1} *e.g.* N-doping which is a substitutional impurity, S, and potentially toxic elements (Cd, Cr, Cu, Mn, Pb)	ICP-MS, ICP-OES
Surface treatment/ functionalisation	Edge or Surface chemical groups Oxidations	XPS/EDX OECD WNT project 1.6: Guidance document on identification and quantification of the surface chemistry and coatings on nano- and microscale materials (OECD 2021b)

Particle size	No. of layers Layer thickness Lateral size	Raman spectroscopy/AFM//XRD OECD TG 125 (OECD 2022c)
	Size distribution[Number based distribution; D10, 50, 90]	Laser diffraction (ISO, 2020)
Shape/Aspect ratio	*e.g.* platelet, spherical, ribbon, fibre, quantum dot	TEM, rheo-SAXS
Crystallinity	(%) crystallite size (diameter (L_a))	XRD/Raman
Assembly structure/Orientation	*e.g.* stacking; Bernal, Rhombohedral, Turbostratic	Raman spectroscopy
Defects (type and distance)	Zero, one or two dimensional defect type I_D/I_G ratio as measure of defect distance	
Surface area, including porosity	**Specific surface area by mass (m^2/g), or volume**	BET method (ISO 9277 (2010)) OECD TG 124 (OECD 2022b)
Density	Bulk density (tapped) (graphene council framework)	Helium pycnometry TG 109 Density of Liquids and Solids (2012); ISO 12154:2014
Hydrophobicity attachment efficiency (α)	Surface hydrophobicity	OECD WNT Project 1.7: New test guideline on determination of surface hydrophobicity of manufactured nanomaterials (OECD 2021b) Maximum particle dispersion (MPD) (Li et al. 2022) Dark-Field microscopy (Valsesia et al. 2018) Dye adsorption method (e.g. rose bengal or nile blue dye partitioning) Contact angle hydrophobic interaction chromatography (HIC)
Solubility: **Rate of dissolution** / Equilibrium solubility*	Test for leaching of components/production products	OECD WNT Project 1.5: Guidance document on determination of solubility and dissolution rate of

		nanomaterials in water and relevant synthetic biological media (OECD 2021b). OECD WNT Project 3.10: New test guideline on dissolution rate of nanomaterials in aquatic environment ongoing (OECD 2021b)
Dispersion stability	Concentration maintenance in dispersion under test conditions Zeta potential measurement **Aggregation/agglomeration state**	OECD TG 318 (OECD 2017), GD 318 (OECD 2021) Zetasizer folded capillary cells Dynamic light scattering
Surface reactivity (redox reactions)		TG 495 OECD (OECD, 2019e) Electron spin resonance (ESR) Ferric reduction ability of serum (FRAS) assay (Gandon et al. 2017) Dichlorodihydrofluorescin diacetate ($DCFH_2$-DA) assay Protein carbonylation
Degradation/ Transformation /Surface chemistry changes	physical breakage, enzymatic reactions, oxidation, hydrolysis, sulfidization, photocatalytic **Degradation or transformation products**	ISO 20814:2019 (ISO,2019); NADH monitoring Rhodamine-B dye degradation OECD TG 316 (OECD 2008) OECD WNT Project 3.16: Guidance Document Environmental abiotic transformation of nanomaterials (OECD 2021b) Degradation halftimes ($t_{1/2}$) (Kümmerer et al. 2011) OECD TG 309 (OECD 2004b), TG 303 (OECD 2001); OECD TG 301 (OECD 1992): BIOLOG MT2 assay (adapted) (Cross et al. 2022) OECD TG 86 (OECD 2018)

Note: properties in bold reflect those specifically required to fulfil obligations under REACH (Annex VI) (EC, 2006)

2.3.2.2 Methods for concentration maintenance

To maintain nominal exposure concentrations throughout testing, approaches already proposed by GD 317 for testing NMs include media modifications (pH, ionic strength/composition), adding turbulence (agitation/shaking), addition of stabilising substances (*e.g.* NOM/DOM) or introduction/modification of water renewals. However, feasible and acceptable approaches differ depending on the specific TG: TG 201 allows agitation while TG 202 should be a static system, and in TG 203 both agitation and an exposure renewal can be used. According to TG 236 water renewals can be used, while none of the approaches are detailed in the test procedure of TG 249 and instead shorter (*e.g.* 4 h) exposures are prescribed for unstable test substances. In the collected studies agitation (hand or orbital shaking and magnetic stirring) of exposure dispersions of graphene materials was often used in algal tests, however, despite this, unstable dispersions and loss of concentrations during the 72-h exposure period were often reported. Specific modifications described in GD 317 for TG 201 when testing NMs relates to agitation of dispersion and the use of pre-tests to determine optimum mixing methods. In one of the collected studies (Barrick et al. 2019) choice of magnetic stirring over other approaches was based on a study by Manier et al. 2016 which compared orbital shaking and magnetic stirring regimens and showed that the magnetic stirring minimized the agglomeration and sedimentation of TiO_2 NMs. However, the result is likely be different for different NMs. In fact, in the study of Barrick et al (2019) magnetic stirring was applied to the three different types of graphene materials being tested and the differences in concentration maintenance for each ranged from 0-94%. In all other studies the rationale for selection of specific agitation methods (*e.g.* shaking by hand 3 times a day) was not provided, stability was not maintained and pre-tests as prescribed by GD 317 may have aided in optimising maintenance of the graphene materials in dispersion.

Such agitation approaches are not advocated for in TG 202, in order to maintain the organism's natural static environment and indeed sedimentation and losses of concentrations were often reported. However, concentration maintenance may not be as critical when testing using TG 202 as *Daphnia,* the test organism, is a filter feeder and it has been observed that any material which sedimented to the bottom of the exposure vessels were still bioavailable and taken up by the organisms (Malina et al. 2020). While not explored in any of the studies using TG 202 to date, an exposure water renewal approach could also be used to facilitate the maintenance of a constant exposure phase. Exposure concentration renewal approaches were used in the majority (8/13) of studies in the fish acute toxicity tests that were performed with graphene materials (Table 3). Exposure renewal approaches were also used in a large number of the studies (10/26) performed using embryos (TG 236) (Table 4). In both of these tests, renewals were more commonly performed

every 24 h, however in some cases longer or shorter (*e.g*. twice daily) intervals were used. In order for such an approach to ensure consistent exposures, pre-tests for stability assessment should be performed and will inform on the frequency of renewal that may be necessary to maintain exposure concentrations of at least ≥ 80% of the nominal starting concentration to be tested. These pre-tests were missing in the studies performed with graphene materials to date and if incorporated into future study designs water renewals with increased frequency may prove a feasible approach for use in TG 203 and TG 236. However, careful considerations must be given to the role of any material that has attached to the organisms during these renewal phases and its contribution to the overall exposure dose.

A standardised test guideline for NM stability assessment in simulated environmental media is available (TG 318, OECD 2017). According to this test guideline, stability assessments are performed in media representing natural surface waters at specific pHs, concentrations of divalent ions and NOM and specific particle concentrations. However, the methodology, while not standardised or validated for stability assessment under specific ecotoxicity test conditions, can be adapted and serve also for testing stability in a range of different test media and at different concentrations. Also to be as representative as possible of test conditions, not only freshly prepared specific test media but also test media which has been held under test conditions and with organisms present (matured media) could be used. Such an approach would introduce also secretions from organism into the systems, which have been shown to have a direct impact on graphene material stability (Lu et al. 2017; Lv et al. 2018). Also these pre-tests can be performed in the same test vessels as prescribed in respective tests to represent test conditions.

Another approach for test concentration maintenance is the use of stabilising substances. According to GD 317, while this approach should be avoided, natural organic matter (NOM)/dissolved organic matter (DOM) may be permitted in certain cases where there is a strong desire to stabilise the test material. Humic acid (HA), the principal constituent of NOM, is used in some protocols for fish acute toxicity (*e.g*. EPA 1996) while recently a standardised NOM (Suwannee River NOM (2R101N)) composed of various constituents (including HA) has been used in an approach to allow the characterisation of NM stability under such conditions (OECD TG 318) (OECD, 2017). However, NOM/DOM use has not been prescribed specifically in any of the OECD TGs discussed in this review for aquatic toxicity assessment. In the collected studies, organic matter has only been used on a few occasions (6 studies) and overall promoted exposure concentration maintenance in the various test media but also mitigations of toxic effects were evidenced. In algal tests the use of HA (20 mg/L) promoted GO colloidal stability and concentrations remained within (or close to) the limit of the 20% reduction of the nominal concentration. However, EC_{50} 72 h values for GO

increased from 66.60 to 242.78 mg/L when tested in the presence of HA (Castro et al. 2018). Other low molecular weight organic acids (LOAs), specifically benzoic acid (BA) and gallic acid (GA), also promoted colloidal stability of graphene materials in a concertation dependent manner, but to different degrees and with distinct effects on algal growth and toxicity (Wang et al. 2016). In tests using TG 202 and incorporating different concentrations of HA (5-25 mg/L) to GO test dispersions, reductions in agglomeration and defects were evidenced in the presence of HA and EC_{50} values for acute toxicity to *D. magna* increased from 84.2 to 111.4 mg/L in a HA concentration dependent manner (Zhang et al. 2019). In fish tests, the addition of Suwannee River NOM (10 mg/L) facilitated the maintenance of exposure concentrations ≥90% over 72 h when testing small FLG, however exposure concentrations of large FLG ≥75 µg/L could not be maintained at or above 80% (Lu et al. 2017), highlighting that specific considerations and adaptations for different graphene material forms may be needed. Similarly, in fish embryo tests, de Medeiros et al. (2021) have tested GO and GO-AgNPs in zebrafish embryo medium supplemented with 20 mg/L Suwannee River NOM and only evidenced the promotion of maintenance of exposure concentrations of GO over the exposure period (72 h). The presence of NOM did not improve maintenance of GO-AgNPs exposure concentrations and also mitigated the toxic effect of these materials to embryos (LC_{50} from 1.4 to 2.3 mg/L). Clemente et al. (2019) reported also the maintenance of GO exposure concentrations in reconstituted water, and a reduction in toxicity of the GO to zebrafish embryos when HA (20 mg/L) was used. According to GD 317, in cases where distinct EC_{50} values are obtained the most conservative EC_{50} values should be used for hazard assessment.

2.3.2.3 Media interactions

Working test concentration ranges are usually prepared from initial stock dispersions, in relevant test exposure/growth medium that vary in chemistry (*e.g.* ionic strength and ionic species, nutrients etc.) according to the requirements of the organisms/cells used in the specific TGs. There are already excellent articles on the influence of solution chemistry on NM dispersion and toxicity (Gao et al. 2009). Thus, the distinct media formulations used, as well as any supplements, are likely to influence material behaviour (stability) and results. For example, Castro et al. (2018) have provided a detailed characterisation of the stability of GO in a range of standard media used for testing aquatic species including algae and *Daphnia*, demonstrating distinct dispersions and behaviours. Markovic et al. (2020) showed distinct size distributions of the GO test material and toxicity when using MA-MS medium vs. the OECD TG 201 standard medium in tests with algae. The other media used in the TG 201 algal tests performed included: HB-4, ZBB, Oligo, G-11, SE, CSI, Simplified SE, and BG-11 (Table 1). In tests that exposed *Daphnia spp.* the media used included: distilled water, tap water, artificial freshwater, reconstituted water, ASTM hard water, Elendt M4

medium or a simplified Elendt M7 medium (SM7), as well as the standard TG 201 medium recommended for use in algal studies (Table 2). Similarly, in fish studies, the reported exposure media varied from freshwater, tap water (chlorinated or dechlorinated; UV-sterilised or non-sterilised), natural salt water or conditioned water (salts added) (Table 3). While in embryo testing, E3 culture medium was often used, and also deionised and artificial freshwater were utilised (Table 4). Thus, in this wide range of different media used the graphene materials tested likely have distinct and media-composition/condition dependent behaviours that must be fully characterised and understood.

One particular graphene material-media interaction reported in algal toxicity tests was a nutrient availability decrease by the tested GO materials (Malina et al. 2019). The nutrients Ca^{2+} and Mg^{2+} were almost completely removed (88-89% respectively) from the TG 201 medium and adsorbed to GO (Malina et al. 2019). The lower bioavailability of Ca and Mg caused a growth decrease of the algae in algal tests (Zhao et al. 2017), interpreted as evidence of "indirect toxicity" of the tested material. Approaches that have been used to alleviate this effect include pre-conditioning the materials in medium prior to preparation of working suspensions in an "absorption to saturation approach" (Markovic et al. 2020).

Also substances (*e.g.* biomolecules) excreted by organisms during the testing can contribute to the media composition and influence effects. For example, when using TG 203, fish are held in exposure tanks/test water for an acclimatisation period of a minimum of 7 days and thereafter depending on the test setup/dosing protocols/water renewals the condition of the water (including biomolecules) will be modified influencing particle-media interactions and the nanoforms of particles the fish are exposed to. Studies have begun investigating these interactions further and the influence of what has become known as "eco coronas" to reach a deeper understanding of how they may influence NM-organism interaction (Nasser et al. 2020; Ekvall et al. 2021; Nasser and Lynch, 2016; Fadare et al. 2020) or even bio-coronas *in vivo* (Abdolahpur Monikh et al. 2021). This may also explain the wide variability in ecotoxicity data and the need for thorough characterisations of materials and of any changes in properties/nanoforms under controlled test conditions when testing.

Also an influence of serum protein (*e.g.* for instance those present in fetal bovine serum, FBS) used in cell culture medium (fish cell lines included) likely also contributes to the differences in sensitivities among *in vitro* assays used for testing graphene materials (Table 5). While such proteins aid stability (dispersion maintenance), they may also influence cellular interactions. In the newly published TG 249 fish cell line acute toxicity test, a defined, protein and serum-free exposure medium (Leibovitz L-15 medium/ex) is used when preparing working test concentrations, to avoid any possible protein interfering effects. To date this TG has not been followed when testing

graphene materials, and thus the behaviour of graphene materials in this standardised TG 249 exposure medium has yet to be characterised. The use of such a standardised medium will facilitate future comparative studies, without media specific influences complicating interpretation of results.

2.3.2.4 Interferences

The final specific factor to take into account when performing tests with graphene materials is related with the interferences of the graphene test materials with standard testing procedures. As graphene material dispersions are coloured and light absorbing, in tests which rely on absorbance or fluorescence measurements (*e.g.* TG 201 and TG 249) interferences with measurements were evidenced (Kalman et al. 2019; Barrick et al. 2019; Malina et al. 2019; Markovic et al. 2020). This led, in some cases, to impediments in the characterisation of toxic effects (even to the inability to interpret effects) at high concentrations. The necessity to use other and alternative approaches to determine effects (*e.g.* cell counting) became evident and the need for modified methods for extraction and measurement of chl a to overcome interferences (see section 2.1.1). Also in tests with algae, which rely on the penetration of light for algal growth, what has been described as a shading effect was highlighted. It will be important to characterise the contribution of this effect to any growth inhibition and to distinguish it from inherent toxicity. In most studies this was not performed, however reference to specific protocols for testing this effect have been provided (Zhao et al. 2017). Lastly physical interferences resulting from the interaction of aggregated material with algae, inhibiting direct counting of algal cells as a measure of reduction in growth were reported (Markovic et al. 2020), as well as adsorption of aggregates to organism bodies (*e.g.* *Daphnia*) that through a physical effect may contribute to a reduction in immobilisation.

2.3.3 Data analysis and reporting

A thorough characterisation and specific reporting of physicochemical properties is essential to any toxicological evaluation/hazard assessment. Also, from a regulatory perspective any particle characteristics that impact the safety of the substance must be indicated and this includes system dependent properties such as dispersion stability, dissolution, reactivity (biological, photo-reactivity) and potential transformations/degradations (EC, 2020). A framework for the classification of the many different forms, or "grades" of graphene materials and a syntax has been recently developed by the Graphene Council (Graphene Council, 2021) to aid in distinguishing distinct forms and types, and it facilitates a certain degree of standardisation in reporting. Specific properties that have been identified as important for classification as well as describing the unique behaviour of graphene materials include number of layers, lateral size, carbon-to oxygen (C/O) ratio (oxygen content), and structural defects (Wick et al. 2014; Fadeel et al. 2018). The material can be

positively classified as graphene through the identification of sp^2 bonded carbon detection. However, the complete chemical composition of the material must be considered and accounted for, including any residual impurities or byproducts from production processes. Toxicological effects have also been evidenced to vary as a function of these distinct properties or their alteration (Liu et al. 2012; Sydlik et al. 2015; Jiang et al. 2021; Lu et al. 2017; Chen et al. 2021). For example, lateral sheet size seemed to influence adverse effects towards zebrafish embryos in a comparative study, with larger sheets (>200-600 nm) showing increased toxicity through physical interactions and smaller sheets (<200 nm) not showing any effects (Moreira et al. 2021).

In table 8 all relevant material properties, both inherent and system-dependent, are presented building on work by Wick et al. (2014), considering *(i)* information requirements to fulfil reporting obligations by REACH (Annex VI) (EC, 2006), *(ii)* particle properties that are relevant for ecotoxicological hazard assessment in the aquatic environment, and *(iii)* those defined by the graphene classification framework Graphene Flagship and IEC/ISO. Methods that can be used to measure the respective properties are also listed, identifying those which have been applied/validated/developed for NM testing and those that are currently under development. The structural property headings used include chemical composition, impurities, surface treatment/functionalisation, particle size, shape/aspect ratio, crystallinity, assembly structure/orientation/rigidity, defects (type and distance), surface area (including porosity), density, and hydrophobicity/attachment efficiency (α). The ISO/IEC standards, ISO/TS 21356-1:2021 and ISO/TR 19733:2019 can be consulted for methods that can be used to measure structural properties of graphene materials. Such methods include Raman spectroscopy (for defects, exfoliation degree, number of layers characterisation), atomic force microscopy (AFM) and transmission electron microscopy (TEM) (lateral size, thickness characterisation), BET (Brunauer, Emmett and Teller) method for specific surface area measurement and X-ray photoelectron and/or Fourier Transform Infrared spectroscopy for surface chemistry (ISO 2019, ISO 2021). The importance of such standards for the graphene community has been highlighted by Clifford et al. (2021). The Graphene Material Classification framework details also standardised test methods for measuring definitive properties for a minimum set of relevant characteristics of graphene materials to be reported on material specification sheets (Graphene Council, 2021). These characteristics include, among the 19 identified: oxygen content, structural defects, specific surface area, shape, surface charge, bulk density (tapped) and crystallinity. While developed principally for manufacturers for the purpose of fulfilling registration requirements of substances, such a framework will also greatly aid in establishing toxicological profiles and help link intrinsic material properties with apical toxic effects or specific system dependent properties (property-effect relationships).

For some of the properties, standardised guidelines/protocols/methodologies are still under development (*e.g*. hydrophobicity, OECD WNT project 1.7). For example, a maximum particle dispersion (MPD) methodology (and dye absorption method, Li et al. 2022) has been successfully used to measure the hydrophobicity of a graphene nanoplatelet (30.9 mJ/m^2 and 0.8 according to respective methods). Other methods used include a water contact angle method with values of 93 and 79 for a single and multiple layer graphene (Bahl et al. 2020). However, before these values can become meaningful the most appropriate metric scale would need to be developed to classify levels of hydrophobicity and identify thresholds. The attachment efficiency related to the affinity of NMs to attach to other particles or surfaces (heteroagglomeration) has also been proposed as a proxy for hydrophobicity characterisation and has been identified as an important parameter that can determine fate and be used in fate modelling. There are still challenges in calculating a precise attachment efficiency value taking into consideration all the possible interactions (e.g. heteroagglomeration (Praetorius et al. 2020)). However currently attachment efficiency can be derived from dispersion stability testing according to OECD TG 318 and its guidance document (OECD, 2017, 2021c) although also specific test guidelines are being developed.

Another information requirement under REACH regulation (Annex VII, 7.4) is on material density, which is a property not widely reported for the range of graphene materials tested. While perfect graphene sheets have a density the same as crystalline graphite (2.267 g/cm^3), this changes with stacking order. Methods to measure density include helium pycnometry.

Defects are an important graphene material specific property. While visual inspections using TEM can be used to identify, for example, wrinkles/folds/breakages in physical structure (Meyer et al. 2008). The different types of defects at an atomic level that can be evidenced in graphene materials have been discussed in the review paper by Ahmed et al. 2021. The ratio between the intensities of the D and G peaks of a Raman spectra (I_D/I_G) correlate with the mean distance of two defects in graphene (Lucchese et al. 2010). The distance between defects, grain size and relative density of defects can be measured using the shift in the relative position and width of the G-peak, D-peak and 2D-peak of the Raman spectrum (Ferrari et al. 2007, Cançado et al. 2011), and further developments combining techniques are emerging (Raman spectro-electrochemistry, Raman-μSEC). An I_D/I_G value was in fact provided in a number of the collected studies and ranged from 0.49 to 1.31 according to the specific material being tested, with higher ratios representing higher defect levels.

Characterisation of the manufactured material should be distinguished from characterisation of the material post-processing/manipulation (*e.g*. dispersion preparation). Any processing/manipulation is likely to re-arrange the symmetry, could change the charge, stacking, and can create defects and

disorder in the carbon lattice (hetero-structures, grain boundaries, vacancies, and interstitial impurities) as well as irregular/sharp edges. Ultimately, all of this leads to testing of a very dissimilar material to the starting pristine material. These post-processing manipulations can also directly affect toxicity assessments. For example, high-energy sonication of graphene material can create smaller fragments with increased toxicity (Mullick Chowdhury et al. 2014, Jiang et al 2021), while the presence of irregular sharp edges can lead to direct cell membrane destruction (Li et al. 2013). Also any residual impurities could be released from the material through such post processing (Kalman et al. 2019).

The system-dependent properties include solubility, stability, surface reactivity and degradation/transformation and these will be dictated by the specific conditions under which the various aquatic tests are performed. In an environmental setting these properties will directly determine fate and behaviour and what compartments are most likely to be exposed to the NMs (*e.g.* benthic vs. pelagic systems) and may be at greater risk. However, when testing, a controlled system is required/desirable. A dispersion is considered stable, for the purposes of meeting test assay validity criteria, when the concentration of graphene in medium is maintained at least at 80 % of the nominal value, however further considerations may be needed as the understanding of stability can be extended to maintenance of a constant hydrodynamic diameter and polydispersity index with ≤10% deviation. TG 318 outlines a general methodology for stability assessment for NMs which could be adapted, while not prescribed for or described according to the standard operating procedures, to assess the stability of NMs under specific test conditions (*e.g.* in test medium, and for a specific test exposure duration). For example, an extended test monitoring period for the duration of the exposure, according to a specific test (*e.g.* 96 h), could be applied and testing in complete exposure medium at higher concentrations (*e.g.* 100 mg/L). For measuring graphene dispersion stability, approaches based on UV-Vis spectroscopy have been used in the collected studies and reported as % of initial concentration during the experiment. Other approaches for dispersion stability assessment focused on size distribution and include measurements of particle size by dynamic light scattering (DLS) and reporting of the size distributions contained in dispersion in percentiles (90%, 50% and 10%) (i.e. D90, D50, D10 values) (ISO 2020). Also light scattering of a dispersion can be measured using Turbiscan instruments which generate Turbiscan stability indices (Dai et al. 2015). These can be categorised into scales according to stability as proposed by Dai and colleagues, for example; (1-5=well dispersed and stable), (5-20=can be redispersed), (>20=precipitated). Also an approach has been explored and applied for GO characterisation of the mass and number of individual particles or aggregates in suspension using

resonant mass measurements (RMM) that can be used to analyse 2D materials in suspension without the assumptions of spherical models (Circa et al. 2021).

Particular attention must also be given to any changes (degradations/transformations) that may occur under aquatic testing conditions (Zhao et al. 2020). Such transformations can be physical or chemical, abiotic or biotic, and can lead to the creation of new nanoforms with distinct hazard profiles. To highlight the importance of such an assessment, transformed graphene materials and by-products (low molecular weight aromatic compounds) that show higher toxicity following photo-reduction under simulated sunlight irradiation have been detected (Zhao et al. 2020). This transformation aspect is particularly relevant considering that certain naturally occurring enzymes can biodegrade graphene (Kotchey et al. 2011; Liu et al. 2015) and it can be degraded naturally by fungi and bacteria (Candotto Carniel et al. 2021). Specifically, it has been seen that *Shewanella oneidensis* MR-1 (a normal component of the surface flora of fishes) have the ability to reduce GO to rGO (Wang et al. 2011a, b). This has important implications for potential transformations that may occur under environmental and testing conditions.

Various methods that can be used to investigate (bio)degradation have been detailed by Chen et al. (2017). However standardised testing strategies to monitor this property are still needed (Baun et al. 2017) and currently approaches rely on direct visualisations using TEM-EDX or AFM, while other standardised approaches are being developed (*e.g.* OECD, Project 3.16 GD on transformation of nanomaterials in aquatic environmental media will be developed to provide advice on ways to determine abiotic transformations of nanomaterials in the environment (OECD 2021b)).

Raman spectroscopy can be used to monitor degradation according to the appearance of a D-band ($\sim 1350^{-1}$) which can serve as an indicator of the material structural disintegration. Also already standardised tests that may be used for graphene biodegradation assessment include OECD 301F (manometric respirometry). Any possible transformations occurring *in vivo* are also useful for biopersistence/bioaccumulation assessment and may be assessed *in vitro* by monitoring transformation in biological fluids that mimic biological compartments and intracellular environments.

Overall limitations in analytical techniques for material quantification (*e.g.* UV-Vis spectroscopy limits of detection of 0.5 mg/L reported by Martínez-Álvarez (2021)) and a lack of standardised protocols for degradation/transformation likely explains the lack of reporting of degradation/transformation in collected studies and is causing an information gap and uncertainties which need to be addressed in future studies.

3. Conclusion

3.1 Future perspective and overall conclusions on applicability of environmental related OECD TGs for aquatic toxicity hazard classification of graphene materials

The existing OECD TGs 201, 202, 203 that form a test battery for CLP classification or for ecotoxicity assessment under a variety of regulations (e.g. REACH) have been and can be applied for graphene material testing. The overall methodology, procedural approaches, and conventional endpoints of TG 201, 202 and 203 used are sufficiently generic to be applicable to a wide range of substances including 2D graphene materials. However, the studies reviewed here highlighted also some drawbacks, especially for TG 201 that make this TG less robust when applying it to graphene related materials. Indeed, more emphasis must be put on the need for additional assessments (safe guards, quality checks) both prior to conducting and during testing. The absence of this in tests to date has impeded conclusions to be made on the hazards of certain "challenging to test" substances such as graphene materials. These assessments are required to ensure there is no evident change in nanoform under, or directly caused by, pre-processing/experimental conditions, that a certain degree of stability can be maintained under general conditions (or following already detailed adjustments (*e.g.* agitation/aeration/renewal approaches), and that graphene materials properties (*e.g.* opacity, inherent fluorescence) or behaviour (absorptive capacity/media interaction) do not interfere with the performance/readout of the test. Additional assessments include preliminary stability tests extended to the assessment of agglomeration state, transformations and specific media interactions, interference checks and then, if deemed necessary, the use of appropriate adaptations to test design to meet test validity criteria and to overcome specific factors as detailed in this review. Often it is not the performance of the testing itself but other aspects such as the lack of a thorough characterisation of physicochemical properties, including system dependent properties, that reduce the quality of performed studies. Also in most cases any characterisation of, or contribution from, impurities that may be introduced through the various production processes was not considered and must be in future studies using filtrate controls or purified materials.

A critical aspect that must be addressed in future studies is the overall lack of concentration measurements. These are compulsory in the updated TG 203 and therefore to meet future test validity criteria, measurements must be performed and more sophisticated analytical techniques developed for carbonaceous based materials such as graphene.

Also the large number of studies which have used fish embryos and applied TG 236, that can be regarded as new approach methodologies (NAMs) to test graphene materials, points to a valuable source of data that can be used in a WoE approach for fish acute toxicity assessment for graphene

materials. Such alternative NAM tests, together with the standardised test battery, deemed applicable for testing graphene materials according to this review, will play a major role in the testing strategies and future IATA´s to meet regulatory needs.

CRediT authorship contribution statement

M. Connolly: Conceptualization, Methodology, Investigation, Data curation, Writing – original draft, Writing – review & editing. G. Moles: Conceptualization, Methodology, Investigation, Data curation, Visualisation, Writing – review & editing. F. Candotto Carniel, M. Tretiach, G. Caorsi: Methodology, Data curation, Writing – review & editing. E.Flahaut: Methodology, Writing – review & editing. B. Soula: Writing – review & editing. E. Pinelli, L. Gauthier, F. Mouchet: Methodology, Data curation, Writing – review & editing. J.M Navas: Conceptualization, Funding acquisition, Project Administration, Writing – review & editing, Supervision.

Declaration of Competing Interest

The authors declare no competing financial interest.

Acknowledgements

GrapheneCore3 - This project has received funding from the European Union's Horizon 2020 research and innovation programme under grant agreement No. 881603 of the Graphene Flagship. Mona Connolly has received financing granted by the Community of Madrid (2018T2/AMB-11392, Mode 2, Young Doctor Recruitment). Giada Caorsi has also received financing from the Graphene Flagship Core 3 project "Safegraph" funded by the European Commission (Framework Partnership Agreement No. 649953).

References

Abdolahpur Monikh, F., Chupani, L., Karkossa, I., et al. 2021. An environmental ecocorona influences the formation and evolution of the biological corona on the surface of single-walled carbon nanotubes. NanoImpact 22:100315. https://doi.org/10.1016/j.impact.2021.100315

Achawi, S., Pourchez, J., Feneon, B., & Forest, V. 2021. Graphene-Based Materials In Vitro Toxicity and Their Structure-Activity Relationships: A Systematic Literature Review. Chemical research in toxicology 34(9), 2003–2018. https://doi.org/10.1021/acs.chemrestox.1c00243

Ahmad, W., Ullah, Z., Sonil, N.I. et al. 2021. Introduction, production, characterization and applications of defects in graphene. J Mater Sci: Mater Electron 32, 19991–20030. https://doi.org/10.1007/s10854-021-06575-1

Almeida, A.R., Salimian, M., Ferro, M., et al. 2019. Biochemical and behavioral responses of zebrafish embryos to magnetic graphene/nickel nanocomposites. Ecotoxicol Environ Saf., 186:109760. http://doi.org/doi:10.1016/j.ecoenv.2019.109760

Al-Rudainy, K. 2019. Histopathological changes (gills and liver) and clinical signs of common carp, Cyprinus carpio L. exposed to graphene nanoparticles .Iraqi journal of Agricultural Science, 50 (3). https://doi.org/10.36103/ijas.v50i3.706

Amorim, M.J.B., Fernández-Cruz, M.L., Hund-Rinke, K. et al. 2020. Environmental hazard testing of nanobiomaterials. Environ Sci Eur 32, 101. https://doi.org/10.1186/s12302-020-00369-8

An Wong, C.H., Sofer, Z., Kubešová, M., Kučera, J., Matějková, S., Pumera, M., 2014. Synthetic routes contaminate graphene materials with a whole spectrum of unanticipated metallic elements. Proc. Natl. Acad. Sci. U. S. A. 111, 13774–13779. https://doi.org/10.1073/pnas.1413389111

Andrade, L.R., Leal, R.N., Noseda, M, et al. 2010. Brown algae overproduce cell wall polysaccharides as a protection mechanism against the heavy metal toxicity. Mar Pollut Bull. 60:9, 1482-1488. https://doi.org/10.1016/j.marpolbul.2010.05.004

Arvidsson, R., Molander S, Sandén A. B. 2013. Review of Potential Environmental and Health Risks of the Nanomaterial Graphene, Human and Ecological Risk Assessment: An International Journal, 19:4, 873-887. https://doi.org/10.1080/10807039.2012.702039

Audira, G., Lee, J.S., Siregar, P., Malhotra, N., Rolden, M.J., Huang, J., Chen, K.H., Hsu, H., Hsu, Y., Ger, T., & Hsiao, C. 2021. Comparison of the chronic toxicities of graphene and graphene oxide toward adult zebrafish by using biochemical and phenomic approaches. Environ. Pollut. 278, 116907. https://doi.org/10.1016/j.envpol.2021.116907

Avant, B., Bouchard, D., Chang, X., Hsieh, H-S., Acrey, B., Han, Y., Spear, J., Zepp, R., Knightes, C. D. 2019. Environmental fate of multiwalled carbon nanotubes and graphene oxide across different aquatic ecosystems. NanoImpact, 13, 1–12. http://doi.org/10.1016/j.impact.2018.11.001

Bahl, A., Hellack, B., Wiemann, M., Giusti, A., Werle, K., Haase, A., Wohlleben, W. 2020. Nanomaterial categorization by surface reactivity: A case study comparing 35 materials with four different test methods. NanoImpact, 19, 100234. https://doi.org/10.1016/j.impact.2020.100234

Baig, Z., Mamat, O., Mustapha, M., Mumtaz, A., Munir, K. S., & Sarfraz, M. 2018. Investigation of tip sonication effects on structural quality of graphene nanoplatelets (GNPs) for superior solvent dispersion. Ultrason Sonochem, 45, 133–149. https://doi.org/10.1016/j.ultsonch.2018.03.007

Banchi, E., Candotto Carniel, F., Montagner, A., et al. 2019. Graphene-based materials do not impair physiology, gene expression and growth dynamics of the aeroterrestrial microalga Trebouxia gelatinosa. Nanotoxicology, 13(4):492-509. http://doi.org/doi:10.1080/17435390.2019.1570371

Bangeppagari, M., Park, S.H., Kundapur, R.R., Lee, S.J. 2019. Graphene oxide induces cardiovascular defects in developing zebrafish (Danio rerio) embryo model: In-vivo toxicity assessment. Sci. Total Environ, 673:810-820. http://doi.org/10.1016/j.scitotenv.2019.04.082.

Barbolina, I., Woods, C.R., Lozano, N., Kostarelos, K., Novoselov, K.S., Roberts, I.S., 2016. Purity of graphene oxide determines its antibacterial activity. 2D Mater. 3. https://doi.org/10.1088/2053-1583/3/2/025025

Barrick, A., Châtel, A., Manier, N., Kalman, J., Navas, M, J., Mouneyrac, C. 2019. Investigating the Impact of Manufacturing Processes on the Ecotoxicity of Carbon Nanofibers: A Multi-Aquatic Species Comparison. Environ. Toxicol. Chem. https://doi.org/10.1002/etc.4537.

Basei, G, Zabeo, A, Rasmussen, K, Tsiliki,G, Hristozov,D. 2021. A Weight of Evidence approach to classify nanomaterials according to the EU Classification, Labelling and Packaging Regulation criteria. NanoImpact, 24, 100359. https://doi.org/10.1016/j.impact.2021.100359

Baun, A., Sayre, P., Steinhäuser, K. G., Rose, J. 2017. Regulatory relevant and reliable methods and data for determining the environmental fate of manufactured nanomaterials. NanoImpact, 8, 1–10. https://doi.org/10.1016/j.impact.2017.06.004

Belanger, S.E., Lillicrap, A.D., Moe, S.J., Wolf, R., Connors, K., Embry, M.R. 2022. Weight of evidence tools in the prediction of acute fish toxicity [published online ahead of print. Integr Environ Assess Manag. http://doi.org/10.1002/ieam.4581. doi:10.1002/ieam.4581

Boros, B-V., Ostafe, V. 2020. Evaluation of Ecotoxicology Assessment Methods of Nanomaterials and Their Effects. Nanomaterials, 10(4), 610. http://doi.org/10.3390/nano10040610

Botte, E., Vagaggini, P.,Zanoni, I., Gardini, D., Costa, AL., Ahluwalia, A. 2021. An integrated pipeline and multi-model graphical user interface for accurate nano-dosimetry. bioRxiv https://doi.org/10.1101/2021.08.31.458389

Buelke, C., Alshami, A., Casler, J., Lewis, J., AlSayaghi, M., and Hickner, M.A. 2018. Graphene oxide membranes for enhancing water purification in terrestrial and spaceborn applications: state of the art. Desalination 448, 113–132. https://doi.org/10.1016/j.desal.2018.09.008

Cançado, L.G., Jorio, A., Martins-Ferreira, E.H.., Stavale, F., Achete, C.A., Capaz, R.B., Moutinho, M.V.O., Lombardo, A., Kulmala, T.S., Ferrari, A.C. 2011. Quantifying Defects in Graphene via Raman Spectroscopy at Different Excitation Energies. Nano Lett. 2011, 11, 8, 3190–3196. https://doi.org/10.1021/nl201432g

Candotto Carniel, F., Fortuna, L., Zanelli, D., et al. 2021. Graphene environmental biodegradation: Wood degrading and saprotrophic fungi oxidize few-layer graphene. J Hazard Mater. 414:125553. http://doi.org/10.1016/j.jhazmat.2021.125553

Cao, Z., Su, M., Wang, H., et al. 2021. Carboxyl graphene oxide nanoparticles induce neurodevelopmental defects and locomotor disorders in zebrafish larvae. Chemosphere, 270, 128611. http://doi.org/doi:10.1016/j.chemosphere.2020.128611

Castro, V.L., Clemente, Z., Jonsson, C., et al. 2018. Nanoecotoxicity assessment of graphene oxide and its relationship with humic acid. Environ Toxicol Chem. 2018;37(7):1998-2012. http://doi.org/10.1002/etc.4145

Castro, A.K., Dasari, T., & Tchounwou, P.B. 2019. Graphene-Based Nanomaterials Toxicity in Fish. Rev Environ Contam Toxicol, 247, 1–58. https://doi.org/10.1007/398_2018_15

Chen, M., Yin, J., Liang, Y., et al. 2016. Oxidative stress and immunotoxicity induced by graphene oxide in zebrafish. Aquat Toxicol, 174:54-60. http://doi.org/10.1016/j.aquatox.2016.02.015

Chen, M., Qin, X., & Zeng, G. 2017. Biodegradation of Carbon Nanotubes, Graphene, and Their Derivatives. Trends Biotechnol, 35(9), 836–846. http://doi.org/10.1016/j.tibtech.2016.12.001

Chen, Z., Yu, C., Khan, I.A., Tang, Y., Liu, S., Yang, M. 2020. Toxic effects of different-sized graphene oxide particles on zebrafish embryonic development. Ecotoxicol. Environ. Saf. 197, 110608. https://doi.org/10.1016/j.ecoenv.2020.110608.

Chen, Y., Rivers-Auty, J., Crică, L. E., Barr, K., Rosano, V., Arranz, A. E., et al. 2021. Dynamic interactions and intracellular fate of label-free, thin graphene oxide sheets within mammalian cells: role of lateral sheet size. Nanoscale Advances, 3(14), 4166–4185. http://doi.org/10.1039/d1na00133g

Clemente, Z., Silva, G.H., de Souza Nunes, M.C. et al. 2019. Exploring the mechanisms of graphene oxide behavioral and morphological changes in zebrafish. Environ Sci Pollut Res 26, 30508–30523. https://doi.org/10.1007/s11356-019-05870-z

Clifford, C.A., Martins Ferreira, E.H., Fujimoto, T. et al. 2021.The importance of international standards for the graphene community. Nat Rev Phys 3, 233–235. https://doi.org/10.1038/s42254-021-00278-6

Connolly, M., Navas J.M., Coll J. 2021. Prediction of nanographene binding-scores to trout cellular receptors and cytochromes bioRxiv.432107 https://doi.org/10.1101/2021.02.20.432107

Crane, M., Handy, R.D., Garrod, J., Owen, R. 2008. Ecotoxicity test methods and environmental hazard assessment for engineered nanoparticles. Ecotoxicology, 17(5):421-437. http://doi.org/10.1007/s10646-008-0215-z

Crica, L.E., Dennison, T.J., Guerini, E.A., & Kostarelos, K. 2021. A method for the measurement of mass and number of graphene oxide sheets in suspension based on non-spherical approximations. 2D Materials, 8. http://doi.org/10.1088/2053-1583/abfe01

Cross, R., Matzke, M., Spurgeon, D., et al. 2022. Assessing the similarity of nanoforms based on the biodegradation of organic surface treatment chemicals. NanoImpact, 26:100395. http://doi.org/10.1016/j.impact.2022.100395

Cupi, D., Hartmann, N.B., Baun, A. 2015. The influence of natural organic matter and aging on suspension stability in guideline toxicity testing of silver, zinc oxide, and titanium dioxide nanoparticles with Daphnia magna. Environ. Toxicol. Chem. 34, 497–506. http://doi.org/10.1002/etc.2855

d'Amora, M., Camisasca, A., Lettieri, S., Giordani, S. 2017. Toxicity Assessment of Carbon Nanomaterials in Zebrafish during Development. Nanomaterials (Basel), 7(12):414. http://doi.org/10.3390/nano7120414.

Dai, J., Wang, G., Ma, L., Wu, C. 2015. Study on the surface energies and dispersibility of graphene oxide and its derivatives. J. Mater. Sci., 50, 3895-3907. https://doi.org/10.1007/s10853-015-8934-z

Dasmahapatra, A.K., Dasari, T.P.S., Tchounwou, P.B. 2019. Graphene-Based Nanomaterials Toxicity in Fish. Rev Environ Contam Toxicol, 247:1-58. http://doi.org/10.1007/398_2018_15

de Medeiros, A.M.Z., Khan, .LU., da Silva, G.H., et al. 2021. Graphene oxide-silver nanoparticle hybrid material: an integrated nanosafety study in zebrafish embryos. Ecotoxicol Environ Saf, 209, 111776. http://doi.org/10.1016/j.ecoenv.2020.111776

DeLoid, G., Cohen, J., Darrah, T. et al. 2014. Estimating the effective density of engineered nanomaterials for in vitro dosimetry. Nat Commun 5, 3514. https://doi.org/10.1038/ncomms4514

Deng, S., Fu, A., Junaid, M., et al. 2019. Nitrogen-doped graphene quantum dots (N-GQDs) perturb redox-sensitive system via the selective inhibition of antioxidant enzyme activities in zebrafish. Biomaterials, 206:61-72. http://doi.org/10.1016/j.biomaterials.2019.03.028

Dimou, A.E., Maistros, G., Poulin, P., & Alexopoulos, N.D. 2021. In situ control of graphene oxide dispersions with a small impedance sensor. Nanotechnology, 33(5), 10.1088/1361-6528/ac2dc8. https://doi.org/10.1088/1361-6528/ac2dc8

Du, S., Zhang, P., Zhang, R., et al. 2016. Reduced graphene oxide induces cytotoxicity and inhibits photosynthetic performance of the green alga Scenedesmus obliquus. Chemosphere, 164:499-507. http://doi.org/10.1016/j.chemosphere.2016.08.138

EC 2006, Regulation (EC) No 1907/2006 of the European Parliament and of the Council of 18 December 2006 concerning the Registration, Evaluation, Authorisation and Restriction of Chemicals (REACH), establishing a European Chemicals Agency, amending Directive 1999/45/EC and repealing Council Regulation (EEC) No 793/93 and Commission Regulation (EC) No 1488/94 as well as Council Directive 76/769/EEC and Commission Directives 91/155/EEC, 93/67/EEC, 93/105/EC and 2000/21/EC

EC 2009, Regulation (EC) No 1272/2008 of the European Parliament and of the Council of 16 December 2008 on classification, labelling and packaging of substances and mixtures, amending and repealing Directives 67/548/EEC and 1999/45/EC, and amending Regulation (EC) No 1907/2006

EC 2020, Commission Regulation (EU) 2020/878 of 18 June 2020 amending Annex II to Regulation (EC) No 1907/2006 of the European Parliament and of the Council concerning the Registration, Evaluation, Authorisation and Restriction of Chemicals (REACH)

EC 2022. Commission Recommendation of 10.06.2022 on the definition of nanomaterial. Retrieved on 12.07.2022 from https://ec.europa.eu/environment/chemicals/nanotech/pdf/C_2022_3689_1_EN_ACT_part1_v6.pdf

ECHA 2022, Appendix for nanoforms applicable to the Guidance on Registration and Substance Identification Version 2.0, January 2022 ECHA-21-G-06-EN, European Chemicals Agency, 2022

ECHA, 2022a: https://echa.europa.eu/registration-dossier/-/registered-dossier/24678/6/2/2

ECHA, 2022b: https://echa.europa.eu/substance-information/-/substanceinfo/100.227.924

ECHA, 2022c: https://echa.europa.eu/registration-dossier/-/registered-dossier/27774/2/1

ECHA 2022d, https://echa.europa.eu/support/qas-support/browse/-/qa/70Qx/view/ids/1831

Ekvall, M.T., Hedberg, J., Odnevall Wallinder, I. et al. 2021. Adsorption of bio-organic eco-corona molecules reduces the toxic response to metallic nanoparticles in Daphnia magna. Sci Rep 11, 10784. https://doi.org/10.1038/s41598-021-90053-5

EPA 1996. Ecological Effects Test Guidelines OPPTS 850.1085

Evariste, L., Mottier, A., Lagier, L., Cadarsi, S., Barret, M., Sarrieu, C., Soula, B., Mouchet, F., Flahaut, E., Pinelli, E., & Gauthier, L. 2020. Assessment of graphene oxide ecotoxicity at several trophic levels using aquatic microcosms. Carbon, 156, 261-271. https://doi.org/10.1016/j.carbon.2019.09.051

Fadare, O.O., Wan, B., Liu, K., Yang, Y., Zhao, L., & Guo, L. H. 2020. Eco-Corona vs Protein Corona: Effects of Humic Substances on Corona Formation and Nanoplastic Particle Toxicity in Daphnia magna. Environ. Sci. Technol, 54(13), 8001–8009. https://doi.org/10.1021/acs.est.0c00615

Fadeel, B., Bussy, C., Merino, S., et al. 2018. Safety Assessment of Graphene-Based Materials: Focus on Human Health and the Environment. ACS Nano, 12(11):10582-10620. http://doi.org/10.1021/acsnano.8b04758

Fadeel, B., & Kostarelos, K. 2020. Grouping all carbon nanotubes into a single substance category is scientifically unjustified. Nat. Nanotechnol. 15, 164. http://doi.org/10.1038/s41565-020-0654-0

Farkas, J., & Booth, A.M. 2017. Are fluorescence-based chlorophyll quantification methods suitable for algae toxicity assessment of carbon nanomaterials?, Nanotoxicology, 11:4, 569-577. http://doi.org/10.1080/17435390.2017.1329953

Fekete-Kertész, I., László, K., Terebesi, C., Gyarmati, B.S., Farah, S., Márton, R., Molnár, M. 2020. Ecotoxicity Assessment of Graphene Oxide by Daphnia magna through a Multimarker Approach from the Molecular to the Physiological Level including Behavioral Changes. Nanomaterials (Basel), 10(10):2048. http://doi.org/10.3390/nano10102048

Ferrari, A.C. 2007. Raman spectroscopy of graphene and graphite: Disorder, electron-phonon coupling, doping and nonadiabatic effects. Solid State Commun, 143, 47–57. https://doi.org/10.1016/j.ssc.2007.03.052

Franqui, L.S., De Farias, M.A., Portuga,l RV., et al. 2019. Interaction of graphene oxide with cell culture medium: Evaluating the fetal bovine serum protein corona formation towards in vitro nanotoxicity assessment and nanobiointeractions. Mater Sci Eng C Mater Biol Appl., 100, 363-377. http://doi.org/10.1016/j.msec.2019.02.066

Gandon, A., Werle, K., Neubauer, N., & Wohlleben, W. 2017. Surface reactivity measurements as required for grouping and read-across: An advanced FRAS protocol. J. Phys. Conf. Ser., 838. http://doi.org/10.1088/1742-6596/838/1/012033

Gao, J., Youn, S., Hovsepyan, A., Llaneza, V.L., Wang, Y., Bitton, G., Bonzongo, J-C.J. 2009. Dispersion and Toxicity of Selected Manufactured Nanomaterials in Natural River Water Samples: Effects of Water Chemical Composition. Environ Sci Technol., 43(9), 3322–3328. http://doi.org/10.1021/es803315v

Garacci, M., Barret, M., Mouchet, F., Sarrieu, C., Lonchambon, P., Flahaut, E., Gauthier, L., Silvestre, J., Pinelli, E., 2017. Few Layer Graphene sticking by biofilm of freshwater diatom Nitzschia palea as a mitigation to its ecotoxicity. Carbon N. Y. 113, 139–150. https://doi.org/10.1016/j.carbon.2016.11.033

GHS, 2022. Globally Harmonized System of Classification and Labelling of Chemicals, United Nations, New York; Geneva: Ninth revised edition. ST/SG/AC.10/30/Rev.9

Graphene Council 2021. Proposed "Graphene classification framework". Available at : https://cdn.ymaws.com/www.thegraphenecouncil.org/resource/resmgr/standards/Graphene_Classification_Fram.pdf

Guo, X., & Mei, N. 2014. Assessment of the toxic potential of graphene family nanomaterials. J Food Drug Anal, 22(1), 105–115. https://doi.org/10.1016/j.jfda.2014.01.009

Guo, X., Dong, S., Petersen, E.J., Gao, S., Huang, Q., Mao, L. 2013. Biological uptake and depuration of radio-labeled graphene by Daphnia magna. Environ Sci Technol. 47(21):12524-12531. http://doi.org/10.1021/es403230u

Hofmann, U., König, E. 1937. Untersuchungen über Graphitoxyd. Zeitschrift für anorganische und allgemeine Chemie, 234, 311-336. http://doi.org/10.1002/ZAAC.19372340405

Hu, J., Lin, W., Lin, B., Wu, K., Fan, H., Yu, Y. 2019. Persistent DNA methylation changes in zebrafish following graphene quantum dots exposure in surface chemistry-dependent manner. Ecotoxicol Environ Saf., 169:370-375. http://doi.org/10.1016/j.ecoenv.2018.11.053

Hummers, S.W Jr., Offeman, E.R., 1958. Preparation of Graphitic Oxide. J. Am. Chem. Soc. 80, 6, 1339. https://doi.org/10.1021/ja01539a017

Hund-Rinke, K., Sinram, T., Schlich, K., Nickel, C., Dickehut, H.P., Schmidt, M., Kühnel, D. 2020. Attachment Efficiency of Nanomaterials to Algae as an Important Criterion for Ecotoxicity and Grouping. Nanomaterials, 10(6), 1021. http://doi.org/10.3390/nano10061021

Hund-Rinke, K., Schlinkert, R. & Schlich, K. 2022. Testing particles using the algal growth inhibition test (OECD 201): the suitability of in vivo chlorophyll fluorescence measurements. Environ Sci Eur, 34, 41. https://doi.org/10.1186/s12302-022-00623-1

ISO 2014. ISO 12154:2014(en) Determination of density by volumetric displacement — Skeleton density by gas pycnometry.

ISO 2010. ISO 9277:2010. Determination of the specific surface area of solids by gas adsorption - BET method.

ISO 2012. ISO 6341 Water Quality-Determination of the Inhibition of the Mobility of Daphnia magna Straus (Cladocera, Crustacea)-Acute Toxicity Test, ISO 6341;2012

ISO 2017. ISO/TS 80004-13:2017(en) Nanotechnologies — Vocabulary — Part 13: Graphene and related two-dimensional (2D) materials.

ISO 2019. ISO/TR 19733:2019(E), Nanotechnologies — Matrix of properties and measurement techniques for graphene and related two-dimensional (2D) materials.

ISO 2019. ISO 20814:2019 Nanotechnologies — Testing the photocatalytic activity of nanoparticles for NADH oxidation.

ISO 2020. ISO 13320-1 Particle size analysis –Laser diffraction methods.

ISO 2021. ISO/TS 21356-1:2021(E) Nanotechnologies — Structural characterization of graphene — Part 1: Graphene from powders and dispersions.

Jastrzębska, A.M., Olszyna, A.R. 2015.The ecotoxicity of graphene family materials: current status, knowledge gaps and future needs. J Nanopart Res, 17, 40. https://doi.org/10.1007/s11051-014-2817-0

Jensen, K., A., Kembouche, Y., Christiansen, E., Jacobsen, N.R., Wallin, H., Guiot, C., Spalla, O., Witschger, O. 2011. Final protocol for producing suitable manufactured nanomaterial exposure media – Report The generic NANOGENOTOX dispersion protocol – Standard Operation Procedure (SOP) and background documentation. July, 2011.

Jia, P-P., Sun, T., Junaid, M., Xiong, Y., Wang, Y., Liu, L., Pu, S., Pei, D. 2019. Chronic exposure to graphene oxide (GO) induced inflammation and differentially disturbed the intestinal microbiota in zebrafish Environ. Sci.: Nano 6, 2452-246. http://doi.org/10.1039/C9EN00364A

Jiang, T., Amadei, C.A., Lin, Y., et al. 2021. Dependence of Graphene Oxide (GO) Toxicity on Oxidation Level, Elemental Composition, and Size. Int J Mol Sci, 22(19):10578. http://doi.org/10.3390/ijms221910578

Kovtyukhova, N.I., Ollivier, P.J., Martin, B.R. Mallouk, T.E., Chizhik, S.A., Buzaneva, E.V., Gorchinskiy, A.D. 1999. Layer-by-Layer Assembly of Ultrathin Composite Films from Micron-Sized Graphite Oxide Sheets and Polycations. Chem. Mater., 11, 771−778.

Kalman, J., Merino, C., Fernández-Cruz, M.L., & Navas, J.M. 2019. Usefulness of fish cell lines for the initial characterization of toxicity and cellular fate of graphene-related materials (carbon nanofibers and graphene oxide). Chemosphere, 218, 347–358. https://doi.org/10.1016/j.chemosphere.2018.11.130

Kalman, J., Torrent, F., & Navas, J. M. 2022. Cytotoxicity of three graphene-related materials in rainbow trout primary hepatocytes is not associated to cellular internalization. Ecotoxicol Environ Saf, 231, 113227. https://doi.org/10.1016/j.ecoenv.2022.113227

Karthik, V., Selvakumar, P., Senthil Kumar, P. et al. 2021. Graphene-based materials for environmental applications: a review. Environ Chem Lett 19, 3631–3644. https://doi.org/10.1007/s10311-021-01262-3

Kotchey, G.P., Allen, B.L., Vedala, H., Yanamala, N., Kapralov, A.A., Tyurina, Y.Y., Klein-Seetharaman, J., Kagan, V.E., Star, A. 2011. The enzymatic oxidation of graphene oxide. ACS Nano. 5(3):2098-108. https://doi.org/10.1021/nn103265h

Kümmerer, K., Menz, J., Schubert, T., & Thielemans, W. 2011. Biodegradability of organic nanoparticles in the aqueous environment. Chemosphere, 82(10), 1387–1392. https://doi.org/10.1016/j.chemosphere.2010.11.069

Lammel T, Boisseaux P, Fernández-Cruz ML, Navas JM. 2013. Internalization and cytotoxicity of graphene oxide and carboxyl graphene nanoplatelets in the human hepatocellular carcinoma cell line Hep G2. Part Fibre Toxicol. 10:27. doi:10.1186/1743-8977-10-27

Lammel, T., & Navas, J. M. 2014. Graphene nanoplatelets spontaneously translocate into the cytosol and physically interact with cellular organelles in the fish cell line PLHC-1. Aquat Toxicol, 150, 55–65. https://doi.org/10.1016/j.aquatox.2014.02.016

Lanphere, J.D., Rogers, B., Luth, C., Bolster, C.H., Walker, S.L. 2014. Stability and Transport of Graphene Oxide Nanoparticles in Groundwater and Surface Water. Environ Eng Sci. 31(7):350-359. http://doi.org/10.1089/ees.2013.0392

Lee, B.-C., Hong, G., Lee, H., Kim, P., Seo, D.-Y., Hwang, G., Kim, G., Kim, P. 2020. Influence of NOM on the Stability of Zinc Oxide Nanoparticles in Ecotoxicity Tests. Appl. Sci, 10, 6431. https://doi.org/10.3390/app10186431

Li, Y., Yuan, H., von dem Bussche, A., et al. 2013. Graphene microsheets enter cells through spontaneous membrane penetration at edge asperities and corner sites. Proc Natl Acad Sci USA, 110(30):12295-12300. http://doi.org/10.1073/pnas.1222276110

Li, G., Cao, Z., Ho, K.K.H.Y., Zuo, Y.Y. 2022. Quantitative Determination of the Hydrophobicity of Nanoparticles. Anal Chem. 94(4):2078-2086. http://doi.org/10.1021/acs.analchem.1c04172

Liu, J.H., Yang, S.T., Wang, H., Chang, Y., Cao, A., Liu, Y. 2012. Effect of size and dose on the biodistribution of graphene oxide in mice. Nanomedicine (Lond). 7(12):1801-1812. http://doi.org/10.2217/nnm.12.60

Liu, X.T., Mu, X.Y., Wu, X.L., et al. 2014. Toxicity of multi-walled carbon nanotubes, graphene oxide, and reduced graphene oxide to zebrafish embryos. Biomed Environ Sci. 27(9):676-683. http://doi.org/10.3967/bes2014.103

Liu, L., Zhu, C., Fan, M., et al. 2015. Oxidation and degradation of graphitic materials by naphthalene-degrading bacteria. Nanoscale. 7(32):13619-13628. http://doi.org/10.1039/c5nr02502h

Liu, Y., Han, W., Xu, Z., Fan, W., Peng, W., Luo, S. 2018. Comparative toxicity of pristine graphene oxide and its carboxyl, imidazole or polyethylene glycol functionalized products to Daphnia magna: A two generation study. Environ Pollut. 237:218-227. http://doi.org/10.1016/j.envpol.2018.02.021

Loureiro, S., Goncalves, S.F, Goncalves, G., Hortiguela, M.J., Rebelo, S., Ferro, M.C., Vila, M. 2018. Eco-friendly profile of pegylated nano-graphene oxide at different levels of an aquatic trophic chain. Ecotoxicol. Environ. Saf. 162, 192-200. https://doi.org/10.1016/j.ecoenv.2018.06.078

Lu, K., Huang, Q., Wang, P., Mao, L. 2015. Physicochemical Changes of Few-Layer Graphene in Peroxidase-Catalyzed Reactions: Characterization and Potential Ecological Effects. Environ Sci Technol. 49(14):8558-8565. http://doi.org/10.1021/acs.est.5b02261

Lu, K., Dong, S., Petersen, E.J., et al. 2017. Biological Uptake, Distribution, and Depuration of Radio-Labeled Graphene in Adult Zebrafish: Effects of Graphene Size and Natural Organic Matter. ACS Nano, 11, 3, 2872–2885. https://doi.org/10.1021/acsnano.6b07982

Lucchese, M.M., Stavale, F., Ferreira, E.H.M., Vilani, C., Moutinho, M.V.O., Capaz, R.B., et al. 2010. Quantifying ion-induced defects and Raman relaxation length in graphene. Carbon 48:1592–7. https://doi.org/10.1016/j.carbon.2009.12.057

Lv, X., Yang, Y., Tao, Y., Jiang, Y., Chen, B., Zhu, X., Cai, Z., Li, B. 2018. A mechanism study of toxicity of graphene oxide to Daphnia magna: direct link between bioaccumulation and oxidative stress. Environ Pollut 234:953–959. http://doi.org/10.1016/j.envpol.2017.12.034

Malhotra, N., Villaflores, O.B., Audira, G., et al. 2020. Toxicity Studies on Graphene-Based Nanomaterials in Aquatic Organisms: Current Understanding. Molecules. 25(16):3618. http://doi.org/10.3390/molecules25163618

Malina, T., Maršálková, E., Holá, K, Tuček, J., Radek Zbořil M.S., Maršálek, B. 2019. Toxicity of graphene oxide against algae and cyanobacteria: Nanoblade-morphology-induced mechanical injury and self-protection mechanism. Carbon 155, 386-396. http://doi.org/10.1016/j.carbon.2019.08.086

Malina, T., Maršálková, E., Holá, K., Zbořil, R., Maršálek, B. 2020. The environmental fate of graphene oxide in aquatic environment-Complete mitigation of its acute toxicity to planktonic and benthic crustaceans by algae. J Hazard Mater. 399:123027. http://doi.org/10.1016/j.jhazmat.2020.123027

Manier, N., Le Manach, S., Bado-Niles, A., Pandard, P. 2016. Effect of two TiO2nanoparticles on the growth of unicellular green algae using the OECD201 test guideline: Influence of the exposure system. Toxicol. Environ. Chem., 98, 860–876. https://doi.org/10.1080/02772248.2015.1124881

Manjunatha, B., Park, S.H., Kim, K. et al. 2018. In vivo toxicity evaluation of pristine graphene in developing zebrafish (Danio rerio) embryos. Environ Sci Pollut Res, 25, 12821–12829. https://doi.org/10.1007/s11356-018-1420-9

Marković, M.S., Andelkovic, I.B., Shuster, J., Janik, L.J., Kumar, A.K., Losic, D., & Mclaughlin, M.J. 2020. Addressing challenges in providing a reliable ecotoxicology data for graphene-oxide (GO) using an algae (*Raphidocelis subcapitata*), and the trophic transfer consequence of GO-algae aggregates. Chemosphere, 245, 125640. https://doi.org/10.1016/j.chemosphere.2019.125640

Martín-de-Lucía, I., Gonçalves, S.F., Leganés, F., Fernández-Piñas, F., Rosal, R., & Loureiro, S. 2019. Combined toxicity of graphite-diamond nanoparticles and thiabendazole to Daphnia magna. Sci. Total Environ., 688, 1145-1154. http://doi.org/10.1016/j.scitotenv.2019.06.316

Martínez-Álvarez, I., Le Menach, K., Devier, M.H., et al. 2021. Uptake and effects of graphene oxide nanomaterials alone and in combination with polycyclic aromatic hydrocarbons in zebrafish. Sci Total Environ. 775:145669. http://doi.org/10.1016/j.scitotenv.2021.145669

Marcano, D. C., Kosynkin, D. V., Berlin, J. M., Sinitskii, A., Sun, Z., Slesarev, A., Alemany, L. B., Lu, W., & Tour, J. M. 2010. Improved synthesis of graphene oxide. ACS nano, 4(8), 4806–4814. https://doi.org/10.1021/nn1006368

Meyer, J.C., Girit, C.O., Crommie, M.F., Zettl, A. 2008. Imaging and dynamics of light atoms and molecules on graphene. Nature 454, 319–322. http://doi.org/10.1038/nature07094

Mittal, K., Crump, D., Head J.A., Hecker, M., Hickey, G., Maguire, S., Hogan, N., Xia, J., Basu, N. 2022. Resource requirements for ecotoxicity testing: A comparison of traditional and new approach methods. http://doi.org/10.1101/2022.02.24.481630

Montagner, A., Bosi, S., Tenori, E., Bidussi, M., Alshatwi, A.A., Tretiach, M., Prato, M., Syrgiannis, Z. 2017. Ecotoxicological effects of graphene-based materials. 2D Materials, 4, 012001. http://doi.org/10.1088/2053-1583/4/1/012001

Moreira, C.C., Costa, Í.A., Moura, D.S., Grisolia, C.K., Leite, C.A., Souza, P.E., Moreira, S., Pereira-da-Silva, M.A., Braga, J.W., & Paterno, L.G. 2021. Oxidation degree or sheet size: What really matters for the photothermal effect and ecotoxicity of graphene oxide? FlatChem http://doi.org/10.1016/J.FLATC.2021.100231

Mullick Chowdhury, ., Dasgupta, S., McElroy, A.E., Sitharaman, B. 2014. Structural disruption increases toxicity of graphene nanoribbons. J Appl Toxicol. 34(11), 1235-1246. http://doi.org/ doi:10.1002/jat.3066

Nasser, F., Lynch, I., 2019. Updating traditional regulatory tests for use with novel materials: Nanomaterial toxicity testing with Daphnia magna. Saf. Sci. 118, 497-504. http://doi.org/10.1016/j.ssci.2019.05.045

Nasser, F., Constantinou, J., Lynch, I. 2020. Nanomaterials in the Environment Acquire an "Eco-Corona" Impacting their Toxicity to Daphnia Magna-a Call for Updating Toxicity Testing Policies. Proteomics, 20(9), e1800412. https://doi.org/10.1002/pmic.201800412

Nogueira, P.F., Nakabayashi, D., Zucolotto, V. 2015. The effects of graphene oxide on green algae Raphidocelis subcapitata. Aquat Toxicol. 166, 29-35. http://doi.org/10.1016/j.aquatox.2015.07.001

OECD 1992, Test No. 301: Ready Biodegradability, OECD Guidelines for the Testing of Chemicals, Section 3, OECD Publishing, Paris, https://doi.org/10.1787/9789264070349-en

OECD 2001, Test No. 303: Simulation Test - Aerobic Sewage Treatment -- A: Activated Sludge Units; B: Biofilms, OECD Guidelines for the Testing of Chemicals, Section 3, OECD Publishing, Paris, https://doi.org/10.1787/9789264070424-en

OECD 2004a, Test No. 202: Daphnia sp. Acute Immobilisation Test, OECD Guidelines for the Testing of Chemicals, Section 2, OECD Publishing, Paris, https://doi.org/10.1787/9789264069947-en

OECD 2004b, Test No. 309: Aerobic Mineralisation in Surface Water – Simulation Biodegradation Test, OECD Guidelines for the Testing of Chemicals, Section 3, OECD Publishing, Paris, https://doi.org/10.1787/9789264070547-en

OECD 2008, Test No. 316: Phototransformation of Chemicals in Water – Direct Photolysis, OECD Guidelines for the Testing of Chemicals, Section 3, OECD Publishing, Paris, https://doi.org/10.1787/9789264067585-en

OECD 2011, Test No. 201: Freshwater Alga and Cyanobacteria, Growth Inhibition Test, OECD Guidelines for the Testing of Chemicals, Section 2, OECD Publishing, Paris, https://doi.org/10.1787/9789264069923-en.

OECD 2012, Test No. 109: Density of Liquids and Solids, OECD Guidelines for the Testing of Chemicals, Section 1, OECD Publishing, Paris, https://doi.org/10.1787/9789264123298-en.

OECD 2013a. Recommendation of the council on the safety testing and assessment of manufactured nanomaterials. https://legalinstruments.oecd.org/en/instruments/OECD-LEGAL-0400.

OECD 2013b, Test No. 236: Fish Embryo Acute Toxicity (FET) Test, OECD Guidelines for the Testing of Chemicals, Section 2, OECD Publishing, Paris, https://doi.org/10.1787/9789264203709-en.

OECD 2017, Test No. 318: Dispersion Stability of Nanomaterials in Simulated Environmental Media, OECD Guidelines for the Testing of Chemicals, Section 3, OECD Publishing, Paris, https://doi.org/10.1787/9789264284142-en.

OECD 2018. Assessment of Biodurability of nanomaterials and their surface ligands series on the safety of manufactured nanomaterials. Series on the Safety of Manufactured Nanomaterials. No. 86. ENV/JM/MONO(2018)11

OECD 2019a, Guidance document on aqueous-phase aquatic toxicity testing of difficult test chemicals, OECD Series on Testing and Assessment, No. 23 OECD Publishing, Paris, https://doi.org/10.1787/0ed2f88e-en

OECD, 2019b, Guiding principles and key elements for establishing a weight of evidence for chemical assessment. Series on Testing and Assessment No. 311 OECD Publishing, Paris, http://doi.org/10.1787/f11597f6-en

OECD 2019c, Test No. 203: Fish, Acute Toxicity Test, OECD Guidelines for the Testing of Chemicals, Section 2, OECD Publishing, Paris, https://doi.org/10.1787/9789264069961-en

OECD 2019d, Guiding Principles and Key Elements for Establishing a Weight of Evidence for Chemical Assessment, Series on Testing and Assessment No. 311, Environment, Health and Safety Division, Environment Directorate.

OECD 2019e, Test No. 495: Ros (Reactive Oxygen Species) Assay for Photoreactivity, OECD Guidelines for the Testing of Chemicals, Section 4, OECD Publishing, Paris, https://doi.org/10.1787/915e00ac-en

OECD 2021a, Test No. 249: Fish Cell Line Acute Toxicity - The RTgill-W1 cell line assay, OECD Guidelines for the Testing of Chemicals, Section 2, OECD Publishing, Paris, https://doi.org/10.1787/c66d5190-en

OECD 2021b, Work plan for the Test Guidelines Programme (TGP), Available at: https://www.oecd.org/env/ehs/testing/work-plan-test-guidelines-programme-july-2021.pdf

OECD 2021c, Guidance document for the testing of dissolution and dispersion stability of nanomaterials and the use of the data for further environmental testing and assessment strategies. Series on Testing and Assessment No. 318, OECD Publishing, Paris, https://www.oecd.org/officialdocuments/publicdisplaydocumentpdf/?cote=env/jm/mono(2020)9&doclanguage=en

OECD 2022a, Guidance Document on on Aquatic and Sediment Toxicological Testing of Nanomaterials, Series on Testing and Assessment No. 317, OECD Publishing, Paris, https://www.oecd.org/officialdocuments/publicdisplaydocumentpdf/?cote=env/jm/mono(2020)8&doclanguage=en

OECD 2022b, Test No. 124: Determination of the Volume Specific Surface Area of Manufactured Nanomaterials, OECD Guidelines for the Testing of Chemicals, Section 1, OECD Publishing, Paris, https://doi.org/10.1787/abb72f8f-en

OECD 2022c, Test No. 125: Nanomaterial Particle Size and Size Distribution of Nanomaterials, OECD Guidelines for the Testing of Chemicals, Section 1, OECD Publishing, Paris, https://doi.org/10.1787/af5f9bda-en

Paparella, M., Scholz, S., Belanger, S., Braunbeck, T., Bicherel, P., et al. 2021. Limitations and uncertainties of acute fish toxicity assessments can be reduced using alternative methods. ALTEX, 38(1), 20–32. https://doi.org/10.14573/altex.2006051

Pecoraro, R., D'Angelo, D., Filice, S., Scalese, S., Capparucci, F., Marino, F., Iaria, C., Guerriero, G., Tibullo, D., Scalisi, E.M., Salvaggio, A., Nicotera, I., Brundo, M.V. 2018. Toxicity Evaluation of Graphene Oxide and Titania Loaded Nafion Membranes in Zebrafish. Front Physiol. 4(8):1039. http://doi.org/10.3389/fphys.2017.01039

Petersen, E.J., Henry, T.B., Zhao, J., MacCuspie, R.I., Kirschling, T.L., Dobrovolskaia, M.A., Hackley, V., Xing, B., White, J.C., 2014. Identification and avoidance of potential artifacts and misinterpretations in nanomaterial ecotoxicity measurements. Environ. Sci. Technol. 48, 4226–4246. https://doi.org/10.1021/es4052999

Praetorius, A., Badetti, E., Brunelli, A., Clavier, A., Gallego-Urrea, J.A., et al., 2020. Strategies for determining heteroaggregation attachment efficiencies of engineered nanoparticles in aquatic environments. Environ. Sci. Nano 7(2):351-367. http://doi.org/10.1039/C9EN01016E

Qiang, L., Chen, M., Zhu, L-Y., & Wu, W., Wang, Q. 2016. Facilitated Bioaccumulation of Perfluorooctanesulfonate in Common Carp (Cyprinus carpio) by Graphene Oxide and Remission Mechanism of Fulvic Acid. Environ. Sci. Technol. 50, 21, 11627–11636. http://doi.org/10.1021/acs.est.6b02100

Rasmussen, K., González, M., Kearns, P., Sintes, J.R., Rossi, F., Sayre, P. 2016. Review of achievements of the OECD Working Party on Manufactured Nanomaterials' Testing and Assessment Programme. From exploratory testing to test guidelines. Regul Toxicol Pharmacol. 74:147-160. http://doi.org/10.1016/j.yrtph.2015.11.004

Ren, C., Hu, X., Li, X., Zhou, Q. 2016. Ultra-trace graphene oxide in a water environment triggers Parkinson's disease-like symptoms and metabolic disturbance in zebrafish larvae. Biomaterials. 93:83-94. http://doi.org/10.1016/j.biomaterials.2016.03.036

Shamsi, S., Alagan, A.A., Sarchio, S.N.E., Md Yasin, F. 2020. Synthesis, Characterization, and Toxicity Assessment of Pluronic F127-Functionalized Graphene Oxide on the Embryonic Development of Zebrafish (Danio rerio). Int J Nanomedicine 15:8311-8329. http://doi.org/10.2147/IJN.S271159

Shaw, B.J., Liddle, C.C., Windeatt, K.M., Handy, R.D. 2016. A critical evaluation of the fish early-life stage toxicity test for engineered nanomaterials: experimental modifications and recommendations. Arch. Toxicol. 90(9), 2077–2107. https://doi.org/10.1007/s00204-016-1734-7

Skjolding, L.M., Kruse, S., Sørensen, S.N., Hjorth, R., Baun, A. 2020. A Small-Scale Setup for Algal Toxicity Testing of Nanomaterials and Other Difficult Substances. J Vis Exp. 164. http://doi.org/10.3791/61209

Soares, J.C., Pereira, T., Costa, K.M., Maraschin, T., Basso, N.R., Bogo, M.R. 2017. Developmental neurotoxic effects of graphene oxide exposure in zebrafish larvae (Danio rerio). Colloids Surf B Biointerfaces, 157:335-346. http://doi.org/10.1016/j.colsurfb.2017.05.078

Sobanska, M., Scholz, S., Nyman, A.M., Cesnaitis, R., Gutierrez Alonso, S., Klüver, N., Kühne, R., Tyle, H., de Knecht, J., Dang, Z., Lundbergh, I., Carlon, C., De Coen, W. 2018. Applicability of the fish embryo acute toxicity (FET) test (OECD 236) in the regulatory context of Registration, Evaluation, Authorisation, and Restriction of Chemicals (REACH). Environ. Toxicol. Chem, 37(3), 657–670. https://doi.org/10.1002/etc.4055

Sørensen, S. N., Hjorth, R., Delgado, C. G., Hartmann, N. B., & Baun, A. 2015. Nanoparticle ecotoxicity-physical and/or chemical effects? Integr. Environ. Assess. Manag. 11(4), 722–724. http://doi.org/10.1002/ieam.1683

Souza, J.P., Venturini, F.P., Santos, F., Zucolotto, V. 2018. Chronic toxicity in Ceriodaphnia dubia induced by graphene oxide, Chemosphere, 190, 218-224. http://doi.org/10.1016/j.chemosphere.2017.10.018

Souza, J.P., Mansano, A.S., Venturini, F.P. et al. 2019. Antioxidant metabolism of zebrafish after sub-lethal exposure to graphene oxide and recovery. Fish Physiol Biochem 45, 1289–1297. https://doi.org/10.1007/s10695-019-00678-7

Souza, J.P., Baretta, J.F., Santos, F., Paino, I.M.M., Zucolotto, V. 2017. Toxicological effects of graphene oxide on adult zebrafish (Danio rerio). Aquat Toxicol, 186, 11-18. http://doi.org/10.1016/j.aquatox.2017.02.017

Srikanth, K., Sundar, L.S., Pereira, E., Duarte, A.C. 2018. Graphene oxide induces cytotoxicity and oxidative stress in bluegill sunfish cells. J Appl Toxicol. 38(4), 504-513. http://doi.org/10.1002/jat.3557

Staudenmaier, L. 1898. Verfahren zur Darstellung der Graphitsäure. Berichte der deutschen chemischen Gesellschaft, 31, 1481-1499.

Su, Y., Yang, G., Lu, K., Petersen, E. J., & Mao, L. 2017. Colloidal properties and stability of aqueous suspensions of few-layer graphene: Importance of graphene concentration. Environ. Pollut. 220, 469–477. http://doi.org/10.1016/j.envpol.2016.09.089

Sun, J., Zhou, Q., Hu, X. 2019. Integrating multi-omics and regular analyses identifies the molecular responses of zebrafish brains to graphene oxide: Perspectives in environmental criteria. Ecotoxicol Environ Saf. 180:269-279. http://doi.org/10.1016/j.ecoenv.2019.05.011

Sydlik, S.A., Jhunjhunwala, S., Webber, M.J., Anderson, D.G., Langer, R. 2015. In vivo compatibility of graphene oxide with differing oxidation states. ACS Nano. 9(4):3866-3874. http://doi.org/10.1021/acsnano.5b01290

Taurozzi, J.S., Hackley, V.A., Wiesner, M.R. 2013. Ultrasonic dispersion of nanoparticles for environmental, health and safety assessment--issues and recommendations. Nanotoxicology 5(4):711-729. https://doi:10.3109/17435390.2010.528846

Valsesia, A., Desmet, C., Ojea-Jiménez, I. et al. 2018. Direct quantification of nanoparticle surface hydrophobicity. Commun Chem 1, 53. https://doi.org/10.1038/s42004-018-0054-7

Wang, G., Quian, F., Saltikov, C.W., Jiao, Y., Li, Y. 2011a. Microbial reduction of graphene oxide by Shewanella. Nano Res 4:563–570. https://doi.org/10.1007/s12274-011-0112-2

Wang, K., Ruan, J., Song, H., Zhang, J., Woo, Y., Guo, S., Cu,i D. 2011b. Biocompatibility of graphene oxide. Nanoscale Res Lett 6:1–8. http://doi.org/10.1007/s11671-010-9751-6

Wang, Z.G., Zhou, R., Jiang, D., et al. 2015. Toxicity of Graphene Quantum Dots in Zebrafish Embryo. Biomed Environ Sci. 28(5):341-351. http://doi.org/10.3967/bes2015.048

Wang, Z., Gao, Y., Wang, S. et al. 2016. Impacts of low-molecular-weight organic acids on aquatic behavior of graphene nanoplatelets and their induced algal toxicity and antioxidant capacity. Environ Sci Pollut Res 23, 10938–10945. https://doi.org/10.1007/s11356-016-6290-4

Wang, Z., Zhang, F., Vijver, M.G., Peijnenburg, W,J,G,M. 2021. Graphene nanoplatelets and reduced graphene oxide elevate the microalgal cytotoxicity of nano-zirconium oxide. Chemosphere, 276:130015. http://doi.org/10.1016/j.chemosphere.2021.130015

Wick, P., Louw-Gaume, A.E., Kucki, M., et al. 2014. Classification framework for graphene-based materials. Angew Chem Int Ed Engl. 53(30):7714-7718. http://doi.org/10.1002/anie.201403335

Xiong, G., Deng, Y., Liao, X., Zhang, J., Cheng, B., Cao, Z., Lu, H. 2020. Graphene oxide nanoparticles induce hepatic dysfunction through the regulation of innate immune signaling in zebrafish (Danio rerio). Nanotoxicology, 14:5, 667-682. http://doi.org/10.1080/17435390.2020.1735552

Yan, J., Chen, S., Zuo, Z., He, C., Yi, M. 2020. Graphene oxide quantum dot exposure induces abnormalities in locomotor activities and mechanisms in zebrafish (Danio rerio). J Appl Toxicol. 40(6):794-803. http://doi.org/10.1002/jat.3944

Yan, Z., Yang, X., Lynch, I., Cui, F. 2022. Comparative evaluation of the mechanisms of toxicity of graphene oxide and graphene oxide quantum dots to blue-green algae Microcystis aeruginosa in the aquatic environment. J Hazard Mater, 425, 127898. https://doi.org/10.1016/j.jhazmat.2021.127898

Yang, X., Yang, Q., Zheng, G., et al. 2019. Developmental neurotoxicity and immunotoxicity induced by graphene oxide in zebrafish embryos. Environ Toxicol. 34(4), 415-423. http://doi.org/10.1002/tox.22695

Yao, H., Li, X., Zhang, L., Huang, Y., Luo, T., Chen, J. 2018. Effect of different surface functional groups of graphene on oxidative stress in Daphnia magna. Chinese Science Bulletin 64 (4), 419-429. http://doi.org/10.1360/n972018-00960

Ye, N., Wang, Z., Wang, S., Peijnenburg, W.J.G.M. 2018. Toxicity of mixtures of zinc oxide and graphene oxide nanoparticles to aquatic organisms of different trophic level: particles outperform dissolved ions. Nanotoxicology. 12(5):423-438. http://doi.org/10.1080/17435390.2018.1458342

Yin, J., Dong, Z., Liu, Y., Wang, H., Li, A., Zhuo, Z., et al., 2020. Toxicity of reduced graphene oxide modified by metals in microalgae: Effect of the surface properties of algal cells and nanomaterials, Carbon 169, 182-192. http://doi.org/10.1016/j.carbon.2020.07.057

Zhang, H., Peng, C., Yang, J., Lv, M., Liu, R., He, D., et al. 2013. Uniform ultrasmall graphene oxide nanosheets with low cytotoxicity and high cellular uptake. ACS Appl. Mater. Interfaces 5, 1761-1767. https://doi.org/10.1021/am303005j

Zhang, X., Zhou, Q., Zou, W., Hu, X. 2017a. Molecular Mechanisms of Developmental Toxicity Induced by Graphene Oxide at Predicted Environmental Concentrations. Environ Sci Technol. 51(14):7861-7871. http://doi.org/10.1021/acs.est.7b01922

Zhang, J.H., Sun, T., Niu, A., Tang, Y.M., Deng, S., Luo, W., Xu, Q., Wei, D., Pei, D. S. 2017b. Perturbation effect of reduced graphene oxide quantum dots (rGOQDs) on aryl hydrocarbon receptor (AhR) pathway in zebrafish. Biomaterials, 133, 49–59. https://doi.org/10.1016/j.biomaterials.2017.04.026

Zhang Y, Meng T, Guo X, Yang R, Si X, Zhou J. 2018. Humic acid alleviates the ecotoxicity of graphene-family materials on the freshwater microalgae Scenedesmus obliquus. Chemosphere. 197:749-758. doi:10.1016/j.chemosphere.2018.01.051

Zhang, Y., Meng, T., Shi, L., Guo, X., Si, X., Yang, R., & Quan, X. 2019. The effects of humic acid on the toxicity of graphene oxide to Scenedesmus obliquus and Daphnia magna. Sci. Total Environ, 649, 163-171. https://doi.org/10.1016/j.scitotenv.2018.08.280

Zhang, S., Han, J., Luo, X., Wang, Z., Gu, X., Li, N., de Souza, N.R., Garcia Sakai, V., Chu. X.Q. 2021. Investigations of structural and dynamical mechanisms of ice formation regulated by graphene oxide nanosheets. Struct Dyn 8(5), 054901. http//doi.org/10.1063/4.0000111

Zhao, J., Cao, X., Wang, Z., Dai, Y., & Xing, B. 2017. Mechanistic understanding toward the toxicity of graphene-family materials to freshwater algae. Water research, 111, 18–27. https://doi.org/10.1016/j.watres.2016.12.037

Zhao, J., Li, Y., Cao, X., Guo, C., Xu, L., Wang, Z., Feng, J., Yi, H., Xing, B. 2019. Humic acid mitigated toxicity of graphene-family materials to algae through reducing oxidative stress and heteroaggregation. Environmental science. Nano, 6(6):1909-1920. http://doi.org/10.1039/C9EN00067D23

Zhao, J, Ning, F., Cao, X., Yao, H., Wang, Z., Xing, B. 2020. Photo-transformation of graphene oxide in the presence of co-existing metal ions regulated its toxicity to freshwater algae. Water Research, 176, 115735. http:doi.org/10.1016/j.watres.2020.115735

Zhao, Y., Liu, Y., Zhang, X., Liao, W. 2021. Environmental transformation of graphene oxide in the aquatic environment. Chemosphere. 262:127885. http://doi.org/10.1016/j.chemosphere.2020.127885

Aims of the project

Despite the growing body of scientific literature on the ecotoxicological effects of GRMs that applies the TG 201, several questions still remain unanswered. The knowledge gaps mainly concern the poor investigation of GRMs behaviour in aqueous media. The issues regarding the TG 201 applicability to GRMs remain little investigated, including the existing limitation of analytical methods used for a reliable assessment of TG 201 endpoints, together with a robust evaluation of the GDS over time. Furthermore, to date only a few studies focused on evaluating the main factors affecting the GRMs stability. In addition, little is still known about the possible transformation, environmental fate of GRMs, and potential ecotoxicological effects on freshwater organisms, such as algae, under environmental-like conditions.

Addressing these gaps is absolutely necessary to determine if the TG 201 is applicable or not to GRMs as it is, and to develop GDs tailored to GRMs to enhance the reliability of future studies and, most importantly, the relevance of the required risk assessment for freshwater environments.

In this context, my PhD project aimed at addressing and investigating the aforementioned concerns, hence, the three main research objectives of this thesis are:

i) identify proper techniques for conducting ecotoxicological assays, specifically tailored for GRMs;

ii) verify the applicability of the TG 201 to GRMs, suggesting possible adaptations to improve its applicability;

iii) investigate the potential environmental fate of GRMs in natural freshwaters, posing a focus also on the ecotoxicological effects on freshwater green microalgae, primary producers at the base of the trophic chain in freshwater ecosystems.

To achieve these aims, the three most common GRMs, namely FLG, GO, and rGO, having different physicochemical properties, *e.g*. numbers of layers, lateral size, C/O ratio, were used to carry out the experiments. The GRMs Dispersions Stability (GDS) was investigated in both synthetic and natural media providing specific information on agglomeration/aggregation and settling processes throughout the tests. This information is crucial to assess if the main TG 201 applicability criterion is met and to predict the potential environmental fate of GRMs. Furthermore, the effect of GRMs on algal growth inhibition was investigated both following the TG 201, and, for the first time, under environmental-like conditions.

Thesis outline

My PhD research work has been organized for this thesis into three main sections, with the topics covered in each chapter will be presented as follows.

Chapter 1 outlined the work performed to develop a proper methodological approach for TG 201 testing on GRMs, avoiding the biases already reported in the literature. Traditional methods commonly used to evaluate the TG 201 endpoints, *i.e.* counting chamber and spectrophotometer, provided biased results due to strong hetero-agglomeration of GRMs with algal cells. Instead, an innovative approach applying flow-cytometer (FCM), allowed a proper evaluation of both algal and GRMs populations.

Once the proper methodology to carry out the test was established, we verified the applicability of the TG 201 to GRMs and proposed some modification to the standard protocol, as described in chapter 2. Our results showed that the TG 201 is hardly applicable to GRMs in its current for, due to significant aggregation and sedimentation phenomena, hindering the fulfilment of the TG 201 stability requirement. However, it was found that a delayed starting time, allowing GRMs dispersions to attain a stable condition, is needed to fulfill the stability criterion of the TG 201. Furthermore, it has been demonstrated the importance of a comprehensive evaluation of the GDS, as aggregation and sedimentation alter the effective concentration to which the algae are exposed, affecting the GRMs bioavailability, and also their potential fate in real freshwater environments.

Finally, in chapter 3 we further explored this last point by studying the potential environmental fate of GRMs using natural fresh waters. First, the impact of the medium ionic composition on the GDS was investigated by comparing GDS in standard soft media (*i.e.* TG 201 medium and dH_2O) with commercial mineral waters. Then, real natural fresh waters were employed to assess the GRMs behaviour under environmental-like conditions, offering a more realistic perspective than standard laboratory media. Our results showed that ionic, clay, and NOM content significantly affect the GDS, resulting in even more aggregation and sedimentation than previously observed. As a consequence, GRMs in the environment are likely to accumulate in the sediments.

The thesis concludes with an appendix detailing a side projects of the Graphene Flagship, the Spearhead Project called Safegraph, in which I was involved during my doctoral studies. This project was aimed at supporting four projects, namely ChemSens, WearGraph, GICE, and Graphil, by providing an organized and case-to-case adapted authorization framework, necessary for commercializing their GRMs-containing products. My involvement required to provide ecotoxicological information for the risk assessment by applying the TG 201 to the GRMs potentially released by the devices developed in the aforementioned projects. Specifically, I focused on the Graphil device, *i.e.* a system for household filtration of drinkable water enhanced by the

application of GO to the filtering matrix (polysulfone fibers). Applying the TG 201 on waters filtered through the GO-containing cartridge no ecotoxicological effects on the target algae, *Raphidocelis subcapitata*, were observed.

Chapter 1

Test Guideline (TG) 201 and graphene-related materials (GRMs): establishing a robust methodological approach for a reliable assessment of the TG endpoints

Giada Caorsi[1], Fabio Candotto Carniel[1], Emmanuel Flahaut[2], Maurizio Prato[3], Mauro Tretiach[1]

[1] Dipartimento di Scienze della Vita, Università di Trieste, via L. Giorgieri 10, 34127 Trieste, Italia

[2] Centre Interuniversitaire de Recherche et d'Ingénierie des Matériaux - CIRIMAT, Université Paul-Sabatier, 118 Route de Narbonne, Cedex 9, 31062 Toulouse, France

[3] Dipartimento di Scienze Chimiche e Farmaceutiche, Università di Trieste, via L. Giorgieri 1, 34127 Trieste, Italia

Abstract

Environmental risk assessment for graphene-related materials (GRMs) relies on standardised test guidelines (TGs) from the Organisation for Economic Co-operation and Development (OECD), originally designed for water-soluble substances. This raises significant concerns about the applicability of existing algal test guidelines, *i.e.* TG 201, to non-water-soluble nanoparticles, such as GRMs. Key issues include the evaluation of the (*i*) algal cells densities, and (*ii*) TG 201 stability requirement (maintenance of ± 20 % of the nominal initial concentration). This work aims to establish a suitable methodological approach for TG 201 testing on GRMs, addressing the biases reported in the literature. Standard methods, *i.e.* Bürker and Malassez counting chambers, were evaluated and compared to flow cytometer (FCM) as an alternative method, to improve the accuracy and efficiency of the TG 201 results. Out of these methods, FCM resulted to be the most suitable, allowing for accurate detection of algal cell densities, even at low concentration, with high precision. Additionally, FCM enabled the assessment of changes in GRMs flakes particles, allowing the evaluation of their stability.

In conclusion, FCM is suggested as a robust and reliable method for the applicability of TG 201 to GRMs, ensuring accurate evaluation of both the algal and GRMs populations.

Keywords

Graphene-related materials (GRMs), OECD TG 201, algal growth inhibition, GRMs dispersions stability (GDS), standard test guidelines.

1. Introduction

Testing the hazard potential of nanomaterials (NMs) is essential for their risk assessment. According to the Registration, Evaluation, Authorisation, and Restriction of Chemicals (REACH) regulation, standardised test guidelines (TGs) from the Organisation for Economic Co-operation and Development (OECD) are required to determine whether a substance is hazardous or not to the environment [1]. Currently, the test battery for ecotoxicological assessment in aquatic environments includes tests using algae and/or cyanobacteria, invertebrates (crustaceans), and fish, namely TG 201: "Freshwater Algae and Cyanobacteria Growth Inhibition Test" [2], TG 202: "Daphnia Acute Immobilisation Test" [3], TG 203: "Fish Acute Toxicity Test" [4]. These test guidelines were originally developed for water-soluble substances, mandating concentration measurement and stability requirement, *i.e.* the maintenance of ± 20% of the nominal or measured initial concentration throughout the 72-h test period.

However, this is typically unsuitable for NMs, which generally exhibit stability issues primarily due to aggregation/agglomeration and sedimentation phenomena. This raises significant concerns regarding the applicability to NMs of standard test methods in the current form [5,6]. Specifically, the applicability of the existing algal test guidelines is hindered by the fundamental differences between NMs and water-soluble substances. While these tests are considered generally applicable for the testing of many NMs [7,8], doubts have been raised about their applicability when testing specifically "difficult to test" NMs, such as graphene-related materials (GRMs) [9]. In particular, TG 201 proved to be the most challenging when testing GRMs, with respect to TG 202 and TG 203 [9,10].

The TG 201 aims to determine the effects of a substance on the growth of freshwater microalgae and/or cyanobacteria. The test endpoint is the algal growth inhibition, expressed as the logarithmic increase in biomass (dry weight per volume) as a function of time [22]. However, since dry weight is generally difficult to measure and not applicable in the presence of particles, other surrogate parameters are proposed by the TG 201. The most commonly used methods for quantification of biomass are based on cell counting (traditional microscopy or automated counting), cell volume, fluorescence measurements, and optical density [2,11–14]. However, as reviewed by Connoly et al., the existing test methods are not always applicable to GRMs and suitable test methods are missing [9]. Consequently, TG 201 results in the presence of GRMs can be frequently biased.

Both the affinity of algal cells with GRMs and the dynamic nature of the test systems represent major challenges leading to inconsistencies or information gaps. These issues are mainly related to the (*i*) evaluation of the algal growth inhibition, *i.e.* the TG 201 test endpoint, and (*ii*) assessment of the TG 201 stability requirement, *i.e.* maintenance of ± 20 % of the initial concentration.

Regarding the first point, the main issues arise from physical interferences resulting from GRMs hetero-aggregation with algae, hindering direct counting of algal cells and consequently leading to apparent algal growth inhibition [5,15–20]. Furthermore, as GRMs dispersions are coloured and light absorbing, interferences with fluorescence readouts were evidenced in methods that rely on absorbance or fluorescence measurements, such as UV-Vis measurements, and *in vitro* or *in vivo* chlorophyll fluorescence [13,15,21]. Regarding the second point, due to the well-known poor stability of the GRMs dispersions [22–25], the dispersions should be analysed to verify the initial concentration and maintenance of the exposure concentrations during the test. However, there is a lack of analytical measurement of GRMs concentrations in most of the available studies [9], leading to uncertainties and reduced reliability of the TG 201 results. Therefore, is evident the need for additional assessments, alternative approaches, and modified methods.

This work aims to address the aforementioned methodological issues related to the applicability of the TG 201 to GRMs, focusing on the determination of algal cell densities and the stability issues of GRMs. A methodological approach specifically tailored for GRMs is proposed to ensure a fast and reliable evaluation of the TG 201 endpoints. To this end, flow cytometer (FCM) is suggested as a fast and straightforward procedure suitable for testing GRMs, improving the reliability and interpretability of results when applying the TG 201.

2. Materials and methods

2.1. Graphene-related materials preparation and characterization

Few-layers graphene (FLG) was prepared following the method outlined by González-Domínguez et al. [26]. A mixture of 7.5 mg graphite and 22.5 mg melamine was subjected to ball milling at 100 r.p.m. for 30 minutes using a Retsch PM 100 planetary mill (Retsch Technology, DE) and subsequently sonicated for 1 minute in 20 mL of MilliQ distilled water. The suspension was then dialyzed against water to remove melamine and the resulting FLG dispersion was lyophilized.

Graphene oxide (GO), provided by Grupo Antolín Ingeniería (Burgos, ES), was prepared by oxidation of carbon nanofibers (GANF Helical-Ribbon Carbon Nanofibres) using the Hummer's method [27,28]. GO was gently ground with a mortar and pestle to homogenize the as-received powder before preparing the dispersion.

Reduced GO (rGO) was produced from Grupo Antolin's GO by thermal reduction at 200 °C by CIRIMAT-CNRS, Tolouse (FR), using a process detailed by Evariste et al. and Di Mauro et al. [29,30].

The three GRMs were characterized by transmission electron microscopy (TEM), thermogravimetric analysis (TGA), Raman analysis, and quantitative analyses for C, H, N, O, and S (for details see Chap. 2 - S.I.).

2.2. The algal growth rate inhibition tests: determination of the algal cells densities

The algal growth inhibition test procedure was performed according to the OECD Test Guideline 201 [2] using the unicellular freshwater green microalga *Raphidocelis subcapitata* (Korshikov) [31] (formerly known as *Pseudokirchneriella subcapitata* or *Selenastrum capricornutum*) as test organism. Axenic algal stock cultures were cultivated in 100 mL of OECD TG 201 standard medium (see annex 3 of the OECD TG 201 [2] for medium composition) in 250 mL Erlenmeyer's flasks and placed in a thermostatic chamber at 20 ± 1 °C, 65 ± 5 µmol photons m^{-2} s^{-1} under a light:dark cycle of 14:10 h. Prior to each test, a pre-culture in TG 201 standard medium was prepared and left at 21 ± 1 °C under continuous illumination of 75 µmol photons m^{-2} s^{-1}, to adapt the algae to the test conditions.

The TG 201 medium was used to prepare a dilution series of rGO dispersions at concentrations ranging from 5 to 40 mg L^{-1}, aligning with typical EC_{50} values reported in the literature [9]. The rGO was chosen among other GRMs for its high aggregation and sedimentation phenomena, aiming to test the reliability of counting chambers and FCM in the presence of such "difficult to test" NMs.

All rGO dispersions and controls (without rGO) were inoculated with algae in the exponential growth phase to a starting density of $1 \cdot 10^4$ cell mL^{-1} (within the TG 201 specified range of $5 \cdot 10^3$-10^4 cell mL^{-1}). Six replicates (25 mL) for each dispersion were poured in 50 mL Erlenmeyer's flasks and placed in a thermostatic chamber at 21 ± 1 °C on an orbital shaker (M301-OR, MPM Instruments, IT) at 90 r.p.m., and additionally manually shaken three times per day to resuspend any settled cells, and then returned to the orbital shaker to minimize spatial difference in illumination and temperature. The flasks were subjected to continuous illumination of 75 µmol photons m^{-2} s^{-1} from below, provided by daylight lamps (Neon Gro-Lux F18W/T8, Sylvania, DE). Light intensity was measured using an immersion spherical sensor (US-SQS/L Spherical Submersible Micro Quantum Sensor connected to ULM-500 Universal Light Meter & Data Logger, WALZ, DE), measuring the photosynthetically active radiation in the 400-700 nm wavelength range. To assess the actual light conditions experienced by the algae, the sensor was inserted inside the flasks. Tests were conducted at a pH of 8.1, with a drift of < 0.5 pH units for individual samples throughout the 72-h test period.

The effects of rGO dispersions (5-40 mg L^{-1}) were investigated by subjecting the algae to chronic exposure for 72 h. As outlined in the TG 201, algal cell densities should be counted daily to

calculate the algal growth rate (AGR), and from this, the algal growth inhibition (AGI %), *i.e.* the TG 201 endpoint [2], is determined. To this end, algal cell densities were monitored over the 72-h test period using two different counting chambers, *i.e.* Bürker and Malassez counting chambers, and a flow cytometer (FCM). Measurements were performed in parallel on the same samples to allow for a direct comparison of the two methods and to determine the most effective and robust methodology.

2.3. Evaluation of the GRMS dispersion stability (GDS)

According to the aforementioned TG 201 stability requirement, the GRMS dispersion stability (GDS) is a critical factor to assess throughout the test period. To this end, the stability of the GRMs dispersions was tested by flow cytometer (FCM) to monitor the agglomeration/aggregation and changes in complexity of GRMs particles.

The TG 201 medium was used to prepare FLG, GO and rGO dispersions at concentrations ranging from 4 to 20 mg L^{-1}. Six replicates (25 mL) of the GRMs dispersions were left for 72 h in 50 mL Erlenmeyer's flasks and the GRMs flakes populations were monitored throughout the 72-h test period. Additionally, dilution series ranging from 1.25 to 40 mg L^{-1} of GRMs dispersions in TG 201 medium were prepared to test the reliability of FCM in evaluating the initial GRMs concentration.

2.4 Tested techniques

Counting chambers – The algal cell densities in CTRL and treated samples were counted daily using two different counting chambers, namely Bürker, the most commonly used, and Malassez, as proposed at ECHA level [32,33].

Both Bürker and Malassez counting chambers consist of a glass chamber with 2 counting grid patterns etched on its surface. In Bürker counting chamber each grid (3 x 3 mm, depth 0.1 mm) present 9 large squares (1 x 1 mm) of 0.1 mm^3, each containing 16 smaller squares (0.2 × 0.2 mm) of 0,04 mm^3 (Fig. S1A). In Malassez counting chamber, each grid (2 x 2.5 mm, depth 0.2 mm) present 25 large rectangles (0.25 x 0.20 mm) of 0.01 mm^3, each containing 20 smaller squares (0.05 x 0.05 mm) of $5 \cdot 10^{-4}$ mm^3 (Fig. S1B).

To evaluate the algal cell densities, a small volume of the samples was spiked between the chamber and the coverslip, then, under an optical light microscope (Zeiss AxioPlan, DE), algal cells were counted in 4 or 6 large squares/rectangles (both in the upper and lower counting grid) for Bürker and Malassez, respectively. The algal cell density in the original sample was then calculated, using the known volume of the squares/rectangles, by the mean number of algal cells counted in the

squares/rectangles, applying the appropriate conversion factor for Bürker and Malassez counting chambers, in order to express the counted cell count as cells·mL^{-1}.

Flow cytometer (FCM) – FCM is a rapid method for the quantitative measurement of individual cells in a fluid widely applied in medical and oceanographic research [34–36]. Recently it resulted to be also an ideal technology for applications to microalgae as they are single cells containing photosynthetic pigments, such as chlorophyll a [37], which could be detected using proper filters.
The analyses were performed using a Flow Attune™ NxT Flow Cytometer (Invitrogen™, Thermo Fisher Scientific, Massachusetts) equipped with an excitation blue laser (wavelength: 488 nm).
Individual cells or particles moving in a thin capillary pass through a laser beam and measurements of light refracted or scattered and fluorescence properties are collected simultaneously. Light scattered was collected in forward scatter (FSC) or side scatter (SSC). FSC, or low-angle light scatter, is defined as scattered light in the direction of the laser path, and its magnitude provides information on the size of the detected events. SSC, or larger angles light scatter, is defined as scattered light at 90° to the laser path, providing information on the granularity and structural complexity inside the detected events. Fluorescence was acquired using a far-red BL3 filter (λ = 675-715 nm). The acquisition was performed at a flow rate set to 100 µL min^{-1} and the events were counted for 1 minute.
The combination of FSC, SSC, and BL3 filters acquired in logarithmic scale, voltage settings (370, 400, 250 V for FSC, SSC and BL3, respectively), together with the establishment of specific gates designed to maximize the separation of different populations of events, allowed the identification of algae population in gate R2, and GRMs in gate R3 (Fig. S2). Moreover, logarithmic gating was employed to effectively exclude small debris particles from the analysis. The obtained data were initially processed using Attune Cytometric NxT v5.3.0 software and subsequently refined with FlowJo: Flow Cytometry Analysis Software for enhanced gates definition.
This approach enabled the effective assessment of the algal cell density, and the GDS in terms of both changes in the number of suspended flakes/particles and their complexity.

- *Algal cell density*: The algal cell densities were recorded from the FCM outcomes and the results expressed as cells·mL^{-1} by applying a conversion factor to the number of detected events in gate R2.

- *Changes in GRMs flakes/particles population:* GRMs populations in gate R3 were monitored over time to provide insight into both the number of GRMs flakes/particles remaining in dispersion and changes in their complexity.
The number of GRMs suspended flakes/particles (GSP) were expressed as:

$$GSP\ (\%) = \frac{n^\circ \text{ of detected events } t_x}{n^\circ \text{ of detected flakes } t_0}$$

The assessment of the GRMs flakes/particles complexity was evaluated by dividing the GRMs population into 21 gates with increasing events complexity on the basis of the side scatter (SSC), a parameter related to the complexity of the detected events (Fig. 4A).

The GRMs flakes/particles complexity (GFC) was reported as the percentage of events in each gate, on the total of all detected events:

$$GFC\ (\%) = \frac{n^\circ \text{ of flakes gate}_x}{n^\circ \text{ of detected flakes}}$$

To monitor the changes of flakes/particles distribution in the gates over the 72-h test period, the amount of events in gates 1 to 3 (*i.e.* low complexity) and 19 to 21 (*i.e.* high complexity) (Fig. 4A) were compared at the beginning and at the end of the test.

2.5. Statistical analyses

The data showed in this study were expressed as mean ± standard deviation.

Statistical analyses were carried out with R (R version 4.3.1, R Core Team (2023). We used generalized least squares (GLS) models ('nmle' R package), setting each parameter measured (*e.g.* algal cell densities, particles decrease, etc.) as the response variable (*e.g.* material, concentration, time, etc.) and their interaction as the explanatory ones. When homogeneity of variance assumption was violated, we used the "varPower()" variance structure (Pinheiro et al. 2016), while we log transformed the response variable when the normality assumption was violated. When the interaction was statistically significant ($p < 0.05$), differences between groups were tested and p-values were adjusted using the Holm correction through the emmeans (Estimated Marginal Means) function in 'emmeans' R package.

3. Results and discussions

The TG 201 is a guideline commonly used for ecotoxicological risk assessment aimed to assess the dose-dependent inhibitory effects of a test substance on algal growth. For its valid application, a stable exposure concentration (maintenance of ± 20 % of initial concentration) of the test substance has to be ensured throughout the 72 h test period [2]. In this work, we tested the FCM as a proper and robust methodology for a suitable evaluation of the algal cell density (the starting point for the calculation of the algal growth inhibition, *i.e.* the TG 201 test endpoint) in the presence of GRMs.

Additionally, FCM has been suggested for the evaluation of the GRMs stability by monitoring the GRMs flakes population throughout the test period.

3.1 Evaluation of the algal cell density

We chose a starting cell densities in the test vessels at time 0 h of $1 \cdot 10^4$ cell mL^{-1} (within the TG 201 specified range of $5 \cdot 10^3$-10^4 cell mL^{-1}), calculated based on the inoculum cell density values. This procedure is prescribed by OECD as it provides the greatest precision [2].

The algal cell densities in CTRL and treated samples were then monitored over the 72-h test period using two different counting chambers, namely Bürker and Malassez, as well as the FCM, to compare which method provides the most accurate outcomes.

Our results showed that, at time 0 h, Bürker and Malassez counting chambers showed values in the range of 4.2-7.5 and 3.8-7.1·10^3 cell mL^{-1}, respectively, underestimating the starting algal densities (Fig. 1A). Instead, FCM provided algal concentrations in the range of 1.0-1.1·10^4 cell mL^{-1}. This discrepancy between counting chambers and FCM decreases as the algal densities increased over the testing period (Fig. 1B-D), with values after 72 h in the range of 7.2-6.6, 6.7-5.8, and 7.7-7.4·10^5 cell mL^{-1}, for FCM, Bürker, and Malassez respectively (Fig. 1D).

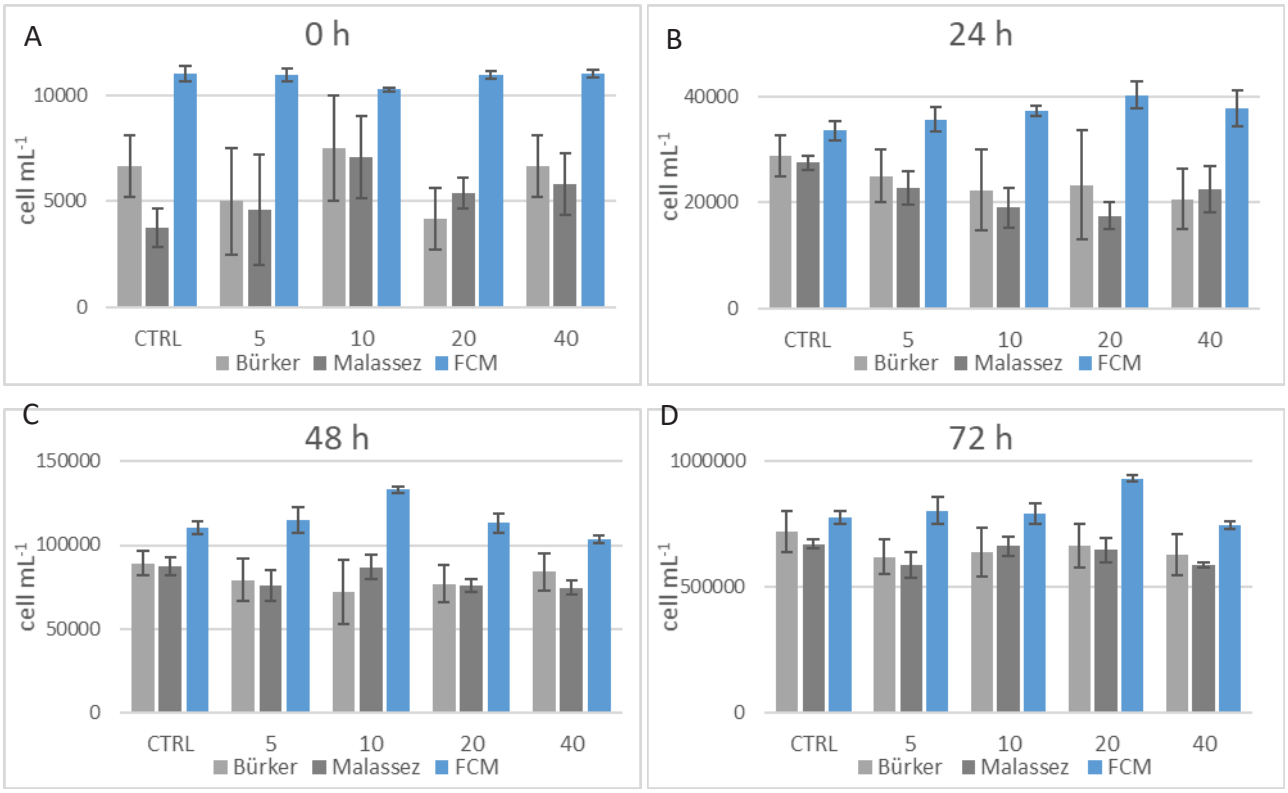

Figure 1. Algal cell densities of *R. subcapitata* exposed to rGO dispersions (0-CTRL, 5, 10, 20, 40 mg mL^{-1}) measured using three different ways: Bürker (light grey) or Malassez (dark grey) counting chambers, and flow cytometer (FCM) (blue) at time (A) 0 h, (B) 24 h, (C) 48 h, (D) 72 h. Data reported as mean ± standard deviation (n= 6).

This trend can be explained by the relatively low sensitivity of both Bürker and Malassez counting chambers at low algal cell densities, *i.e.* at 0 h, probably due to their conversion factor (10^4 and 10^5, respectively) [2,14]. As algal densities increase, the number of counted cells also increase, enhancing the reliability of the results obtained.

On the contrary, FCM has been reported to have sufficient sensitivity to analyze cells at low cell densities, even as low as 100 cells mL^{-1} [38], thus allowing for a reliable evaluation of the algal densities already from the very beginning of the test.

It should be noted that the initial algal cell densities have a strong influence on the estimation of the algal growth inhibition, therefore an error in determining the initial biomass could be one of the most significant sources of error in the evaluation of the algal growth inhibition [14].

Moreover, higher discrepancies in algal cell densities were observed between the two counting chambers and FCM in treated samples compared to the controls (Fig. 1).

This can be caused by the interactions of aggregated rGO particles with algal cells, resulting in the formation of hetero-aggregates (Fig. 2), a well-documented issue in several studies [13,15,39,40]. This phenomenon results in the masking of algal cells during the counting with the two chambers, leading to the observed underestimation of cell densities due to the localization of algal cells inside rGO aggregates.

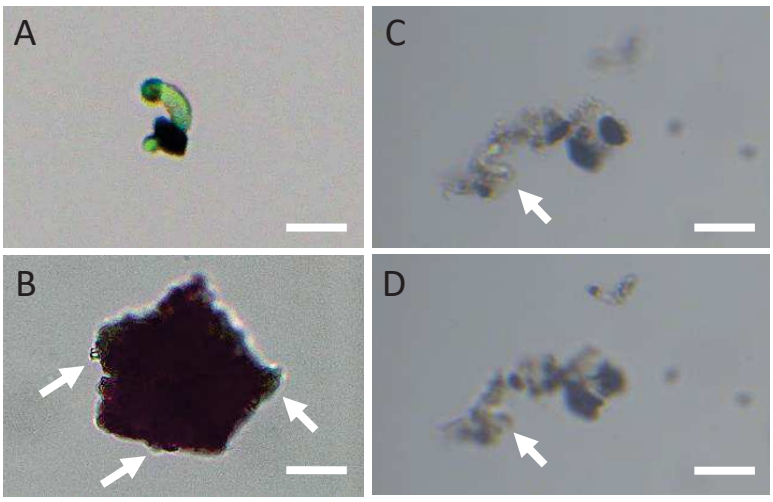

Figure 2. Brightfield images of *Raphidocelis subcapitata* in the presence of rGO showing strong hetero-aggregation. White arrows indicate the masking effect of rGO, underestimating the manual counting of algal cells performed with commonly used counting chambers. In particular (C) and (D) show the same algal cell partially concealed by an rGO aggregate. Scale bars: A = 5 µm; B = 25 µm; C, D = 15 µm.

This issue, can be successfully addressed by employing FCM. Indeed, *Raphidocelis subcapitata*, is a single-celled green microalga containing photosynthetic pigments, such as chlorophyll a [37,41]. When excited by blue light at 488 nm, *i.e.* the excitation laser used in FCM, this pigment fluoresces at 660-700 nm and can be easily detected by the far-red BL3 filter (λ = 675-715 nm) within the designed R2 gate. Therefore, by carefully selecting appropriate filters and adjusting the voltage

settings to maximize the signal-to-noise ratio, FCM allowed to put the algae population in the specifically-designed gate, enabling a fast and reliable evaluation of algal cell densities, even at low algal concentrations and in the presence of GRMs. Furthermore, FCM results also provided higher precision, as evidenced by standard deviation values lower than those obtained by counting chambers (Fig. 1).

Lastly, it is important to highlight that FCM took just one minute to process each sample, saving a significant amount of time compared to manual cell counting with counting chambers. This efficiency allows for a substantial increase in the number of samples that could be analysed.

In conclusion, especially when dealing with low algal concentrations and/or in the presence of GRMs, the use of FCM provided more reliable algal densities, higher precision, and faster results, making it the preferred choice over traditional counting chambers.

3.2 Evaluation of the GDS

As before mentioned, FCM also allowed to monitor the changes over time of the GRMs dispersions.

Focusing on gate R3, specifically designed for the evaluation of the GRMs populations, a decrease in the number of suspended GRMs particles over time was observed (Fig. 3). This finding highlights the stability issues of GRMs and aligns well with data reported in the literature [9,24,25].

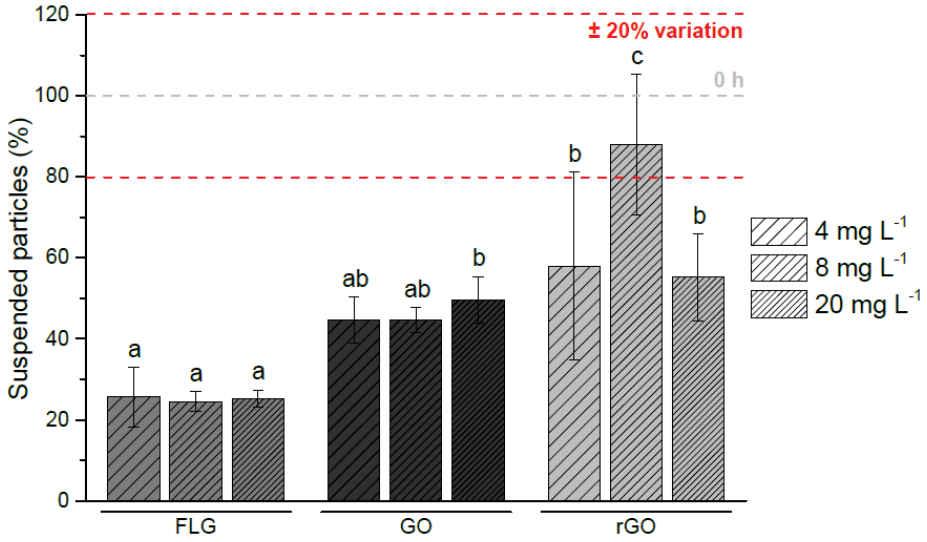

Figure 3. Suspended particles (%) of FLG (grey), GO (dark grey) and rGO (light grey) remaining in dispersion after 72 h of testing at concentrations of 4, 8 and 20 mg L-1 in TG 201 medium under shaking condition (90 r.p.m.). The grey dash line indicates the condition at 0 h (100 % suspended particles). The red dash lines indicate the ± 20% variation in concentration allowed by the TG 201 stability requirement with respect to the initial concentration. Data are reported as mean ± 1 standard deviation (n= 6). Statistically different groups are marked with different letters (GLS analysis, emmeans post-hoc test) (flow cytometry analysis).

Furthermore, FCM provided valuable insight in terms of changes in GMs flakes complexity, reporting a general decrease of flakes/particles distribution in gates with lower SSC (1-3), and instead an increase in gates with higher SSC (19-21) over time (Fig. 4B).

This is a relevant aspect to take into account, as it could strongly affect the GRMs bioavailability [22–25,42], and thus the outcome of the eco-toxicological assessment. These interesting features regarding the particles decrease and change in complexity will be further investigated in the following chapters (2 and 3), posing special attention to the factors that can affect the GDS.

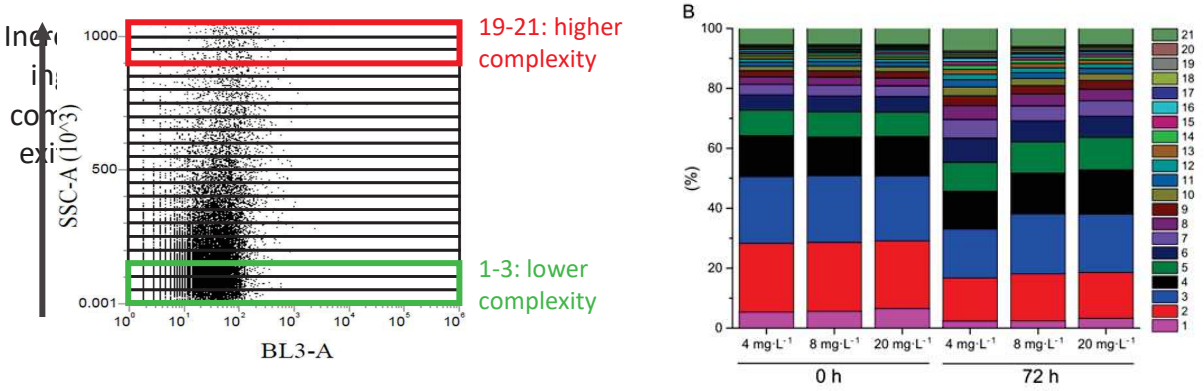

Figure 4. (A) Flow cytometer (FCM) outcome: GRMs population divided in 21 gates determined from the SSC (complexity) range obtained through flow cytometry analysis with increasing complexity from base to top, (B) distribution (%) of flakes/particles in the 21 gates of GO dispersions (4, 8 and 20 mg L^{-1}) at 0 h and after 72 h of testing, showing a decrease of flakes/particles distribution in gates with lower SSC (1-3), and instead an increase in gates with higher SSC (19-21) over time.

Finally, GRMs concentrations ranging from 1.25 to 40 mg L^{-1} were analysed. When plotting the number of detected events in gate R3 at 0 h against the nominal starting concentration, a strong correlation was observed, especially in the case of GO, with R^2 values quite close to 1 (Fig. 5). This indicates a linear relationship between nominal starting concentrations and GRMs particle counts, even at lower GRMs concentrations.

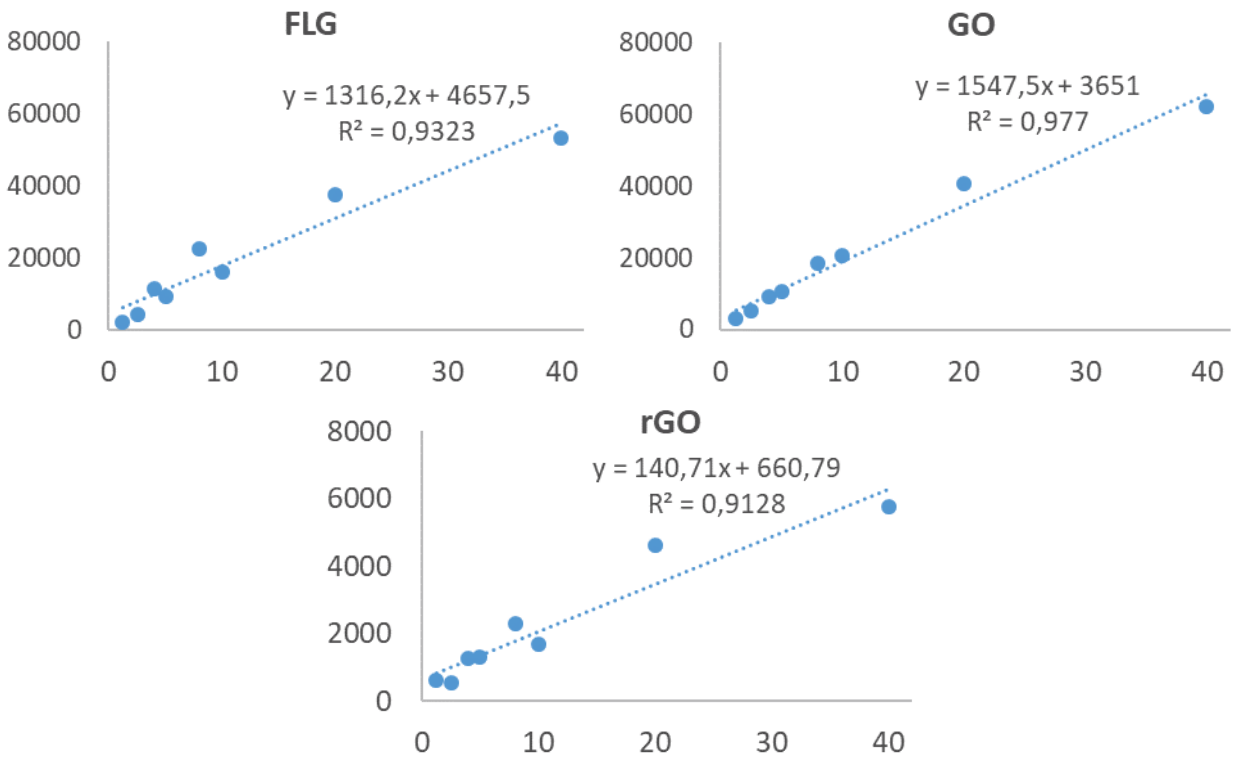

***Figure 5**. Correlation among the nominal concentration with the number of particles of (A) FLG, (B) GO, and (C) rGO counted in the gate R3 (n=6).*

Thus, FCM could be satisfactory used for the assessment of the starting GRMs concentrations. However, due to the observed changes in the GRMs flakes/particles complexity, this method should be cautiously used for assessment of the GRMs concentration throughout the test period, as some biases could be introduced.

4. Conclusions

To date, methodological limitations outlined in existing literature have hindered the possibility to draw conclusions regarding the hazards of certain "difficult to test" substances, such as GRMs.

Therefore, within this paper we reported and described the effort undertaken to establish a suitable methodological approach for TG 201 testing on GRMs, avoiding the biases reported in the literature. Standard methods, *i.e.* Bürker and Malassez counting chambers, were evaluated and compared to FCM as an alternative technique, to improve the accuracy and efficiency of the TG 201.

Our results outlined that cell counting chambers are a time-consuming method that may not accurately reflect algal cell densities at low concentrations and/or in the presence of GRMs. On the contrary, FCM enabled a precise evaluation of algal cell densities already from the very beginning of the test. Additionally, FCM provided valuable insight into GRMs populations, reporting a

general decrease in GRMs particles and an increase in particles complexity over time, suggesting an ongoing aggregation process that will be further investigated in the following chapters.
In conclusion, FCM is suggested as a reliable and time-saving method, ensuring a proper evaluation of both the algal and GRMs populations. Therefore, it should be implemented in the TG 201 testing for the risk assessment associated with GRMs, ensuring improved precision, and high reliability of the results. This is a crucial consideration, as "difficult to test" NMs entering the market, such as GRMs, necessitate information on such endpoints for regulatory compliance. Hence, it is important to have efficient and time-saving testing methods that could be readily employed by testing laboratories and industries.

5. Conflicts of interest

There are no conflicts of interest to declare.

6. Acknowledgements

This work was supported by the Horizon 2020 Graphene Flagship Core 3 (grant agreement no. 881603), which covered the activity of Dr. Fabio Candotto Carniel. Graphene Flagship Core 3 Spearhead project "Safegraph" (grant agreement no. 649953) and University of Trieste DOTTAMBIENTEVITA36 covered the activity of Giada Caorsi.

7. References

1 EC, 2020. Commission Regulation (EU) 2020/878 of 18 June 2020 amending Annex II to Regulation (EC) No 1907/2006 of the European Parliament and of the Council concerning the Registration, Evaluation, Authorisation and Restriction of Chemicals (REACH).

2 OECD, Test No. 201: Freshwater Alga and Cyanobacteria, Growth Inhibition Test, OECD Guidelines for the Testing of Chemicals, Section 2. OECD Publishing, Paris, 2011.

3, OECD, Test No. 202: Daphnia sp. Acute Immobilisation Test, OECD Guidelines for the Testing of Chemicals, Section 2. OECD Publishing, Paris, 2004.

4, OECD, Test No. 203: Fish, Acute Toxicity Test, OECD Guidelines for the Testing of Chemicals, Section 2. OECD Publishing, Paris, 2019.

5 A. B. Hartmann, N. B., F. Von der Kammer, T. Hofmann, M. Baalousha, S. Ottofuelling, *Toxicology*, 2010, 269, 190–197.

6 K. Tiede, M. Hassellöv, E. Breitbarth, Q. Chaudhry and A. B. A. Boxall, *J. Chromatogr. A*, 2009, 1216, 503–509.

7 K. Rasmussen, H. Rauscher, P. Kearns, M. González and J. Riego Sintes, *Regul. Toxicol. Pharmacol.*, 2019, 104, 74–83.

8 OECD, Recommendation of the Council on the Safety Testing and Assessment of Manufactured Nanomaterials.

9 M. Connolly, G. Moles, F. C. Carniel, M. Tretiach, G. Caorsi, E. Flahaut, B. Soula, E. Pinelli, L. Gauthier, F. Mouchet and J. M. Navas, *NanoImpact*, , DOI:10.1016/J.IMPACT.2022.100447.

10 OECD, *Oecd No. 137.*, 2022, 66.

11 P. F. M. Nogueira, D. Nakabayashi and V. Zucolotto, *Aquat. Toxicol.*, 2015, 166, 29–35.

12 J. Zhao, F. Ning, X. Cao, H. Yao, Z. Wang and B. Xing, *Water Res.*, 2020, 176, 115735.

13 T. Malina, E. Maršálková, K. Holá, J. Tuček, M. Scheibe, R. Zbořil and B. Maršálek, *Carbon N. Y.*, 2019, 155, 386–396.

14 N. B. Hartmann, C. Engelbrekt, J. Zhang, J. Ulstrup, K. O. Kusk and A. Baun, *Nanotoxicology*, 2013, 7, 1082–1094.

15 M. Markovic, I. Andelkovic, J. Shuster, L. Janik, A. Kumar, D. Losic and M. J. McLaughlin, *Chemosphere*, 2020, 245, 125640.

16 R. D. Handy, N. Van Den Brink, M. Chappell, M. Mü, R. Behra, M. Dušinská, P. Simpson, J. Ahtiainen, A. N. Jha, J. Seiter, A. Bednar, A. Kennedy, T. F. Fernandes, M. Riediker, R. D. Handy, Á. A. N. Jha, N. Van Den Brink, M. Chappell, Á. J. Seiter, Á. A. Bednar, Á. A. Kennedy, M. Mühling, R. Behra Eawag, M. Dušinská, J. Ahtiainen, T. F. Fernandes and M. Riediker, *Ecotoxicology*, 2012, 21, 933–972.

17 F. Schwab, T. D. Bucheli, L. P. Lukhele, A. Magrez, B. Nowack, L. Sigg and K. Knauer, *Environ. Sci. Technol.*, 2011, 45, 6136–6144.

18 V. Aruoja, H. C. Dubourguier, K. Kasemets and A. Kahru, *Sci. Total Environ.*, 2009, 407, 1461–1468.

19 A. L. Janssen, Karen Van Hoecke, Joris T. K. Quik, Joanna Mankiewicz-Boczek, Karel A.C. De Schamphelaere, Andreas Elsaesser, Paul Van der Meeren, Clifford Barnes, George McKerr, C. Vyvyan Howard, Dik Van De Meent, Konrad Rydzyńsk, Kenneth A. Dawson, Anna Salvat, *Env. Sci Technol*, 2009, 43, 4537–4546.

20 S. M. Hund-Rinke K, *Env. Sci Pollut Res Int*, 2006, 13, 225–232.

21 A. Barrick, A. Châtel, N. Manier, J. Kalman, J. M. Navas and C. Mouneyrac, *Environ. Toxicol. Chem.*, 2019, 38, 2314–2325.

22 Y. Gao, X. Zeng, W. Zhang, L. Zhou, W. Xue, M. Tang and S. Sun, *Sci. Total Environ.*, , DOI:10.1016/J.SCITOTENV.2021.150942.

23 J. Zhao, X. Cao, Z. Wang, Y. Dai and B. Xing, *Water Res.*, 2017, 111, 18–27.

24 V. L. Castro, Z. Clemente, C. Jonsson, M. Silva, J. H. Vallim, A. M. Z. de Medeiros and D. S. T. Martinez, *Environ. Toxicol. Chem.*, 2018, 37, 1998–2012.
25 J. Yin, Z. Dong, Y. Liu, H. Wang, A. Li, Z. Zhuo, W. Feng and W. Fan, *Carbon N. Y.*, 2020, 169, 182–192.
26 J. M. González-Domínguez, V. León, M. I. Lucío, M. Prato and E. Vázquez, *Nat. Protoc.*, 2018, 13, 495–506.
27 W. S. Hummers and R. E. Offeman, *J. Am. Chem. Soc.*, 1958, 80, 1339.
28 B. Lobato, C. Merino, V. Barranco and T. A. Centeno, *RSC Adv.*, 2016, 6, 57514–57520.
29 L. Evariste, L. Lagier, P. Gonzalez, A. Mottier, F. Mouchet, S. Cadarsi, P. Lonchambon, G. Daffe, G. Chimowa, C. Sarrieu, E. Ompraret, A. M. Galibert, C. M. Ghimbeu, E. Pinelli, E. Flahaut and L. Gauthier, *Nanomater. 2019, Vol. 9, Page 584*, 2019, 9, 584.
30 G. Di Mauro, R. Rauti, R. Casani, G. Chimowa, A. M. Galibert, E. Flahaut, G. Cellot and L. Ballerini, *Nanomaterials*, 2021, 11, 2161.
31 L. Krienitz, C. Bock, H. Nozaki and M. Wolf, *J. Phycol.*, 2011, 47, 880–893.
32 https://echa.europa.eu/it/registration-dossier/-/registered-dossier/19786/6/2/6 (acccessed on 18/07/2023)
33 https://echa.europa.eu/it/registration-dossier/-/registered-dossier/26848/6/2/6 (acccessed on 18/07/2023)
34 M. C. Pernice and J. M. Gasol, *Front. Microbiol.*, 2023, 13, 1064112.
35 D. L. Jaye, R. A. Bray, H. M. Gebel, W. A. C. Harris and E. K. Waller, *J. Immunol.*, 2012, 188, 4715–4719.
36 R. Marcos-Fernández, B. Sánchez, L. Ruiz and A. Margolles, *Crit. Rev. Microbiol.*, 2023, 49, 556–577.
37 F. Leliaert, D. R. Smith, H. Moreau, M. D. Herron, H. Verbruggen, C. F. Delwiche and O. De Clerck, *CRC. Crit. Rev. Plant Sci.*, 2012, 31, 1–46.
38 J. L. Stauber, N. M. Franklin and M. S. Adams, *Trends Biotechnol.*, 2002, 20, 141–143.
39 J. Zhao, Y. Li, X. Cao, C. Guo, L. Xu, Z. Wang, J. Feng, H. Yi and B. Xing, *Environ. Sci. Nano*, 2019, 6, 1909–1920.
40 J. Farkas and A. M. Booth, *Nanotoxicology*, 2017, 11, 569–577.
41 D. Franqueira, M. Orosa, E. Torres, C. Herrero and A. Cid, in *Science of the Total Environment*, Elsevier Science Publishers B.V., 2000, vol. 247, pp. 119–126.
42 M. Markovic, A. Kumar, I. Andjelkovic, S. Lath, J. K. Kirby, D. Losic, G. E. Batley and M. J. McLaughlin, *Environ. Toxicol. Chem.*, 2018, 37, 1340–1348.

Supplementary information

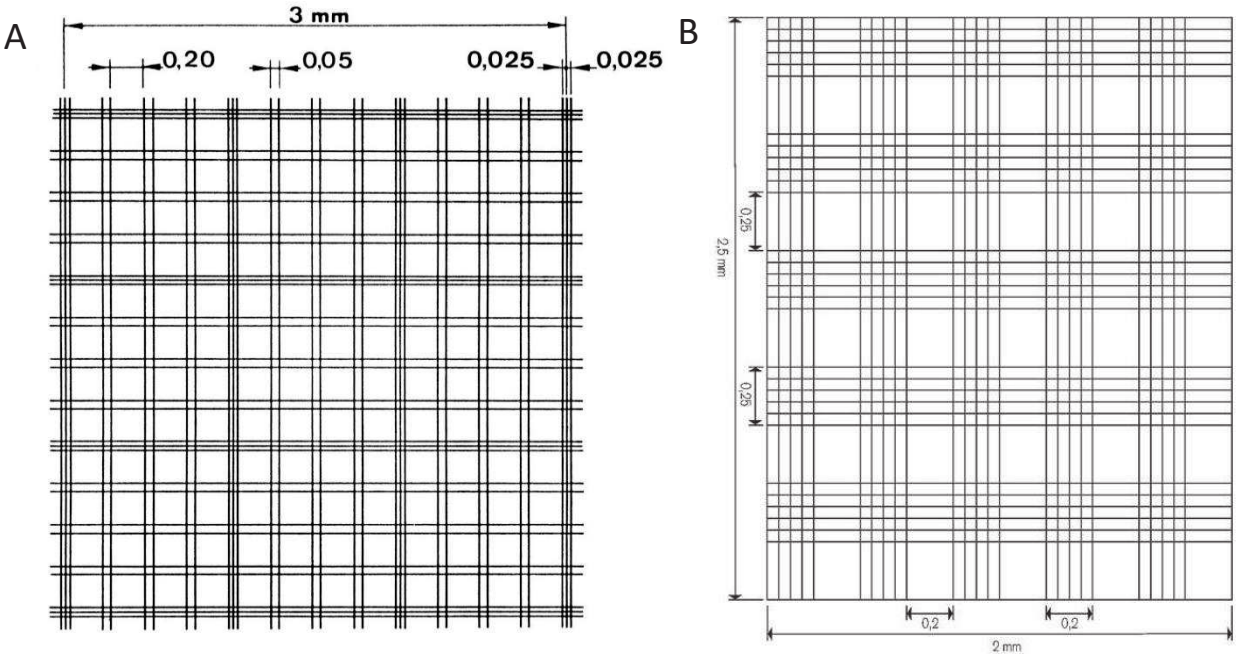

Figure S1. Counting grid of (a) Bürker counting chamber (3 x 3 mm, depth 0.1 mm) presenting 9 large squares (1 x 1 mm) of 0.1 mm^3, each containing 16 smaller squares (0.2 × 0.2 mm) of 0,04 mm^3; (b) Malassez counting chamber (2 x 2.5 mm, depth 0.2 mm) presenting 25 large rectangles (0.25 x 0.20 mm) of 0.01 mm^3, each containing 20 smaller squares (0.05 x 0.05 mm) of $5 \cdot 10^{-4}$ mm^3.

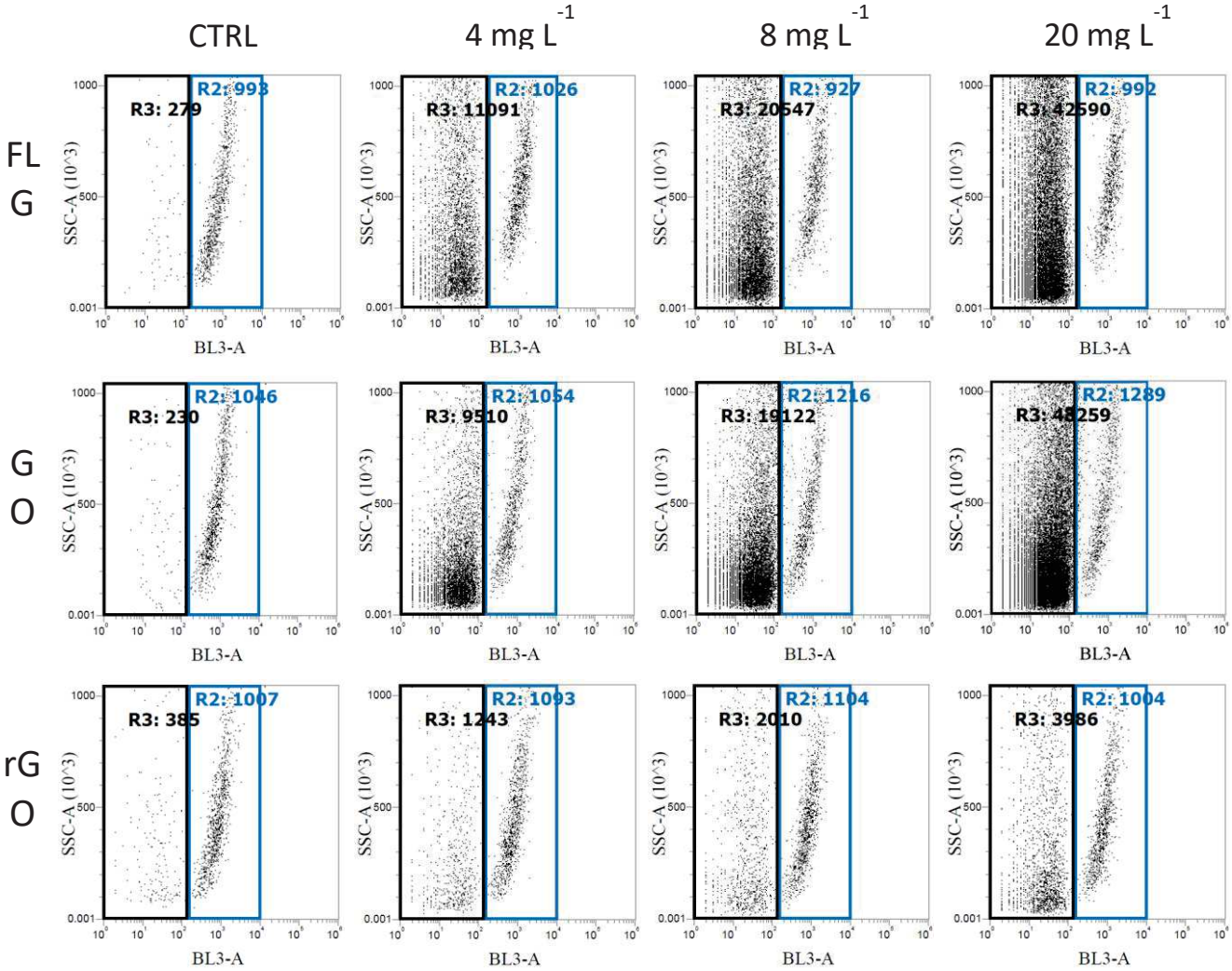

Figure S2. Flow cytometry (FCM) outcomes of algae population (R2, in blue frame) in the presence of FLG, GO and rGO dispersions (R3, in black frame) at 0 (CTRL), 4, 8, and 20 mg L^{-1} in TG 201 medium. The two different gates have been designed to maximize the separation among the two populations. Fluorescence was acquired using a far-red BL3 filter (λ = 675-715 nm). Both SSC and BL3 are reported in logarithmic scale.

Chapter 2

Applicability of the OECD Test Guideline 201 to graphene-related materials: new insights into dispersion stability

Under revision in Environmental Toxicology

Giada Caorsi[1], Fabio Candotto Carniel[1], Morgan Légnani[2], Emmanuel Flahaut[2], Viviana Jehová González [3], Ester Vázquez[3,4], Maurizio Prato[5], Mauro Tretiach[1]

[1] Dipartimento di Scienze della Vita, Università di Trieste, via L. Giorgieri 10, 34127 Trieste, Italia

[2] Centre Interuniversitaire de Recherche et d'Ingénierie des Matériaux - CIRIMAT, Université Paul-Sabatier, 118 Route de Narbonne, Cedex 9, 31062 Toulouse, France

[3] Instituto Regional de Investigación Científica Aplicada (IRICA), Universidad de Castilla-La Mancha, Avda. Camilo José Cela, 13071 Ciudad Real, Spain.

[4] Departamento de Química Inorgánica, Orgánica y Bioquímica, Facultad de Ciencias y Tecnologías Químicas, Universidad de Castilla-La Mancha, Avda. Camilo José Cela 1B, 13071 Ciudad Real, Spain

[5] Dipartimento di Scienze Chimiche e Farmaceutiche, Università di Trieste, via L. Giorgieri 1, 34127 Trieste, Italia

Abstract

Graphene-related materials (GRMs) are used in many innovative applications for their physico-chemical properties. Their possible release could have critical consequences for the environment. According to a European Union regulation, one of the test guidelines (TG) that must be applied to check the environmental hazard of new substances is the TG 201. It was developed for water-soluble substances, whereas GRMs are not: dispersed in aqueous media, they tend to aggregate and settle, changing their bioavailability. This work aims to evaluate the applicability of the TG 201 to GRMs by investigating the stability of GRMs dispersions (GDS) in TG 201 medium, focusing on the stability criterion of TG 201, *i.e.* maintaining ± 20 % of the nominal initial concentration. Based on flow-cytometry, Turbiscan and Utermöhl sedimentation chamber measurements, the following factors were tested: (*i*) different carbon/oxygen ratio of GRMs; (*ii*) particles concentration; (*iii*) application of turbulence; (*iv*) addition of dispersants; (*v*) presence/absence of the target organisms. Strong agglomeration/aggregation and sedimentation phenomena were observed for all materials under all tested conditions, thus the stability criterion of TG 201 was not met. Nevertheless, this can be satisfied by allowing an adequate period of time (approx. 6 hours) for the GRM dispersion to stabilize after its preparation. Only then, a detailed physico-chemical characterization of the suspended material is required, which must be reiterated at the end of the test.

Keywords

Graphene-related materials (GRMs), OECD TG 201, GRMs dispersions stability (GDS), *R. subcapitata*

1. Introduction

In the European Union (EU), all new substances are subject to a specific Regulation, "Registration, Evaluation, Authorisation and Restriction of Chemicals" (REACH) [1], issued by the European Chemicals Agency (ECHA). REACH requires that information on safety of substances for human health and the environment be provided [2]. Annex VII also lists specific Test Guidelines (TG) that must be applied for specific mass intervals of manufactured or imported substances in order to make a reliable statement about their environmental impact. For quantities of 10 to 100 tonnes, the TGs are: TG 201 Freshwater Alga and Cyanobacteria, Growth Inhibition Test [3], TG 202 Daphnia Acute Immobilisation Test [4], TG 203 Fish Acute Toxicity Test [5], and TG 301 Ready Biodegradability [6]. Originally developed by the Organisation for Economic Co-operation and Development (OECD), these TG were specifically designed for water-soluble substances that are expected to remain dissolved in water under the test conditions [3]. Conversely, many nanomaterials (NM) are not water-soluble: once dispersed in aqueous media, they tend to aggregate and settle, altering their bioavailability. This behaviour conflicts with the applicability requirement that the exposure concentration of the target substance must remain within ± 20% of the initial concentration throughout the test period.

As early as 2012, it was noted that the OECD TGs should be implemented to be applicable to NMs [7]. Some OECD experts went further, and suggested that TGs and Guidance Documents (GD) specific for NMs are needed to address the issues related to dissolution rate and dispersion stability (agglomeration/aggregation, settling and transformation) of NMs [8]. Significant efforts have already been made to update some TGs and develop new GDs, especially for aquatic environments [7,9–12].

Among NMs, the graphene family is becoming increasingly important. Graphene is a carbon allotrope consisting of a single layer of carbon atoms arranged in a honeycomb network and exhibiting unique properties [13]. Since its discovery in 2004 [14], numerous other graphene-related materials (GRMs) have been developed: the most representative members are few-layers graphene (FLG), graphene oxide (GO), and reduced GO (rGO) [15]. Thanks to their excellent physico-chemical properties, GRMs are widely used for industrial applications in many different and innovative fields, such as transportation, energy storage and electronics, sports equipment, food, sensors, desalination, biomedicine etc. [16–19].

The growing production and development of GRMs-containing products [20,21] worldwide could lead to unintentional release of GRMs during the manufacturing processes, transportation, use, and disposal of GRMs products [15]. This raises concerns about potential environmental impacts, and thus a number of studies have been conducted to address various aspects of the fate of GRM in the environment, ranging from degradation by [22] to pollination ecology [23–25], and hazard assessment for

bacteria [26–28], animals [29,30], and vascular plants [25,31] (more references in Fadeel et al. [32] and Lin et al. 2024 [33]). Cyanobacteria and algae were also studied, with most of the works following the exposure protocols of TG 201. However, as reviewed by Connolly et al. [34], their results were frequently biased by poor stability of GRM dispersions, GRM hetero-aggregation with the cells of the target organisms, interference with fluorescence readouts, and limitations in renewing media throughout the test period. Furthermore, specific characterisation of the tested GRMs and their transformation during bioassays/treatments were often lacking, although evaluation and reporting of any change in GRM nanoform during the experiment is crucial for the evaluation of their ecotoxicological properties, as the toxicity of GRMs is altered by the formation of agglomerates/aggregates [35–39].
Based on these observations, one might wonder whether TG 201 is indeed applicable to GRMs in order to obtain robust data on their potential environmental impact. Therefore, the aim of this work is to verify the applicability of TG 201 to three GRMs (namely, few-layers graphene, FLG; graphene oxide, GO; reduced GO, rGO), which differ in the carbon to oxygen ratio (C/O), using the unicellular green alga *Raphidocelis subcapitata* as the target organism. The dispersion stability (GDS) of the three GRMs was characterized in aqueous media under the conditions of TG 201 to obtain specific information on dispersibility, agglomeration/aggregation and settling processes. In addition, a comprehensive characterisation of the GRMs throughout the test period was presented. Finally, possible modifications and adaptations to the test protocol TG 201 are discussed in detail, to make the data obtained fully adequate and robust.

2. Materials and methods

2.1 Graphene-related materials preparation and characterization

Few-layers graphene (FLG) was prepared by ball-milling treatment, following the method outlined by González-Domínguez et al. [40]. A mixture of graphite (7.5 mg of SP-1 graphite powder from Bay Carbon, USA) and melamine (22.5 mg of 1,3,5-triazine-2,4,6-triamine from Sigma-Aldrich, DE) was subjected to ball milling at 100 r.p.m. for 30 minutes using a Retsch PM 100 (Retsch Technology, DE) planetary mill. The resulting solid mixture was suspended in 20 mL of MilliQ distilled water and sonicated for 1 minute. The suspension was then dialyzed against water to remove melamine, and the liquid fraction, consisting in suspended graphene sheets (FLG), was allowed to stabilize for 5 days before being separated from the poorly exfoliated graphene precipitate. The FLG dispersion was lyophilized, and when needed, the material was re-suspended in water to achieve a final concentration of 100 mg L^{-1}.

Graphene oxide (GO), provided by Grupo Antolín Ingeniería (Burgos, ES), was prepared by oxidation of carbon nanofibers (GANF Helical-Ribbon Carbon Nanofibres) using the Hummer's method [41,42]. GO was gently ground with a mortar and pestle to homogenize the as-received powder before preparing the dispersion.

Reduced GO (rGO) was produced from Grupo Antolin's GO by thermal reduction at 200 °C by CIRIMAT-CNRS, Tolouse (FR), using a process detailed by Evariste et al. and Di Mauro et al. [43,44]. This process ensured a direct comparison between GO and rGO. Briefly, it was obtained from the partial reduction of GO in H_2 atmosphere (hydrogen flow rate: 5 $L \cdot h^{-1}$) at 200 °C for 2 h, keeping most of the oxygen in the material, with minimal effects on material morphology, lateral size, and numbers of layers. This ensures a direct comparison of rGO with the starting GO material, except for the surface chemistry and wetting properties, modified by the reduction treatment.

The three GRMs were characterized by transmission electron microscopy (TEM), thermogravimetric analysis (TGA), Raman analysis, and quantitative analyses for C, H, N, O, and S.

For TEM, seven µL of the dispersions was drop-cast onto nickel or copper grids (3 mm, 200 or 400 mesh, Lacey carbon film), dried under vacuum and observed with a JEM 2100 high-resolution transmission electron microscope (HR-TEM) (JEOL JEM-2100F, JP) at an accelerating voltage of 200 kV. Images were analyzed with Fiji software to calculate the lateral size distribution.

For TGA, FLG powders were characterized with a TGA Q50 (TA Instruments, USA) under nitrogen atmosphere, while GO and rGO were characterized with a TAG16 (SETARAM) under inert Argon atmosphere, from RT to 1000 °C at 10 °C per minute.

For RAMAN, an aliquot of the GRMs dispersion was drop-cast onto a Si wafer or glas slide and analyzed with an in Via Raman Microscope (Renishaw, UK or Labram HR 800 Yvon Jobin, JP). At least 30 Raman measurements were collected in different locations with a 100x objective at 532 nm and an incident power of 1 mW μm^{-2} (FLG) or at 633 nm and an incident power of 0.8 mW μm^{-2} (GO, rGO). The data were normalized towards G band intensity.

Quantitative elemental analyses for C, H, N, O, and S were carried out with a LECO CHNS-932 elemental analyzer (LECO Corporation, USA) for FLG or with X-ray photoelectron spectroscope with K-Alpha (Thermo Fisher Scientific, USA) system using Al-Kα radiation (hν = 1486.6 eV) from a monochromatized source for GO, and rGO.

2.2. Preparation of the TG 201 medium and GRMs dispersions

The TG 201 medium was prepared according to the annex 3 of the OECD TG 201 [3]. The medium was sterilized in autoclave at 121 °C for 21 minutes, cooled to room temperature, equilibrated with

the atmospheric CO_2 by bubbling with sterile air for 2 h, and then stored in the dark at 4 °C until use.

Preparation of the GRMs working-dispersions – Stock dispersions (100 mg L^{-1}) of sole GRMs and GRMs with dispersants were always prepared fresh before the experiments. GRMs powders were dispersed directly in the TG 201 medium or in the TG 201 medium enriched with dispersants, as appropriate, and sonicated in an ultrasonic bath (Elma Transsonic T 310 Ultrasonic bath, ELMA, DE), FLG for 1 minute, hand-shaking the bottle every 10 seconds [40], while GO and rGO for 30 minutes, hand-shaking the bottle every 10 minutes. Aliquots of the stock dispersions were then diluted to the desired final concentrations to obtain the working GRMs dispersions.

Dispersants and preparation of stock solutions – Three biocompatible dispersants were selected to test their effects on the GDS: carboxymethyl-cellulose (CMC) [45], sodium deoxycholate (SDC) [46], and Suwannee River natural organic matter (SRNOM) [47], as a standard for humic acids (HA) [48]. CMC (ultra-low viscosity) and SDC (BioXtra) were purchased from Sigma-Aldrich (Merck, USA). Stock solutions (100 mg L^{-1}) of both dispersants were prepared dissolving CMC and SDC powders in the TG 201 medium (hereafter referred as TG 201+C and TG 201+S, respectively), and used to prepare GRMs dispersions with a 1:1 concentration ratio.

HA was purchased from the International Humic Substance Society (IHSS, USA). It is commonly added to standard mineral nutrients to simulate the presence of organic carbon found in natural waters [49–52] and is explicitly suggested by OECD guideline 318 and 225. These HA have been thoroughly characterised for their elemental content, acidic functional groups, amino-acidic and carbohydrate composition, amongst all (for details see at: https://humic-substances.org/carbohydrate-compositions-of-ihss-samples/). The HA stock solution (100 mg L^{-1}) was prepared according to the TG 318 [47]: HA powder was dissolved in the TG 201 medium by vigorous magnetic stirring for 24 h, after adjustment of pH to 8 to accelerate the dissolution. The solution was filtered with a 0.22 μm polyether-sulfone (PES) membrane filter (MF-Millipore®, DE) to remove any undissolved material, and the pH of the solution checked again. The TG 201 medium containing HA (hereafter referred to as TG 201+H) was used to prepare the GRMs dispersions with a final HA concentration of 20 mg L^{-1}. This HA concentration was chosen accordingly to literature, as it is an environmentally-relevant concentration in freshwater environments [49–52].

2.3. Evaluation of the GRMS dispersion stability (GDS)

The GDS of the target materials during the TG 201 testing was assessed considering the following factors: (*i*) the particles composition and (ii) concentration; (*iii*) the application of turbulence; (*iv*) the addition of dispersants and (*v*) the presence of the target organism.

Over the 72 h test period, the GDS was evaluated by: (1) visual inspection; (2) flow cytometry (FCM); (3) transmittance characterization through Turbiscan; (4) mass quantification of GRMs sedimentation in Utermöhl chamber.

Visual inspection – Flasks and Utermöhl sedimentation chambers were visually inspected, and photographs and/or videos were taken at each time point to monitor the behaviour of GRMs dispersion within the testing period.

FCM analyses – The GRMs agglomeration/aggregation and sedimentation was analysed with a Flow Attune™ NxT Flow Cytometer (Invitrogen™, Thermo Fisher Scientific, USA) equipped with an excitation blue laser (wavelength: 488 nm). The acquisition was performed at a flow rate set to 100 µL min^{-1} and the events were counted for 1 minute. Light scattered was collected in forward scatter (FSC), *i.e*. scattered light in the direction of the laser path, providing information on the size of the detected events, and side scatter (SSC), *i.e*. scattered light at 90° to the laser path providing information on the events granularity. Fluorescence was acquired using a far red BL3 filter (λ = 675-715 nm). The combination of FSC, SSC and BL3 filter allows the detection and separation of different populations of events, *e.g*. GRMs vs algae. The data were analysed with Attune Cytometric NxT v5.3.0 software and subsequently with FlowJo: Flow Cytometry Analysis software for further gates definition. Prior to the analyses, the calibration of the instrument was verified using the ApogeeMix beads.

Turbiscan analyses – The GRMs dispersion behaviour in the exposure media was analyzed by monitoring the changes in turbidity over time using a Turbiscan™ LAB Stability Analyzer (Formulaction SA, Toulouse, FR). The GRMs dispersions (20 mL) were prepared as described above (see section 2.2), poured into Turbiscan flasks and placed in the measurement chamber at room temperature. Transmittance measurements were taken at 0, 3, 6, 24, 48, 72 h (the time intervals had been determined in a series of preliminary stability tests) with 1 scan per minute for 5 minutes by measuring during each scan the transmittance of the GRMs dispersion. Transmission and backscattering of the near infrared light source (880 nm) were measured every 40 µm of the sample/vial height. For the analyses, mean of data from 10 to 30 mm were considered, to avoid biases of measurements due to meniscus and bottom of the flasks (Fig. S1).

Mass quantification of GRMs sedimentation in Utermöhl chamber – To quantify the GRMs mass settled during the TG 201 testing, the Utermöhl sedimentation chamber (USC) (Thalassia, Trieste, IT) was used. This device is normally used for phyto- and micro-zooplankton quantification and identification [53]. It is made of 2 separated parts: a cylindrical sedimentation chamber of 4 × 25 (internal diameter) mm, capacity 2 mL, carved in the thickness of a 42 × 42 × 5 mm plaquette of plexiglass, which is positioned at the bottom of the upper column, USC (Fig. S4), a cylinder made

in plexiglass, 97 mm high, with internal diameter of 25 mm. The USC is filled up to the brim with 50 mL of dispersion and covered with a glass lid. After the sedimentation period, the upper column is shifted laterally onto a solid plaquette of the same height of the sedimentation chamber. The settled materials within the sedimentation chamber are carefully recovered and transferred into handcrafted aluminium foil vessels, previously weighed. Then, they are placed in the oven at 50 °C to dry out, providing a mass-based quantification of the settled GRMs. From this, the resulting concentration of GRMs remaining in dispersion in the upper part of the chamber is calculated by subtracting the amount of settled material to the initial quantity.

2.4. Factors affecting the GRMS dispersion stability (GDS)

2.4.1. Particle composition and concentration: TG 201 standard protocol

The TG 201 test was performed as described in the guideline: 25 mL of the GRMs dispersions at 0 (CTRL), 4, 8 and 20 mg L^{-1} were left for 72 h in 50 mL Erlenmeyer's flasks under orbital shaking at 90 r.p.m. (M301-OR orbital shaker, MPM Instruments, IT) in the presence or absence (blanks) of the target alga *R. subcapitata*. Every 24 h, flasks were visually inspected, and photographs were taken. At the same time-points, the changes in GRMs flakes/particles population and eventually in algae population were monitored by flow cytometry in blanks (without algae), CTRL and treated samples.

The algal cell densities were measured daily to calculate the algal growth rate (AGR); then, the algal growth inhibition (%) (AGI), *i.e.* the TG 201 endpoint, was calculated by dividing the specific growth rates of the treatments by the average growth rate of the controls, according to the TG 201 instructions. Negative AGI values mean an algal growth stimulation.

Changes in the GRMs population were expressed as per cent GRMs flakes/particles decrease (GFD):

$$\text{GFD (\%)} = -\frac{\text{n. of detected events } t_x - \text{n. of detected events } t_0}{\text{n. of detected flakes } t_0}$$

The assessment of the GRMs flakes/particles complexity was evaluated by dividing the GRMs population in 21 gates with increasing complexity of events on the basis of the side scatter (SSC), a parameter related to the complexity of the detected events (Fig. S2).

The GRMs flakes/particles complexity (GFC) in the TG 201 medium at 0 and 72 h was expressed as the percentage of events in each gate, on the total of all detected events:

$$\text{GFC (\%)} = \frac{\text{n. of flakes gate}_x}{\text{n. of detected flakes}}$$

To monitor the changes of flakes/particles distribution in the gates over the 72 h test period, the amount of events in gates 1 to 3 (*i.e.* low complexity) and 19 to 21 (*i.e.* high complexity) were compared at 0 and 72 h.

The changes of the turbidity of the dispersions in blank samples at minimum and maximum GRMs concentration (4 and 20 mg L^{-1}) were analysed as changes of transmittance by Turbiscan at 0, 3, 6, 24, 48, 72 h to describe the kinetic of the sedimentation phenomena. The time-points have been chosen on the basis of a sedimentation curve made by following the changes in transmittance of GRMs dispersions (4, 8, and 20 mg L^{-1}) continuously over the 72 h test period under static condition (Fig. S3).

The variation (Δ) in transmittance (T) of GRMs dispersions (G) over time (t = 0, 3, 6, 24 and 72 h) were expressed as:

$$\Delta T_{G} = \frac{(T_G\ t_x - T_G\ t_0)}{(T_{TG\,201} - T_G\ t_0)}$$

where:

$T_G\ t_x$ = transmittance of GRMs dispersions at time x

$T_{TG\,201}$ = transmittance of blank, *i.e.* TG 201 medium alone

Variations of dispersion transmittance during the test period are related to the level of GRMs stability: greater transmittance variation corresponds to lower stability, while lower transmittance variation means higher stability.

2.4.2. Alternative methods to apply turbulence

The following methods to generate turbulence inside the dispersions were tested to increase the GDS: orbital shaking at 150 r.p.m. (M301-OR orbital shaker, MPM Instruments, IT), magnetic stirring at 300 r.p.m. (20 mm magnet, VMS-D magnetic stirrer, VWR, UK), bubbling (8-channel bubbling system of a Multi-Cultivator MC 1000-OD, Photon Systems Instruments, CZ). The turbulence methods were applied to GRMs dispersions (25 mL) at 4, 8, 20 mg L^{-1} into Erlenmeyer's flasks for 6 h. Visual inspection and FCM analyses were conducted to monitor the GRMs populations. The results obtained using different turbulence methods were compared to static conditions. Turbiscan analyses were performed for the GRMs dispersions (4, 8, 20 mg L^{-1}) under static conditions to observe the GRMs sedimentation curve over the 72 h test period (Fig. S3).

2.4.3. Addition of dispersants

The dispersants CMC, SDC, and HA were tested to increase the GDS. The effects of these dispersants on the GDS were evaluated by monitoring the changes in transmittance of the GRMs dispersions at 4 and 20 mg L^{-1} over the 72 h by Turbiscan analysis both under static and shaking conditions.

The variation (Δ) in transmittance (T) of GRMs dispersions (G) + dispersants (d) over time (t = 0, 3, 6, 24 and 72 h) were expressed as:

$$\Delta T_{G+d} = \frac{(T_{G+d\ t_x} - T_{G+d\ t_0})}{(T_{TG201+d} - T_{G+d\ t_0})}$$

The effects of dispersants (E_d) on the transmittance of GRMs dispersions over time were expressed as:

$$E_d = \frac{(\Delta T_{G+d} - \Delta T_G)}{\Delta T_G}$$

Potential negative effects of the three dispersants on the algae were verified applying the TG 201 and using a 20 mg L^{-1} concentration of dispersants, *i.e.*, the highest used, to test the worst-case scenario.

The dispersant ensuring the best GDS and no toxic effects on algae was used to verify its suitability for the application of TG 201. According to the TG 201 protocol, the test was conducted subjecting the target alga to six GRMs concentrations arranged in a geometric series with a factor of 2: 1.25, 2.5, 5, 10, 20, 40 mg L^{-1}. The test was performed in Erlenmeyer's flasks containing 25 mL of the GRMs dispersions in TG 201 enriched with the best dispersant (20 mg L^{-1}), under static condition. Visual inspection and FCM analyses were conducted to monitor both the populations of GRMs flakes and algae.

2.4.4. Presence of the algae

Cultures of Raphidocelis subcapitata

The test organism was the unicellular freshwater green alga *Raphidocelis subcapitata* (Korshikov) [54] (also known as *Pseudokirchneriella subcapitata* or *Selenastrum capricornutum*), strain 61.81, purchased from the Collection of Algal Cultures (SAG, University of Göttingen, Germany). Axenic algal stock cultures were cultivated in 100 mL of OECD TG 201 standard medium in 250 mL Erlenmeyer's flasks and placed in a thermostatic chamber at 20 ± 1 °C, 65 ± 5 µmol photons m^{-2} s^{-1} under a light : dark cycle of 14 : 10 h. Prior to the beginning of each test, an inoculum culture in the TG 201 standard medium was prepared and left at 21 ± 1 °C under continuous illumination of 75

μmol photons m^{-2} s^{-1}, to adapt the algae to the test conditions. After approximately 3 days, when in exponentially growth phase, the algae were harvested for the experiment inoculum.

Exposure of the algae to the treatments

The algae cultures in exponentially growing phase have been exposed to the treatment in sterile 50 mL conical flasks containing 25 mL of medium at a start density of $1 \cdot 10^4$ cells mL^{-1}.

The effects of GRMs and/or dispersants were investigated by subjecting the algae to chronic exposure for 72 h. The test exposures were placed in a thermostatic chamber at 21 ± 1 °C under continuous illumination of 75 μmol photons m^{-2} s^{-1} from below provided by daylight lamps (Neon Gro-Lux F18W/T8, Sylvania, DE). An immersion spherical light probe (US-SQS/L Spherical Submersible Micro Quantum Sensor, WALZ, DE) has been used for the light measurement inside the flasks. All flasks were shaken 3 times per day to resuspend any settled cell and repositioned daily on the transparent plate to minimize any possible spatial difference in illumination and temperature. Flasks exposed under shaking condition were placed on an orbital shaker (M301-OR, MPM Instruments, IT) at 90 r.p.m., and additionally shaken by hand three times per day to resuspend any settled cells, and then returned to the orbital shaker.

Exposure concentrations were in a range from 0 (CTRL) to 40 mg L^{-1} of GRMs in the presence or absence of dispersants. Each concentration was done in six replicates and the tests were repeated at least twice.

To validate the experimental set-up, a test with the reference substance $K_2Cr_2O_7$ (potassium dichromate, Sigma Aldrich, USA) was performed every 6 months, as suggested by the TG 201 [3].

2.5. Quantification of the sedimentation

50 mL of 40 mg L^{-1} GRMs dispersions were poured in the USC and left at laboratory conditions for up to 78 h. Sedimentation of all the materials was evaluated after 6, 72, and 72+6 h, for GO also after 6 weeks (Fig. S15). The settled GRMs were quantified under static condition in absence or presence of the algae (to determine if the growth of algae could affect the sedimentation) by weighing GRMs settled at the bottom of the chamber (see 2.3) and by FCM measurements of the GRMs dispersions collected in the sedimentation chamber and in the middle of the upper column. The effect of the algal weight was also considered by testing the sole TG 201 medium with algae. Following the 72-h sedimentation in the USC, no influence of settled algal biomass was observed (0.217 ± 0.006 mg), consistent with the expected cell dry weight of 2-3 x 10^{-8} mg/cell (c. 4×10^7 cells/L to achieve 1 mg/L) as reported in the OECD TG 201 [3].

The quantification of GRMs sedimentation was calculated as:

$$\text{GRMs sedimentation} = \frac{\text{settled GRMs } t_x}{\text{GRMs in the chamber}}$$

$$\text{Concentration of GRMs remaining in dispersion} = \frac{(\text{GRMs in the chamber} - \text{settled GRMs } t_x)}{V_{USC}}$$

where:

GRMs in the chamber = total amount of GRMs present in the chamber (2 mg)

V_{USC} = 50 mL

To characterize both settled and suspended GRMs fraction, Raman and TEM analyses have been performed. Concentrations lower than 40 mg L^{-1} GRMs did not ensure reliable results due to scale limitations.

2.6. Statistical analyses

The data showed in this study were expressed as mean ± standard deviation, unless otherwise specified.

Statistical analyses were carried out with R (R version 4.3.1, R Core Team (2023)). We used generalized least squares (GLS) models ('nmle' R package), setting each parameter measured (*e.g.* particles decrease, algal growth inhibition, sedimentation, etc.) as the response variable (*e.g.* material, concentration, time etc.) and their interaction as the explanatory ones. When homogeneity of variance assumption was violated, we used the "varPower()" variance structure [55], while we log transformed the response variable when the normality assumption was violated. When the interaction was statistically significant ($p < 0.05$), differences between groups were tested and p-values were adjusted using the Holm correction through the emmeans (Estimated Marginal Means) function in 'emmeans' R package.

3. Results and discussions

3.1. Characterization of the tested GRMs

The physico-chemical characteristics of the three tested materials are detailed in Fig. S5 and Table S1.

The FLG flakes had an average lateral size of 510 ± 423 nm (Tab. S1), and had a high degree of purity, with 93.58 ± 0.31 % C, 0.55 ± 0.01 % H, 0.50 ± 0.01 % N (wt % melamine (% N) = 0.75 %), 4.82 ± 0.08 % O, and 0.55 ± 0.01 % S. This was confirmed also by TGA: FLG displayed a

weight loss of c. 10% (Fig. S5 E), an expected result when the analysis is conducted in an inert atmosphere [40]. The weight loss corresponds to the melamine content and a low concentration of oxygen groups, created during the ball-milling treatment [40]. The Raman spectrum of FLG was characterized by one intense peak at ~1580 cm^{-1}, the G band, and two additional less intense peaks at ~1345 and ~2700 cm^{-1}, the D and 2D bands respectively (Fig. S5 D). The ratio between the intensity (I) of D and G bands, *i.e.* an indicator of the presence of defects on the graphene lattice, was I(D)/I(G) = 0.36, confirming a low level of defects, usually attributed to the edges of the micrometer sheets [56]. Furthermore, the I(2D)/I(G) = 0.51 is consistent with values (< 1) reported in the literature for this material [57,58].

The GO and rGO flakes had an average lateral size of 200 to 8000 nm (Tab. S1). TGA analyses showed a higher mass loss for GO (- 55 wt. %) compared to rGO (- 40 wt. %), as expected due to the thermal reduction process applied to produce rGO (loss of carbon and oxygen) (Fig. S5 E). Elemental composition was obtained from XPS analysis (data are expressed after conversion of at. % to wt. %) and showed average values of 61.7 wt. % C, 36.4 wt. % O, 0.4 wt. % N, and 1.5 wt. % S for GO, and 78.4 wt. % C, 21.15 wt. % O, and 0.45 wt. % S for rGO. Raman spectroscopy revealed the two characteristic D and G bands of GO and rGO, with their peaks located at ~1350 and ~1600 cm^{-1}, respectively, with higher value of D band for rGO (ID/IG intensity ratio strongly increased from 1.1 to 1.7). X-ray diffraction (XRD) analysis (Scherrer equation) revealed flakes with a thickness in a range of 1-5 layers (Tab. S1). It also revealed that the expected initial (002 line) peak at 11.07 ° in GO [59] is absent in rGO, but also that the reduction at 200 °C was not complete, as shown by the shape and intensity of the (002) line of rGO, which peaked at 24.7 ° instead of 26.4 ° as expected in graphite (Fig. S5 F) (see ICDS N° 01-075-1621).

3.2. Evaluation of the GDS

3.2.1. Particle composition and concentration: TG 201 standard protocol

In order to evaluate the effects of particle composition and concentration, the GDS was tested under shaking conditions (90 r.p.m.), as recommended in the TG 201. Visual inspection showed that a strong aggregation and sedimentation occurred in all samples even though clear differences were observed among materials (Fig. S6). FLG dispersions showed loose agglomerates at the bottom of the flasks, easily broken by pipetting/shaking. Differently, GO dispersions seemed the most stable, exhibiting a homogeneous, concentration-dependent (darker) coloration, with less visible aggregates than FLG. rGO showed numerous stable aggregates, unbreakable even when pipetting, and already present at the bottom of the flasks during the preparation of dispersions.

FCM measurements showed that the number of events (each event representing a flake/particle) in FLG and GO dispersions progressively decreased over time in respect to the initial number but to different extents: FLG events decreased of c. 65 %, and 75 % at all the concentrations after 24 and 72 h, respectively (Fig. S8 and Fig. 1), while GO events decreased from c. 35 % after 24 h and up to 55 % after 72 h (Fig. S8 and Fig. 1). rGO dispersions showed high variability with significant changes among concentrations (Fig. S8 and Fig. 1) and, in agreement with visual inspections, the number of events in dispersion measured by FCM was much lower than the one detected for GO already from time 0 h, suggesting that rGO was much less dispersible (Fig. S9).

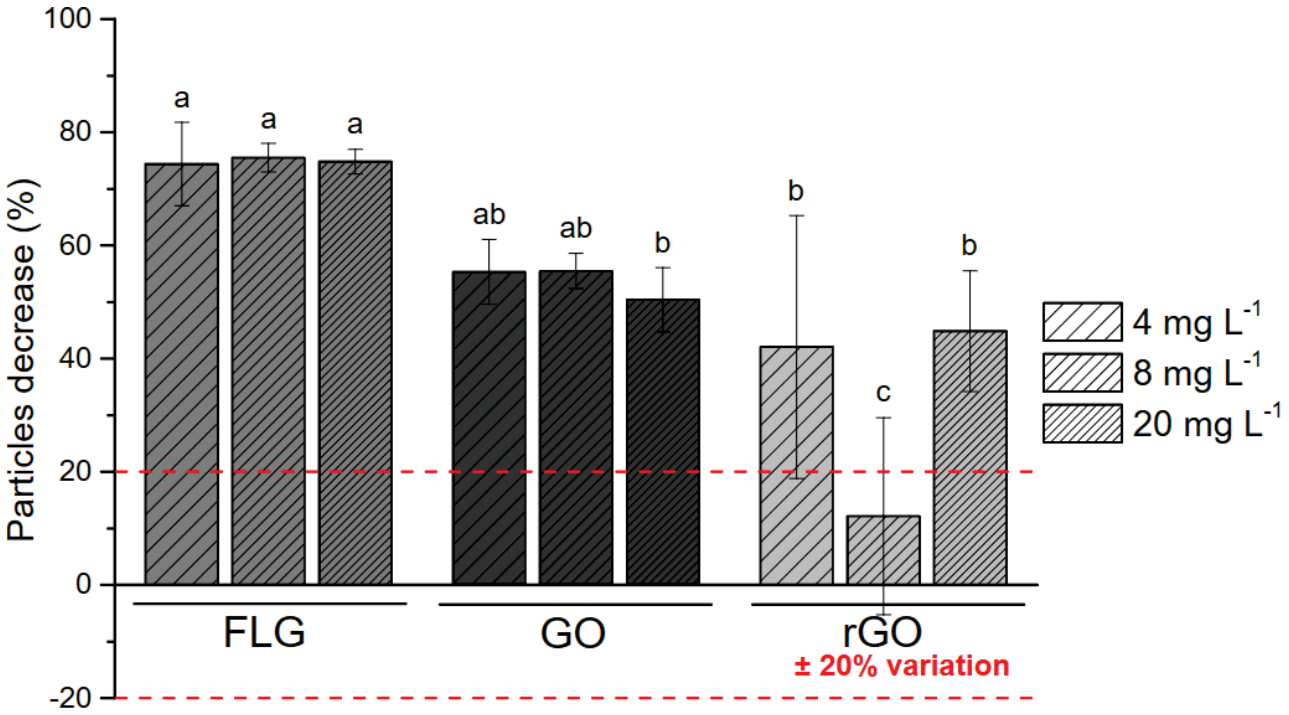

Figure 1. Per cent decrease of FLG (grey), GO (dark grey) and rGO (light grey) particles observed after 72 h of testing at concentrations of 4, 8 and 20 mg L^{-1} in TG 201 medium under shaking condition (90 r.p.m.). The red dash lines indicate the ± 20% variation in concentration allowed by the TG 201 stability requirement in respect to the initial concentration. Data are reported as mean ± 1 standard deviation (n= 6). Statistically different groups are marked with different letters (GLS analysis, emmeans post-hoc test) (flow cytometry analysis).

The FCM measurements also provided an important insight on the changes occurring to the morphology of the flakes/particles during the testing period. The scatterplots showed that after 72 h the cloud of events was denser in gates with high SSC values than at 0 h, indicative of a change in flakes/particle morphology towards higher complexity (Fig. S10). Over the 72 h, there was a general decrease in the number of flakes/particles included in gates with lower SSC (1-3) and a corresponding increase in gates with higher SSC (19-21). The relative abundance of flakes/particles in gates from 1 to 3 (lower complexity) decreased from 18.67 % to 6.64 %, from 50.79 % to 38.07 % and from 6.43 % to 2.61 % for FLG, GO and rGO, respectively (20 mg L^{-1} in Fig. 2, 4-8 mg L^{-1}

in Fig. S10). Instead, the relative abundance of events in gates from 19 to 21 (higher complexity) increased from 38.03 % to 55.14 %, from 6.24 % to 6.52 % and from 45.97 % to 54.12 % for FLG, GO and rGO, respectively (20 mg L^{-1} in Fig. 2, 4-8 mg L^{-1} in Fig. S10). Therefore, the decrease in the number together with the increased complexity suggests that there was an aggregative process throughout the 72 h test period even for the apparently more stable GO dispersions. This phenomenon might have a strong effect on the GRMs bioavailability [35–39]. Indeed, the size of flakes/particles is a strong determinant of their interactions with cells and hence it can influence their overall toxicity [60–62].

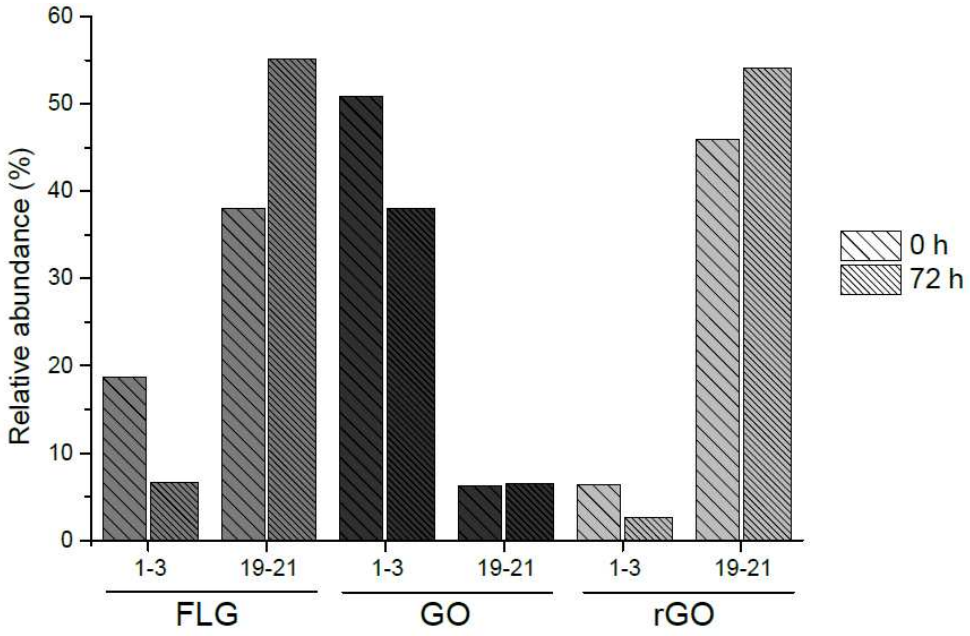

Figure 2. Percentage (%) of FLG (grey), GO (dark grey) and rGO (light grey) particles (20 mg L^{-1} in TG 201 dispersion) in low- (1-3) and high-complexity (19-21) gates determined from the analysis of the side scatter parameter obtained through flow cytometry analysis at 0 h and after 72 h of testing under shaking condition (90 r.p.m.).

Turbiscan measurements showed a variation in the transmittance of GRMs dispersions over the 72 h and the trend was similar between the tested concentrations (*i.e.* 4 and 20 mg L^{-1}, lower and upper ones) (Fig. S12 and Fig. 3). The variation was stronger in the first 6 h for both FLG and GO, then it progressively slowed down during the following hours reaching a plateau after 72 h.

The transmittance of the dispersions increased by 52 % and 85 % for FLG, and by 32 % and 49 % for GO after 6 and 72 h, respectively, compared to the initial values. Differently, rGO dispersions exhibited the highest transmittance already from time 0 h showing a very small variation in transmittance over time, with values similar to those of blank (74.6 vs. 79.6) (Fig. 3).

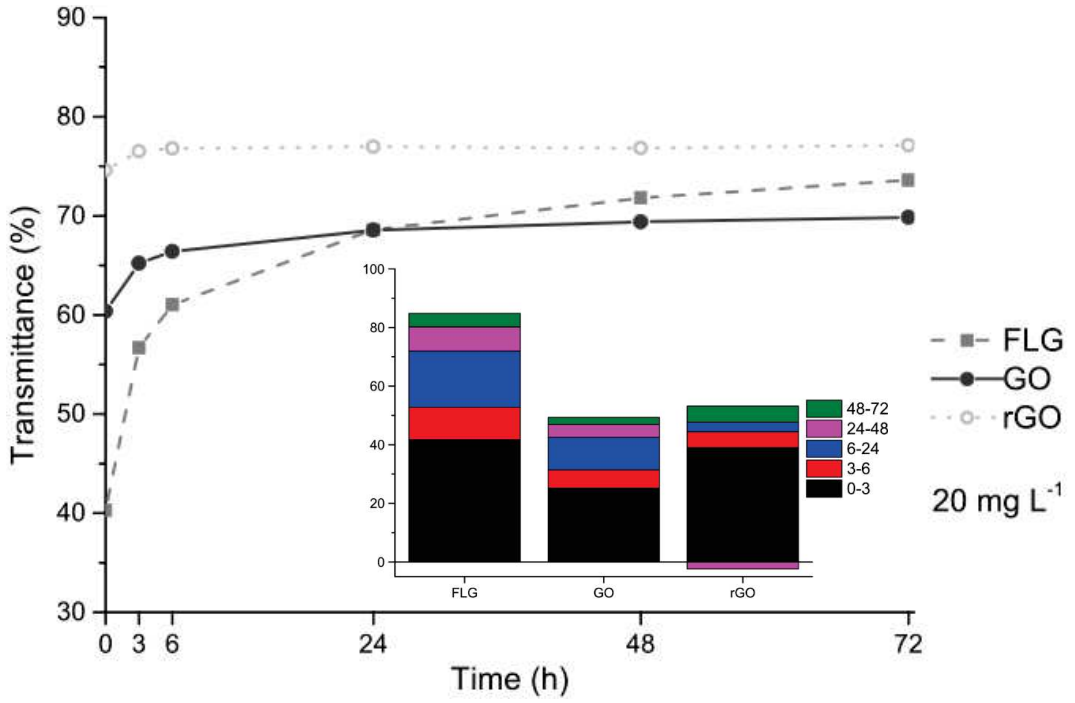

Figure 3. Per cent transmittance variation of FLG, GO and rGO dispersions (20 mg L^{-1} in TG 201 medium) under shaking condition (90 r.p.m.) observed at 0, 3, 6, 24, 48 and 72 h of testing. Insert: stacked histogram representing the percentage of per cent transmittance variation occurring after 3, 6, 24, 48, and 72 h (Turbiscan analysis).

In good agreement with visual inspections and the FCM analyses, these transmittance variations reflect the decrease in density of GRMs flakes in the medium over time as a consequence of aggregation/agglomeration followed by sedimentation processes. Importantly, the particle composition (*i.e.* FLG, GO and rGO), was the main factor affecting these processes, being predominant over the concentration, particularly for FLG and GO (Tab. S2A). FLG, being made by more than 90% of C (Tab. 1), lacks oxygen functional groups, making it a particularly hydrophobic material [63,64]. Differently, the surface of GO consists of hydrophobic islands presenting hydrophilic regions made by numerous oxygen functional groups (*i.e.* carbonyl, hydroxyl, and epoxide) and having a high negative charge density [65]. These characteristics ensure an improved hydrophilicity [15] and thus a better GDS than FLG in aqueous solutions [65]. In the case of GO, the formation of loose agglomerates and their consequent sedimentation depends on the presence of divalent cations in the medium, which can bind to negatively charged sites of GO (*e.g.*, deprotonated carboxylic and hydroxyl groups) forming ionic bonds between flakes [37]. Instead, the apparent stability of rGO is misleading, only indicating that the small fraction that remained in dispersion was rather stable, while most of the flakes/particles either agglomerate/aggregate and settled down very quickly or they formed aggregates very difficult to disperse. The poor dispersibility and stability of rGO in aqueous media is due to the high level of aggregation of the powder used to prepare the dispersion,

and the pronounced hydrophobicity, caused by the significant decrease of the oxygen functional groups after reduction of GO (O content of 16.81 % vs 30.37 % for rGO and GO, respectively) [15].

To sum up, performing the standard TG 201 protocol revealed that during testing the GRMs population undergoes change in the density and complexity of flakes/particles over time due to agglomeration/aggregation and sedimentation phenomena. Importantly, the majority of FLG and GO flakes/particles settled down in the first 6 h even though to different extents, with GO being the most stable. Including the poor dispersibility of rGO, these results suggest that the main applicability requirement of the TG 201 might not be met depending on the GRMs under analysis.

3.3. Modification to the standard TG 201 protocol to increase the GDS

3.3.1. Alternative methods to apply turbulence

To increase the GDS, alternative methods to apply turbulence, namely orbital shaking at 150 r.p.m., bubbling, and magnetic stirring, have been tested and compared to static condition. However, already from visual inspection, it was clear that with the alternative methods there was an increase of the settled materials in respect to the static condition (*e.g.* Fig. S6 vs. Fig. S7).

FCM analysis showed that FLG events decreased by 65.9 % under shaking (150 r.p.m.), 61.4 % for bubbling, 28.9 % for magnetic stirring, and 26.4 % for static in respect to time 0 h. GO events decreased by 22.0 % under shaking (150 r.p.m.), 54.8 % for bubbling, 1.7 % for magnetic stirring and 1.6 % under static. rGO showed a decrease in the number of events by 32.2% under shaking (150 r.p.m.), 5.1 % for bubbling, 34.9 % for magnetic stirring and 37.9 % under static (Fig. S11). In this case as well, FLG exhibited the strongest decrease in the number of flakes/particles remaining in suspension.

Shaking is commonly being used to keep colloidal suspension homogeneous in the medium. However, here we show that this is not always the case, especially when applying it to GRMs, and despite increasing the intensity, no significant improvements were obtained. Despite providing good results, the application of magnetic stirring might lead to some technical issues such as possible algal damage induced by the spinning anchor, but, more importantly, the heating of the medium due to the running magnetic stirrer.

Physical factors, like the water flow type and intensity, play a dominant role on the NPs stability [66,67]. Turbulence conditions can lead to increased probability of flakes collision, forming weak bonds between surface charges of the particle and, consequently, increasing formation of agglomerates and sedimentation. Thus, it is an important factor to consider, especially when dealing with GRMs, as it can lead to a detrimental effect on the GDS. The FCM results revealed that (*i*)

none of the tested turbulence methods helped to increase GDS significantly and without drawbacks, and (*ii*) the static condition ensured values of dispersed flakes/particles within (or close to) the stability threshold throughout the testing period, especially for GO, thus this condition should be preferred.

Following this last result, Turbiscan measurements have been performed to investigate the GDS over time under static condition. FLG dispersions exhibited the highest transmittance variation, which increased by 48.5 % and 80.9 % after 6 and 72 h in respect to 0 h, respectively. Transmittance of GO dispersions showed the lowest variation, which increased by 25.3 % and 44.5 % after 6 and 72 h, respectively. Again, rGO showed the highest transmittance value (74.8) at time 0 h, close to the one of blank (79.5) (Fig. S12).

These results are in contrast with the decrease in the number of GRMs particles observed with FCM under static condition. These discrepancies warrant attention and should be attributed to the different sampling procedures applied for the two methodologies. Indeed, Turbiscan measurements were performed on as-they-are samples, settled down for the desired period, while FCM analyses were performed on resuspended samples, thus breaking the loose GRMs agglomerates through pipetting. This crucial difference accounts for the surprisingly low values observed with FCM in the decrease in the number of GRMs particles. Therefore, Turbiscan provided a more realistic perspective on the kinetic of the GRMs sedimentation curve over time.

By comparing Turbiscan results under static and shaking conditions, almost no differences among the respective sedimentation curves were observed. This suggests the importance of the dimensions of the vessel. Indeed, also from visual inspection, it was clear that the effect of the orbital shaking on the dispersions inside an Erlenmayer flask or a Turbiscan flask was quite different, even under the same shaking conditions (90 r.p.m.), due to the different flask diameter.

3.3.2. Addition of dispersants: effects on GDS and toxicity assessment on algae

According to GD 317 and GD 318, the standard TG 201 protocol can be modified to increase the stability of colloidal dispersions by using natural, non-toxic dispersants. In this work, carboxymethyl-cellulose (CMC), Suwannee River natural organic matter (HA) and sodium deoxycholate (SDC), have been used for their capability in increasing the stability of nanomaterials [68–71].

The tested dispersants differed in their capacity to stabilize the dispersions over the 72 h test period, as shown by Turbiscan measurements. Compared to the pristine dispersions, CMC increased the transmittance variation (*i.e.* decreased the stability) by 8.3 % and 12.4 % for FLG and rGO, respectively, and decreased it (*i.e.* increased the stability) by 23.6 % for GO. HA decreased the

transmittance variation by 12.0 % and 87.7 % for FLG and GO, respectively, and increased it by 1.7 % for rGO. SDC increased the transmittance variation by 112.2 % and 6.2 for FLG and rGO, respectively, and decreased it by 54.1 % for GO (Fig. S13, Tab. S3). Almost the same trend was observed under shaking condition, with slightly higher transmittance variations. In summary, HA was the best dispersant for stabilizing GRMs dispersions, especially for GO, both under static and shaking conditions.

A stabilizing effect of HA on GRMs dispersions has already been reported [15,37,49,72,73], but only for GO and rGO and it is mainly due to the adsorption of HA on GRMs causing steric repulsion [15,74]. The fact that HA can stabilize GO dispersions to a greater extent in respect to FLG and rGO might indicate a different mode of interaction of HA with materials differing in their surface chemistry. Supporting this, Hartono et al. reported that GO can adsorb NOM via hydrogen bonds, Lewis acid-base, and π-π interactions [75].

Before implementing dispersants in the TG 201 protocol, their toxicity has been tested towards algae. After 72 h, AGI values of - 4.96 ± 8.39 %, - 31.04 ± 3.09 % and 0.68 ± 3.00 % in the presence of CMC, HA and SDC, respectively, were observed (Tab. S5). Therefore, none of the tested dispersants had a significant toxic effect, but HA significantly stimulated the algal growth.

According to these results, the TG 201 has been applied to GRMs using HA to increase the GDS, as also suggested by the OECD (*e.g.* in TG 318, and GD 317).

FCM analysis showed that the number of GRMs events decreased similarly during the 72 h of testing in both FLG and GO dispersions, while high variability was reported for the rGO ones, which did not allow to determine a clear pattern (Fig. S14 C). The decrease in FLG events differed significantly among the concentrations tested, with a maximum of 75.8 % at 10 mg L^{-1}, while it was lower at higher and lower concentrations, with a minimum of 39.1 % at 1.25 mg L^{-1} (Fig. S14 A). A similar trend was observed for GO events, with a maximum decrease of 81.9 % at 5 mg L^{-1} and a minimum of 42.7 % at 1.25 mg L^{-1} (Fig. S14 B).

Instead, performing the TG 201 without HA, FLG dispersions showed a significant decrease in the number of events of 51.8 % at 1.25 mg L^{-1} increasing up to 74.4 % at 10 mg L^{-1} and down to 65.1 % at 40 mg L^{-1} (Fig. S14 A). Similarly, the decrease in the number of GO events varied from 53.5 % at 1.25 mg L^{-1} up to 67.8 % at 10 mg L^{-1} and down to 54.0 % at 40 mg L^{-1} (Fig. S14 B). Thus, the presence of the algae limited the stabilizing effect of HA, especially for GO dispersions, previously observed by Turbiscan measurements on GRMs dispersions without algae.

In this case as well, the presence of HA stimulated the algal growth. After 72 h, the AGI values for GO dispersions in the absence of HA were from 36.7 ± 5.0 to 81.1 ± 5.7 % (at minimum and maximum concentration) and were found to be statistically different from those in the presence of

HA, from - 5.1 ± 7.3 to 63.4 ± 8.2 % (at minimum and maximum concentration). The same trend, with increased algal growth stimulation, was observed for FLG, while high variability was reported for rGO (Tab. S6). Considering that GO had an inhibitory effect on the algal growth (Tab. S6), these results suggest that HA can mitigate this inhibitory effect of GO, with AGI values even becoming negative at lower concentrations.

One of the key mechanisms for toxicity mitigation by HA involves diminishing membrane damage. This is achieved both through reducing oxidative stress and minimizing direct interactions between GRMs and algae [76]. The negatively charged algal cell surface [38] could lead to the electrostatic repulsion between algal cells and HA-coated GRMs in a stronger manner than GRMs alone [77]. Zhang et al. and Zhao et al. suggested that this effect might result in diminished interaction between GRMs and algal cells, less physical penetration and damage caused by a decreased deposition of GRMs on cells through interaction with HA, or GRMs behaving like antioxidants [77,78]. Furthermore, the GRMs-HA interaction decreased the adsorption of nutrient on the GRMs surface, especially Ca^{++}, Mg^{++}, P and N, in turns, these macroelements become bioavailable for the algae and algal growth is enhanced [34,38,77,79,80].

Thus, when performing the TG 201 in the co-presence of GRMs and HA, the algal growth was stimulated, and the stabilizing effect of HA was nullified, suggesting that the exo-polysaccharides secreted by the algae affect the GDS [38,81–83].

According to these results, HA and dispersants in general should be verified in advance because they might not significantly improve the GDS, as in the case of CMC and SDC or lead to unreliable results due to mitigation of the GRMs toxicity. These results also raise the attention towards the behavior of GRMs in natural freshwater environments, where dissolved organic carbon/molecules of very variable composition are present [15,36,52,84].

3.4. Quantification of mass sedimentation during the TG 201 testing and dimensional re-characterization of dispersed GRMs flakes/particles

Since the testing performed under static condition was the one yielding the best stability results, the TG201 stability requirement of ± 20 % was verified quantitatively by using the Utermöhl sedimentation chamber (USC). Sedimentation of FLG was of 82.8 ± 4.7 % (1.66 mg settled out of the starting 2 mg) after 6 h, and 89.5 ± 2.5 % after 72 h (1.79 mg settled). GO showed a 43.0 ± 5.9 % sedimentation (0.86 mg settled) and 60.3 ± 2.3 % (1.21 mg settled) after 6 h and 72 h, respectively. Instead, for rGO the sedimentation was 64.2 ± 18.0 % (1.28 mg settled) and 66.3 ± 11.5 % (1.33 mg settled) after 6 h and 72 h, respectively (Fig. 4). The effect of the presence of the

algae has also been tested: after 72 h a slight, not significant, increase in sedimentation for FLG and GO (89.7 ± 1.7 % and 61.8 ± 5.3 %, for FLG and GO, respectively) was observed, while a significantly different increase in sedimentation was observed for rGO (88.7 ± 11.0 %) (Fig. 4).

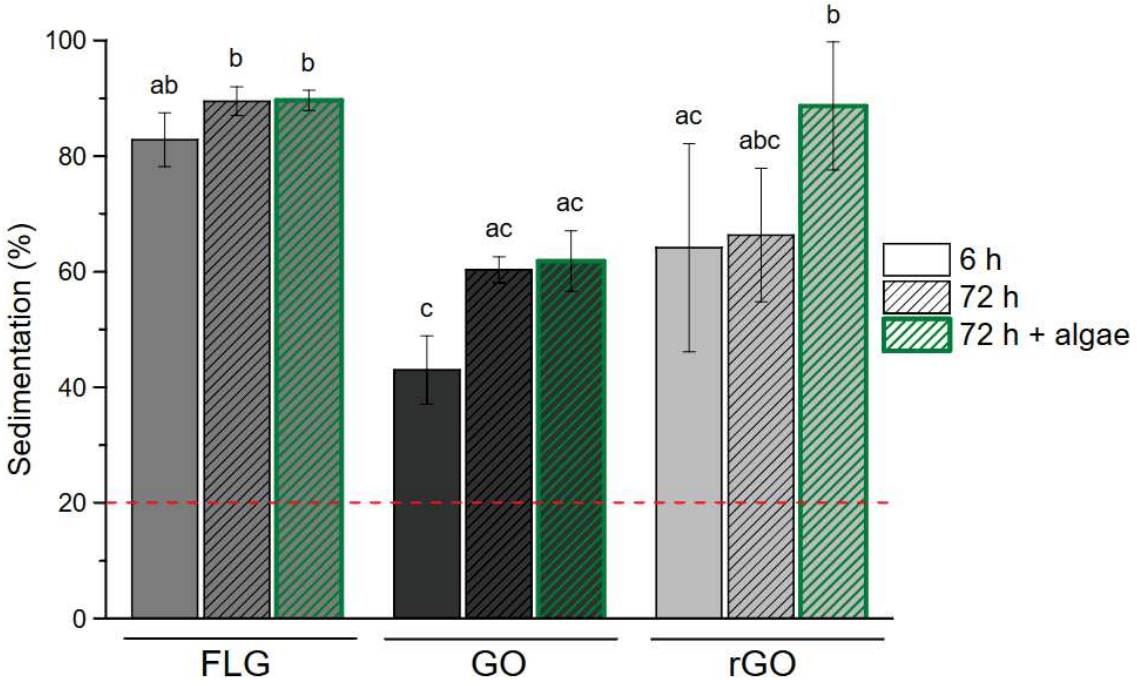

Figure 4. Per cent sedimentation of FLG (grey), GO (dark grey) and rGO (light grey) particles (40 mg L^{-1} in TG 201 medium) after 6 and 72 h, without or with algae (green) in the Utermöhl sedimentation chambers. The red dash lines indicate the ± 20% variation in concentration allowed by the TG 201 stability requirement. Data are reported as mean ± 1 standard deviation (n= 6). Statistically different groups are marked with different letters (GLS analysis, emmeans post-hoc test).

As a consequence, from the initial concentration of 40 mg L^{-1} for all the three GRMs, the concentrations of GRMs remaining in dispersion in the upper part of the USC were 4.9, 4.2 and 4.1 mg L^{-1} after 6 h, 72 h, and 72 h + algae, respectively, for FLG; 22.8, 15.9 and 15.3 mg L^{-1} for GO; and 14.3, 13.3 and 3.9 mg L^{-1} for rGO (Tab. S7).

By comparing those results in USC in the absence of the algae with the ones obtained under static condition with Turbiscan, a consistent trend is observed. Although Turbiscan and USC are the most directly comparable methods, Turbiscan results indicate a potential underestimation of the actual sedimentation occurring over time in the samples. This might be addressed to the low sensitivity of photometric methods in the detection of concentration variation, especially at the lowest concentration. Markovic et al. reported a good correlation between the absorbance of GO and the exposure concentration, but the limit of detection (LOD) and the limit of quantification (LOQ) were 1.06 mg L^{-1} and 3.21 mgL^{-1}, respectively [80], close to the concentration of FLG dispersions over the test period.

As already reported in the literature, it is quite known that GRMs tend to aggregate and settle down in the aquatic compartment [34,35,49]. However, to date, only few studies investigated the GRMs stability when applying the TG 201. Castro et al. and Yin et al. reported an absorbance time-dependent decrease of around 40 % already after 24 h for GO and up to 55 % for rGO nanocomposites after settling for 96 h in aqueous phase, respectively [37,39]. On the contrary, Markovic et al. reported a high stability (detected using UV-vis technique) of GO dispersions at 16 and 32 mg L^{-1} after a 96 h test period [80]. However, this readout could be biased due to scarce or improper stability evaluation, and the main reasons could be addressed to GRMs hetero-agglomeration with algae and biases in the measurements due to interferences with fluorescence readouts [34].

In conclusion, by quantifying the GRMs sedimentation (and the resulting concentrations of GRMs remaining in dispersion), we evidenced values up to 90 % (for FLG) and in any case none below 20% after the 72 h test period, due to agglomeration/aggregation and sedimentation phenomena. These data confirm that under these conditions the TG 201 stability requirement is never met, thus the TG 201 is hardly applicable to GRMs, due to the afore mentioned stability issues.

3.4.1. Dimensional characterization of the suspended and settled fractions after 72 h

Sedimentation is primarily due to the larger and agglomerated fraction of the GRMs particle population while the smallest and thinnest fraction remains in suspension. Particle size particularly affects bioavailability, alga-particle interactions and thus potential toxicity [35,60,61]. Therefore, the two fractions obtained from the use of USC, *i.e.* suspended and settled ones, were dimensionally re-characterized.

HR-TEM observations showed a progressive decrease in lateral size of GRMs flakes remained in dispersion throughout the 72 h of testing: mean values significantly decreased from 394.4 nm to 239.2, 217.8, 352.3 nm after 0, 6, 72 and 72+6 h, respectively, for FLG; from 688.7 nm to 519.9, 331.8 and 415.4 nm, for GO; from 1588.6 nm to 790.4, 544.2, 528.9 nm, for rGO (Fig. 5). In contrast, GRMs flakes/particles settled down in the sedimentation chamber were found to have significantly ($p< 0.05$) larger lateral size for FLG and GO, with mean values of 496.5 and 1362.9 nm, respectively, while settled rGO particles had almost the same size of those measured at time 0 h with mean value of 1410.6 nm (Fig. 5).

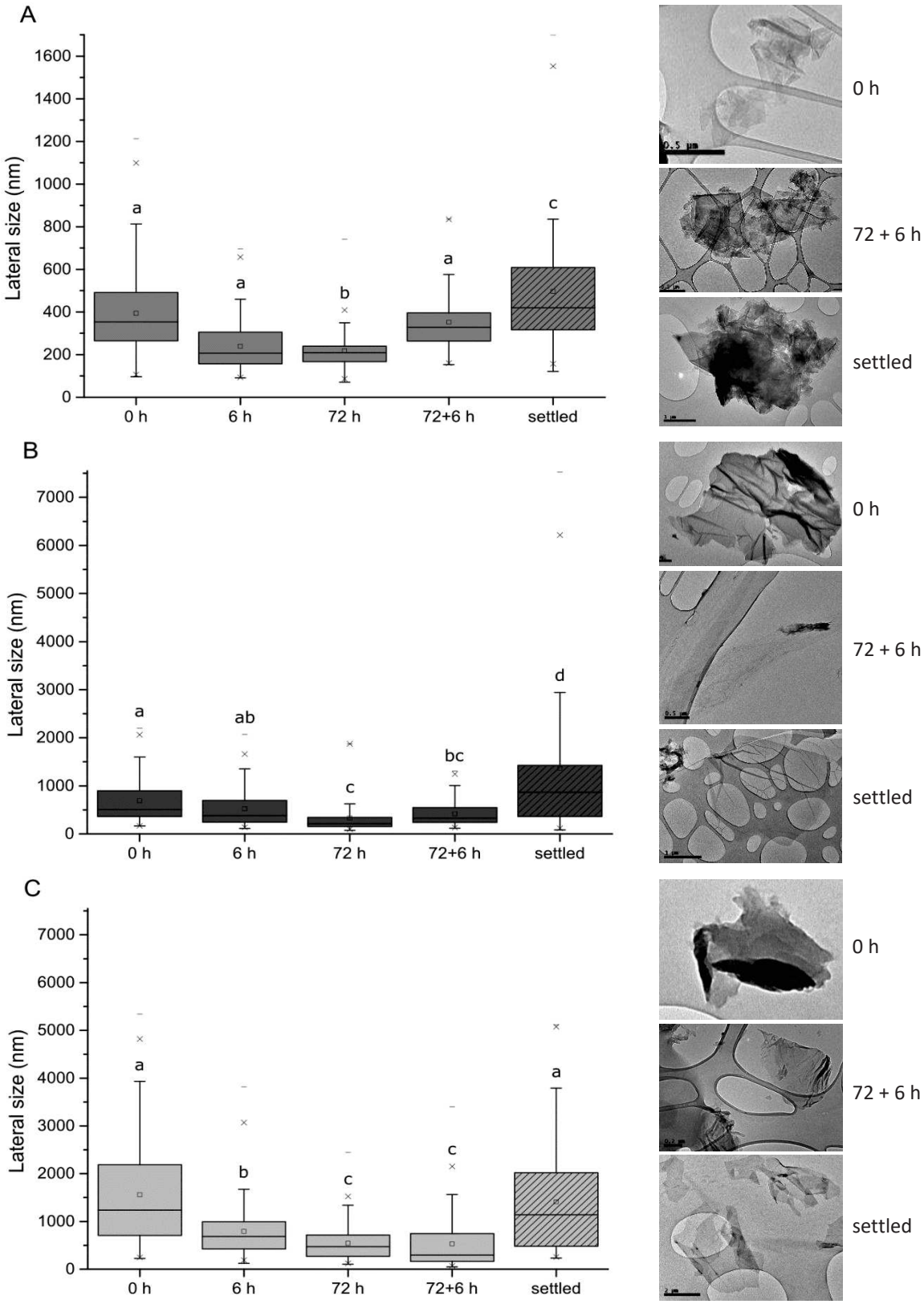

Figure 5. Lateral size (nm) distribution of FLG (A), GO (B) and rGO (C) particles in TG 201 medium remaining in dispersion in the upper part of the Utermöhl sedimentation chamber at 0, 6, 72 and 72+6 h (full bars) as compared to the lateral size distribution of the particles settled down at the bottom of the chamber after 72+6 h (patterned bars). Boxplots represent the 25-75 percentile with median as a line, and mean as small square; minimum and maximum values are represented as short lines, 1 and 99% as small x (n= 101-104). Statistically different groups are marked with different letters (GLS analysis, Bonferroni post-hoc test). On the right side, HR-TEM images of representative particles of the corresponding GRM suspended at 0 h, 72+6 h and settled are reported.

The lateral dimension of rGO flakes already from 0 h (1588.6 nm) was much bigger than the range expected from the first characterization (200-800 nm, Tab. 1) and it was very close to the value of the settled flakes after 72+6 h (1410.6 nm), confirming that this material had very poor dispersibility despite using standard preparation protocols of GRMs suspensions.

These results underscore the importance of recharacterizing the materials in the test medium, as the presence of ions could lead to the formation of agglomerates/aggregates with greater dimensions than expected, and consequent sedimentation [34,37]. Therefore, in addition to a change in concentration over time, algae are also exposed to a GRMs population that changes progressively in terms of size.

3.5. Progress and problems with the application of the TG 201 to GRMs

Among the OECD TGs developed for the ecotoxicological risk assessment in freshwater environments, TG 201 is the most challenging for testing GRMs, due to the nature of both the test organisms and the materials. All target organisms of TG 201 (the green algae *Raphidocelis subcapitata* and *Desmodesmus subspicatus*, the diatom *Navicula pelliculosa*, the cyanobacteria *Anabaena flos-aquae* and *Synechococcus leopoliensis*) have no flagella or cilia, and tend to self-settle, like the GRMs, whereas the target organisms of TG 202 (young daphnids, aged less than 24 hours) and TG 203 (a variety of method approved fish species, including rainbow trout and zebra fish) are motile, and their movements resuspend the material and limit its agglomeration [34]. However, only few studies have dealt with the quantitative evaluation of the stability of GRMs dispersions. According to the recent review by Connolly et al. [34], out of the 13 studies based specifically on the TG 201, only three have done so: two of them reported high sedimentation values for GO and rGO dispersions [34,36], while the other reported high stability of GO [80]. Importantly, only one provided detailed information on the sampling methods of the dispersions for the subsequent UV/vis spectrophotometric measurements [34]. However, as shown earlier, these methods could lead to an underestimation of the sedimentation, as the correlation between transmittance values and quantitative sedimentation measurements is generally poor (Figs. 3, 4).

Data on the quantification of sedimentation and size of GRMs flakes remaining in dispersion and settled are of crucial importance in an ecotoxicological assay. They should always be provided, as they strongly influence the bioavailability of the tested material and determine the actual exposure concentration to which the organisms are exposed. The lack of quantitative GDS data and check of actual concentration at the end of the test makes the EC_{50} eventually provided *de facto* highly questionable. To our knowledge, this study is the first to provide a comprehensive evaluation of the behaviour of GRMs dispersions, by presenting a direct mass-based quantification of aggregation

and sedimentation, and characterization of the flakes/particles settled vs. still in suspension at the end of the test period. This knowledge is essential to obtain meaningful data for the hazard assessment of GRMs, a procedure that will be increasingly required by the EU authorities for human health and environmental safety (*e.g.* ECHA, EFSA, etc.) as a result of the increasing massive use of these materials in the nearby future [20,21].

Our study has shown that material instability is a major limiting factor for the application of TG 201 for GRMs testing. Approaches to improve material stability and maintenance were not effective: strong agglomeration/aggregation and sedimentation phenomena were observed for all materials under all tested conditions, thus the stability criterion of TG 201 was never met. The general conclusion is that TG 201 is only suitable for testing GRMs concentrations that can be kept stable in the system. This can be achieved by allowing an adequate period of time for the dispersion to stabilize after the preparation of the GRM dispersion. Only then a detailed physico-chemical characterization of the suspended material is required, which must be reiterated at the end of the 72-hour test. Moreover, a direct assessment of the actual mass concentration is required. In our case, a stabilization time of approximately 6 hours ensured that our FLG and GO dispersions lost the coarser fraction, and then remained relatively stable and homogeneous over time, at least for the test period. This stabilization time should be determined in advance and tailored to the tested material on a case-by-case basis, as the lateral size, number of layers, C/O ratio, presence of any chemical function, etc. exert a strong influence on the GDS [15,52,85].

Data such as those provided in this study are relevant from an environmental perspective as they allow predictions to be made about the fate of GRMs in the natural environment. Hydrophobic GRMs, like FLG, tend to settle rapidly in aqueous dispersions and become bioavailable to benthic organisms, such as polychaetes[86], oligochaetes [62], chironomid larvae [87–90], etc., leading to adverse effects even at concentration as low as 0.5 mg L^{-1}. Failure to account for this aspect could lead to an underestimation of the potential risk posed by these materials to freshwater environments. Considering the number of TGs offered by OECD and the need for a robust aquatic toxicity assessment, it seems reasonable to integrate the minimum battery of TGs required by REACH with others specifically designed to determine potential ecotoxicity to benthic organisms such as TG 225 [91] (on oligochaetes), TG 233 [92] (on chironomids) or TG 239 [93] (on vascular plants), which are already prescribed for substances manufactured or imported in quantities of 1000 tonnes or more.

4. Conclusions and environmental relevance

In this study, a careful investigation of the applicability of the OECD TG 201 to three representative member of the GRMs family, namely FLG, GO and rGO, was conducted, with emphasis on the maintenance of the nominal initial concentration (± 20 %). Strong agglomeration/aggregation and sedimentation phenomena were observed in the TG 201 medium under standard test conditions and the above criterion was not met by any of the tested materials. Modifications to increase the GRMs dispersion stability, including the application of different types and intensities of turbulence and the addition of dispersants (CMC, HA, and SDC) failed, albeit in different ways depending on the particle composition and their intrinsic properties. These facts undermine the applicability of TG 201 to the three tested materials and possibly to other GRMs. Nevertheless, a period of stabilization of the freshly prepared dispersions could be introduced prior to the testing to separate the coarser and most instable fractions of the GRMs population from that remaining in dispersion. This stable fraction needs an *ad hoc* physico-chemical characterization both in terms of population size and mass concentration, to be repeated at the end of the 72-hour test period. Furthermore, when dealing with materials undergoing sedimentation phenomena, such as GRMs, the implementation of other TGs specifically designed for the benthic compartment, such as TG 225, TG 233 and TG 239 is suggested for a comprehensive evaluation of the potential adverse effect of these materials in the freshwater environments.

5. Conflicts of interest

There are no conflicts of interest to declare.

6. Acknowledgements

This work was supported by the Horizon 2020 Graphene Flagship Core 3 (grant agreement no. 881603), which covered the activity of Dr. Fabio Candotto Carniel, and by Spanish government (project PID2020-113080RB-I00). Graphene Flagship Core 3 Spearhead project “Safegraph” (grant agreement no. 649953) and University of Trieste DOTTAMBIENTEVITA36 covered the activity of Giada Caorsi.

7. References

1 EC, 2020. Commission Regulation (EU) 2020/878 of 18 June 2020 amending Annex II to Regulation (EC) No 1907/2006 of the European Parliament and of the Council concerning the Registration, Evaluation, Authorisation and Restriction of Chemicals (REACH).

2 EC, 2006. Regulation No 1907/2006 of the European Parliament and of the Council of 18 December 2006 concerning the Registration, Evaluation, Authorisation and Restriction of Chemicals (REACH), establishing a European Chemicals Agency, amending Directive 1999/45/EC and repealing Council Regulation (EEC) No 793/93 and Commission Regulation (EC) No 1488/94 as well as Council Directive 76/769/ EEC and Commission Directives 91/155/EEC, 93/67/EEC, 93/105/EC and 2000/ 21/EC.

3 OECD, Test No. 201: Freshwater Alga and Cyanobacteria, Growth Inhibition Test, OECD Guidelines for the Testing of Chemicals, Section 2. OECD Publishing, Paris, 2011.

4 OECD, Test No. 202: Daphnia sp. Acute Immobilisation Test, OECD Guidelines for the Testing of Chemicals, Section 2. OECD Publishing, Paris, 2004.

5 OECD, Test No. 203: Fish, Acute Toxicity Test, OECD Guidelines for the Testing of Chemicals, Section 2. OECD Publishing, Paris, 2019.

6 OECD, Test No. 301: Ready Biodegradability, OECD Guidelines for the Testing of Chemicals, Section 3. OECD Publishing, Paris, 1992.

7 R. D. Handy, N. Van Den Brink, M. Chappell, M. Mü, R. Behra, M. Dušinská, P. Simpson, J. Ahtiainen, A. N. Jha, J. Seiter, A. Bednar, A. Kennedy, T. F. Fernandes, M. Riediker, R. D. Handy, Á. A. N. Jha, N. Van Den Brink, M. Chappell, Á. J. Seiter, Á. A. Bednar, Á. A. Kennedy, M. Mühling, R. Behra Eawag, M. Dušinská, J. Ahtiainen, T. F. Fernandes and M. Riediker, *Ecotoxicology*, 2012, 21, 933–972.

8 Series on the Safety of Manufactured Nanomaterials No. 40 - Ecotoxicology and Environmental Fate of Manufactured Nanomaterials: Test Guidelines - Expert Meeting Report. OECD, Environment Directorate, 2014.

9 OECD, Guidance Document on Aquatic and Sediment Toxicological Testing of Nanomaterials. Series on Testing and Assessment No. 317. OECD Publishing, Paris, 2022.

10 OECD, Guidance document for the testing of dissolution and dispersion stability of nanomaterials and the use of the data for further environmental testing and assessment strategies. Series on Testing and Assessment No. 318. OECD Publishing, Paris, 2021.

11 E. J. Petersen, S. A. Diamond, A. J. Kennedy, G. G. Goss, K. Ho, J. Lead, S. K. Hanna, N. B. Hartmann, K. Hund-Rinke, B. Mader, N. Manier, P. Pandard, E. R. Salinas and P. Sayre, *Environ. Sci. Technol.*, 2015, 49, 9532–9547.

12 D. Kühnel and C. Nickel, *Sci. Total Environ.*, 2014, 472, 347–353.

13 K. S. Novoselov, V. I. Fal'Ko, L. Colombo, P. R. Gellert, M. G. Schwab and K. Kim, *Nature*, 2012, 490, 192–200.

14 K. S. Novoselov, A. K. Geim, S. V. Morozov, D. Jiang, Y. Zhang, S. V. Dubonos, I. V. Grigorieva and A. A. Firsov, *Science*, 2004, 306, 666–669.

15 K. He, G. Chen, G. Zeng, M. Peng, Z. Huang, J. Shi and T. Huang, *Nanoscale*, 2017, 9, 5370–5388.

16 A. Bianco, *Angew. Chem. Int. Ed. Engl.*, 2013, 52, 4986-97.

17 X. Guo and N. Mei, *J. Food Drug Anal.*, 2014, 22, 105–115.

18 N. Malhotra, O. B. Villaflores, G. Audira, P. Siregar, J. S. Lee, T. R. Ger and C. Der Hsiao, *Mol.*, 2020, 25, 3618.

19 V. C. Sanchez, A. Jachak, R. H. Hurt and A. B. Kane, *Chem. Res. Toxicol.*, 2012, 25, 15–34.

20 D. G. Goodwin, A. S. Adeleye, L. Sung, K. T. Ho, R. M. Burgess and E. J. Petersen, *Environ. Sci. Technol.*, 2018, 52, 4491–4513.

21 H. Hong, F. Part and B. Nowack, *Environ. Sci. Technol.*, 2022, 56, 13798–13809.

22 F. Candotto Carniel, L. Fortuna, D. Zanelli, M. Garrido, E. Vázquez, V. J. González, M. Prato and M. Tretiach, *J. Hazard. Mater.*, 2021, 414, 125553.

23 D. Zanelli, F. Candotto Carniel and M. Tretiach, *Appl. Sci.*, 2021, 11, 6150.

24 D. Zanelli, F. Candotto Carniel, L. Fortuna, E. Pavoni, V. Jehová González, E. Vázquez, M. Prato and M. Tretiach, *Chemosphere*, 2023, 312, 137138.

25 D. Zanelli, F. Candotto Carniel, L. Fortuna, E. Pavoni, V. Jehová González, E. Vázquez, M. Prato and M. Tretiach, *Sci. Total Environ.*, 2022, 830, 154625.

26 L. V. Efremova, A. S. Vasilchenko, E. G. Rakov and D. G. Deryabin, *Biomed Res. Int.*, 2015, 869361.

27 S. Gurunathan, J. W. Han, A. Abdal Dayem, V. Eppakayala and J. H. Kim, *Int. J. Nanomedicine*, 2012, 7, 5901–5914.

28 S. Liu, T. H. Zeng, M. Hofmann, E. Burcombe, J. Wei, R. Jiang, J. Kong and Y. Chen, *ACS Nano*, 2011, 5, 6971–6980.

29 L. Q. Chen, P. P. Hu, L. Zhang, S. Z. Huang, L. F. Luo and C. Z. Huang, *Sci. China Chem.*, 2012, 55, 2209–2216.

30 X. T. Liu, X. Y. Mu, X. L. Wu, L. X. Meng, W. B. Guan, Y. Q. Ma, H. Sun, C. J. Wang and X. F. Li, *Biomed. Environ. Sci.*, 2014, 27, 676–683.

31 F. Candotto Carniel, D. Gorelli, E. Flahaut, L. Fortuna, C. Del Casino, G. Cai, M. Nepi, M. Prato and M. Tretiach, *Environ. Sci. Nano*, 2018, 5, 1608–1617.

32 B. Fadeel, C. Bussy, S. Merino, E. Vázquez, E. Flahaut, F. Mouchet, L. Evariste, L. Gauthier, A. J. Koivisto, U. Vogel, C. Martín, L. G. Delogu, T. Buerki-Thurnherr, P. Wick, D. Beloin-Saint-Pierre, R. Hischier, M. Pelin, F. Candotto Carniel, M. Tretiach, F. Cesca, F. Benfenati, D. Scaini, L. Ballerini, K. Kostarelos, M. Prato and A. Bianco, *ACS Nano*, 2018, 12, 10582–10620.

33 H. Lin, T. Buerki-Thurnherr, J. Kaur, P. Wick, M. Pelin, A. Tubaro, F. Candotto Carniel, M. Tretiach, E. Flahaut, D. Iglesias, E. Vázquez, G. Cellot, L. Ballerini, V. Castagnola, F. Benfenati, A. Armirotti, A. Sallustrau, F. Taran, M. Keck, C. Bussy, S. Vranic, K. Kostarelos, M. Connolly, J. M. Navas, F. Mouchet, L. Gauthier, J. Baker, B. Suarez-Merino, T. Kanerva, M. Prato, B. Fadeel*, A. Bianco, *ACS Nano*, 2024, 18, 8, 6038–6094

34 M. Connolly, G. Moles, F. C. Carniel, M. Tretiach, G. Caorsi, E. Flahaut, B. Soula, E. Pinelli, L. Gauthier, F. Mouchet and J. M. Navas, *NanoImpact*, 2023, 29, 10447.

35 Y. Gao, X. Zeng, W. Zhang, L. Zhou, W. Xue, M. Tang and S. Sun, *Sci. Total Environ.*, 2022, 806, 150942.

36 M. Markovic, A. Kumar, I. Andjelkovic, S. Lath, J. K. Kirby, D. Losic, G. E. Batley and M. J. McLaughlin, *Environ. Toxicol. Chem.*, 2018, 37, 1340–1348.

37 J. Zhao, X. Cao, Z. Wang, Y. Dai and B. Xing, *Water Res.*, 2017, 111, 18–27.

38 V. L. Castro, Z. Clemente, C. Jonsson, M. Silva, J. H. Vallim, A. M. Z. de Medeiros and D. S. T. Martinez, *Environ. Toxicol. Chem.*, 2018, 37, 1998–2012.

39 J. Yin, Z. Dong, Y. Liu, H. Wang, A. Li, Z. Zhuo, W. Feng and W. Fan, *Carbon N. Y.*, 2020, 169, 182–192.

40 J. M. González-Domínguez, V. León, M. I. Lucío, M. Prato and E. Vázquez, *Nat. Protoc.*, 2018, 13, 495–506.

41 W. S. Hummers and R. E. Offeman, *J. Am. Chem. Soc.*, 1958, 80, 1339.

42 B. Lobato, C. Merino, V. Barranco and T. A. Centeno, *RSC Adv.*, 2016, 6, 57514–57520.

43 L. Evariste, L. Lagier, P. Gonzalez, A. Mottier, F. Mouchet, S. Cadarsi, P. Lonchambon, G. Daffe, G. Chimowa, C. Sarrieu, E. Ompraret, A. M. Galibert, C. M. Ghimbeu, E. Pinelli, E. Flahaut and L. Gauthier, *Nanomater.*, 2019, 9, 584.

44 G. Di Mauro, R. Rauti, R. Casani, G. Chimowa, A. M. Galibert, E. Flahaut, G. Cellot and L. Ballerini, *Nanomater.*, 2021, 11, 2161.

45 C. G. Van Ginkel and S. Gayton, *Environ. Toxicol. Chem.*, 1996, 15, 270–274.

46 L. Lagier, F. Mouchet, C. Laplanche, A. Mottier, S. Cadarsi, L. Evariste, C. Sarrieu, P. Lonchambon, E. Pinelli, E. Flahaut and L. Gauthier, *Carbon N. Y.*, 2017, 119, 72–81.

47 H. Mohan, M. Bartkowski and S. Giordani, *Appl. Sci.*, 2021, 11, 10565.

48 OECD, Test No. 318: Dispersion Stability of Nanomaterials in Simulated Environmental Media, OECD Guidelines for the Testing of Chemicals, Section 3. OECD Publishing, Paris, 2017.

49 Z. Clemente, V. L. S. S. Castro, L. S. Franqui, C. A. Silva and D. S. T. Martinez, *Environ. Pollut.*, 2017, 225, 118–128.

50 Frimmel, F.H., 2004. Aquatic Humic Substances. v.1, Cap 10. En: Steinbüchel a. Biopolymers.

51 A. Sharma and R. Anthal, *Int. J. Innov. Res. Sci. Eng. Technol.*, 2018, 5, 18462–18470.

52 H. Utermöhl, *SIL Proceedings*, 1931, 5, 567–596.

53 Y. Jiang, R. Raliya, P. Liao, P. Biswasa, J. D. Fortner, *Environ. Sci.: Nano*, 2017, 4, 1484-1493.

54 J. Pinheiro, D. Bates, S. DebRoy, D. Sarkar, R Core Team. 2019, linear and nonlinear mixed effects models. available online: https://cran.r-project.org/package=nlme.

55 L. Krienitz, C. Bock, H. Nozaki, M. Wolf, *J Phycol*, 2011, 47, 880–893.

56 F. Torrisi, T. Hasan, W. Wu, Z. Sun, A. Lombardo, T. S. Kulmala, G.-W. Hsieh, S. Jung, F. Bonaccorso, P. J. Paul, D. Chu and A. C. Ferrari, *ACS Nano*, 2012, 6, 2992–3006

57 A. C. Ferrari, J. C. Meyer, V. Scardaci, C. Casiraghi, M. Lazzeri, F. Mauri, S. Piscanec, D. Jiang, K. S. Novoselov, S. Roth and A. K. Geim, *Phys. Rev. Lett.*, 2006, 97, 187401.

58 U. Mogera, R. Dhanya, R. Pujar, C. Narayana and G. U. Kulkarni, *Phys. Chem. Lett.*, 2015, 6, 4437–4443.

59 L. Stobinski, B. Lesiak, A. Malolepszy, M. Mazurkiewicz, B. Mierzwa, J. Zemek, P. Jiricek, I. Bieloshapka, *J. Electron Spectros. Relat. Phenomena*, 2014, 195, 145-154.

60 X. Hu, L. Mu, J. Kang, K. Lu, R. Zhou and Q. Zhou, *Environ. Sci. Technol.*, 2014, 48, 6919–6927.

61 X. Hu, S. Ouyang, L. Mu, J. An and Q. Zhou, *Environ. Sci. Technol.*, 2015, 49, 10825–10833.

62 L. Mao, C. Liu, K. Lu, Y. Su, C. Gu, Q. Huang and E. J. Petersen, *Carbon N. Y.*, 2016, 109, 566–574.

63 P. A. Denis and F. Iribarne, *Phys. Chem. C*, 2011, 115, 1, 195–203.

64 Y. Su, G. Yang, K. Lu, E. J. Petersen and L. Mao, *Environ. Pollut.*, 2017, 220, 469–477.

65 A. E. Aboubaraka, E. F. Aboelfetoh and E. Z. M. Ebeid, *Chemosphere*, 2017, 181, 738–746.

66 A. A. Mohana, S. M. Farhad, N. Haque and B. K. Pramanik, *Chemosphere*, 2021, 284, 131430.

67 H. Sun, R. Jiao and D. Wang, *Environ. Pollut.*, 2021, 268, 115942.

68 A. L. Alpatova, W. Shan, P. Babica, B. L. Upham, A. R. Rogensues, S. J. Masten, E. Drown, A. K. Mohanty, E. C. Alocilja and V. V. Tarabara, *Water Res.*, 2010, 44, 505–520.

69 S. H. Othman, S. Abdul Rashid, T. I. Mohd Ghazi and N. Abdullah, *Nanomater.*, 2012, 718214.

70 L. Zhang, Z. Zhang, C. He, L. Dai, J. Liu and L. Wang, *ACS Nano*, 2014, 8, 6663–6670.

71 Q. Zhao, X. Liu, S. Veldhuis and I. Zhitomirsky, *Colloids Surfaces A: Physicochem. Eng. Asp.*, 2020, 588, 124382.

72 H. Hyung and J.-H. KIM, *Environ. Sci. Technol.*, 2008, 42, 4416–4421.

73 G. Hwang, A. Gomez-Flores, S. A. Bradford, S. Choi, E. Jo, S. B. Kim, M. Tong and H. Kim, *Colloids Surfaces A: Physicochem. Eng. Asp.*, 2018, 554, 306–316.

74 I. Chowdhury, M. C. Duch, N. D. Mansukhani, M. C. Hersam and D. Bouchard, *Environ. Sci. Technol.*, 2013, 47, 6288–6296.

75 T. Hartono, S. Wang, Q. Ma and Z. Zhu, *Colloid Interface Sci.*, 2009, 333, 114–119.

76 J. Zhao, Y. Li, X. Cao, C. Guo, L. Xu, Z. Wang, J. Feng, H. Yi and B. Xing, *Environ. Sci. Nano*, 2019, 6, 1909–1920.

77 Y. Zhang, T. Meng, X. Guo, R. Yang, X. Si and J. Zhou, *Chemosphere*, 2018, 197, 749–758.

78 A. Debroy, N. Roy, S. Giri, M. Pulimi, N. Chandrasekaran, W. J. G. M. Peijnenburg, A.Mukherjee, *Environ. Pollut.*, 2024, 341, 123015.

79 T. Malina, E. Maršálková, K. Holá, J. Tuček, M. Scheibe, R. Zbořil and B. Maršálek, *Carbon N. Y.*, 2019, 155, 386–396.

80 M. Markovic, I. Andelkovic, J. Shuster, L. Janik, A. Kumar, D. Losic and M. J. McLaughlin, *Chemosphere*, 2020, 245, 125640.

81 L. Hazeem, *Water*, 2022, 14, 2669.

82 M. Garacci, M. Barret, F. Mouchet, C. Sarrieu, P. Lonchambon, E. Flahaut, L. Gauthier, J. Silvestre and E. Pinelli, *Carbon N. Y.*, 2017, 113, 139–150.

83 F. Schwab, T. D. Bucheli, L. P. Lukhele, A. Magrez, B. Nowack, L. Sigg and K. Knauer, *Environ. Sci. Technol.*, 2011, 45, 6136–6144.

84 J. Zhao, Z. Wang, J. C. White and B. Xing, *Environ. Sci. Technol.*, 2014, 48, 9995–10009.

85 Y. Jiang, R. Raliya, P. Liao, P. Biswas and J. D. Fortner, *Environ. Sci. Nano*, 2017, 4, 1484–1493.

86 M. M. Gudarzi, *Langmuir*, 2016, 32, 5058–5068.

87 A. Pires, E. Figueira, M. S. S. Silva, C. Sá and P. A. A. P. Marques, *Environ. Pollut.*, 2022, 299, 118869.

88 L. Evariste, A. Mottier, L. Lagier, S. Cadarsi, M. Barret, C. Sarrieu, B. Soula, F. Mouchet, E. Flahaut, E. Pinelli and L. Gauthier, *Carbon N. Y.*, 2020, 156, 261–271.

89 R. Martin-Folgar, A. Esteban-Arranz, V. Negri and M. Morales, *Sci. Total Environ.*, 2022, 815, 152465.

90 L. Evariste, L. Lagier, C. Chary, A. Mottier, S. Cadarsi, E. Pinelli, E. Flahaut, L. Gauthier and F. Mouchet, *Toxics*, 2022, 10, 588.

91 R. Martin-Folgar, A. Esteban-Arranz, V. Negri and M. Morales, *Nanomater.*, 2023, 13, 967.

92 OECD, Test No. 225: Sediment-Water *Lumbriculus* Toxicity Test Using Spiked Sediment, OECD Guidelines for the Testing of Chemicals. OECD Publishing, Paris, 2007.

93 OECD, Test No. 233: Sediment-Water Chironomid Life-Cycle Toxicity Test Using Spiked Water or Spiked Sediment, OECD Guidelines for the Testing of Chemicals. OECD Publishing, Paris, 2010.

94 OECD, Test No. 239: Water-Sediment *Myriophyllum Spicatum* Toxicity Test, OECD Guidelines for the Testing of Chemicals. OECD Publishing, Paris, 2010.

Supplementary information

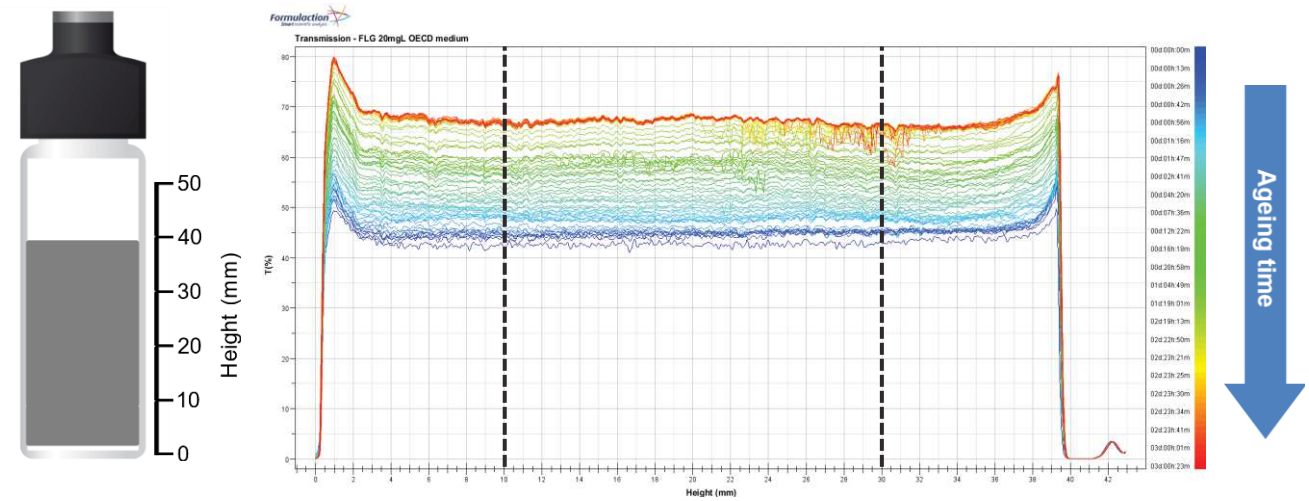

Figure S1. Turbiscan flask with height (mm) and the outcome of Turbiscan measurements. For the results, only the section comprised between 10 and 30 mm has been considered, to avoid biases due to the bottom of the flask or meniscus.

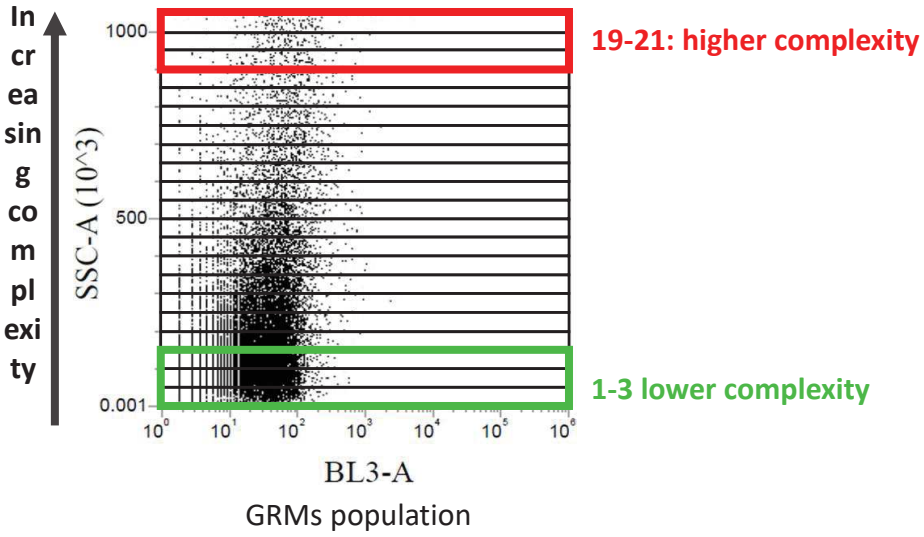

Figure S2. Flow cytometer (FCM) outcome: GRMs population divided in 21 gates with increasing complexity from base to top, based on the side scatter (SSC) parameter.

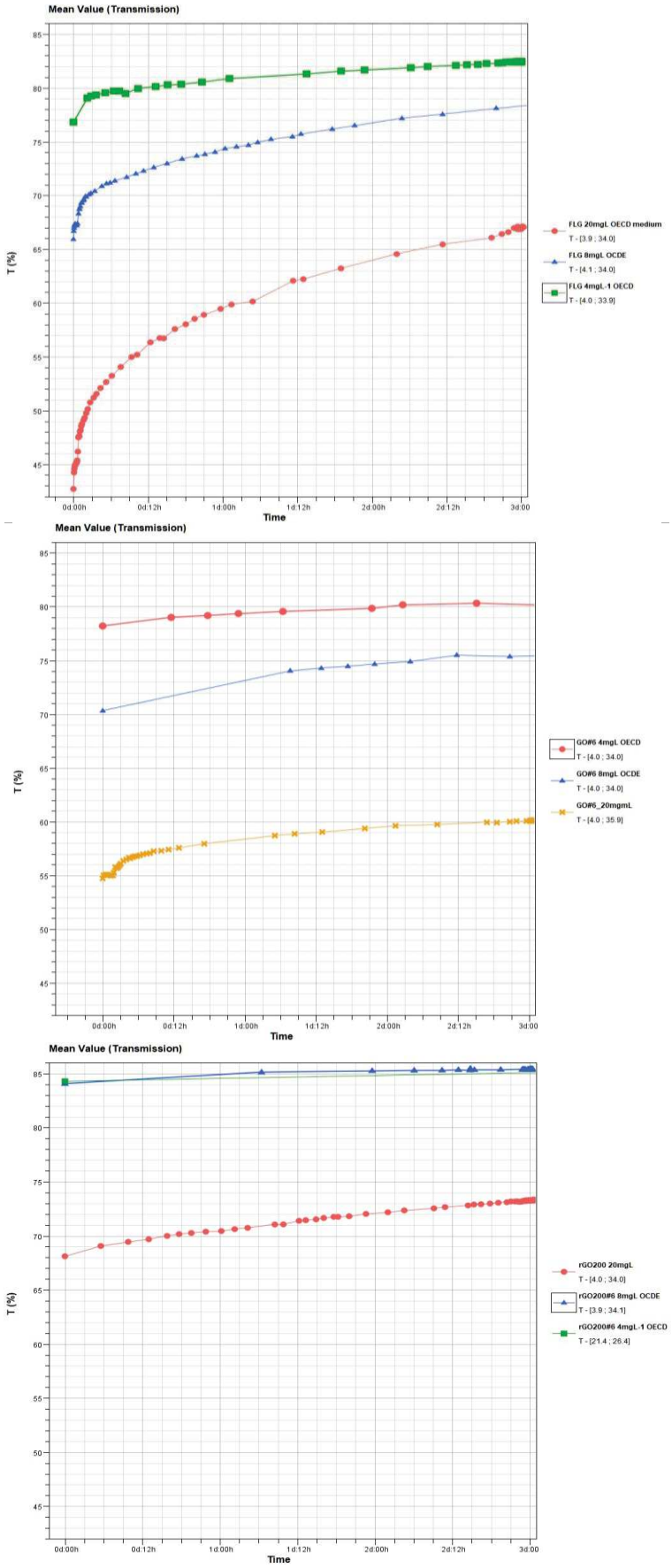

Figure S3. Transmittance variation of FLG (A), GO (B), and rGO (C) dispersions at 4, 8, 20 mg L^{-1} in TG 201 medium under static condition observed throughout the 72 h of testing (Turbiscan analysis).

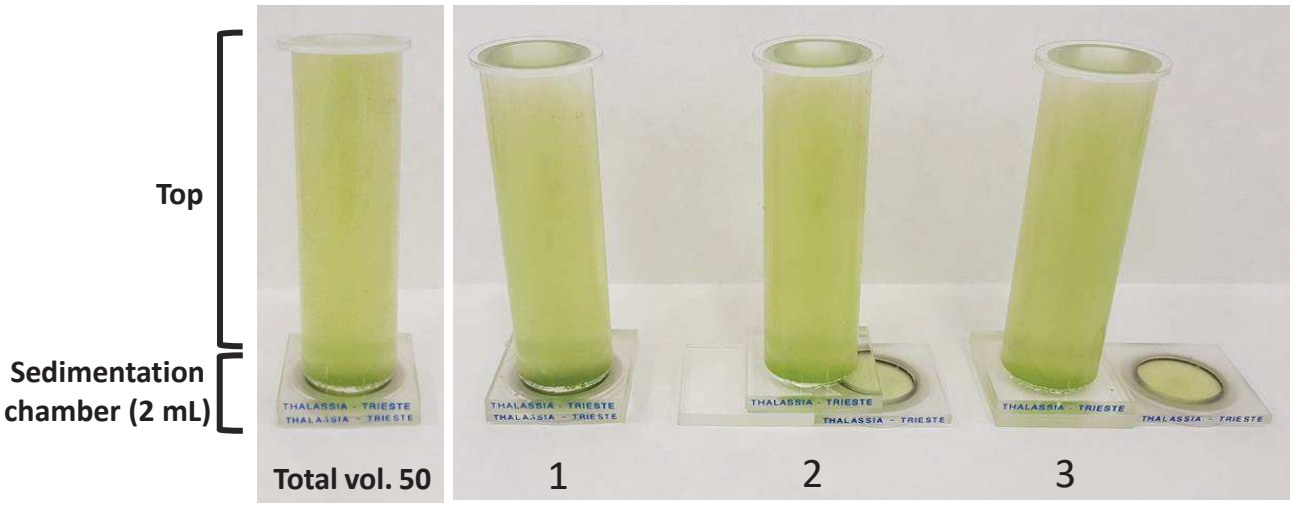

Figure S4. *Functioning of the Utermöhl sedimentation chambers (USC).*

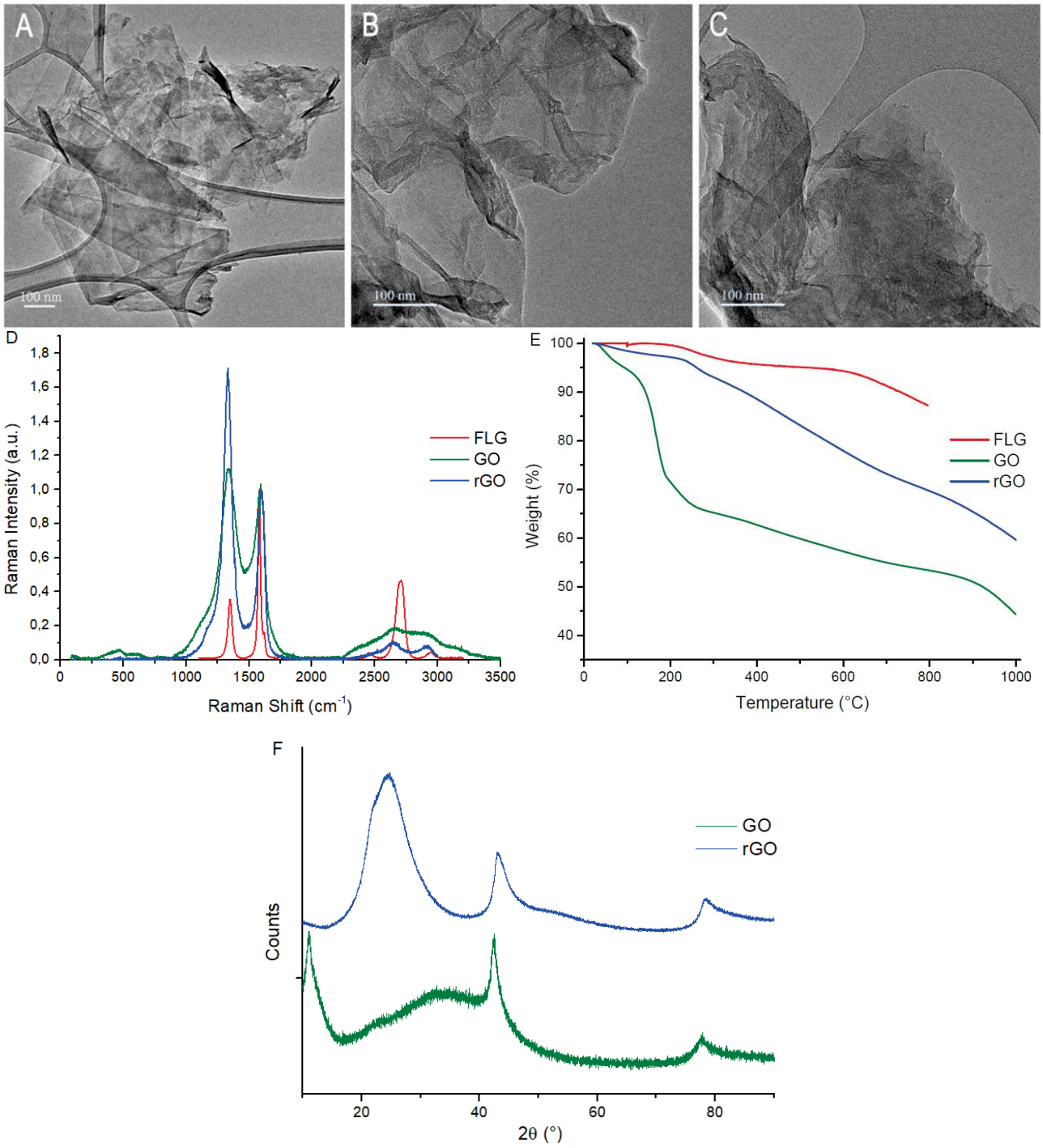

Figure S5. Physico-chemical characterization of pristine few-layers graphene (FLG), graphene oxide (GO), and reduced GO (rGO). Representative TEM images of FLG (A), GO (B), and rGO (C). Scale bar: 100 nm. Raman spectra (D); Thermogravimetric analyses (TGA) (E); and X-ray diffraction (XRD) of GO and rGO (F).

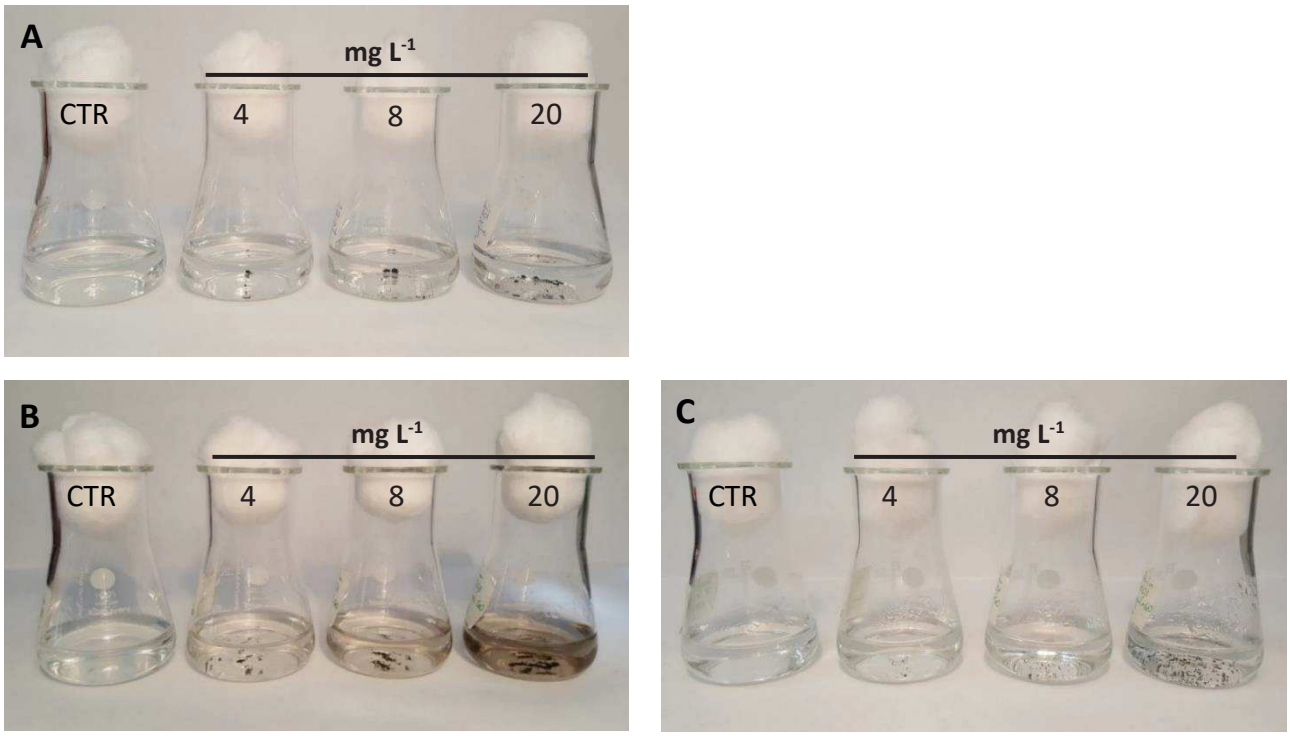

Figure S6. Visual inspection of FLG (A), GO (B), and rGO (C) dispersions at 4, 8, 20 mg L^{-1} in TG 201 medium under shaking condition (90 r.p.m.) after 72 h.

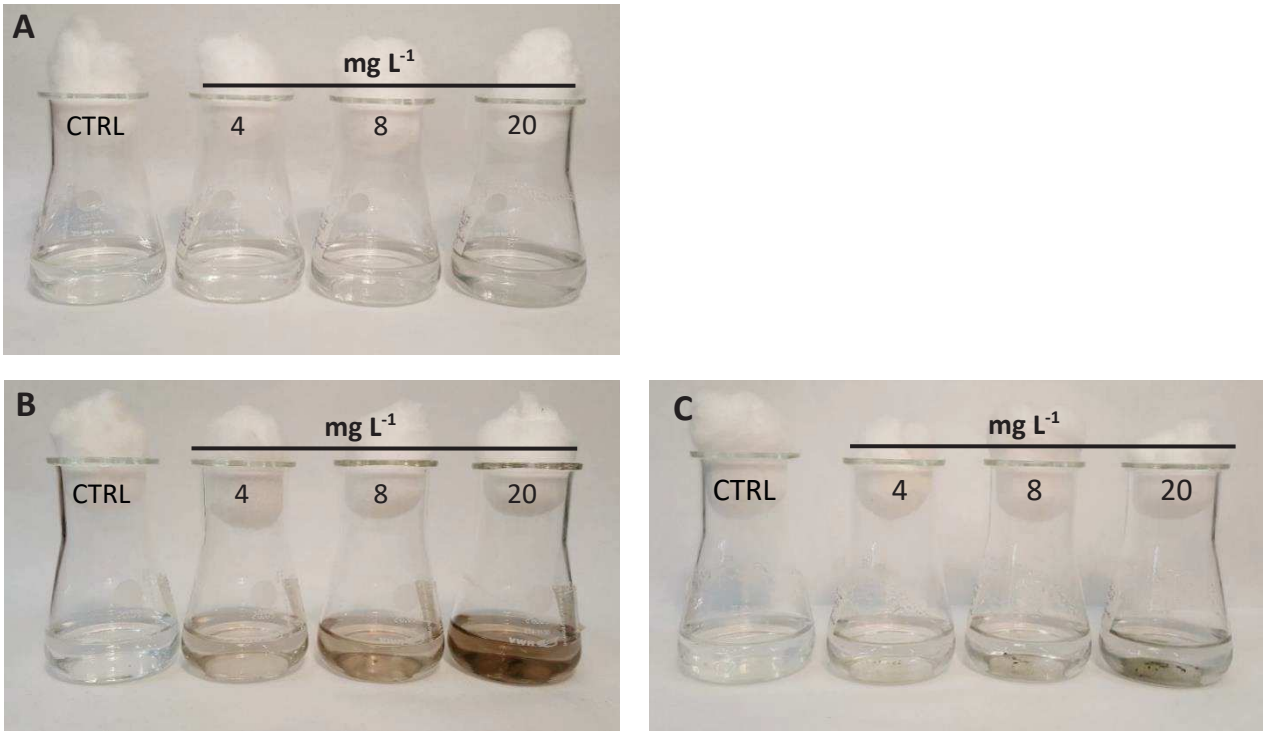

Figure S7. Visual inspection of FLG (A), GO (B), and rGO (C) dispersions at 4, 8, 20 mg L^{-1} in TG 201 medium under static condition after 72 h.

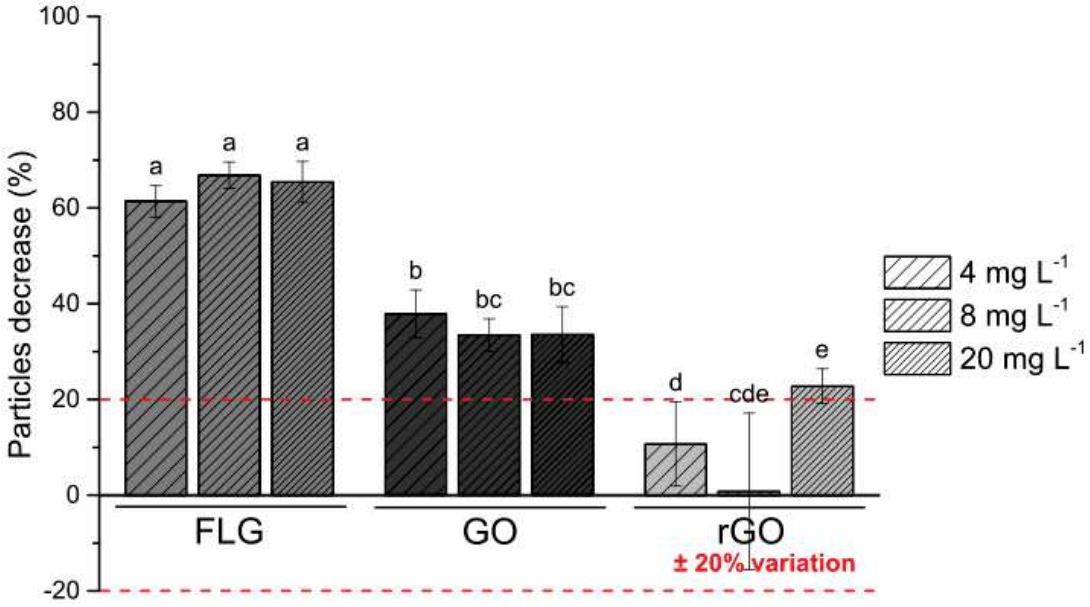

Figure S8. Per cent decrease in the number of GRMs particles (for details see section 2.4.1) observed after 24 h of testing in respect to 0 h of FLG (grey), GO (dark grey), and rGO (light grey) particles at concentrations of 4, 8 and 20 mg L^{-1} in TG 201 medium (flow cytometry analysis). The red dash lines indicate the ± 20% variation in concentration allowed by the TG 201 stability requirement. Data are reported as mean ± 1 standard deviation (n= 6). Statistically different groups are marked with different letters (GLS analysis, emmeans post-hoc test).

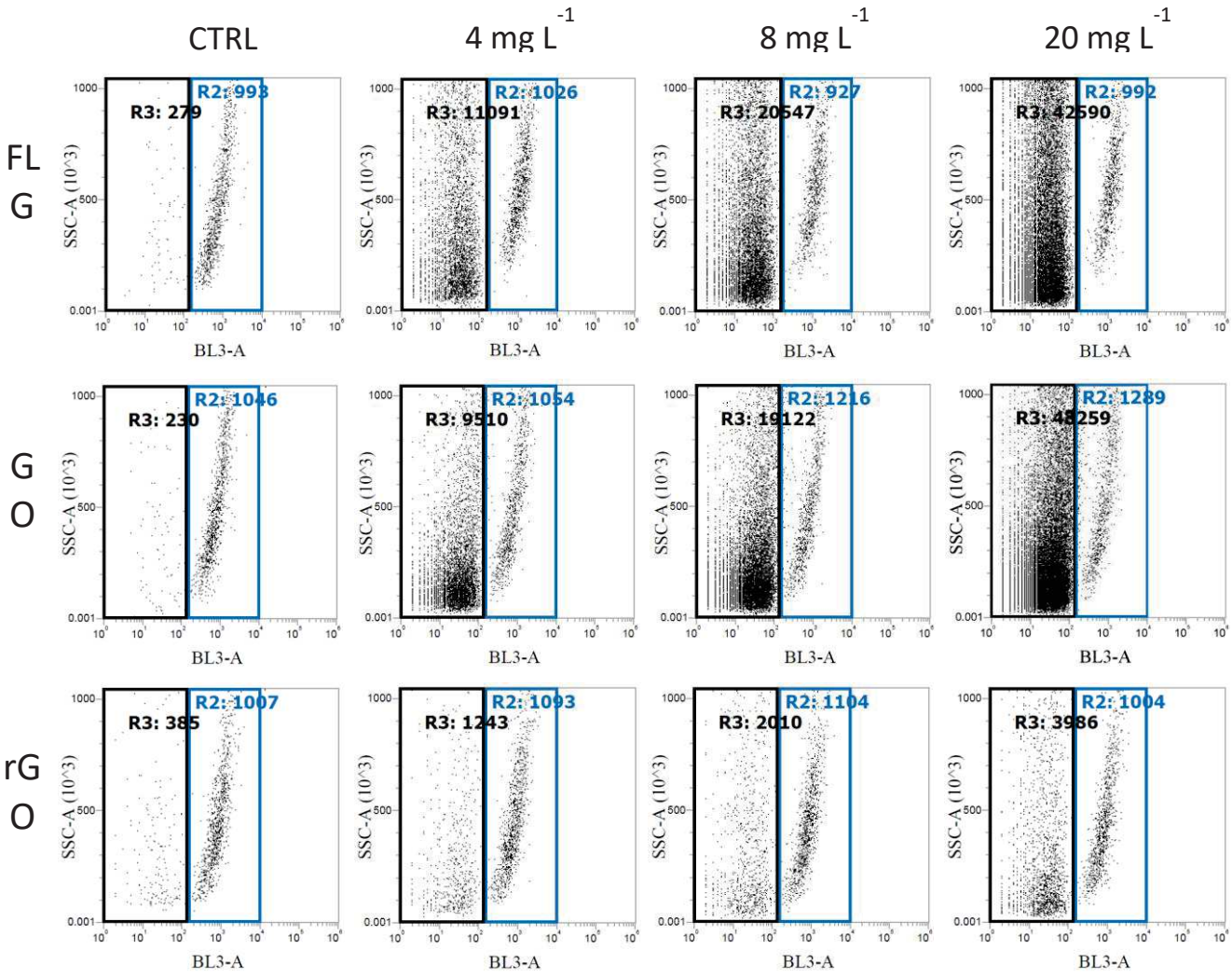

Figure S9. Flow cytometer (FCM) outcomes of FLG, GO, and rGO population (into black frame) in TG 201 medium at 0 (CTRL), 4, 8, and 20 mg L^{-1} in the presence of the algae population (into blue frame). Fluorescence was acquired using a far red BL3 filter (λ = 675-715).

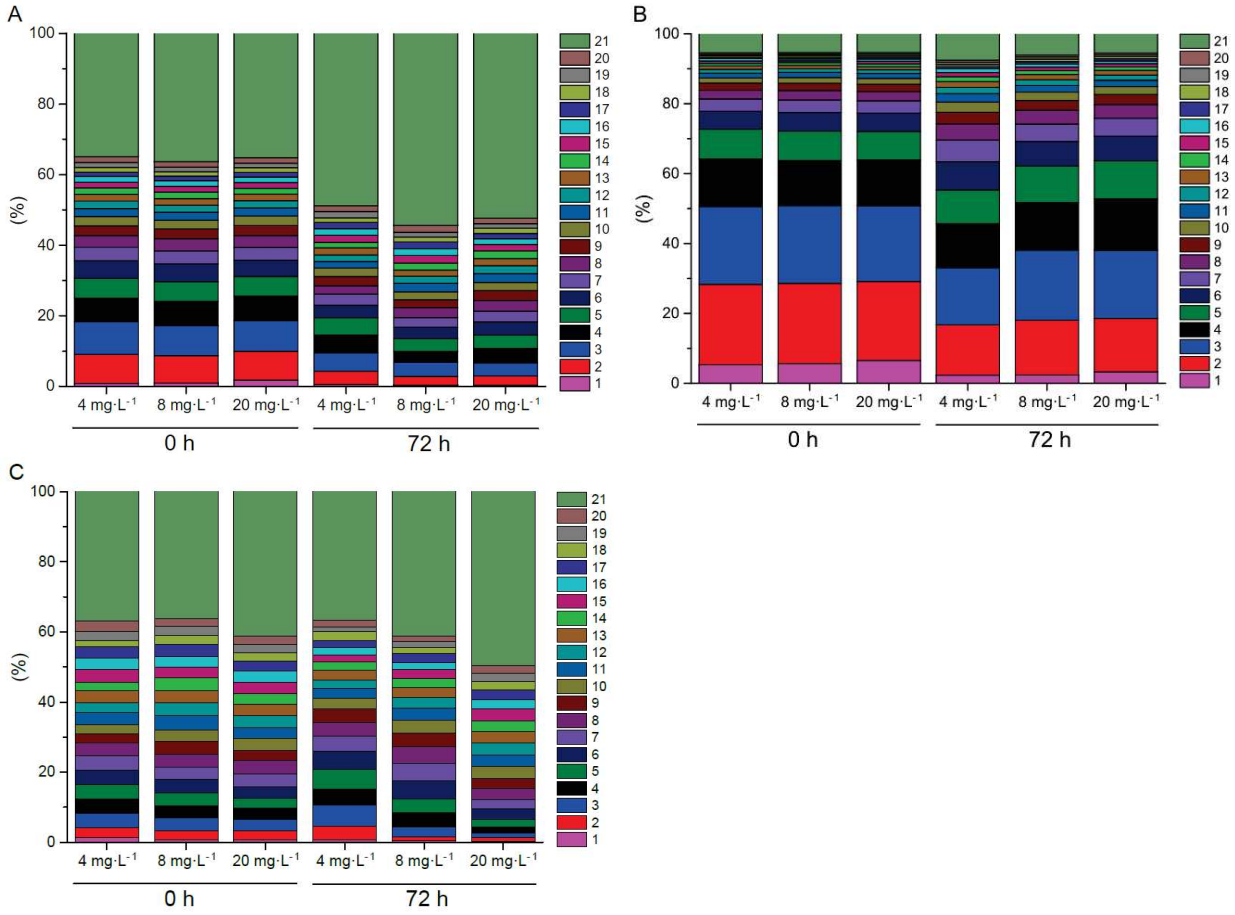

Figure S10. Per cent distribution of particles in the 21 gates determined from the side scatter (complexity) range obtained through flow cytometry analysis (for details see section 2.4.1) of FLG (A), GO (B), and rGO (C) dispersions (4, 8 and 20 mg L^{-1} in TG 201 medium) at 0 h and after 72 h of testing.

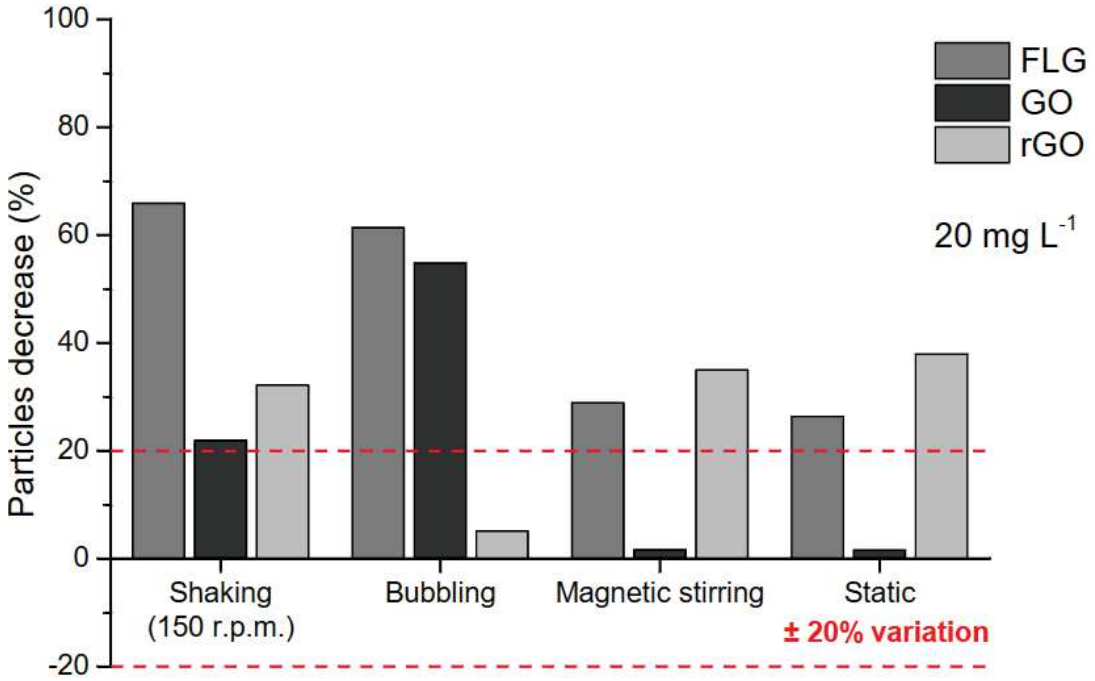

Figure S11. Per cent decrease in the number of GRMs particles (for details see section 2.4.1) in TG 201 medium dispersions (20 mg L^{-1}) subjected to various type and intensities of turbulence, namely shaking at 150 r.p.m., bubbling and magnetic stirring, and to static condition. The red dash lines indicate the ± 20% variation in concentration allowed by the TG 201 stability requirement (FCM analysis).

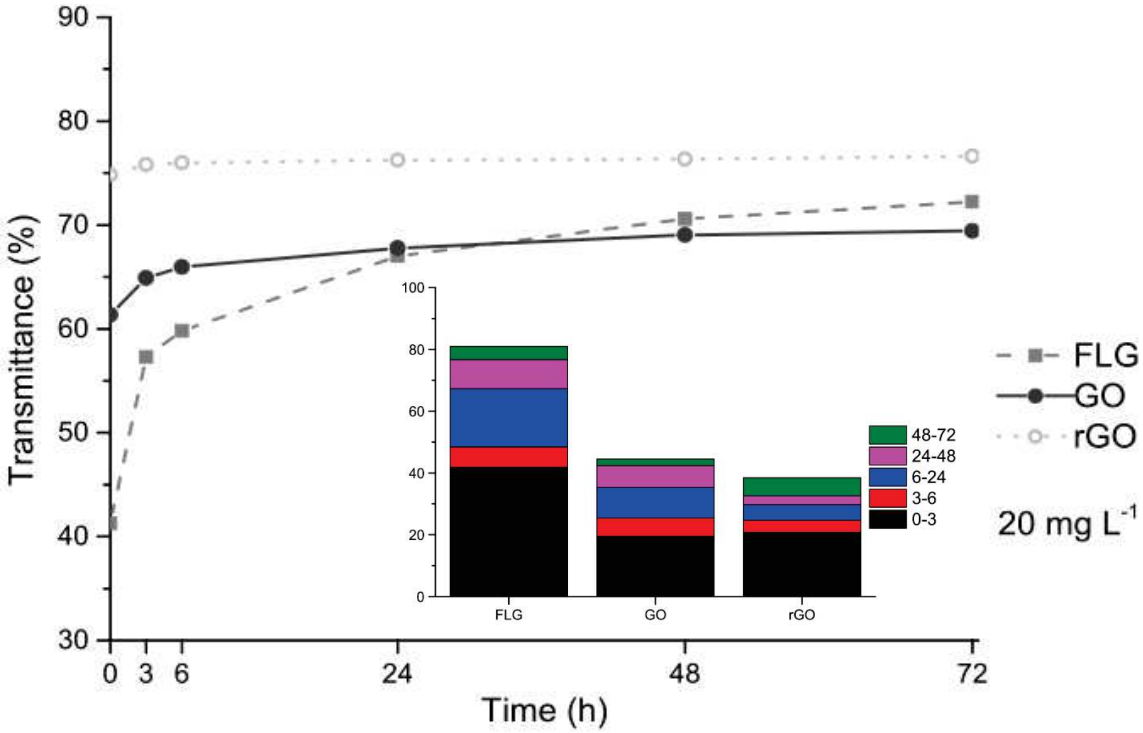

Figure S12. Transmittance variation of FLG, GO, and rGO dispersions (20 mg L^{-1}) in TG 201 medium under static condition observed at 0, 3, 6, 24, 48 and 72 h of testing. Insert: stacked histogram representing the percentage of transmittance variation occurring after 3, 6, 24, 48, and 72 h (Turbiscan analysis).

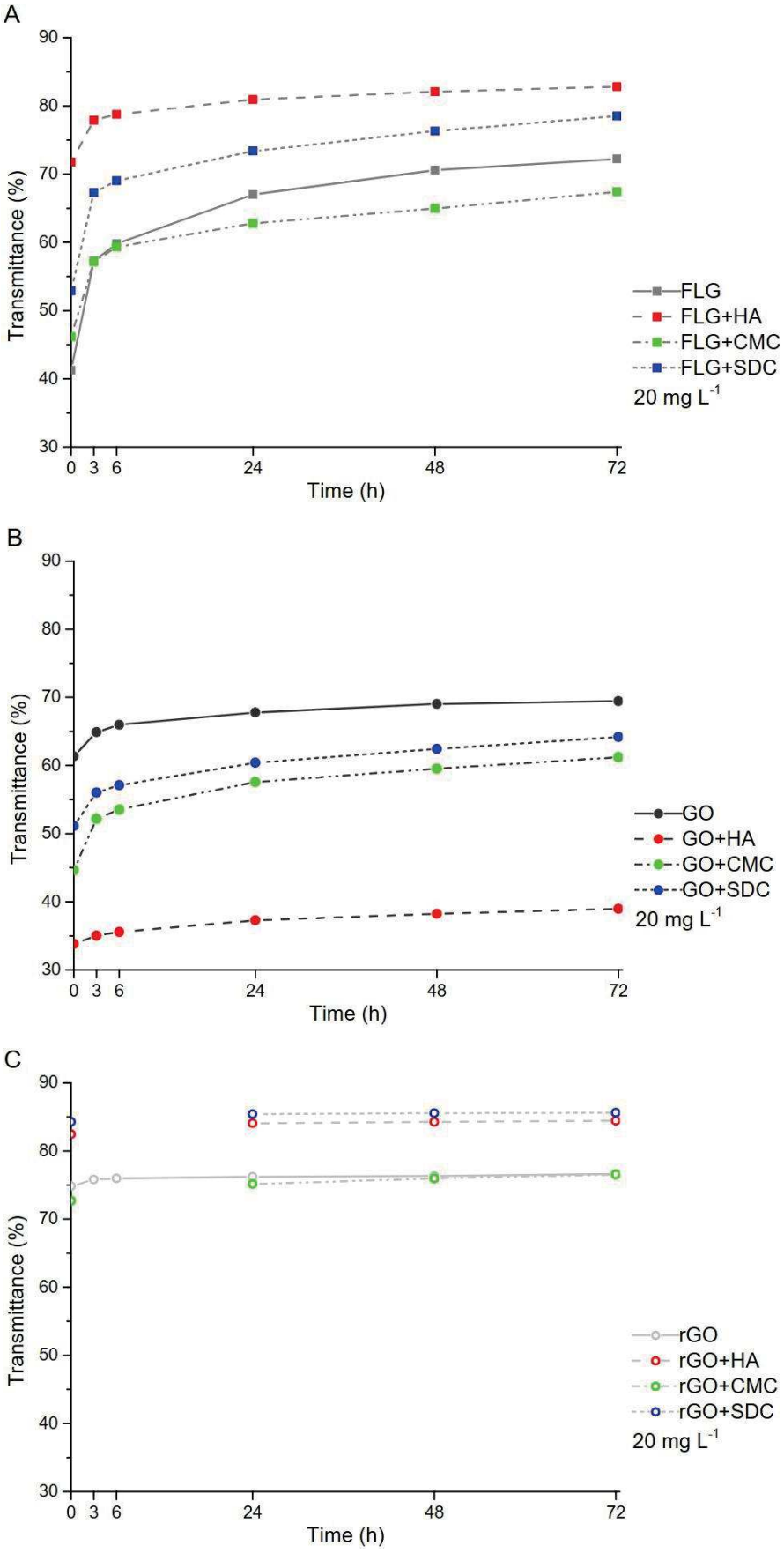

Figure S13. Per cent transmittance variation of FLG (A), GO (B), and rGO (C) dispersions (20 mg L^{-1} in TG 201 medium) observed at 0, 3, 6, 24, 48 and 72 h of testing, in absence (grey solid line) or presence of HA (dash line with red symbols), CMC (dash-dots-dots line with green symbols) or SDC (short dash line with blue symbols) (Turbiscan analysis).

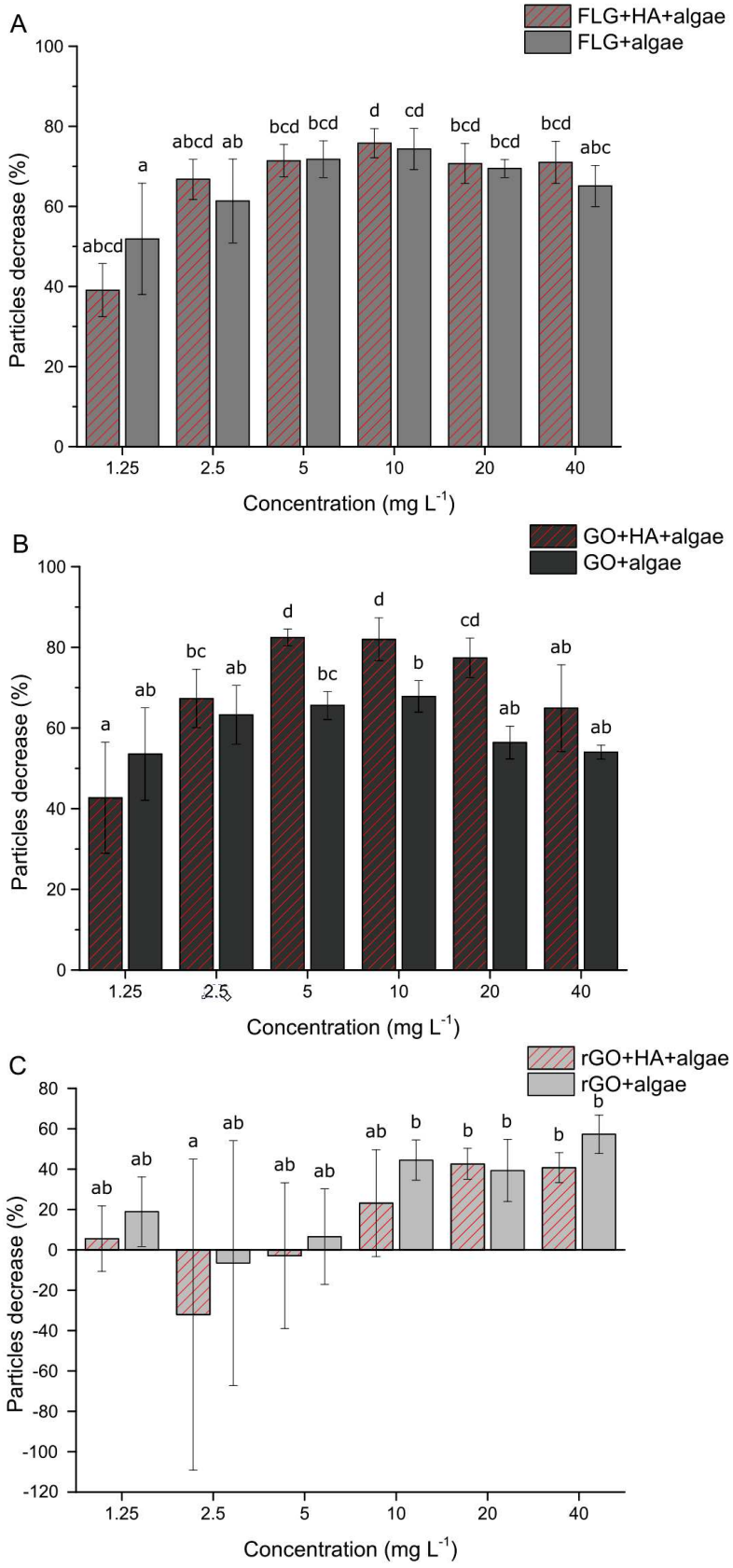

Figure S14. Per cent decrease in the number of GRMs particles (for details see section 2.4.1)in TG 201 + humic acids (HA) (red lines-patterned bars) or TG 201 (full bars) observed after 72 h of testing, both in co-presence of algae (flow cytometry analysis). The tested materials are FLG (A), GO (B), and rGO (C) at concentrations of 1.25, 2.5, 5, 10, 20, and 40 mg L^{-1} in TG 201 medium. Data are reported as mean ± 1 standard deviation (n = 6). Statistically different groups are marked with different letters (GLS analysis, emmeans post-hoc test).

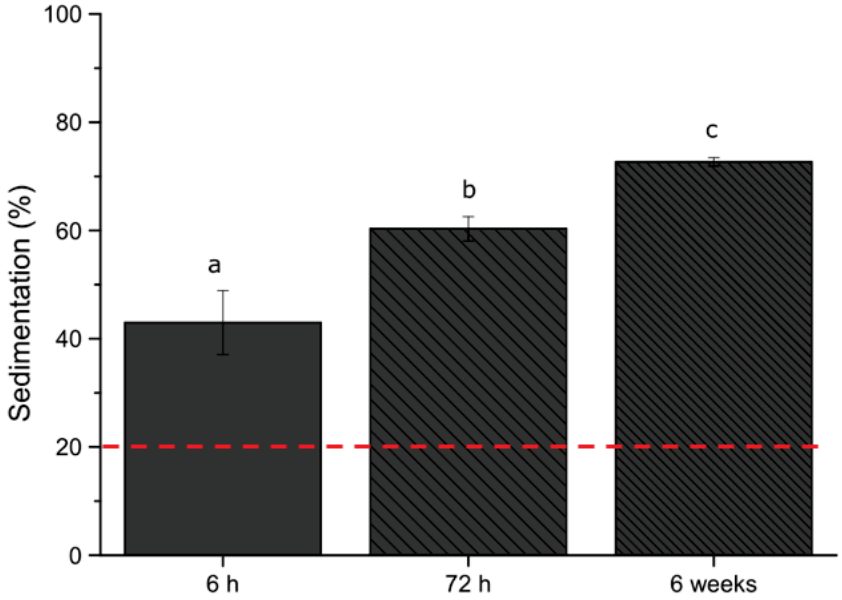

Figure S15. Sedimentation (%) of GO particles (40 mg L^{-1} in TG 201 medium dispersions) after 6 h, 72 h and 6 weeks in the Utermöhl sedimentation chambers. The red dash lines indicate the ± 20% variation in concentration allowed by the TG 201 stability requirement. Data are reported as mean ± 1 standard deviation (n= 3). Statistically different groups are marked with different letters (ANOVA analysis, Scheffe's post-hoc test).

Table S1. Physico-chemical characteristics of few-layers graphene (FLG), graphene oxide (GO), and reduced GO (rGO). Data are reported as mean ± 1 standard deviation.

	FLG	GO	rGO
Lateral size (nm)	510 ± 423	200-8000	200-8000
Number of layers	4*	1-5	1-5
C content (wt %)	93.58 ± 0.31	61.7	78.4
O content (wt %)	4.82 ± 0.08	36.4	21.15
C/O	19.4	2.2	5.2

* Calculated according to Paton et al., Nature Materials, 2014, 13, 624–630 (DOI: 10.1038/nmat3944)

Table S2. Tables of analysis of deviance of the statistical analyses relative to figures and tables presented in the paper. Signif. codes: 0 '***'; 0.001 '**'; 0.01 '*'; 0.05 '.'

A - Fig. 1

	Df	Chisq	Pr(>Chisq)	
(Intercept)	1	2.1411e+05	< 2.2e-16	***
Material	2	5.0056e+01	1.35e-11	***
Concentration	2	2.1420e-01	0.8984	
Material:Concentration	4	4.9878e+00	0.2886	

B - Fig. 4

	Df	Chisq	Pr(>Chisq)	
(Intercept)	1	337.0695	< 2.2e-16	***
Material	2	25.8742	2.407e-06	***
Time	2	1.5368	0.46376	
Material:Time	4	8.6695	0.06991	.

C - Fig. 5

A (FLG)

	Df	Chisq	Pr(>Chisq)	
(Intercept)	1	409.11	< 2.2e-16	***
Time	4	178.80	< 2.2e-16	***

B (GO)

	Df	Chisq	Pr(>Chisq)	
(Intercept)	1	130.555	< 2.2e-16	***
Time	4	87.896	< 2.2e-16	***

C (rGO)

	Df	Chisq	Pr(>Chisq)	
(Intercept)	1	191.35	< 2.2e-16	***
Time	4	133.96	< 2.2e-16	***

D - Fig. S8

	Df	Chisq	Pr(>Chisq)	
(Intercept)	1	1618.7703	< 2.2e-16	***
Material	2	275.3236	< 2.2e-16	***

Concentration	2	7.0205	0.02989	*
Material:Concentration	4	24.1293	7.525e-05	***

E - Tab. S4

	Df	**Chisq**	**Pr(>Chisq)**	
(Intercept)	1	4.9768	0.02569	*
Dispersant	2	110.7878	< 2e-16	***

F - Fig. S17

A (FLG)

	Df	**Chisq**	**Pr(>Chisq)**	
(Intercept)	1	176.6147	< 2.2e-16	***
Concentration	5	39.6785	1.734e-07	***
HA	1	2.5362	0.1113	
Concentration:HA	5	6.6058	0.2516	

B (GO)

	Df	**Chisq**	**Pr(>Chisq)**	
(Intercept)	1	219.6777	< 2.2e-16	***
Concentration	5	21.1345	0.0007640	***
HA	1	2.8929	0.0889733	.
Concentration:HA	5	25.5264	0.0001102	***

C (rGO)

	Df	**Chisq**	**Pr(>Chisq)**	
(Intercept)	1	2.0241	0.154817	
Concentration	5	16.2544	0.006154	**
HA	1	0.4040	0.525023	
Concentration:HA	5	1.6598	0.893919	

G - Tab. S5

B (GO)

	Df	**Chisq**	**Pr(>Chisq)**	
(Intercept)	1	147.284	< 2.2e-16	***
Concentration	5	161.873	< 2.2e-16	***
HA	1	94.596	< 2.2e-16	***

Concentration:HA	5	106.969	< 2.2e-16	***

C (rGO)

	Df	Chisq	Pr(>Chisq)	
(Intercept)	1	8145.9307	<2e-16	***
Concentration	5	5.3426	0.3755	
HA	1	0.8735	0.3500	
Concentration:HA	5	5.1326	0.3999	

H - Fig. S18

	Time	Residuals
Sum of Squares	0.13326667	0.00808333
Deg. of Freedom	2	6
Residual standard error	0.03670453	

Table S3. Effect of dispersants (CMC, HA, and SDC, 20 mg L^{-1}) on the GRMs stability (%) after 72 h, as a function of transmittance variation in respect to CTRL (sole GRMs), under static condition. Negative values indicating an increase in stability.

	FLG	GO	rGO
CMC	+ 8.3	- 23.6	+ 12.4
HA	-12.0	- 87.7	+ 1.7
SDC	+ 112.2	- 54.1	+ 6.2

Table S4: Algal Growth Inhibition (AGI) percentage (%) in TG+C/H/S (20 mg L^{-1}). Positive values (in red) mean a growth inhibition, while negative values (in green) mean a growth stimulation in respect to CTRL. Data are reported as mean ± 1 standard deviation (n= 6).

	CMC	HA	SDC
AGI	-4.96 ± 8.39 **a**	-31.04 ± 3.09 **b**	0.68 ± 3.00 **a**

Table S5. Algal Growth Inhibition (AGI; % in respect to control values) of FLG, GO, and rGO at 1.25, 2.5, 5, 10, 20 and 40 mg L^{-1} in TG 201 medium in the absence (-) or presence (+) of HA (20 mg L^{-1}). Positive values (in red) mean a growth inhibition, while negative values (in green) mean a growth stimulation. Data are reported as mean ± s. d. (n = 6). Data are reported as mean ± 1 standard deviation (n= 6). Statistically different groups are marked with different letters (GLS analysis, emmeans post-hoc test).

	FLG		GO		rGO	
mg·L^{-1}	**- HA**	**+ HA**	**- HA**	**+ HA**	**- HA**	**+ HA**
1.25	-0.9 ± 6.1	-5.9 ± 8.7	36.7 ± 5.0 **c**	-5.1 ± 7.3 **a**	9.5 ± 19.8 **a**	-0.6 ± 6.7 **a**
2.5	-5.2 ± 7.7	-26.6 ± 13.8	57.7 ± 4.7 **d**	-7.3 ± 7.2 **a**	-5.8 ± 31.0 **a**	-8.1 ± 5.6 **a**
5	-13.2 ± 15.8	-23.3 ± 10.3	65.2 ± 3.0 **def**	0.5 ± 6.7 **ab**	-0.1 ± 22.3 **a**	-9.6 ± 5.8 **a**
10	-7.5 ± 9.8	-18.2 ± 9.9	80.0 ± 9.2 **fg**	16.0 ± 9.7 **b**	0.0 ± 31.9 **a**	-6.6 ± 4.5 **a**
20	2.3 ± 13.1	-3.6 ± 10.7	77.3 ± 5.7 **efg**	42.5 ± 12.0 **c**	-4.3 ± 27.0 **a**	3.8 ± 11.4 **a**
40	-3.1 ± 5.3	4.9 ± 18.0	81.1 ± 5.7 **g**	63.4 ± 8.2 **de**	-8.3 ± 38.3 **a**	10.8 ± 8.7 **a**

Table S6. Concentrations of GRMs remaining in dispersion (for details see section 2.5) in the upper part of the Utermöhl sedimentation chambers after 6 and 72 h, and after 72 h in the presence of the algae.

	FLG	GO	rGO
6 h	6.9 ± 1.9	22.8 ± 2.4	14.3 ± 7.2
72 h	4.2 ± 1.0	15.9 ± 0.9	13.5 ± 4.6
72 h + algae	4.1 ± 0.7	15.3 ± 2.1	4.5 ± 4.4

Chapter 3

Graphene oxide (GO) behaviour in reconstituted and natural freshwater systems: when dispersion stability matters

Caorsi G.[1], Candotto Carniel F.[1], Crosera M. [2], Marussi G. [2], Flahaut E.[3], Prato M.[2], Tretiach M.[1]

[1]Dipartimento di Scienze della Vita, Università di Trieste, via L. Giorgieri 10, 34127 Trieste, Italia

[2]Dipartimento di Scienze Chimiche e Farmaceutiche, Università di Trieste, via L. Giorgieri 1, 34127 Trieste, Italia

[3]Centre Interuniversitaire de Recherche et d'Ingénierie des Matériaux- CIRIMAT, Université Paul-Sabatier, 118 Route de Narbonne, Cedex 9, 31062 Toulouse, France

Abstract

The widespread application of graphene-related materials (GRMs) in various innovative fields and their resulting release during the life-cycle of GRMs-containing products raise potential environmental issues that have not been yet sufficiently researched. Aquatic environments are considered the primary receptors of GRMs release, although GRMs in aqueous dispersions are unstable, leading to agglomeration/aggregation and eventual consequent sedimentation. This work aims to assess the potential fate of graphene oxide (GO), one of the most common and hazardous GRMs, in freshwater environments by investigating its dispersion stability (GODS) in reconstituted and natural fresh waters. GODS was tested in five commercial mineral waters with different ionic content and eight natural fresh waters from Friuli-Venezia Giulia (North-East Italy), in comparison with dH_2O and the standard medium recommended by the OECD Test Guideline (TG) 201. Additionally, the effect of GO dispersions on the growth inhibition of the green microalga *Raphidocelis subcapitata* was evaluated in these natural fresh waters, to verify its behaviour under more realistic environmental conditions compared to the TG 201 standard medium. Strong GO agglomeration/aggregation and sedimentation phenomena were observed in all media, especially in almost all natural fresh waters to a much greater extent than in synthetic soft media (*i.e.* dH_2O and the TG 201 medium). Physicochemical properties of water, particularly clay and ions content, accounted for the significant differences observed among the various natural freshwaters. Moreover, high GO toxicity was observed in nearly all natural waters tested, potentially exacerbated by the well-known adsorption properties of GO, which may acts as an efficient *carrier* for environmental pollutants in freshwater systems. Overall, these findings demonstrated that, given the differences in physicochemical composition between natural fresh waters and the most commonly used synthetic medium, the TG 201 could not be the best representative for assessing the environmental risk of GRMs in real freshwater conditions. Therefore, for a consistent ecotoxicological assessment of GRMs in freshwater environments, it is essential to account for and further investigate the potential ecotoxicological consequences to benthic organisms.

Keywords

Natural fresh waters, Graphene-Related Materials (GRMs), GO Dispersion Stability (GODS), environmental fate, ecotoxicology.

1. Introduction

Since graphene was first isolated in 2004, it has garnered intense research interest within both scientific and industrial communities, being considered one of the most outstanding achievements of the 21st century [1,2]. Thanks to its potential in a wide range of applications, numerous different graphene-related materials (GRMs) with unique physicochemical properties have been developed, triggering high expectations for the development of new technological applications [3,4]. Consequently, GRMs production continuously increased over the recent years, with a steep projected increase after 2024 and an estimated production in 2030 of 3461 tonnes, a remarkable 24-fold increase from 2020 [5]. As a result, these GRMs are forecasted to be mass-produced and are likely to be released into the environment and accumulated throughout their entire life cycle, from production to recycling [6]. GRMs, as other engineered NMs, may enter into freshwater environments as a result of human activities, through manufacturing and run-off events from industrial processes, accidental spills during production or transportation, leaching out during use and disposal of enriched products, or improper disposal in wastewater treatment plants [5,7–10].

Graphene oxide (GO) is one of the most exploited GRMs, with a graphene market share of more than 60% [11,12]. More than 80% of all manufactured GO could enter aqueous environments [13,14]. Thus, understanding the behaviour of GO in natural freshwater systems, such as rivers and lakes, is of pivotal importance to predict its environmental fate [11].

Moreover, GO is considered one of the most hazardous GRMs due to its reactivity and (relative) stability in aqueous suspensions [15–20], thus the presence of GO in the environment raises concerns about the potential adverse outcomes on living organisms, especially microorganisms. In particular, freshwater microalgae are highly ecologically relevant as primary producers, at the basis of the trophic food chain in aquatic ecosystems, being the primary food source for crustaceans, molluscs, and fish larvae [3,21,22]. Furthermore, due to their sensitivity to various pollutants, including NMs, they serve as vulnerable indicator organisms for assessing environmental health [23,24].

According to a number of regulations, *e.g.* the REACH regulation [25], current hazard assessments for aquatic toxicity testing often relies on standardised test guidelines (TGs) established by the Organisation for Economic Co-operation and Development (OECD). The test on growth inhibition of algae and cyanobacteria, *i.e.* TG 201 [26] is included in the basic battery of bioassays for the ecotoxicological assessment of the aquatic environment. So far, considerable research on GRMs has been conducted under controlled laboratory settings and using standardised protocols. An increasing number of studies, applying the TG 201 or similar protocols, reported adverse effects (*e.g.* algal growth inhibition, oxidative stress, genotoxicity, cell wall damages, etc.) of GRMs on algae (references in Connolly et al. [17]), and some authors also reported the poor GRMs stability in

aqueous media [27,28]. However, laboratory conditions are often much less complex than those found under real environmental ones. Therefore, there remains a remarkable gap in effectively evaluating and providing concrete evidence on GRMs risks in real water environments [11].

Following the release into the environment, the fate and transport of GRMs undergo significant changes influenced by both their intrinsic physicochemical properties and surrounding aqueous conditions, including ionic strength, ion valence, and presence of natural organic matter (NOM) [11,29–33]. Differently than guidelines standard media, freshwater environments can comprise dissolved and suspended natural organic matter (NOM), humic and fulvic acids, salts and ions, clays, heavy metals, or other contaminants [10,34]. These constituents can interact with GRMs and be adsorbed on the surface, altering GRMs behaviour. Thus, it becomes crucial to investigate the behaviour of GRMs under more realistic environmental conditions [35]. However, to date the GRMs hazard toward these environments is still poorly understood with a limited number of published research on the GRMs fate in fresh waters [10,27,34].

Following on with our previous work (Chap. 2), in which strong GRMs aggregation and sedimentation phenomena have been documented under the OECD TG 201 conditions, here the attention was narrowed down to GO for its wide potential usage and its identified toxicity. This work aims to evaluate the possible environmental fate of GO in natural freshwaters and assess its potential ecotoxicological effects on the freshwater alga *Raphidocelis subcapitata* under more realistic environmental conditions as compared to the standard OECD TGs.

2. Materials and methods

2.1 Graphene oxide (GO) preparation and characterization

The experiments were carried out using graphene oxide (GO) prepared by oxidation of carbon nanofibers (GANF Helical-Ribbon Carbon Nanofibres) by Grupo Antolín Ingeniería (Burgos, ES) using the Hummer's method [36,37]. GO was gently ground with a mortar and pestle to homogenize the as-received powder before preparing the dispersion. The material was characterized by transmission electron microscopy (TEM), thermogravimetric analysis (TGA), Raman analysis, and quantitative analyses for C, H, N, O, and S (Fig. S1).

Preparation of the GO stock- and working-dispersions

Stock dispersions (100 mg L^{-1}) of GO in the desired medium were always prepared fresh before the experiments by sonication for 30 minutes, hand-shaking the bottle every 10 minutes, in an ultrasonic bath (Elma Transsonic T 310 Ultrasonic bath, ELMA, DE). Aliquots of the stock

dispersions were then diluted to the desired final concentrations (20 or 40 mg L^{-1}) to obtain the working dispersions.

The TG 201 medium was prepared according to Annex 3 of the OECD TG 201 [26]. Commercial mineral waters were used as they were, directly from the commercially available bottles, while natural fresh waters were filtered through 0.2 µm PES filters after collection to remove undissolved and biotic components, ensuring no contamination.

2.2. GO behaviour in natural and synthetic media: evaluation of the GO dispersion stability (GODS)

The GO dispersion Stability (GODS) in aqueous media is a critical factor to investigate the asses the environmental fate of GO in aquatic environments.

To study the effect of ion composition and ion concentration on the GODS, five commercial mineral waters were chosen on the basis of their chemistry (Tab. 1). In a second series of experiments, eight natural waters sampled in different freshwater basins in Friuli Venezia Giulia (NE Italy) were tested to evaluate the fate of GO in real natural fresh waters (Fig. S2, Tab. S1).

The GODS was evaluated by visual inspection, by examining the GO flakes/particles decrease and changes in complexity using flow cytometry (FCM), and by mass-based quantification of the GO sedimentation using Utermöhl sedimentation chambers (USC) [38].

2.2.1 Effect of the ionic content on the GODS

Five commercial mineral waters, namely Sant'Anna, Levissima, Rocchetta, Vitasnella, and Fonte Essenziale (chemical properties detailed in Tab. 1), were selected on account of their different content in Ca^{2+}, Mg^{2+}, HCO_3^-, and Na^+, known to interfere with the GODS [11,39–41], and compared to dH_2O and TG 201 medium.

For the experimental procedure, 25 mL of GO dispersions (20 mg L^{-1}) in the selected media were left up to 72 h in 50 mL Erlenmeyer's flasks under orbital shaking at 90 r.p.m. (M301-OR orbital shaker, MPM Instruments, Italy). At each time-point (0, 3, 6, 24, 48 and 72 h), the GO populations were monitored by visual inspection and FCM to evaluate the changes in flakes/particles number and complexity.

2.2.2 Environmental fate of GO: natural fresh waters

Sampling sites

Natural fresh waters were collected from eight sampling sites in various freshwater basins in Friuli Venezia Giulia (NE Italy) (Fig. S2, Tab. S1), to encompass a broad variability of environmental situations.

Most of the sampling sites, with the exception of site 8 (*i.e.* the discharge channel in the Lagoon area), were selected also considering the results of a monitoring survey carried out by the regional agency for environmental protection (ARPA FVG).

Three water samples for each sampling site were collected from the water surface (approximately 30 cm depth) in either clear or dark glass bottles (depending on the analyses to carry out) filled to the brim. Water temperature was taken on-site and then the samples, stored in insulated bags, were promptly transported to the laboratory.

Subsamples of the collected waters were analysed by an accredited analysis laboratory (Gaiambiente S.r.l.). The analyses were conducted on water samples filtered through 0.2 µm PES filters unless otherwise specified. The following parameters were analysed: pH (20 °C), O_2 in saturation (%), dissolved O_2 (mg L^{-1}), C tot (mg L^{-1}), C organic (mg L^{-1}), BOD (mg L^{-1}), COD (mg L^{-1}), Turbidity (NTU), both before (_pre) and after sample filtration, and the concentration (mg L^{-1}) of Ca^{2+}, Mg^{2+}, K^{+}, Na^{+}, N tot, HCO_3^{-} (mEq L^{-1}), PO_4^{3-}, NO_3^{-}, NO_2^{-}, and SiO_2 (specific protocols used for the analyses are reported in Tab. 2). Details on the sampling sites are given in SI (Fig. S2; Table S1).

GO sedimentation and ecotoxicity assessment

To conduct these experiments, tests in Erlenmeyer's flasks and USC were performed in parallel, to both quantify the sedimentation of GO dispersions, and assess ecotoxicological effect of GO dispersions on the algal growth inhibition.

The quantification of GO sedimentation in dispersions in the eight natural freshwaters (all filtered prior to the analyses, see section 2.1) and, for comparison, H_2O and TG 201 standard medium, were conducted using the Utermöhl sedimentation chamber (USC) (Thalassia, IT). 50 mL of the afore mentioned GO dispersions (40 mg L^{-1}) were poured into the USC to the brim, the chamber was sealed and left at laboratory conditions (concentrations lower than 40 mg L^{-1} GO did not ensure reliable results due to scale limitations). After 72 h, the GO settled in the lower part of the chambers (see Chap. 2, Fig. S4) was carefully recovered and transferred into pre-weighed handcrafted aluminium foil vessels (see the method reported in Chap. 2, section 2.3). Then, they were placed in an oven at 50 °C to dry out and weighed at an analytical scale to quantify the settled mass of GO.

At the same time, different aliquots of the same GO dispersions were used to assess the potential ecotoxicity of GO when dispersed in natural fresh waters. 25 mL of GO dispersions (40 mg L^{-1}) were poured into 50 mL Erlenmeyer flasks and left for 72 h in the presence or absence (blanks) of the target alga *R. subcapitata*, the most commonly used green alga suggested by the TG 201. Moreover, at the beginning and the end of the experiment, both the GO and algae populations were monitored by FCM in blanks (without algae), CTRL (without GO), and treated samples to evaluate the decrease in the number of GO flakes/particles, changes in GO flakes/particles complexity, and algal growth inhibition (AGI %).

Exposure of the algae to the treatments

Algae were harvested from the pre-culture when in exponentially growing phase and exposed to the treatment in sterile 50 mL conical flasks containing 25 mL of desired medium at a starting algal density of $1 \cdot 10^4$ cells mL^{-1}. The test exposures were placed in a thermostatic chamber at 21 ± 1 °C under continuous illumination of 75 µmol photons m^{-2} s^{-1} from below, provided by daylight lamps (Neon Gro-Lux F18W/T8, Sylvania). All flasks were shaken 3 times per day to resuspend any settled cell and repositioned daily on the transparent plate to minimize any possible spatial difference in illumination and temperature.

The algal cell densities were measured daily to calculate the algal growth rate (AGR); then, the algal growth inhibition (AGI %), was obtained by dividing the specific growth rates of the treatments by the average growth rate of the controls in TG 201 medium, according to the TG 201 instructions (OECD, 2011). The AGI (%) was calculated to evaluate the effect of both sole natural freshwaters and GO dispersions in the tested media.

2.3. Statistical analyses

The data showed in this study were expressed as mean ± standard deviation (s.d.), unless otherwise specified.

Statistical analyses were carried out with R (R version 4.3.1, R Core Team (2023). We used generalized least squares (GLS) models ('nmle' R package), setting each parameter measured (*e.g.* particles decrease, sedimentation, algal growth inhibition, etc.) as the response variable (*e.g.* medium, sites, physicochemical parameters, etc.) and their interaction as the explanatory ones. When homogeneity of variance assumption was violated, we used the "varPower()" variance structure [42], while we log transformed the response variable when the normality assumption was violated. When the interaction was statistically significant ($p < 0.05$), differences between groups were tested and p-values were adjusted using the Holm correction through the emmeans (Estimated Marginal Means) function in 'emmeans' R package.

A Principal Component Analysis (PCA) was conducted to investigate the variation in chemical parameters across the different sampling sites. The dataset included measurements of various water quality parameters (*i.e.* pH, C tot (mg L^{-1}), Ca^{2+} (mg L^{-1}), Mg^{2+} (mg L^{-1}), K^{+} (mg L^{-1}), Na^{+} (mg L^{-1}), N tot (mg L^{-1}), HCO_3^{-} (mEq L^{-1}), NO_3^{-} (mg L^{-1}), SiO_2 (mg L^{-1})). The data were aggregated by computing the mean and standard deviation for each site, and the PCA was performed on these aggregated values after ensuring that there were no constant columns, which could lead to errors during scaling. The biplot provides a visual representation of the PCA results, where each point represents a sampling site positioned according to its principal component scores. The relative positioning of the sites indicates the similarity or dissimilarity in terms of the measured environmental parameters. Additionally, the sedimentation scores for each site were included in the biplot and represented by circles of different size, with smaller circles indicating lower sedimentation values.

A Redundancy Analysis (RDA) was conducted to identified the physicochemical parameters (*i.e.* pH, C tot (mg L^{-1}), Ca^{2+} (mg L^{-1}), Mg^{2+} (mg L^{-1}), K^{+} (mg L^{-1}), Na^{+} (mg L^{-1}), N tot (mg L^{-1}), HCO_3^{-} (mEq L^{-1}), NO_3^{-} (mg L^{-1}), SiO_2 (mg L^{-1})) that most explain the variance in the observed sedimentation values across the eight sampling sites. The RDA was performed using the vegan package in R, with the response variable being the sedimentation rate and the predictors being the physicochemical parameters. Axis scores for the sites (samples) and environmental variables were extracted and converted into data frames for visualization using ggplot2. A biplot was created to visualize the RDA results, representing the sites and environmental variables in a 2-D plane.

3. Results and discussions

The potential environmental fate of GO is not only determined by its intrinsic physicochemical properties, but is also influenced by different environmental conditions [11,29–31]. Therefore, the GODS of GO has been investigated in both natural and synthetic media. Furthermore, the ecotoxicological effect of GO on algal growth inhibition under environmental-like conditions has been evaluated.

3.1. Evaluation of the GODS

3.1.1. Effects of the ionic content

To understand the effects of the ionic content on the GODS, the focus was posed on those ions, mostly divalent, known to exert a greater impact on the stability of NMs, *i.e.* Ca^{2+}, Mg^{2+}, Na^{+}, and HCO_3^{-} [11,30,39–41]. There was a clear difference between slightly mineralized water (*i.e.* Sant'Anna)

and oligomineral, medium mineral, and rich in mineral waters (*i.e.* Levissima and Rocchetta, Vitasnella, and F. Essenziale respectively). Notably high variation in concentration ranges of Ca^{2+} (3.3 vs 23.1-593 mg L^{-1}), Mg^{2+} (0.45 vs 1.8-102 mg L^{-1}), Na^{+} (1.5 vs 2.1-14.9 mg L^{-1}), and HCO_3^{-} (11 vs 57.9-279 mg L^{-1}) was reported (Tab. 1).

Table 1. Chemical composition (as obtained from the bottle labels and manufacturers' websites) of the five commercial mineral waters used in this study (Sant'Anna, Levissima, Rocchtta, Vitasnella, Fonte Essenziale) with increasing ionic content from top to bottom, compared to the standard TG 201 medium.

mg L^{-1}	Ca^{2+}	Mg^{2+}	Na^{+}	K^{+}	HCO_3^{-}	NO_3^{-}	SiO_2	Solid residue
Sant'Anna	3.3	-	1.5	0.20	11	0.88	-	22
Levissima	23.1	1.8	2.1	1.8	57.9	1.4	5.9	83.0
Rocchetta	56.8	4.00	4.31	0.42	182.0	1.34	5.8	178.4
Vitasnella	96	29	3.5	1.2	313	2.9	10	422
F. Essenziale	593	102	14.9	-	279	<0.5	-	2490
TG 201	4.9	2.9	13.7	0.36	36.32	18.60	-	122.9

Already from visual inspection of the GO dispersions in the different tested media, it was evident that following the 72 h test period, waters with higher ionic content (*i.e.* Levissima, Rocchetta, Vitasnella and Fonte Essenziale) induced more pronounced sedimentation of GO compared to media with lower ionic content (*i.e.* Sant'Anna, TG 201 medium and dH_2O), characterised by a darker coloured dispersions and reduced amount of settled GO at the bottom of the flasks (Fig. 1).

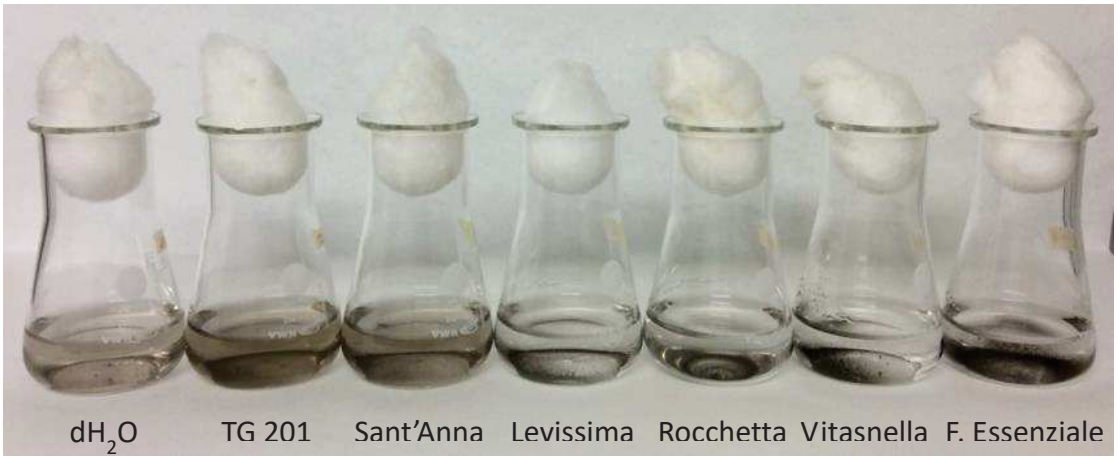

Figure 1. Visual inspection of GO dispersions (20 mg L^{-1}) in dH_2O, TG 201 medium, Sant'Anna, Levissima, Rocchetta, Vitasnella and Fonte Essenziale, after 72 h.

FCM results on the changes in GO flakes/particles complexity over the 72 h confirmed a different trend between low- (*i.e.* TG 201 medium, dH_2O and Sant'Anna) and high-ionic content media (*i.e.* Rocchetta, Vitasnella and Fonte Essenziale). As the ionic content of the medium increase, there was

a general decrease in the relative abundance of particles in gates 1-3 (low-complexity) already at time 0 h, while an increase was observed in gates 19-21 (high-complexity).

In detail, FCM analyses revealed that over the 72 h the relative abundance of low-complexity events decreased from around 45 to 30-40 % in Sant'Anna, TG 201 medium, and dH_2O, and from around 5-10 to 3-6 % in Levissima, Rocchetta, Vitasnella, and Fonte Essenziale. Instead, the relative abundance of high-complexity events increased from around 6 % to 10-20 % in Sant'Anna, TG 201 medium, and dH_2O, and from around 10-20 % to 30 % in Levissima, Rocchetta, Vitasnella, and Fonte Essenziale (Fig. 2).

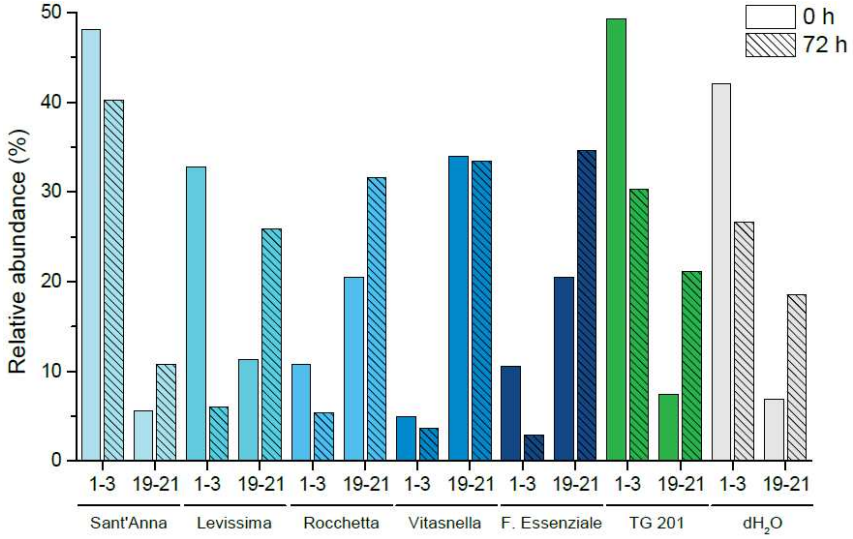

Figure 2. Percentage (%) of flakes/particles of GO dispersions (20 mg L^{-1}) under shaking conditions in five commercial mineral waters, TG 201 medium, and dH_2O in low- (1-3) and high-complexity (19-21) gates, determined from the analysis of the SSC parameter obtained through flow cytometry analysis at 0 h and after 72 h of testing.

These FCM results provided an important insight into the changes occurring to the morphology of GO flakes/particles in the different tested media. Strong differences can be observed in particles distribution between low- and high-ionic content media. Sant'Anna, TG 201 medium and dH_2O displayed a consistent pattern, where the relative abundance of low-complexity particles was predominant over the high-complexity both at the beginning and after 72 h of testing. This stands in stark contrast to Rocchetta, Vitasnella, and F. Essenziale, where the relative abundance of high-complexity particles was predominant over the low-complexity both at the beginning and after 72 h. Levissima, on the other hand, exhibited an intermediary behaviour. At the beginning of the test, the relative abundance of low-complexity particles was predominant over high-complexity ones, but after 72 h, this trend reversed, with high-complexity particles becoming predominant over low-complexity ones. These observed changes in particles complexity in a medium-dependent manner highlighted that high-ionic content media can exert a negative impact on the stability of GO dispersions. This behaviour can be attributed to the interaction of positively charged ions, present in a higher amount in Rocchetta, Vitasnella and F. Essenziale, with the negatively charged sites of GO

(*e.g.*, deprotonated carboxylic and hydroxyl groups), leading to the formation of bigger aggregates/agglomerates and the subsequent sedimentation observed in this study [13,33]. Gao et al. highlighted that in natural surface water, strong-affinity cations (*i.e.* Ca^{2+}), can move across the electrical double-layer (EDL) of GO and interact with oxygen-containing functional groups and aromatic planes. This destabilises GO flakes and initiates the aggregation process of GO primarily through complexation. Subsequently, this aggregation is further facilitated and condensed by cations with weaker affinity, including Mg^{2+} and Na^{+}, as well as by excess strong-affinity cations like Ca^{2+}, achieved through the suppression of the EDL. These results indicate that aggregation of GO in natural surface water is not only induced by a single cation or mechanism, but by complex cationic conditions [11]. Furthermore, according to Wu et al., the aggregation of GO sheets was found to be more effectively induced by Ca^{2+} and Mg^{2+} compared to Na^{+}. This phenomenon was attributed to the cross-linking mechanism facilitated by the divalent cations. Specifically, these ions act as "bridges" between the functional groups located at the edges of the GO sheets, leading to enhanced aggregation [31].

These findings confirmed the hypothesis regarding the pivotal role of the ionic composition in the GO dispersion stability, reporting a higher abundance of particles with higher complexity in waters with higher ionic content, especially Ca^{2+} and Mg^{2+}, and consequent greater sedimentation. Importantly, the higher flakes/particles complexity observed in this study could have a strong effect both on the potential environmental fate and ecotoxicological effect of GO. Indeed, the size of flakes/particles can alter the GO bioavailability by affecting its reactivity, interaction mechanism with cells, and hence the overall toxicity [11,16,27,34,43].

3.1.2. GO behaviour in natural freshwaters and its potential environmental fate

Building on the aforementioned results on the influence of ions content on GO stability, the behaviour of GO was investigated in waters from eight sampling sites selected from different freshwater basins within the Friuli Venezia Giulia region (NE Italy) with different physicochemical properties (Tab. 2) and compared to TG 201 medium and dH_2O.

Table 2. Physicochemical analyses of natural fresh waters collected in site 1 (Dimon Lake - Treppo), 2 (Tagliamento - Forni di Sotto), 3 (Tagliamento - Cornino), 4 (Tagliamento - Belgrado), 5 (Tagliamento - Latisana), 6 (Torre- Zompitta), 7 (Resurgence - S. Giorgio), 8 (Lagoon - Staranzano). Results are expressed as mean ± standard deviation (unless otherwise specified, n= 3)

	1	2	3	4	5	6	7	8	Protocol used
pH (20°C)	8.59 ± 0.27	7.94 ± 0.04	7.52 ± 0.03	7.83 ± 0.02	7.79 ± 0.04	8.28 ± 0.07	7.70 ± 0.04	7.22 ± 0.02	APAT CNR IRSA 2060 Man 29 2003
Temp. (°C)	11.00 ± 0.00	13.00 ± 0.00	14.00 ± 0.00	20.83 ± 0.29	21.50 ± 0.87	17.00 ± 0.00	17.00 ± 0.00	21.00 ± 0.00	APAT CNR IRSA 2100 Man 29 2003
O_2 in saturation (%)	101.03 ± 1.61	103.73 ± 2.29	97.80 ± 0.82	99.37 ± 0.40	101.03±1.67	13.40 ± 5.69	91.93 ± 5.36	78.57±11.15	APAT CNR IRSA 4120 A4 Man 29 2003
Dissolved O_2	8.68 ± 0.05	9.06 ± 0.09	8.58 ± 0.09	8.51 ± 0.13	9.60 ± 0.54	9.21 ± 0.50	8.19 ± 0.80	7.08 ± 0.94	
C tot (mg L^{-1})	11.87 ± 0.45	26.47 ± 1.69	29.10 ± 1.04	36.00 ± 0.40	36.53 ± 0.90	24.13 ± 0.85	51.87 ± 0.12	47.50 ± 0.85	APAT CNR IRSA 5040 Man 29 2003
C organic (mg L^{-1})	<0.1	<0.1	<0.1	<0.1	<0.1	<0.1	<0.1	<0.1	
BOD (mg L^{-1})	<2	<2	<2	<2	<2	<2	<2	<2	APAT CNR IRSA 5120 vol.2 Man 29 2003
COD (mg L^{-1})	<5	<5	<5	<5	<5	<5	<5	<5	APAT CNR IRSA 5130 Man 29 2003
Turbidity_pre (NTU)	6.67 ± 1.15	2.00 ± 1.73	4.33 ± 0.58	1.00 ± 0.00	6.33 ± 0.58	5.67 ± 2.52	3.00 ± 0.00	15.67 ± 0.58	APAT CNR IRSA 2110 Man 29 2003
Turbidity (NTU)	<0.1	<0.1	<0.1	<0.1	<0.1	<0.1	<0.1	<0.1	
Ca^{2+} (mg L^{-1})	15.8 ± 0.26	82.80 ± 1.48	76.27 ± 0.35	77.07 ± 2.70	79.20 ± 8.34	37.57 ± 1.16	81.50 ± 1.15	69.33 ± 0.75	UNI EN ISO 17294-2:2016
Mg^{2+} (mg L^{-1})	5.23 ± 0.15	20.47 ± 0.15	20.97 ± 0.15	20.00 ± 0.35	24.43 ± 2.87	10.63 ± 0.29	31.70 ± 0.00	23.57 ± 0.85	
K^{+} (mg L^{-1})	0.20 ± 0.00	0.70 ± 0.00	0.90 ± 0.00	0.90 ± 0.00	1.03 ± 0.06	0.50 ± 0.10	1.00 ± 0.00	1.77 ± 0.06	
Na^{+} (mg L^{-1})	0.93 ± 0.15	2.17 ± 0.29	3.63 ± 0.06	2.77 ± 0.06	3.60 ± 0.10	1.63 ± 0.15	4.87 ± 0.06	36.20 ± 0.62	
N tot (mg L^{-1})	<0.5	1.10 ± 0.00	1.70 ± 0.00	1.87 ± 0.15	2.80 ± 0.92	1.00 ± 0.00	7.43 ± 1.54	5.67 ± 6.81	APAT CNR IRSA 4060 Man 29 2003
HCO_3^- (mEq L^{-1})	1.65 ± 0.00	3.50 ± 0.00	3.62 ± 0.00	4.21 ± 0.10	4.22 ± 0.07	2.91 ± 0.00	5.75 ± 0.09	5.49 ± 0.23	APAT CNR IRSA 2010 Man 29 2003
PO_4^{3-} (mg L^{-1})	<0.1	<0.1	<0.1	<0.1	<0.1	<0.1	<0.1	<0.1	APAT CNR IRSA 4020 Man 29 2003

NO_3^- (mg L^{-1})	<0.1	2.20 ± 0.00	3.60 ± 0.00	3.77 ± 0.06	4.50 ± 0.00	2.30 ± 0.10	25.00 ± 0.00	0.95 ± 0.03	
NO_2^- (mg L^{-1})	<0.1	<0.1	<0.1	<0.1	<0.1	<0.1	<0.1	<0.1	
SiO_2 (mg L^{-1})	72.00	84.00	82.00	87.00	93.00	76.00	101.00	100.00	APAT CNR IRSA 3020 Man 29 2003

The PCA results (Fig. 3) identified the primary drivers of variation in water quality parameters across the eight sampling sites, highlighting distinct patterns among them, with the first two principal components capturing a significant portion of the variance. The PC1 and PC2 accounted for 67.38% of the total variance in the dataset, with PC1 explaining 47.97% and PC2 explaining 19.41%. The PC1 component was primarily driven by variations in Ca^{2+}, Mg^{2+}, Na^{+}, and N tot. The PC2 component highlights differences in HCO_3^- and NO_3^- concentrations.

Sites 1 and 6 are located on the negative side of both PC1 and PC2, suggesting lower concentrations of most measured parameters. Sites from 2 to 5 form a cluster near the centre of the plot, indicating moderate levels of the measured parameters. Site 7 is positioned towards the positive side of PC1, indicating higher levels of Ca^{2+} and HCO_3^-, while site 8 is a distinct outlier on the positive side of PC1, characterized by its unique chemical composition, particularly its high Na^{+} concentration, high turbidity, and low O_2 saturation and dissolved O_2.

These results were consistent with the geographical distribution of the eight sampling sites in the Friuli Venezia Giulia region. Sites 2-5, collected along the Tagliamento River, were clustered together, indicating a high degree of similarity among them. Similarly, the two sites located in the southeast part of the region, *i.e.* sites 7 and 8, were closer to each other on the PC1, but on opposite parts of the PC2 for the high concentration of Na^{+} in site 8, due to the presence of a saline wedge.

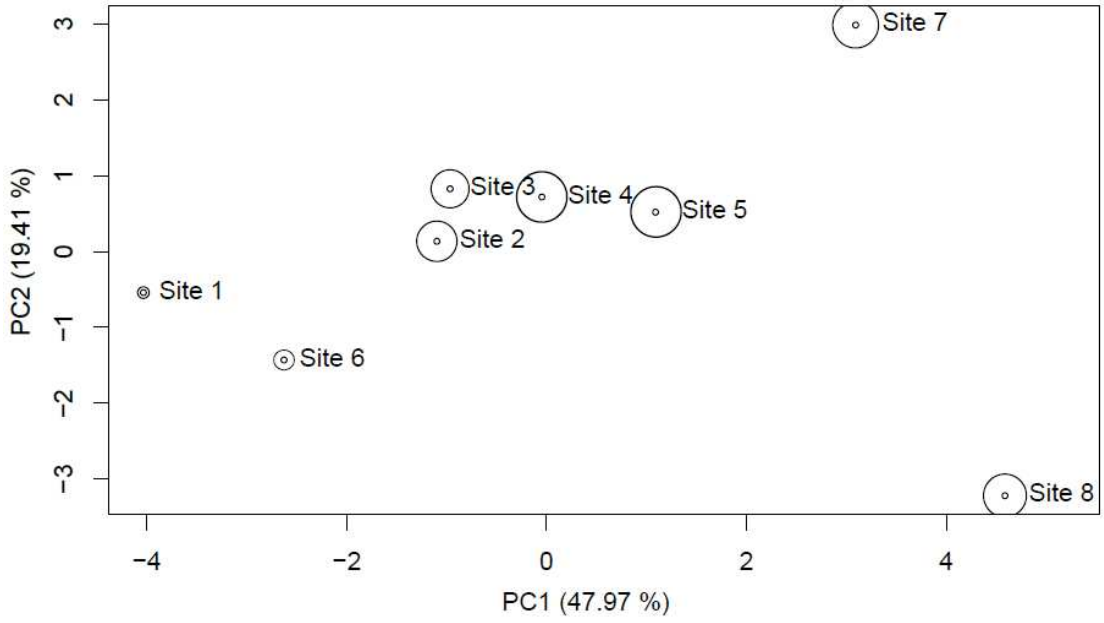

Figure 3. Biplot of score and loadings from principal component analysis (PCA) applied to water quality parameters (*i.e.* pH, C tot, Ca^{2+}, Mg^{2+}, K^{+}, Na^{+}, N tot, HCO_3^-, NO_3^-, SiO_2) for sites 1 to 8. The biplot represents the result of PCA applied to the sampling sites basing on the means ± st. dev. of the water quality parameters. (n= 3). The values of sedimentation of each site are included in the biplot and are identified by a circle (smaller circle= lower sedimentation value).

Following the release into natural fresh waters, the stability of GO might be altered not only by its intrinsic physicochemical properties, but also by the conditions in the receiving water bodies [20]. Therefore, GO behaviour in the 8 different fresh waters, TG 201 medium and dH_2O was tested.

Visual inspection of the GO dispersions in USC filled with the natural water samples showed pronounced sedimentation in nearly all of them within 72 h, resulting in the apparent removal of all GO particles from the water column. Notably, exceptions were samples from site 1, exhibiting a behaviour quite close to that of the TG 201 medium, site 6 and site 3, with a slightly enhanced stability compared to the others. Nevertheless, the GO dispersion in dH_2O exhibited the highest stability (Fig. 4).

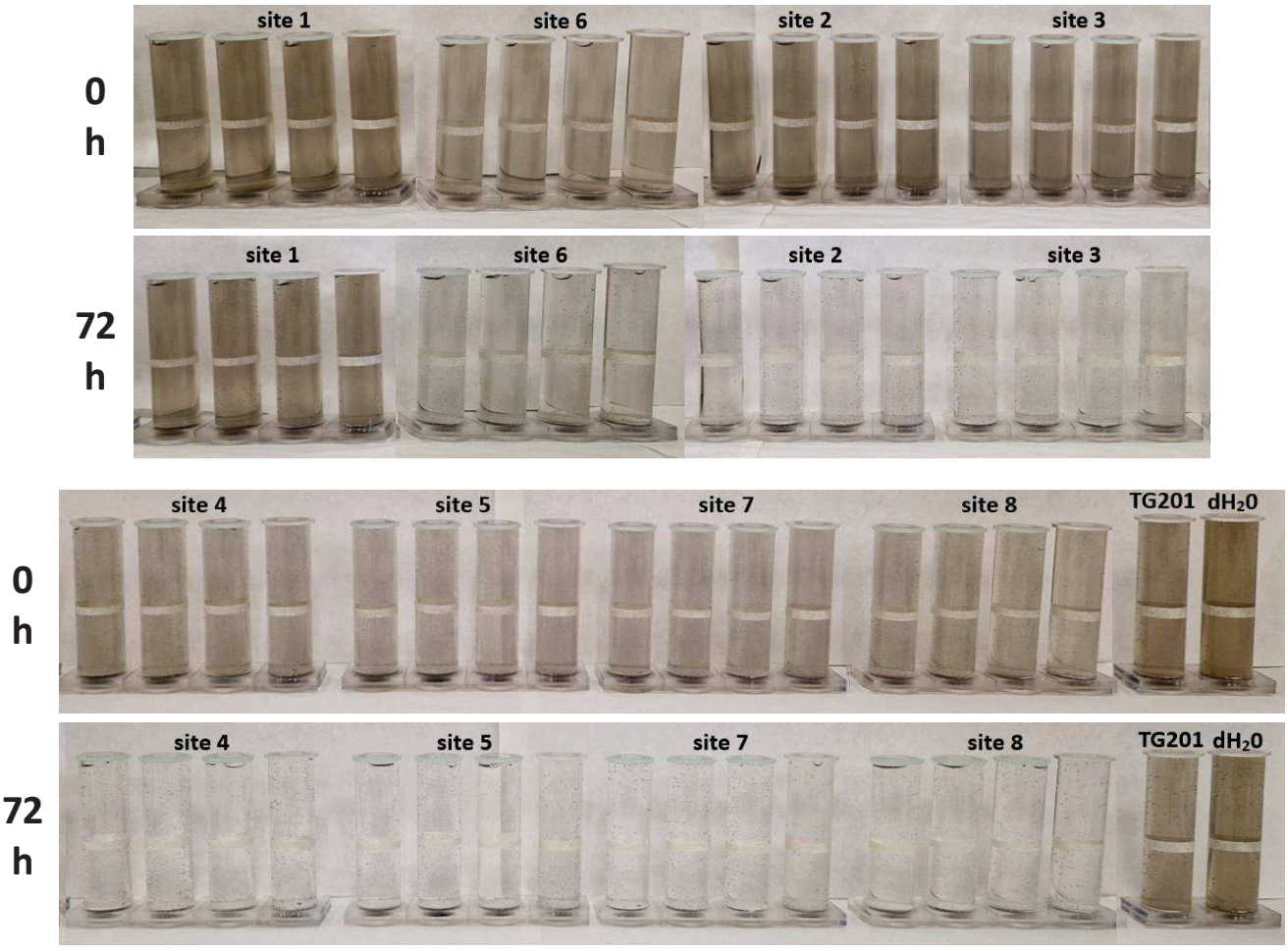

Figure 4. Visual inspection of GO dispersions (40 mg L^{-1}) in natural fresh waters from the eight sampling sites, TG 201 medium, and dH_2O, at 0 h and after 72-h settling in the Utermöhl sedimentation chambers (USC).

After 72 h, the mass-based quantification in USC reported a GO sedimentation ranging from 112.8 ± 6.7, (sites 1) to 248.9 ± 13.5 (site 4) against 66.7 ± 12.9, and 46.2 ± 8.5 % for the TG 201 medium and dH_2O, respectively (Fig. S2).

The mass-based sedimentation values in sites from 1 to 8 exceeded 100 %. Specifically, site 1 (112.8 ± 6.7) reported the lowest value, followed by site 6 (136.4 ± 20.4). These sites also exhibited

the lowest ions, total carbon, and silica content. On the contrary, site 4 (286.1 ± 8.7) and site 7 (248.9 ± 13.5) reported the highest mass-based sedimentation. These sites also exhibited some of the highest levels of ions, total carbon, and silica content. Therefore, the observed mass-based sedimentation values might have been strongly affected by the presence of salts, NOM, clay, or other components in the waters, settling on their own and/or potentially absorbed onto the settling GO particles, as previously described in section 3.1.1 [11,13,19,31,33].

As a consequence, the actual extent of sedimentation was overestimated, leading to biased results.

To overcome this issue, the evaluation of GO particles decrease in the upper column of USC was provided by FCM analysis. Following the 72 h period, the observed decrease was from 71.5 ± 6.3, and 81.2 ± 2.9 for sites 1 and 6, up to around 98 % for sites 4 to 8, against 72.2 ± 3.0, and 52.8 ± 4.9 % for TG 201 medium and dH_2O, respectively (Fig. 5).

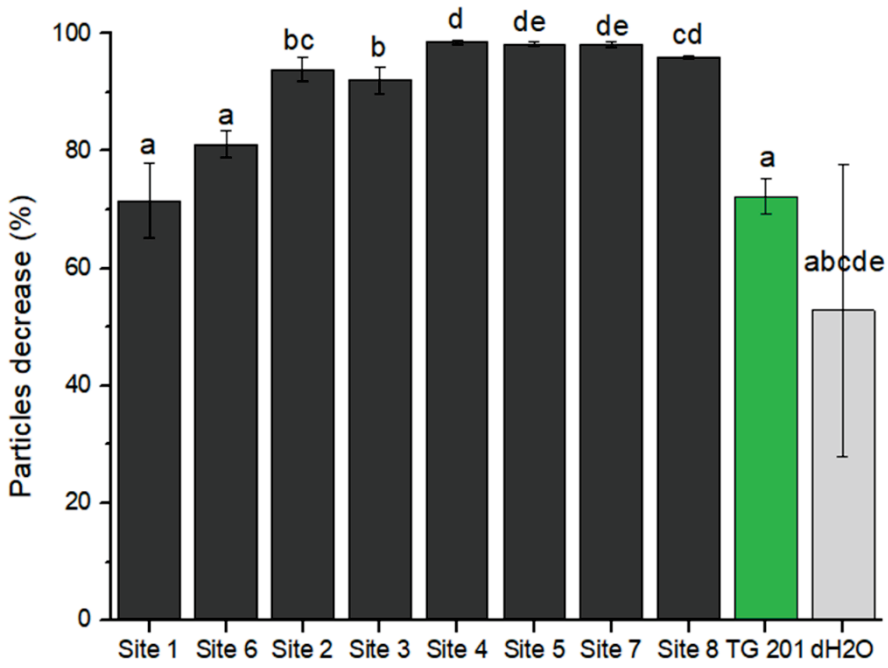

Figure 5. Decrease of GO flakes/particles (% in respect to 0 h) remaining in dispersion in the upper part of the Utermöhl sedimentation chambers (USC) in water samples from sites 1-8, TG 201 medium and dH_2O after 72 h of testing. Data are reported as mean ± s.d. (n= 4). Statistically different groups are marked with different letters (GLS analysis, emmeans post-hoc test).

As expected, both visual inspection and FCM analyses showed the highest GO stability in dH_2O. This stability is attributed to the negatively charged carboxylic groups on the GO particles, that create repulsive electrostatic interactions overcoming the van der Waals attractive forces, thereby enhancing the colloidal stability of GO [20,44].

According to visual inspection, FCM analyses reflected the same sedimentation trend, with the samples from site 3, showing a slight significant reduction in particles decrease. Notably, the

samples from sites 1, 6, and the TG 201 medium exhibited a similar behaviour with a less significant particle decrease in comparison to the others.

The redundancy analysis (RDA) model, performed to identify the physicochemical parameters that better explain the variance in the sedimentation across the eight sampling sites as described by the FCM results, showed a significant portion of the variance explained by the first RDA axis (RDA1), with an eigenvalue of 86.33 representing 94 % of the total explained variance (Fig. S3). A strong correlation between sedimentation rate and chemical parameters such as Ca^{2+}, Mg^{2+}, HCO_3^-, and K^+, with correlation values of 0.96, 0.91, 0.85, 0.73, respectively, were observed, while a value of 0.28 was observed for Na^+. Therefore, the lower sedimentation values observed in sites 1 and 6 were strongly correlated by the reduced amount of ions in the waters. These findings confirm the before mentioned results (see 3.1.1), and are consistent with existing literature [11,39–41].

Supporting this, Chowdhury et al. reported that $CaCl_2$ destabilized GO more aggressively than $MgCl_2$ and NaCl, indicating that Ca^{2+} has a greater binding capacity with hydroxyl and carbonyl functional groups on GO surface, compared to Mg^{2+} ions, which reduces the surface charge of GO [33,44]. Similar findings were reported by Gao et al., explaining in detail the different mechanisms elicited by different ions on GO particles: Ca^{2+} mainly interacts with carboxylic groups, while Mg^{2+} has a greater effect on hydroxyl groups on the GO surface, enhancing the bridging between GO sheets [11]. Therefore, although the presence of the O-containing functional groups on the GO surface makes it extremely hydrophilic, ionized functional groups caused by electrolytes in natural fresh waters generate an electrical double-layer (EDL). Electrolytes can compress this EDL, screening the surface charge of GO and promoting irreversible homoaggregation [20]. Conversely, Na^+ and K^+ have less effect on the oxygen-containing functional group but decrease the C/O ratio, inducing aggregation via EDL compression [11,31].

Upon release into waters, GO may also interact with natural colloids such as clay minerals and natural organic matter, leading to heteroaggregation. This process is considered to be dominant in governing GO transport, rather than GO homoaggregation [20,29,30].

Notably, strong correlation was also observed between sedimentation and the Si content (correlation value of 0.82), *e.g.* sites 1 and 6 having both the lowest decrease of GO flakes/particles and silica content. This parameter serves as a valuable indicator of the clay mineral content, commonly found in various freshwater environments [45,46]. Clay minerals are primarily composed of phyllosilicates, such as kaolinite, ($Al_2Si_2O_5(OH)_4$), montmorillonite ($(Na,Ca)_{0,3}(Al,Mg)_2Si_4O_{10}(OH)_2 \cdot n(H_2O)$), and illite ($((K,H_3O)(Al,Mg,Fe)_2(Si,Al)_4O_{10}[(OH)_2,(H_2O)]$), presenting different surface charge properties and geometric dimensions [30,47]. The latter two are notably rich in Ca^{2+}, Mg^{2+}, and Na^+, among other ions. Clay minerals often contain positively charged edges, which could account for the strong

sedimentation observed in this study, by interacting with the negatively charged surface of GO. Additionally, the oxygen functional groups of both GO and clay minerals could also affect their attachment [45]. Supporting this, Lu et al. studied the interactions between GO and three ubiquitous clay minerals (including montmorillonite, kaolinite, and diatomite) under various chemistry conditions. The affinity followed the order of montmorillonite > kaolinite > diatomite, indicating surface charge and surface area of clay minerals played important roles in the attachment of GO to clay minerals [45]. Zhao et al. reported that for negatively charged kaolinite, heteroaggregation with GO occurred through Lewis acid-base and hydrogen-bonding interactions after overcoming charge repulsions [29]. Furthermore, within the context of saturated porous media, it has been found that GO transport was significantly hindered in the presence of clay minerals [47].

Finally, a good correlation was observed between sedimentation and C tot, with a value of 0.8260. Surprisingly, natural freshwaters with higher amount of C tot, *i.e.* sites 7 and 8, were among the sites exhibiting a greater GO sedimentation.

As discussed in the literature, natural organic matter (NOM) molecules, widely present in natural aquatic environments, have been reported to be adsorbed on GO via hydrogen bonds, Lewis acid-base, and π–π interactions. This should lead to decreased particles aggregation through electrostatic repulsive forces and steric repulsion, increasing the GO stability [10,20,48].

However, the behaviour of GO in natural freshwater environments with high ion content can vary. Chowdhury et al. observed two opposing processes influencing the interactions between NOM and GO in synthetic surface water. First, NOM can bind with GO, providing steric repulsion and thereby increasing its stability. Conversely, in the presence of divalent cations (*e.g.* Ca^{2+}, Mg^{2+}), NOM can facilitate binding with GO functional groups through the formation of bridges between Ca^{2+} and carboxyl functional groups on GO (NOM-divalent cation bridging). This process can lead to an increased aggregation of GO flakes, reducing its stability. Therefore, GO tends to settle out in synthetic surface water in the co-presence of NOM and divalent ions, whereas the removal of divalent ions significantly enhances the stability of GO. These findings confirm the critical role of divalent ions in determining the fate of GO in aquatic environments [33].

Thus, understanding the fate of GO in freshwater systems remains challenging due to the combined effects of various environmentally-relevant conditions. Our results highlighted the significant influence of ions, especially divalent (*i.e.* Ca^{2+} and Mg^{2+}), and clay content, which detrimentally affect GO stability, thereby bearing potential implications for the environmental fate of GO. Therefore, it is essential to investigate the dispersibility and fate of GO in freshwater environments, as significant differences in stability were highlighted across different natural fresh waters. In summary, these findings indicate that once GO is released into natural fresh water, it will form

aggregates and end up in sediment in most instances. This will result in varying bioavailability and toxicity. Indeed, changes in size and shape resulting from agglomeration may subsequently alter GO stability, mobility as well as its reactivity and toxicity (*e.g.*, to algal cells) [49,50].

3.2. Effects on the algal growth inhibition

The effect of GO dispersions on algal growth inhibition (AGI) was evaluated in natural freshwaters, to test more environmental-like conditions with respect to the standard TG 201 medium. The AGI induced by both sole natural fresh waters and GO was evaluated.

Our results showed that after 72 h-exposure, the sole tested media, in the absence of GO, caused a pronounced inhibition of algal growth with respect to TG 201 medium with AGI (%) values ranging from a minimum of 42.63 ± 5.93 (site 7) to a maximum of 55.34 ± 2.19 (site 1), when AGI in dH_2O was 76.36 ± 7.76 %, due to the absence of nutrients (Fig. 8, light blue bars).

The low content of nutrients in site 1 (Tab. 2), easily explain the high AGI value because all macronutrients have to be present in adequate quantities, and in bioavailable chemical form in the medium to allow the proper growth of algae [51,52].

Furthermore, Pastorino et al. reported the presence on potentially toxic elements in the sediments collected in site 1 (Zn: 138.8 ± 0.6; Pb: 109.6 ± 1.2; As: 39.5 ± 0.7; Cd: 0.61 ± 0.02 mg kg^{-1}) [53]. The possible presence of these heavy metals in the water column, and thus in our water samples, could further explain the significant inhibition of algal growth observed in site 1 [54,55].

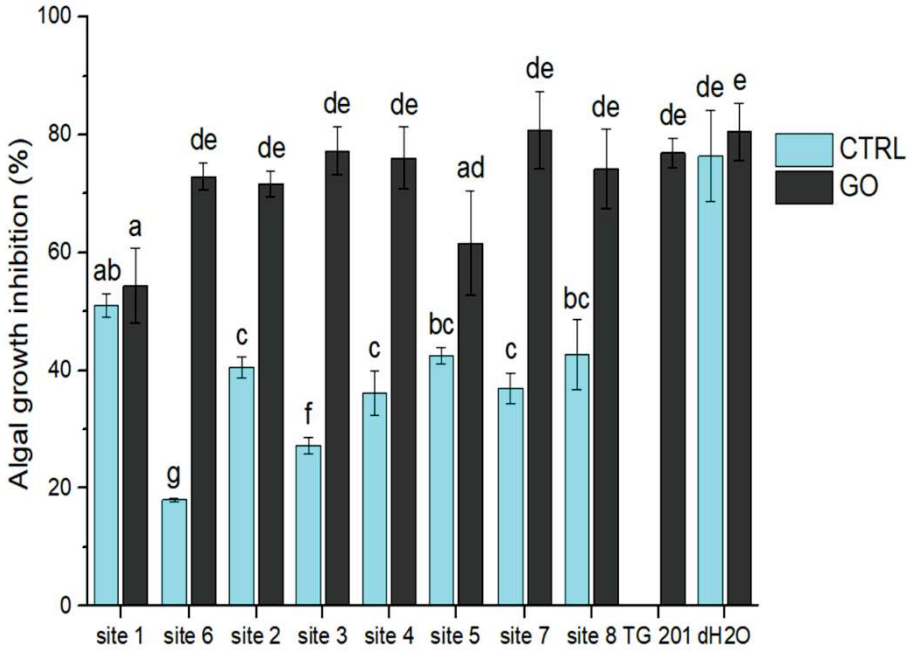

Figure 8. Algal growth inhibition (AGI %) after 72 h of testing in CTRL, *i.e.* the sole medium (light blue), and GO dispersions (40 mg L^{-1}) in sites 1 to 8, TG 201 medium and dH_2O (light grey). Data are reported as mean ± standard deviation (n= 4). Statistically different groups are marked with different letters (GLS analysis, emmeans post-hoc test).

As expected, a generally high GO toxicity was observed in almost all the waters, with AGI values exceeding 70 % in almost all the cases (Fig. 8, grey bars). The only exception were site 1 (54.4 ± 6.4 %) and site 5 (61.6 ± 8.8 %) with significantly lower AGI values. These findings are in good accordance with literature data, reporting GO as one of the most toxic graphene material [15,17,18,20].

The most intriguing aspect of our results lies in the significant increase in AGI values observed in the water samples from sites 6, 3, and 7, with a delta between controls and GO-containing waters of 54.9, 50.0, and 43.8 %, respectively. This suggests that the presence of GO in the natural fresh waters exerted a more detrimental effect on the algal growth, possibly due to the interactions with other pollutants present. Interestingly, these sampling sites were classified by ARPA as having a non-good chemical status due to the presence of nickel (site 6), benzo(α)pyrene (site 3), and glyphosate, tributyltin (TBT), and triphenyltin (TPhT) compounds (as cations) (site 7).

These findings suggest a potential absorption of environmental pollutants onto the GO surface, supporting the hypothesis that GO could act as an efficient *carrier* for pollutants within natural freshwater systems. This interaction might intensify the harmful effects on algal growth inhibition, indicating a complex relationship between GO and other co-occurring environmental pollutants.

Supporting this, among the GRMs family, GO stands out for its excellent absorption capabilities, as reported by a number of publications [56–61]. During the last few years, it has been explored for the adsorption of many environmental pollutants including oil, heavy metals, dyes, and organics [62–65]. Due to the presence of oxygen-containing groups, GO was negatively charged and hence electrostatic attraction plays an important role in the adsorption of positively charged pollutants [32]. The specific interactions for each type of pollutant may be different, and several interactions exist between GO and adsorbed pollutants including electrostatic attraction, hydrogen bonding, π bonding interaction, and Lewis acid-base interaction [66,67]. Thus, it is of pivotal importance to better explore this aspect with further research efforts.

To the best of our knowledge, this is a novelty in the GO scenario, as it is the first time that the ecotoxicological effect of GO on freshwater algae has been tested using real natural freshwaters that contain a mixture of contaminants, under conditions closer to the natural environment, as compared to the standard protocols applied with the TGs conditions. While we are aware that the tested concentration of GO is far from the levels expected in future environmental scenarios, these preliminary data could be significant in predicting the effects of potential accidental spill events.

4. Conclusions and environmental relevance

Within this study, an evaluation of the possible environmental fate of GRMs in natural fresh waters was performed by considering the impact on the GODS both under controlled (*i.e.* sole effect of ionic composition) and semi-natural conditions (*i.e* natural fresh waters). As far as we know, this is a novelty in the scenario of GO ecotoxicity, as it is the first time that the behaviour of GO effects on freshwater algae were tested under environmental-like conditions, using real natural freshwaters having different physicochemical properties and pollutants contaminations.

Our results revealed high GO agglomeration/aggregation and sedimentation phenomena in all the tested media. Notably, to a significantly greater extent in almost all natural fresh waters, compared to synthetic soft media (*i.e.* TG 201 medium and dH_2O). Significant differences among different natural fresh water were due to intrinsic water physicochemical properties. Greater complexity of GO flakes/particles and decreasing number in the water column were observed in waters with higher ions and clay content, which is an important aspect to consider, as it strongly affects the behaviour and environmental fate of the particles and, most importantly, the bioavailability for the organisms and thus the ecotoxicological effect.

As expected, a generally high GO toxicity was observed in almost all the natural waters tested, but the presence of other environmental micropollutants, both organic and inorganic, exacerbated the inhibitory effect on the algal growth of GO, given the well-known adsorption properties of GO, which may become an effective *carrier* for pollutants in natural freshwater systems.

Overall, this work demonstrated that, given the differences in physicochemical composition between natural fresh waters and the standard TG 201 medium, the TG 201 is not the most suitable tool for assessing the environmental hazard of GO in real freshwater conditions. On a positive note, due to high aggregation and sedimentation phenomena, GO – and potentially other GRMs – may remain in the water column only for a limited time. However, they are likely to accumulate in the sediment compartment, potentially exerting a detrimental impact on benthic organisms. Therefore, for a comprehensive ecotoxicological assessment of GRMs in freshwater environments, it is essential to account for and further investigate also the potential ecotoxicological consequences to benthic organisms.

7. References

1 K. S. Novoselov, V. I. Fal'Ko, L. Colombo, P. R. Gellert, M. G. Schwab and K. Kim, *Nat,* 2012, 490, 192-200.

2 K. S. Novoselov, A. K. Geim, S. V. Morozov, D. Jiang, Y. Zhang, S. V. Dubonos, I. V. Grigorieva and A. A. Firsov, *Science,* 2004, 306, 666-669.

3 L. Evariste, P. Braylé, F. Mouchet, J. Silvestre, L. Gauthier, E. Flahaut, E. Pinelli and M. Barret, *Front. Microbiol.*, 2021, 12, 598.

4 D. G. Goodwin, A. S. Adeleye, L. Sung, K. T. Ho, R. M. Burgess and E. J. Petersen, *Environ. Sci. Technol.*, 2018, 52, 4491-4513.

5 H. Hong, F. Part and B. Nowack, *Environ. Sci. Technol.*, 2022, 56, 13798-13809.

6 A. Mottier, M. Légnani, F. Candaudap, E. Flahaut, F. Mouchet, L. Gauthier and L. Evariste, *Chemosphere*, 2023, 335, 139140.

7 K. He, G. Chen, G. Zeng, M. Peng, Z. Huang, J. Shi and T. Huang, *Nanoscale*, 2017, 9, 5370-5388.

8 A. Freixa, V. Acuña, J. Sanchís, M. Farré, D. Barceló and S. Sabater, *Sci. Total Environ.*, 2018, 328-337.

9 T. Y. Sun, N. A. Bornhöft, K. Hungerbühler and B. Nowack, *Environ. Sci. Technol.*, 2016, 50, 4701-4711.

10 J. Zhao, Z. Wang, J. C. White and B. Xing, *Environ. Sci. Technol.*, 2014, 48, 9995-10009.

11 Y. Gao, X. Zeng, W. Zhang, L. Zhou, W. Xue, M. Tang and S. Sun, *Sci. Total Environ.*, 2022, 806, 150942.

12 Global Industry Analysts I, 2021. Graphene - global market trajectory & analytics. Re- search and Markets.

13 J. D. Lanphere, B. Rogers, C. Luth, C. H. Bolster and S. L. Walker, *Environ. Eng. Sci.*, 2014, 31, 350-359.

14 M. Li, J. Zhu, M. Wang, H. Fang, G. Zhu and Q. Wang, *Chemosphere*, 2019, 236, 124834.

15 A. Debroy, N. Roy, S. Giri, M. Pulimi, N. Chandrasekaran, W. J. G. M. Peijnenburg and A. Mukherjee, *Environ. Pollut.*, 2024, 341, 123015.

16 J. Zhao, X. Cao, Z. Wang, Y. Dai and B. Xing, *Water Res.*, 2017, 111, 18-27.

17 M. Connolly, G. Moles, F. C. Carniel, M. Tretiach, G. Caorsi, E. Flahaut, B. Soula, E. Pinelli, L. Gauthier, F. Mouchet and J. M. Navas, *NanoImpact*, 2023, 29, 100447.

18 H. Lin, T. Buerki-Thurnherr, J. Kaur, P. Wick, M. Pelin, A. Tubaro, F. C. Carniel, M. Tretiach, E. Flahaut, D. Iglesias, E. Vázquez, G. Cellot, L. Ballerini, V. Castagnola, F. Benfenati, A. Armirotti, A. Sallustrau, F. Taran, M. Keck, C. Bussy, S. Vranic, K. Kostarelos, M. Connolly, J. M. Navas, F. Mouchet, L. Gauthier, J. Baker, B. Suarez-Merino, T. Kanerva, M. Prato, B. Fadeel and A. Bianco, *ACS Nano*, 2024, 18, 6038-6094.

19 T. Malina, E. Maršálková, K. Holá, J. Tuček, M. Scheibe, R. Zbořil and B. Maršálek, *Carbon N. Y.*, 2019, 155, 386-396.

20 J. Ali, Y. Li, E. Shang, X. Wang, J. Zhao, M. Mohiuddin and X. Xia, *Chinese Chem. Lett.*, 2023, 34, 107327.

21 Z. Yan, X. Yang, I. Lynch and F. Cui, *J. Hazard. Mater.*, 2022, 425, 127898.

22 P. A. Neale, Å. K. Jämting, E. O'malley, J. Herrmann and B. I. Escher, *Cite this Environ. Sci*, 2014, 2,

86.

23 Z. Wang, Y. Gao, S. Wang, H. Fang, D. Xu and F. Zhang, *Environ. Sci. Pollut. Res.*, 2016, 23, 10938-10945.

24 F. Schwab, T. D. Bucheli, L. P. Lukhele, A. Magrez, B. Nowack, L. Sigg and K. Knauer, *Environ. Sci. Technol.*, 2011, 45, 6136-6144.

25 EC, 2006. Regulation No 1907/2006 of the European Parliament and of the Council of 18 December 2006 concerning the Registration, Evaluation, Authorisation and Restriction of Chemicals (REACH), establishing a European Chemicals Agency, amending Directive 1999/45/EC and repealing Council Regulation (EEC) No 793/93 and Commission Regulation (EC) No 1488/94 as well as Council Directive 76/769/ EEC and Commission Directives 91/155/EEC, 93/67/EEC, 93/105/EC and 2000/ 21/EC.

26 OECD, Test No. 201: Freshwater Alga and Cyanobacteria, Growth Inhibition Test, OECD Guidelines for the Testing of Chemicals, Section 2. OECD Publishing, Paris, 2011.

27 V. L. Castro, Z. Clemente, C. Jonsson, M. Silva, J. H. Vallim, A. M. Z. de Medeiros and D. S. T. Martinez, *Environ. Toxicol. Chem.*, 2018, 37, 1998-2012.

28 J. Yin, W. Fan, J. Du, W. Feng, Z. Dong, Y. Liu and T. Zhou, *Environ. Pollut.*, 2020, 260, 113847.

29 J. Zhao, Z. Wang, J. C. White and B. Xing, *Environ. Sci. Technol.*, 2014, 48, 9995-10009.

30 J. Zhao, F. Liu, Z. Wang, X. Cao and B. Xing, *Environ. Sci. Technol.*, 2015, 49, 2849-2857.

31 L. Wu, L. Liu, B. Gao, R. Muñoz-Carpena, M. Zhang, H. Chen, Z. Zhou and H. Wang, *Langmuir*, 2013, 29, 15174-15181.

32 Y. Zhao, Y. Liu, X. Zhang and W. Liao, *Chemosphere*, 2021, 262, 127885.

33 I. Chowdhury, N. D. Mansukhani, L. M. Guiney, M. C. Hersam and D. Bouchard, *Environ. Sci. Technol.*, 2015, 49, 10886-10893.

34 M. Markovic, A. Kumar, I. Andjelkovic, S. Lath, J. K. Kirby, D. Losic, G. E. Batley and M. J. McLaughlin, *Environ. Toxicol. Chem.*, 2018, 37, 1340-1348.

35 Y. Jiang, R. Raliya, P. Liao, P. Biswas and J. D. Fortner, *Environ. Sci. Nano*, 2017, 4, 1484-1493.

36 W. S. Hummers and R. E. Offeman, *J. Am. Chem. Soc.*, 1958, 80, 1339.

37 B. Lobato, C. Merino, V. Barranco and T. A. Centeno, *RSC Adv.*, 2016, 6, 57514-57520.

38 H. Utermöhl, *https://doi.org/10.1080/03680770.1931.11898492*, 1931, 5, 567-596.

39 W. C. Hou, I. Chowdhury, D. G. Goodwin, W. M. Henderson, D. H. Fairbrother, D. Bouchard and R. G. Zepp, *Environ. Sci. Technol.*, 2015, 49, 3435-3443.

40 OECD, *Oecd No. 137.*, 2022, 66.

41 M. M. Gudarzi, *Langmuir*, 2016, 32, 5058-5068.

42 J. Pinheiro, D. Bates, S. DebRoy, D. Sarkar, R Core Team. 2019, linear and nonlinear mixed effects models. available online: https://cran.r-project.org/package=nlme.

43 J. Yin, Z. Dong, Y. Liu, H. Wang, A. Li, Z. Zhuo, W. Feng and W. Fan, *Carbon N. Y.*, 2020, 169, 182-192.

44 I. Chowdhury, M. C. Duch, N. D. Mansukhani, M. C. Hersam and D. Bouchard, *Environ. Sci. Technol.*, 2013, 47, 6288-6296.

45 X. Lu, T. Lu, H. Zhang, Z. Shang, J. Chen, Y. Wang, D. Li, Y. Zhou and Z. Qi, *Environ. Sci. Process. Impacts*, 2019, 21, 506-513.

46 H. J. Kim, T. Phenrat, R. D. Tilton and G. V. Lowry, *J. Colloid Interface Sci.*, 2012, 370, 1-10.

47 T. Lu, T. Xia, Y. Qi, C. Zhang and W. Chen, *Environ. Toxicol. Chem.*, 2017, 36, 655-660.

48 L. Natarajan, M. A. Jenifer and A. Mukherjee, *Environ. Res.*, 2021, 194, 110669.

49 Y. Su, G. Yang, K. Lu, E. J. Petersen and L. Mao, *Environ. Pollut.*, 2017, 220, 469-477.

50 X. Hu, M. Zhou and Q. Zhou, *Environ. Sci. Technol.*, 2015, 49, 3410-3418.

51 G. Procházková, I. Brányiková, V. Zachleder and T. Brányik, *J. Appl. Phycol.*, 2014, 26, 1359-1377.

52 G. Markou, D. Vandamme and K. Muylaert, *Water Res.*, 2014, 65, 186-202.

53 P. Pastorino and M. Prearo, *Divers. 2020, Vol. 12, Page 260*, 2020, 12, 260.

54 L. de O. G. Alho, R. C. Gebara, K. de A. Paina, H. Sarmento and M. da G. G. Melão, *Ecotoxicol. Environ. Saf.*, 2019, 169, 950-959.

55 J. F. Lukavský and V. Cepák, *Algol. Stud. für Hydrobiol. Suppl. Vol.*, 2003, 110, 127-141.

56 S. Dayana Priyadharshini, S. Manikandan, R. Kiruthiga, U. Rednam, P. S. Babu, R. Subbaiya, N. Karmegam, W. Kim and M. Govarthanan, *Environ. Pollut.*, 2022, 306, 119377.

57 S. Khaliha, A. Bianchi, A. Kovtun, F. Tunioli, A. Boschi, M. Zambianchi, D. Paci, L. Bocchi, S. Valsecchi, S. Polesello, A. Liscio, M. Bergamini, M. Brunetti, M. Luisa Navacchia, V. Palermo and M. Melucci, *Sep. Purif. Technol.*, 2022, 300, 121826.

58 S. Singh, T. S. S. K. Naik, N. Shehata, L. Aguilar-Marcelino, K. Dhokne, S. Lonare, V. Chauhan, A. Kumar, J. Singh, P. C. Ramamurthy, A. H. Khan, N. A. Khan and M. H. Dehghani, *J. Mol. Liq.*, 2023, 369, 120821.

59 S. Wang, H. Sun, H. M. Ang and M. O. Tadé, *Chem. Eng. J.*, 2013, 226, 336-347.

60 K. C. Kemp, H. Seema, M. Saleh, N. H. Le, K. Mahesh, V. Chandra and K. S. Kim, *Nanoscale*, 2013, 5, 3149-3171.

61 D. Zhang, S. Wei, C. Kaila, X. Su, J. Wu, A. B. Karki, D. P. Young and Z. Guo, *Nanoscale*, 2010, 2, 917-919.

62 Y. Cao and X. Li, *Adsorption*, 2014, 20, 713-727.

63 T. M. M. Marso, C. S. Kalpage and M. Y. Udugala-Ganehenege, *Fuel*, 2017, 199, 47-64.

64 L. Chen, Q. Han, W. Li, Z. Zhou, Z. Fang, Z. Xu, Z. Wang and X. Qian, *Environ. Sci. Pollut. Res.* 2018, 25, 25840–25861.

65 Y. Qi, M. Yang, W. Xu, S. He and Y. Men, *J. Colloid Interface Sci.*, 2017, 486, 84-96.

66 G. Wei, Y. E. Miao, C. Zhang, Z. Yang, Z. Liu, W. W. Tjiu and T. Liu, *ACS Appl. Mater. Interfaces*, 2013, 5, 7584-7591.

67 J. Zhao, Z. Wang, J. C. White and B. Xing, *Environ. Sci. Technol.*, 2014, 48, 9995-10009.

Supplementary information

GO characterisation

For TEM, seven µL of the dispersions was drop-cast onto nickel or copper grids (3 mm, 200 or 400 mesh, Lacey carbon film), dried under vacuum and observed with a JEM 2100 high-resolution transmission electron microscope (HR-TEM) (JEOL JEM-2100F, JP) at an accelerating voltage of 200 kV. Images were analyzed with Fiji software to calculate the lateral size distribution.

For RAMAN, an aliquot of the GO dispersion was drop-cast onto a Si wafer or glass slide and analyzed with an in Via Raman Microscope (Renishaw, UK or Labram HR 800 Yvon Jobin, JP). At least 30 Raman measurements were collected in different locations with a 100 × objective at 633 nm and an incident power of 0.8 mW μm^{-2}. The data were normalized towards G band intensity.

For TGA, GO was characterized with a TAG16 (SETARAM) under inert Argon atmosphere, from RT to 1000 °C at 10 °C per minute.

Quantitative elemental analyses for C, H, N, O, and S were carried out with X-ray photoelectron spectroscope with K-Alpha (Thermo Fisher Scientific, USA) system using Al-Kα radiation (hν = 1486.6 eV) from a monochromatized source.

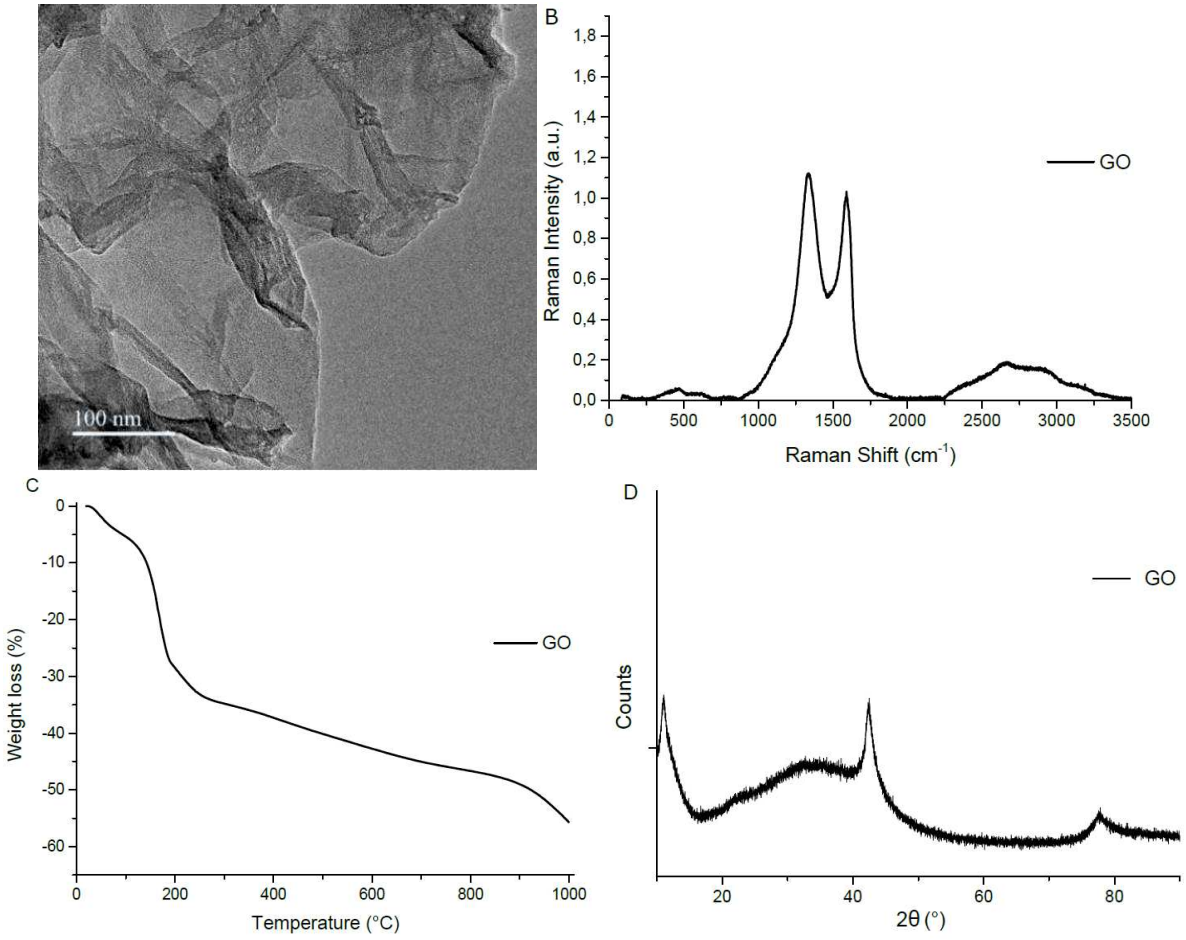

Figure S1. Physico-chemical characterization of graphene oxide (GO): representative TEM images (A), scale bar: 100 nm; Raman spectra (B); thermogravimetric analyses (TGA) (C); X-ray diffraction (XRD) (D).

Sampling sites for natural freshwater samples

Natural fresh waters were collected from eight sampling sites in various freshwater basins in Friuli Venezia Giulia (NE Italy), two in the mountain watershed (sites 1 and 2), one on the west side of the morainic amphitheater, at the border among the Friulian Prealps and the High Friulian Plain (site 3), two in the Low plain (sites 4 and 5), one in the east side of the High Plain, within the Isonzo basin (site 6), one in the resurgence belt (site 7), and one in the Lagoon area (site 8).

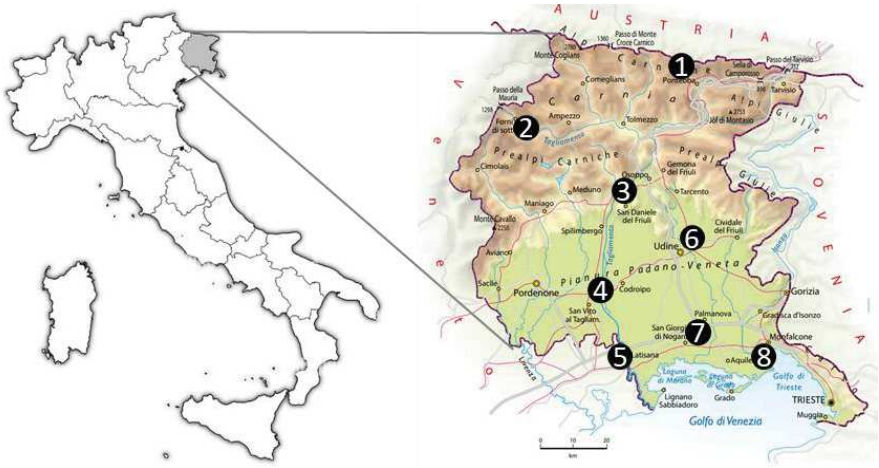

***Figure S2**: Study area and sampling sites presented in this work.*

***Table S1**: Geographical coordinates of each sampling site presented in this work.*

Site	Latitude	Longitude
1. Treppo	46°34′05.4″ N	13°03′45.8″ E
2. Forni di sotto	46°23'40.4016" N	12°41'15.7452" E
3. Cornino	46°12'51.426" N	13°0'56.916" E
4. Belgrado	45°52.728600' N	12°57.724860' E
5. Latisana	45°46.347840' N	12°59.793480' E
6. Zompitta	46°10'42.3192" N	13°15'34.398" E
7. S. Giorgio	45°49' 55.938" N	13°12'55.6812" E
8. Ris. Alberoni	45°46'11.4" N	13°30'40.8"E

Site 1 - Dimon Lake: it is a high-mountain lake located in the Carnic Alps (municipality of Ligosullo, province of Udine, Italy) at 1872 m a.s.l. This lake covers an area of 0.6 hectares, boasts a maximum depth of 4.27 meters, and its bed is constituted of sandstone and volcanic rocks [1]. Nestled in the Carnic Alps, this lake experiences very limited direct anthropogenic impacts, except for trekking and pasturing activities, and physico-chemical parameters indicate oligotrophic water [2]. Dimon lake is typical glacial-origin lake included as a Site of Community Interest and Special Areas of Conservation (SCI/SAC-IT3320002 “Monti Dimon e Paularo”).

Sites 2-5 - Tagliamento River: it flows mostly in Friuli-Venezia Giulia (NE Italy, 46°N, 12°30'E), connecting the Alps and the Adriatic Sea with its approximately 172 km-long course, not altered by human intervention [3-6]. Thus, the Tagliamento River system constitutes an invaluable resource not only as a reference site for the Alps, but as a model ecosystem for large European rivers [7,8].

Four sampling sites have been selected along its course: two in the mountain section (sites 2 and 3), and two in the plain (sites 4 and 5).

Site 2. The first selected site along the Tagliamento River is located quite close to the source, at Ponte di Sacrovint (municipality of Forni di sotto (Udine), Friuli Venezia Giulia Region, NE Italy), in the Natural Park of the Friulian Dolomites. The site is located in a mountainous area downstream of a natural gorge, near the industrial zone of Forni di Sotto. Anthropogenic impacts on this water body, even if not significant, are primarily attributed to the upstream discharge from urban wastewater treatment plants. The monitoring of the water body carried out by ARPA FVG simultaneously with the chemical status, provided good classification of the water body and analysis of priority substances has resulted in a good chemical status.

Site 3. The second sampling site along the Tagliamento River is located at Cornino (municipality of Forgaria nel Friuli-San Daniele del Friuli (Udine), Friuli Venezia Giulia Region, NE Italy), at the boundary between the Friulian Prealps and the high plain. The assessment of river functionality in this stretch is considered good. The monitoring of the water body carried out by ARPA FVG simultaneously with the chemical status, provided good classification of the water body. However, the presence of benzo(α)pyrene resulted in a non-good chemical status.

Site 4. The third sampling site along the Tagliamento River is located at Belgrado (municipality of Varmo (Udine), Friuli Venezia Giulia Region, NE Italy). The water body is located downstream of a long intermittent stretch and begins with the re-emergence of water from the sub-channel. The primary anthropogenic pressure is attributed to gravel extraction activities and the predominantly agricultural use of the surrounding land.

Site 5. The fourth sampling site along the Tagliamento River passes through the inhabited centre of Latisana (municipality of Latisana (Udine), Friuli Venezia Giulia Region, NE Italy). The monitored stretch is located downstream of the inflow of the Varmo River and upstream of the beginning of the saline wedge. The main anthropogenic pressures are attributed to agricultural land use, extensive bank protection works, and significant morphological alterations to the riverbed, both longitudinally and transversely.

The ecological status of both sites 4 and 5, monitored by ARPA FVG, is considered sufficient, with a worsening compared to the past.

Site 6. Within the hydrographic basin of the Isonzo River, a site along the Torre stream (municipality of Povoletto (Udine), Friuli Venezia Giulia Region, NE Italy) in the high plain was selected. The monitored stretch is located between the villages of Zompitta and Savorgnano del Torre, downstream of the confluence of the Cornappo stream, near the AMGA aqueduct intake structures. The primary anthropogenic pressure in this stretch is the presence of urban discharges. ARPA FVG reported an overall assessment of river functionality as good. The substance causing the non-good chemical status is nickel.

Site 7. Within the resurgence belt, a site along the Corno River (municipality of San Giorgio di Nogaro (Udine), Friuli Venezia Giulia Region, NE Italy), in the drainage basin of the Grado and Marano Lagoon, was selected. The significant anthropogenic pressures on this water body are primarily represented by intensive agricultural activities, urban discharges from the inhabited centre of San Giorgio di Nogaro, wastewater treatment plants, and the simplification of the riverbed. ARPA FVG reported an ecological status of the water body deemed sufficient primarily due to glyphosate, tributyltin (TBT), and triphenyltin (TPhT) compounds (as cations) contamination, and a consequent non-good chemical status.

Site 8. Within the Lagoon area (*i.e*. area between the mouths of the Tagliamento and Isonzo Rivers), a discharge channel exhibiting a saline wedge was selected. It is located in the Riserva Alberoni (municipality of Staranzano (Gorizia), Friuli Venezia Giulia Region, NE Italy), close to the mouths of the Isonzo River.

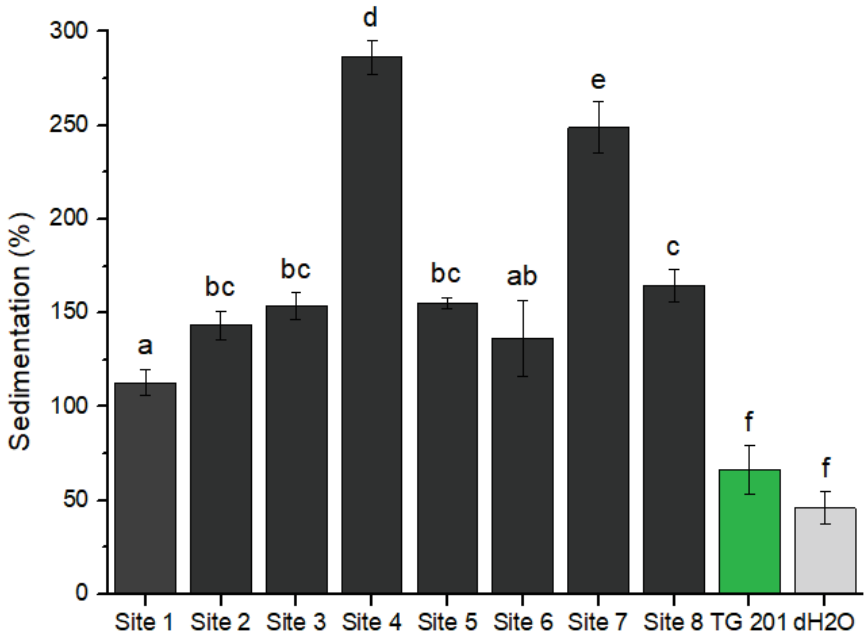

Figure S2. Sedimentation (%) of GO dispersions (40 mg L^{-1}) in water samples from sites 1 to 8, TG 201 medium, and dH_2O, after 72 h of testing in the Utermöhl sedimentation chambers. Data are reported as mean ± standard deviation (n= 4). Statistically different groups are marked with different letters (GLS analysis, emmeans post-hoc test).

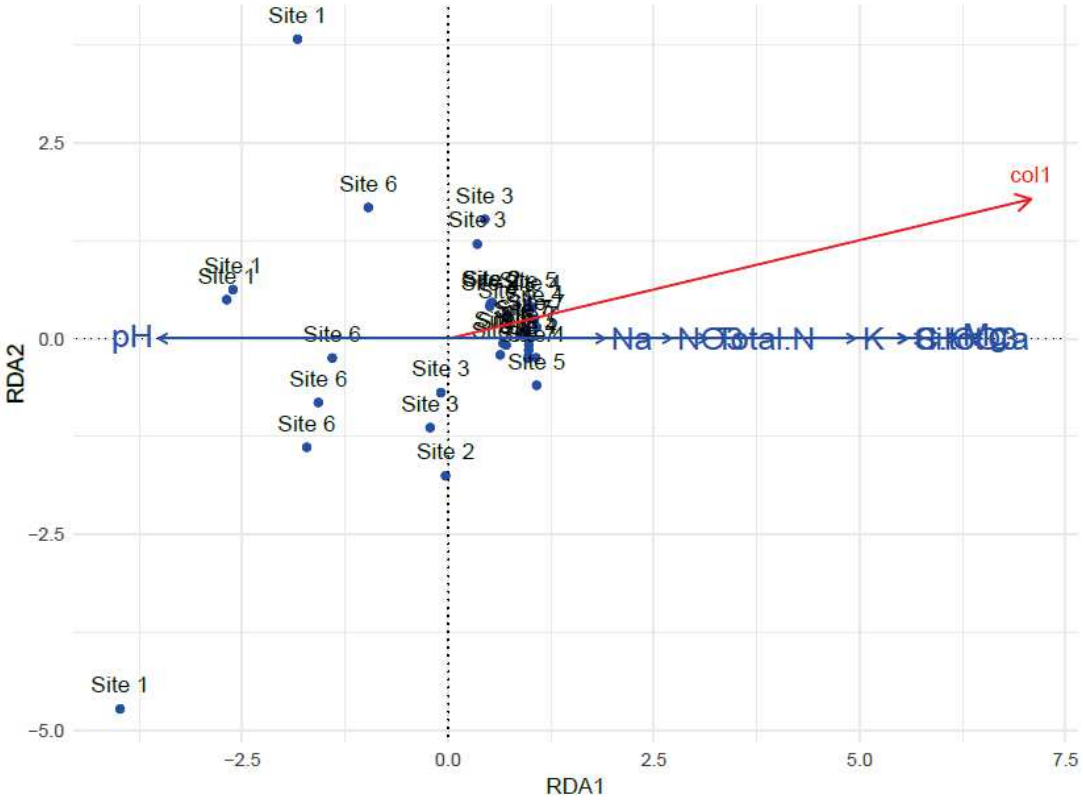

Figure S3. Redundancy analysis (RDA) of sedimentation (%) of GO dispersions (40 mg L^{-1}) in water samples from sites 1 to 8, exhibiting different physicochemical parameters (*i.e.* pH, C tot (mg L^{-1}), Ca^{2+} (mg L^{-1}), Mg^{2+} (mg L^{-1}), K^{+} (mg L^{-1}), Na^{+} (mg L^{-1}), N tot (mg L^{-1}), HCO_3^{-} (mEq L^{-1}), NO_3^{-} (mg L^{-1}), SiO_2 (mg L^{-1})) (n= 4).

Preliminary test: natural fresh waters from Doberdò lake

As a preliminary study, the GRMs dispersion stability (GDS) of FLG, GO, and rGO was evaluated in freshwaters collected from two sampling sites within the Doberdò Lake (Municipality of Doberdò, Friuli Venezia Giulia, NE Italy), located in the "Regional Natural Reserve of Doberdò and Pietrarossa Lakes", in a Special Area of Conservation (SAC IT3340006) and in a Special Protection Area (SPA IT3341002). The lake is one of the most important examples of a lentic karst freshwater system in Europe and is recognised as a site of international interest in the Friuli Venezia Giulia Region [9,10]. Doberdò lake is part of a spring system with an approximately surface area extension of 20 km^2. Underground water supply comes from springs in the western and north-western portion of the Doberdò polje (*i.e.* a large flat specifically found in karst plain), and mainly depends on groundwater inflow from the Isonzo River [11] and to a less extent the Vipava stream and rainfall [10,12,13]. For this study, two distinct sites were selected for examination. First site (45°49′59.05″ N, 13°33′15.05″ E) is located at the main spring, where the influence of groundwater is highest, while the second (45°49′43.03″ N, 13°33′57.92″ E) is at the main shallow-hole, characterized by abundance of floating hydrophytes, hereafter referred to as Dob.1 and Dob.2, respectively (Fig. S5). For the experimental procedure, 25 mL of GRMs dispersions (20 mg L^{-1}) in Dob.1 and Dob.2 were left up to 24 h in 50 mL Erlenmeyer's flasks under orbital shaking at 90 r.p.m. (M301-OR orbital shaker, MPM Instruments, Italy) or under static conditions. The GRMs populations were monitored by FCM to evaluate both the GRMs particles decrease and changes in complexity at time 0, 6 and 24 h.

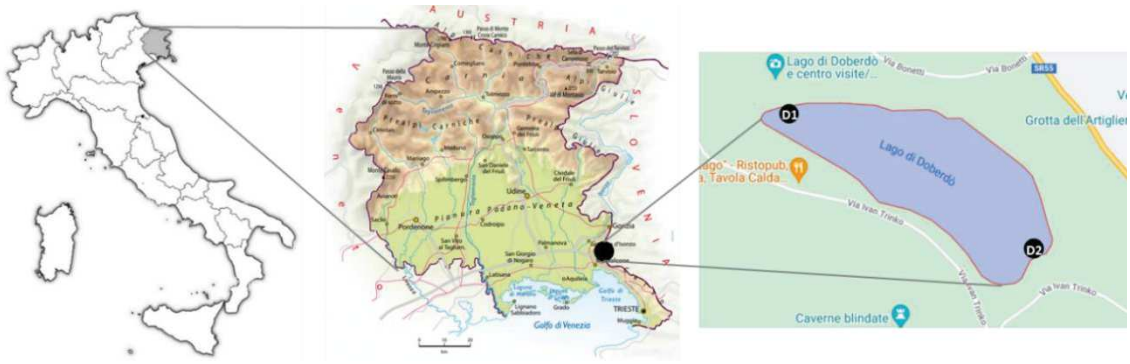

***Figure S5**: Study area and sampling sites of Doberdò lake.*

Table S2. Physicochemical analyses of natural fresh waters collected from the two sites of Doberdò lake, *i.e.* Dob. 1 and Dob. 2.

	Dob. 1	Dob. 2
pH (20°C)	7,38	7,31
Temp. (°C)	13,8	14,9
O_2 in saturation (%)	61,0	88,0

Dissolved O_2 (mg L^{-1})	6,30	8,90
PO_4^{3-} (mg L^{-1})	0,16	0,03
NO_3^- (mg L^{-1})	3,30	3,60
NH_4^+	0,20	0,16

Results and discussion

Visual inspection showed that aggregation and sedimentation phenomena occurred in all samples even though the tested materials showed differences among different media (Fig. S6). FLG dispersions showed agglomerates/aggregates at the bottom of the flasks in a similar manner in all the tested media, with the only exception of dH_2O, were smaller agglomerates/aggregates were observed (Fig. S6A).

Differently, GO dispersions showed quite strong differences in particles aggregation and sedimentation in a medium-dependent manner, exhibiting a more stable behaviour in soft media (*i.e.* TG 201 medium and dH_2O), than in Dob. 1 and Dob. 2. Furthermore, huge differences have been observed in Dob. 1 and Dob. 2, comparing shaking and static conditions (Fig. S6B). Instead rGO, as expected from our previous work (Chap. 2), was the least dispersed, independently from the media (Fig. S6C).

The FCM measurements provided an important insight on the changes occurring to the morphology of the flakes/particles during the testing period in the four different media. Over the 24 h, no significant changes have been observed for FLG dispersions in natural and synthetic media, both under shaking and static conditions (Fig. S7A-B, S8A-B). The same has been observed also for rGO, with just a slight increase in the abundance of flakes/particles in gates 1-3 (low-complexity) dispersed in Dob. 2 and TG 201 medium (Fig. S7E-F, S8E-F). Differently, GO exhibited significant differences in particles distribution between natural and synthetic media. In natural fresh water, the relative abundance of high-complexity particles (c. 30 %) was predominant already at time 0 h over the low-complexity (less than 10 %), in stark contrast to the relative abundance of high-complexity particles found in TG 201 and dH_2O (c. 10 %) over the c. 40 % of low-complexity. In detail, the relative abundance of events in gates 1-3 (low-complexity) decreased from c. 6.5 %, 7.5 %, and 43 % to 1.5 %, 1.8 %, and 38 %, in Dob. 1, Dob. 2, and TG 201, respectively, under shaking conditions, and to 2 %, 3 %, and 40 % under static conditions. While it slightly increased from c. 32 % to c. 37% in dH_2O both under shaking and static conditions. Instead, the relative abundance of events in gates 19-21 (high-complexity) increased from c. 30 %, 27 %, and 8.5 % to 42.5 %, 36.5 %, and 9 % in Dob. 1, Dob. 2, and TG 201 respectively, under static conditions, and to 51.5 %, 50.5 %, and 9.5 %, under shaking conditions. While it slightly decreased from c. 8 % to c. 6 % and c. 7 % in dH_2O under static and shaking conditions (Fig. S7C-D, S8C-D).

These first results, showing changes in particles complexity in a medium-dependent manner, highlighted that natural fresh waters, characterized by physicochemical properties quite different from TG 201 and dH_2O, can exert a negative impact on the stability of GRMs dispersions. This behaviour, particular pronounced for GO, could be attributed to the interaction of ions, present in a higher amount in Dob.1 and Dob.2, with the negatively charged sites of GO (*e.g.*, deprotonated carboxylic and hydroxyl groups), leading to the formation of bigger aggregates/agglomerates and the subsequent observed sedimentation [14,15]. This behaviour was further exacerbated under shaking condition due to the increased probability of GRMs particles collision, consistent with our previous results (Chap. 2).

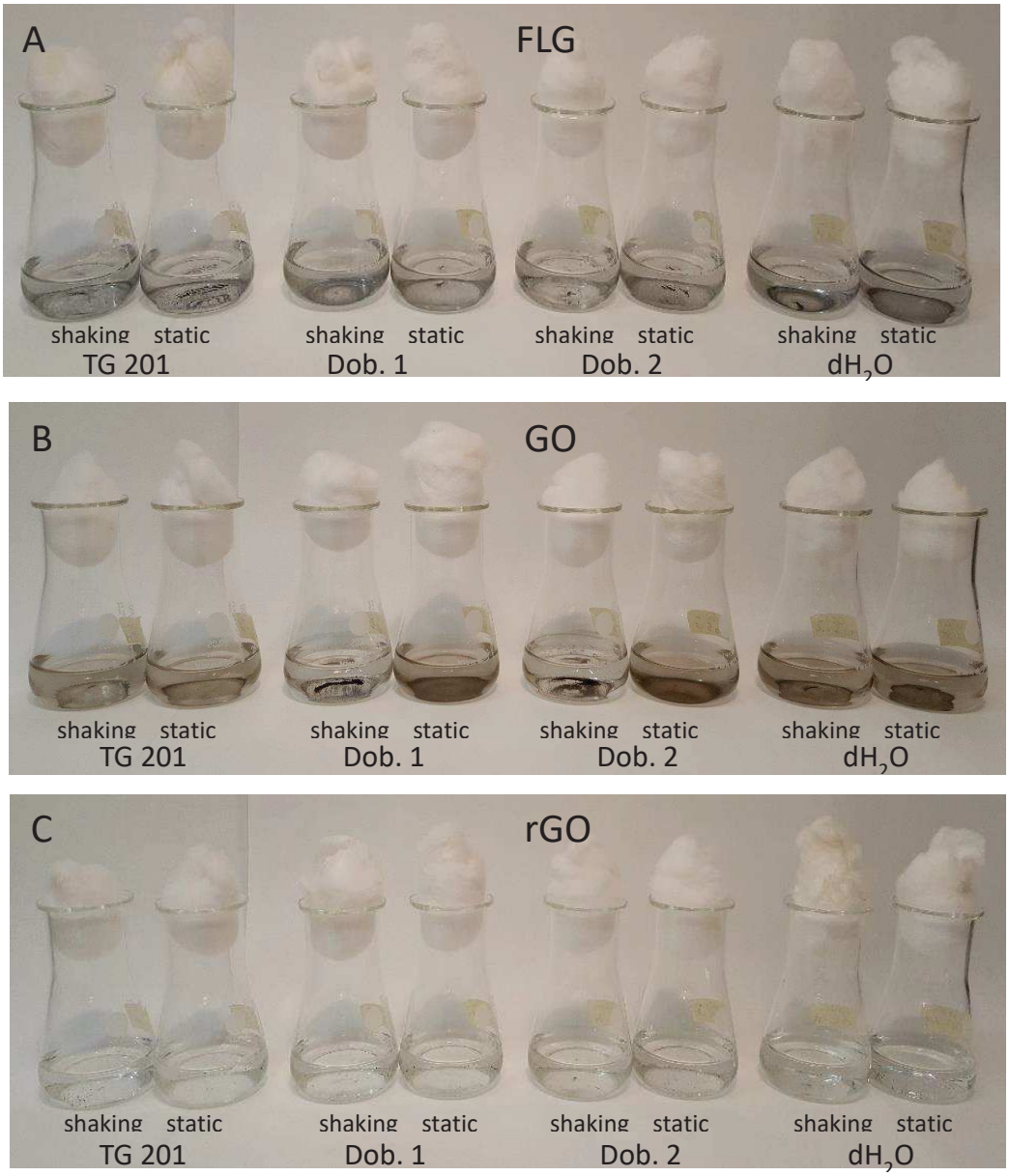

Figure S6. Visual inspection of (A) FLG, (B) GO and (C) rGO dispersions (20 mg L^{-1}) in TG 201 medium, Dob. 1, Dob. 2, or dH_2O under shaking or static condition, after 24 h.

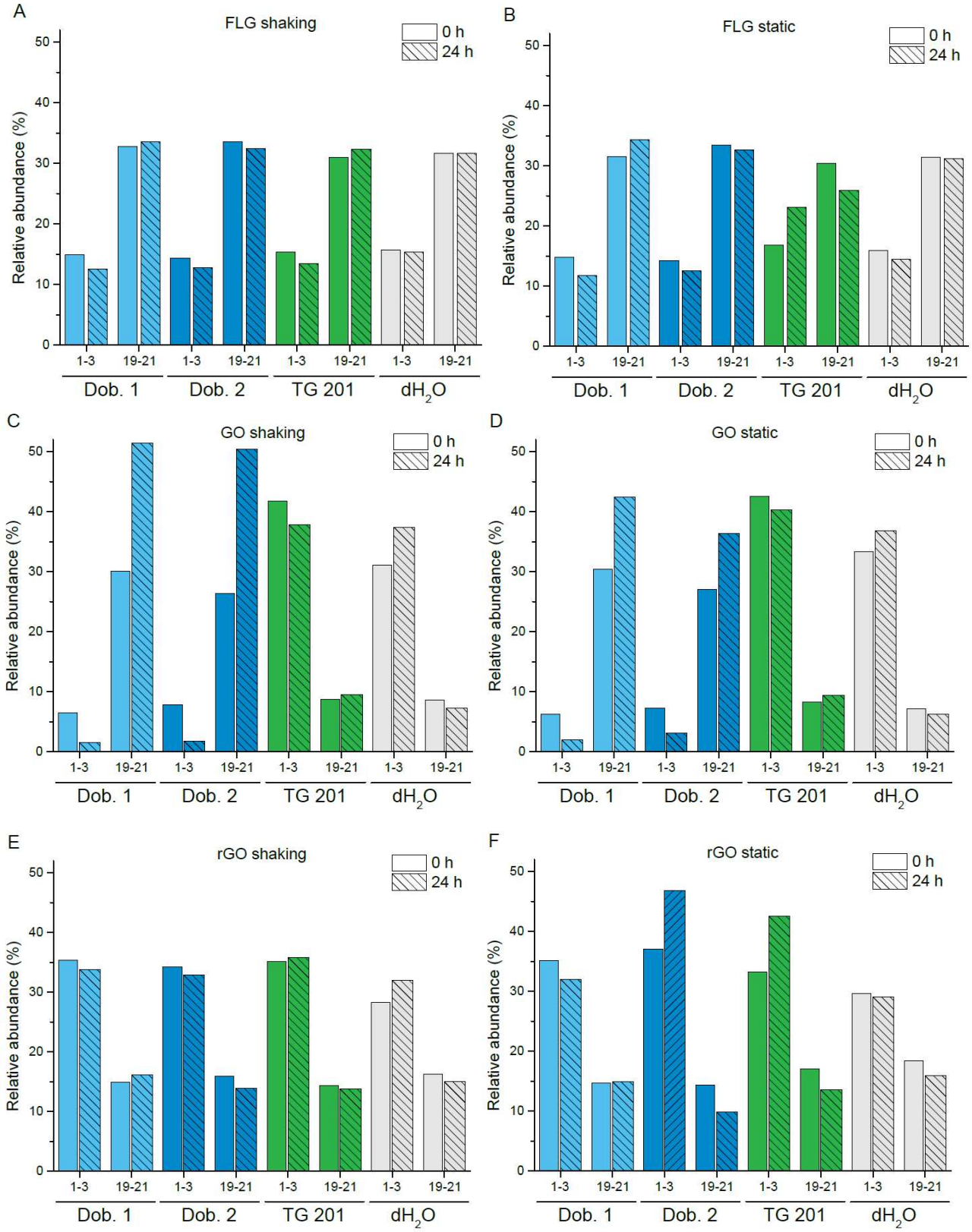

Figure S7. Percentage (%) of flakes/particles of FLG (A-B, under shaking and static, respectively), GO (C-D, under shaking and static, respectively) and rGO (E-F, under shaking and static, respectively) dispersions (20 mg L^{-1}) in Dob. 1 (light blue), Dob. 2 (dark blue), TG 201 medium (green), and dH_2O (light grey) in low- (1-3) and high-complexity (19-21) gates, determined from the analysis of SSC parameter obtained through flow cytometry analysis at 0 h and after 24 h of testing.

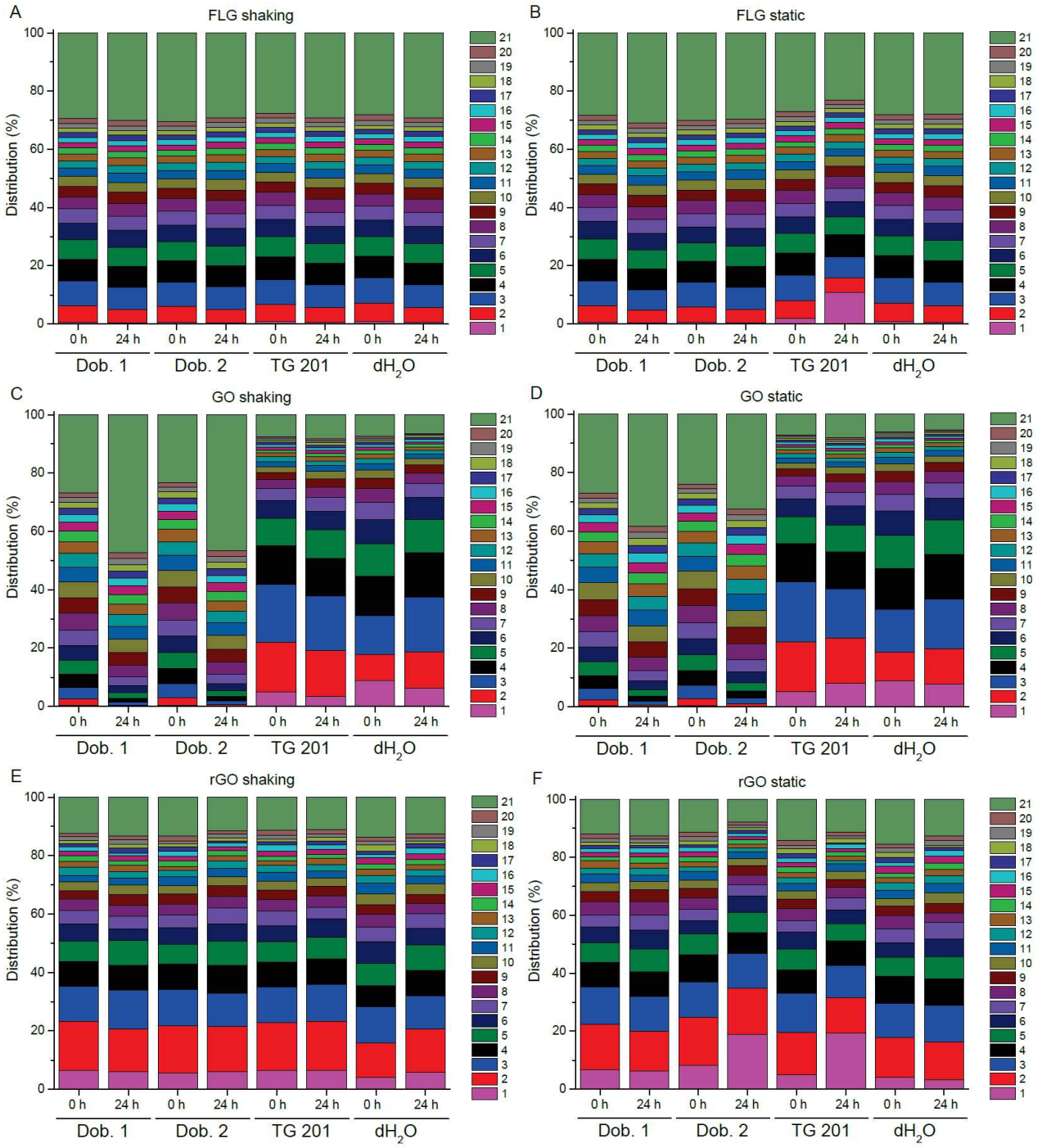

Figure S8. Distribution (%) of flakes/particles in the 21 gates determined from the SSC (complexity) range obtained through flow cytometry analysis of FLG (A-B, under shaking and static, respectively), GO (C-D, under shaking and static, respectively) and rGO (E-F, under shaking and static, respectively) dispersions (20 mg L^{-1}) n Dob. 1, Dob. 2, TG 201 medium, and dH_2O at 0 h and after 24 h of testing.

References

1 P. Pastorino, F. Polazzo, M. Bertoli, M. Santi, M. Righetti, E. Pizzul and M. Prearo, *Turkish Journal of Fisheries and Aquatic Sciences, 2020,* 20, 01-08.

2 P. Pastorino, P. Brizio, M. C. Abete, M. Bertoli, A. G. Oss Noser, G. Piazza, M. Prearo, A. C. Elia, E. Pizzul and S. Squadrone, *Sci. Total Environ.*, 2020, 698, 134282.

3 T. S. and G. V. Lippert, W., N. Müller, S. Rossel, *J. Ver. z. Sch. Bergw.*, 1995, 60, 11-70.

4 N. Müller, *Arch. Hydrobiol. Suppl.*, 1995, 477-512.

5 A. Ward, J. V., K. Tockner, P. J. Edwards, J. Kollmann, G. Bretschko and G. Gurnell, *Regul. Rivers Res. Manag.*, 1999, 15, 63-75.

6 K. Tockner, J. V. Ward, D. B. Arscott, P. J. Edwards, J. Kollmann, A. M. Gurnell, G. E. Petts and B. Maiolini, *Aquat. Sci.*, 2003, 65, 239-253.

7 J. V Ward, K. Tockner and F. Schiemer, *Risers Res. Mgmt*, 1999, 15, 125-139.

8 A. M. Gurnell, G. E. Petts, D. M. Hannah, B. P. G. Smith, P. J. Edwards, J. Kollmann, J. V. Ward and K. Tockner, *Geomorphology*, 2000, 34, 55-72.

9 M. Castello, L. Poldini and A. Altobelli, *Plant Sociol.*, 2021, 58, 75-106.

10 M. Bertoli, F. Franz, P. Pastorino, M. Prearo and E. Pizzul, *Hydrobiol.*, 2020, 847, 2123-2140.

11 C. Calligaris, F. Cucchi, A. Deana, F. Treu, E. Zavagno, L. Zini, D. Iervolino and F. Lippi, *Water hydrogeological Balance in the FVG Plain*

12 M. Bertoli, D. Lesa, A. Merson, P. Pastorino, M. Prearo and E. Pizzul, *Diversity*, 2022, *14*(6), 460.

13 D. Samez, G. Casagrande, F. Cucchi, L. Zini, E. D. I. Pietrarossa, C. Classico, R. Con, L. E. Piene, D. E. I. Fiumi and V. E. Timavo, 2005, 40, 133-152.

14 J. D. Lanphere, B. Rogers, C. Luth, C. H. Bolster and S. L. Walker, *Environ. Eng. Sci.*, 2014, 31, 350-359.

15 I. Chowdhury, N. D. Mansukhani, L. M. Guiney, M. C. Hersam and D. Bouchard, *Environ. Sci. Technol.*, 2015, 49, 10886-10893.

General conclusions and future perspectives

In summary, this PhD thesis provided a deep investigation into the behaviour of GRMs in aqueous media, addressing most of the key gaps related both to a reliable application of the TG 201 to GRMs and also to the potential environmental fate of GRMs in freshwater ecosystem.

The main output of the first study has been the identification of a suitable methodological approach needed for a reliable testing of TG 201 to GRMs, avoiding the biases reported in the literature. This innovative methodological approach suggest the employment of flow cytometry (FCM) analyses as a fast and reliable tool for a proper evaluation of the algal growth inhibition, *i.e.* the TG 201 test end-point, and also for monitoring the GRMs behaviour in aqueous media.

In the second study, focused on the verification of the applicability of the TG 201 to GRMs, a delayed starting time of the test, which should be tailored case-by-case, has been suggested in order to ensure a more stable and homogeneous GRMs dispersions and thus to improve the applicability of the TG 201 to GRMs and the robustness of the ecotoxicological results. Furthermore, the aggregation and sedimentation phenomena observed raised concerns on the EC_{50} values reported in a number of publications (Connolly et al. 2023, and references therein), which could be strongly underestimated.

These data on TG 201 applicability to GRMs will be used to generate documents explaining the limitations of this TG and the possible solutions to improve its applicability to GRMs and robustness. So far, this work has been proposed at the OECD level, the proposal has been approved by the OECD Working Party on Manufactured Nanomaterials (WPMN) and the Working Group of the National Coordinators of the Test Guidelines Programme (WNT), and it was included in their program of work. The final outcome will consist on one or several annexes to the Guidance Document 317 ("Guidance Document on Aquatic and Sediment Toxicological Testing of Nanomaterials"), referring to the applicability of the three mentioned TGs to nanomaterials taking also into account the case of GRMs.

Finally, since standard protocols using controlled laboratory settings represent a much less complex system than real environmental settings, the results obtained by TG 201 testing could not be representative of a real condition in the environment. Thus, within the last chapter, the potential environmental fate of GRMs in natural fresh waters has been assessed.

Overall, the whole dataset clearly demonstrated that, given the differences in physicochemical composition between natural fresh waters and the TG 201 medium (*e.g.* NOM, ions and clay content), a significantly greater agglomeration/aggregation and sedimentation of GRMs occurred in natural fresh waters as compared to synthetic soft media (*i.e.* TG 201 and dH_2O). Thus, the TG 201 might not be the best representative for assessing the environmental risk of GRMs to freshwater

environments, and instead potential ecotoxicological consequences to benthic organisms should be considered.

Furthermore, the observed changes in particles complexity is another important aspect to take into account, as it strongly affects both the behaviour and environmental fate of the particles, and the bioavailability for the organisms, altering the ecotoxicological effect.

The last important aspect that has been considered and investigated is the combined ecotoxicological effect of GRMs and natural fresh waters on algal growth inhibition. As far as we know, this is a novelty in the GRMs scenario, as it is the first time that the ecotoxicological effect of GO on freshwater algae has been tested under environmental-like conditions, using real natural freshwaters.

These findings provide an interesting starting point that offers various insights to be further explored in the future. Considering the well-known adsorption properties of GO with contaminants, it will be worth investigating the role played by GO as a vector for pollutants in natural freshwater systems. While GO could act sequestering pollutants from water column, the flip side of the coin is that, considering its sedimentation behaviour, it could potentially lead to an accumulation in the sediments.

References

1 P. R. Wallace and P. R. W. Ace, *The Band Theory of Graphite*, 1947, vol. 71.

2 W. McClure, *Phys. Rev.*, 1956, 104, 666–671.

3 G. W. Semenoff, *Condensed-Matter Simulation of a Three-Dimensional Anomaly*, 1984.

4 R. Peierls, *Ann. l'institut Henri Poincaré*, 1935, 5, 177–222.

5 L. D. Landau, *Phys. Zeitschrift der Sowjetunion*, 1937, 11, 26–35.

6 N. D. Mermint, *Crystalline Order in Two Dimensions~*, vol. 176.

7 K. S. Novoselov, A. K. Geim, S. V. Morozov, D. Jiang, Y. Zhang, S. V. Dubonos, I. V. Grigorieva and A. A. Firsov, *Science (80-.).*, 2004, 306, 666–669.

8 A. Bianco, *Angew. Chem. Int. Ed. Engl.*, 2013, 52, 4986-97.

9 X. Guo and N. Mei, *J. Food Drug Anal.*, 2014, 22, 105–115.

10 N. Malhotra, O. B. Villaflores, G. Audira, P. Siregar, J. S. Lee, T. R. Ger and C. Der Hsiao, *Mol.,* 2020, 25, 3618.

11 K. S. Novoselov, V. I. Fal'Ko, L. Colombo, P. R. Gellert, M. G. Schwab and K. Kim, *Nature*, 2012, 490, 192–200.

12 V. C. Sanchez, A. Jachak, R. H. Hurt and A. B. Kane, *Chem. Res. Toxicol*, 2012, 25, 15–34.

13 K. He, G. Chen, G. Zeng, M. Peng, Z. Huang, J. Shi and T. Huang, *Nanoscale*, 2017, 9, 5370–5388.

14 M. J. Nine, M. A. Cole, D. N. H. Tran and D. Losic, *J. Mater. Chem. A*, 2015, 3, 12580–12602.

15 K. S. Novoselov, V. I. Fal'Ko, L. Colombo, P. R. Gellert, M. G. Schwab and K. Kim, *Nat.,* 2012, 490, 192–200.

16 B. Fadeel, C. Bussy, S. Merino, E. Vázquez, E. Flahaut, F. Mouchet, L. Evariste, L. Gauthier, A. J. Koivisto, U. Vogel, C. Martín, L. G. Delogu, T. Buerki-Thurnherr, P. Wick, D. Beloin-Saint-Pierre, R. Hischier, M. Pelin, F. Candotto Carniel, M. Tretiach, F. Cesca, F. Benfenati, D. Scaini, L. Ballerini, K. Kostarelos, M. Prato and A. Bianco, *ACS Nano*, 2018, 12, 10582–10620.

17 T. Kuila, S. Bose, P. Khanra, A. K. Mishra, N. H. Kim and J. H. Lee, *Biosens. Bioelectron.*, 2011, 26, 4637–4648.

18 S. Aman, M. Z. Ansari, M. Abdullah, A. G. Abid, I. Bashir, M. Un Nisa, S. Manzoor, A. M. Shawky, S. Znaidia and H. M. Tahir Farid, *Inorg. Chem. Commun.*, 2022, 146, 110136.

19 P. Wick, A. E. Louw-Gaume, M. Kucki, H. F. Krug, K. Kostarelos, B. Fadeel, K. A. Dawson, A. Salvati, E. Vázquez, L. Ballerini, M. Tretiach, F. Benfenati, E. Flahaut, L. Gauthier, M. Prato and A. Bianco, *Angew. Chemie Int. Ed.*, 2014, 53, 7714–7718.

20 H. Döscher and T. Reiss, *2D Mater.*, 2021, 8, 022004.

21 R. Ikram, B. M. Jan and W. Ahmad, *J. Mater. Res. Technol.*, 2020, 9, 11587–11610.

22 H. Hong, F. Part and B. Nowack, *Environ. Sci. Technol.*, 2022, 56, 13798–13809.

23 J. R. Peralta-Videa, L. Zhao, M. L. Lopez-Moreno, G. de la Rosa, J. Hong and J. L. Gardea-Torresdey, *J. Hazard. Mater.*, 2011, 186, 1–15.

24 S. Khaliha, A. Bianchi, A. Kovtun, F. Tunioli, A. Boschi, M. Zambianchi, D. Paci, L. Bocchi, S. Valsecchi, S. Polesello, A. Liscio, M. Bergamini, M. Brunetti, M. Luisa Navacchia, V. Palermo and M. Melucci, *Sep. Purif. Technol.*, 2022, 300, 121826.

25 R. Polo-Mendoza, T. Navarro-Donado, D. Ortega-Martinez, E. Turbay, G. Martinez-Arguelles and R. Peñabaena-Niebles, *Nanomater. 2023, Vol. 13, Page 955*, 2023, 13, 955.

26 R. Arvidsson, S. Molander and B. A. Sandén, *Hum. Ecol. Risk Assess. An Int. J.*, 2013, 19, 873–887.

27 X. Wang, H. Xie, Z. Wang and K. He, *Colloids Surfaces B Biointerfaces*, 2019, 173, 632–638.

28 X. Liu, J.; Zhao, Q.; Zhang, *Appl. Clay Sci.*, 2017, 145, 44–52.

29 D. An, B. Liu, L. Yang, T. J. Wang and C. Kan, *Chem. Eng. J.*, 2017, 311, 318–325.

30 S. Kabiri, F. Degryse, D. N. H. Tran, R. C. Da Silva, M. J. McLaughlin and D. Losic, *ACS Appl. Mater. Interfaces*, 2017, 9, 43325–43335.

31 D. Andelkovic, I.B.; Kabiri, S.; Tavakkoli, E.; Kirby, J.K.; McLaughlin, M.J.; Losic, *J. Clean. Prod.*, 2018, 185, 97–104.

32 T. Maliyekkal, S.M.; Sreeprasad, T.S.; Krishnan, D.; Kouser, S.; Mishra, A.K.; Waghmare, U.V.; Pradeep, *Small*, 2012, 9, 273–283.

33 L. Evariste, P. Braylé, F. Mouchet, J. Silvestre, L. Gauthier, E. Flahaut, E. Pinelli and M. Barret, *Front. Microbiol.*, 2021, 12, 598.

34 E. J. Petersen, T. B. Henry, J. Zhao, R. I. MacCuspie, T. L. Kirschling, M. A. Dobrovolskaia, V. Hackley, B. Xing and J. C. White, *Environ. Sci. Technol.*, 2014, 48, 4226–4246.

35 M. Connolly, G. Moles, F. C. Carniel, M. Tretiach, G. Caorsi, E. Flahaut, B. Soula, E. Pinelli, L. Gauthier, F. Mouchet and J. M. Navas, *NanoImpact*, 2023, 29, 10447.

36 OECD, Test No. 201: Freshwater Alga and Cyanobacteria, Growth Inhibition Test, OECD Guidelines for the Testing of Chemicals, Section 2. OECD Publishing, Paris, 2011.

37, OECD, Test No. 202: Daphnia sp. Acute Immobilisation Test, OECD Guidelines for the Testing of Chemicals, Section 2. OECD Publishing, Paris, 2004.

38, OECD, Test No. 203: Fish, Acute Toxicity Test, OECD Guidelines for the Testing of Chemicals, Section 2. OECD Publishing, Paris, 2019.

39, OECD, Test No. 301: Ready Biodegradability, OECD Guidelines for the Testing of Chemicals, Section 3. OECD Publishing, Paris, 1992.

40 K. Rasmussen, H. Rauscher, P. Kearns, M. González and J. Riego Sintes, *Regul. Toxicol. Pharmacol.*, 2019, 104, 74–83.

41 OECD, Guidance Document on Aquatic and Sediment Toxicological Testing of Nanomaterials. Series on Testing and Assessment No. 317. OECD Publishing, Paris, 2022.

42 P. F. M. Nogueira, D. Nakabayashi and V. Zucolotto, *Aquat. Toxicol.*, 2015, 166, 29–35.

43 J. Zhao, F. Ning, X. Cao, H. Yao, Z. Wang and B. Xing, *Water Res.*, 2020, 176, 115735.

44 T. Malina, E. Maršálková, K. Holá, J. Tuček, M. Scheibe, R. Zbořil and B. Maršálek, *Carbon N. Y.*, 2019, 155, 386–396.

45 M. Markovic, I. Andelkovic, J. Shuster, L. Janik, A. Kumar, D. Losic and M. J. McLaughlin, *Chemosphere*, 2020, 245, 125640.

46 A. Barrick, A. Châtel, N. Manier, J. Kalman, J. M. Navas and C. Mouneyrac, *Environ. Toxicol. Chem.*, 2019, 38, 2314–2325.

47 Y. Gao, X. Zeng, W. Zhang, L. Zhou, W. Xue, M. Tang and S. Sun, *Sci. Total Environ.*, 2022, 806, 150942.

48 J. Zhao, X. Cao, Z. Wang, Y. Dai and B. Xing, *Water Res.*, 2017, 111, 18–27.

49 V. L. Castro, Z. Clemente, C. Jonsson, M. Silva, J. H. Vallim, A. M. Z. de Medeiros and D. S. T. Martinez, *Environ. Toxicol. Chem.*, 2018, 37, 1998–2012.

50 J. Yin, Z. Dong, Y. Liu, H. Wang, A. Li, Z. Zhuo, W. Feng and W. Fan, *Carbon N. Y.*, 2020, 169, 182–192.

51 M. C. Pernice and J. M. Gasol, *Front. Microbiol.*, 2023, 13, 1064112.

52 D. L. Jaye, R. A. Bray, H. M. Gebel, W. A. C. Harris and E. K. Waller, *J. Immunol.*, 2012, 188, 4715–4719.

53 R. Marcos-Fernández, B. Sánchez, L. Ruiz and A. Margolles, *Crit. Rev. Microbiol.*, 2023, 49, 556–577.

54 F. Leliaert, D. R. Smith, H. Moreau, M. D. Herron, H. Verbruggen, C. F. Delwiche and O. De Clerck, *CRC. Crit. Rev. Plant Sci.*, 2012, 31, 1–46.

55 J. L. Stauber, N. M. Franklin and M. S. Adams, *Trends Biotechnol.*, 2002, 20, 141–143.

56 J. Zhao, Y. Li, X. Cao, C. Guo, L. Xu, Z. Wang, J. Feng, H. Yi and B. Xing, *Environ. Sci. Nano*, 2019, 6, 1909–1920.

57 J. Farkas and A. M. Booth, *Nanotoxicology*, 2017, 11, 569–577.

58 D. Franqueira, M. Orosa, E. Torres, C. Herrero and A. Cid, *Science of the Total Environment*, 2000, 247, 119–126.

59 M. Markovic, A. Kumar, I. Andjelkovic, S. Lath, J. K. Kirby, D. Losic, G. E. Batley and M. J. McLaughlin, *Environ. Toxicol. Chem.*, 2018, 37, 1340–1348.

Appendix

Graphene Flagship Spearhead Projects: SafeGraph

Regulatory Pathway and Safety Assessment of Graphene-based products

The Graphene Flagship Spearhead Projects (SHPs) are industry-led initiatives with well-defined, application-oriented objectives, designed to improve the development of industrial prototypes using graphene. The main goal of SHPs is to bring graphene out of the laboratory and onto the market, by increasing the Technology Readiness Level (TRL) of graphene-based technologies.

However, bringing any product to market requires specific regulation and legislative frameworks. The regulatory strategies and authorisation pathway for new materials, such as nano-enabled products and graphene, are still being developed. This regulatory lack could hinder the mass-scale production of highly beneficial and marketable graphene-based products. To address these challenges, the SafeGraph Spearhead Project aimed to develop a sustainable, fast, and accessible pathway to market for GRMs and GRMs-based devices, by formulating regulatory compliance, standard practices, and a clear authorization framework needed for commercialization.

In this context, SafeGraph has selected four SHPs with potentially high impact on the quality of life of users, promoting the environmental sustainability, and advancing health monitoring and protection.

The four SHPs supported by SafeGraph are the following:

1. **ChemSens**: developing skin-applied sensors for medical applications. This project is expected to significantly impact the med-tech industry. In this project, the evaluation of risk assessment for both workers and patients has been particularly relevant;
2. **Weargraph**: developing wearable energy generators. This project is envisaged to have a high impact on the market, with potential clients already interested. In this project, the evaluation of risk assessment on human health and the end-of-life (recyclability) of this device has been highly relevant;
3. **GICE**: developing lighter and better-performing ice protection operating systems for aircrafts. This project will have potentially high market impact, promoting safer and environmentally friendlier aircrafts. In this project, the risk assessment for workers (both during maintenance, and at the end-of-life), environment (release of GRMs during usage), and end-of-life (recyclability) has been considered and investigated;
4. **Graphil**: designing and fabricating point-of-use filters for household drinking water treatment and portable water purification. This project will have a very high impact on the sustainability of water resources, environmental sustainability, and users quality of life, potentially reducing

water-borne diseases and contaminations by persistent pollutants. In this project, the risk assessment on human and environmental health due to the release of GRMs during usage has been evaluated.

The devices developed by these projects were used by SafeGraph as case-studies to develop regulatory compliance frameworks covering from the research prototype phase to the market launch.

The main output of SafeGraph has been the development of a regulatory strategy and market authorization pathway, coupled with an occupational, consumer, and environmental risk assessment, to support the SHPs in reaching the market and paving the way for future products.

To date, SafeGraph has produced a preliminary roadmap for complex electronic GRMs-containing devices for medical and consumer applications, which is still under revision, and will be soon available. It is intended to be a useful tool that allows European developers who want to market a device containing graphene to follow the correct procedures to meet the requirements of European regulations.

Thanks to SafeGraph efforts, these four projects are set for safe industrial application and mass-scale production in a cost- and timely-efficient manner. Most importantly, this resulting framework is intended to be adopted also in future graphene projects to ensure faster to-market times and sustainable (safe-by-design) products.

Graphil filtering system: paving the way for commercialization

One of the biggest challenges of the 21st century is to provide access to safe, clean water for everyone, and to reduce the plastic waste resulting from bottled water consumption. In Europe, water quality is generally high, however the occurrence of the so called “emerging contaminants” (ECs) in surface, ground and even drinking water is increasing every day [1,2]. Many of these contaminants are resistant to conventional depuration strategies and no current technology is able to remove all of them [3]. The European Commission has recently published the new Drinking Water Directive (EU 2020/2184) [4], which regulates the water quality for human consumption, establishing specific parameters and limits for various substances in drinking water to ensure its safety and potability. To this end, Graphil committed to manufacturing a compact filtration system that can be easily connected to a household sink, or used as a portable water purifying device, ensuring easy access to safe and clean drinking water.

Among nanomaterials, graphene derivatives have garnered increasing interest in this field, primarily due to their wide commercial availability, high surface area and promising performances in both adsorption and filtration scenarios [5-7].

A recent study conducted by Graphil project partners has demonstrated the possibility to exploit graphene oxide (GO) to enhance the adsorption functionality of existing commercially available polysulfone hollow fiber filtration system, thus improving their application range for adsorbing ECs from drinking water [8].

Taking into account these data, an improved household filtration system was crafted within the Graphil project. The Graphil filter (Fig. A1), developed by Medica, consists of GraphiSulfone® membrane, *i.e*. polysulfone hollow fibers (PSU-HFs) membranes featuring surface pores and macrovoids of porosity in the range 5-100 nm, and graphene oxide (GO) which is embedded into the membranes through an ad hoc developed industrial pilot plants (Medica S.p.A). This newly developed filter combines membrane ultrafiltration and absorption mechanisms to remove both microbiological and inorganic contaminants from water. The membranes act as a filter allowing the ultrafiltration, effectively removing microbiological contaminants, such as bacteria, viruses, and endotoxins, with high levels retention (9 LRV for bacterial and 8 LRV for viruses). Meanwhile GO, thanks to its strong chemical affinity, enables the removal of molecular-level emerging contaminants, including antibiotics, pesticides, PFAs, heavy metals, drugs, and personal care by-products [9].

Figure A1. Graphil In-Line Filter: PSU-GO cartridge for filtration of drinking water

During my PhD period, I was involved in the SafeGraph project, and my involvement required the application of the TG 201 protocol to the GRMs present in real case studies, *i.e*. the devices developed by these projects, in order to provide the ecotoxicological information for the environmental risk assessment. In detail, I was tasked to assess the ecotoxicity of drinking waters filtered through the Graphil cartridges caused by potential release of GO during use conditions, which might end in freshwater environments.

To this end, the Graphil cartridge was subjected to an ecotoxicological assessment applying the OECD TG 201 (for methodological details, see Chapter 2). The aim was to verify the possible GO release from the cartridge containing GO-enriched PSU-HFs during water filtration, by evaluating the algal growth inhibition. The TG 201 testing has been performed on waters filtered through a GO-free (already commercially available), and a GO-containing PSU-cartridge, with unfiltered

bidistilled commercial water as a control. Then algae have been exposed to these migrates enriched with the salts necessary to recreate the TG 201 standard medium. The test did not evidence any significant effect on the algal growth inhibition, *i.e.* the endpoint of the test, either using waters filtered through the GO-enriched cartridge or through the standard one made of sole PSU-HFs membranes (already approved for commercialization and readily available) (Fig. A2).

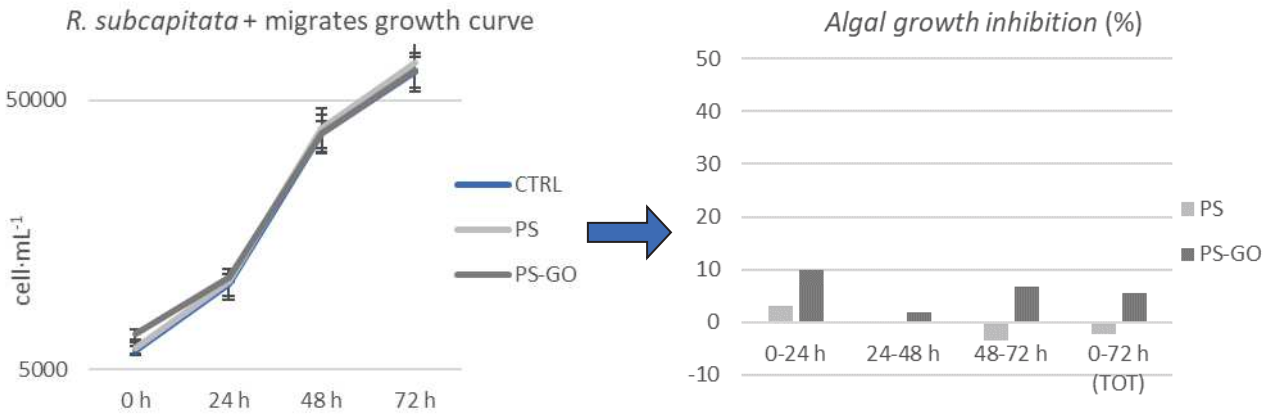

Figure A2. Growth curve and growth inhibition (%) of algae exposed to the migrates from a GO-free (already commercially available) and a GO-containing PSU-cartridge under the TG 201 test conditions (n=6)..

Thanks to the efforts of SafeGraph, Graphil filters have been tested to ensure compliance with the EU Drinking Water Directive (EU 2020/2184) [4] and DM 174, guaranteeing their compatibility with food and drinking water applications. As a result, the first Graphil In-Line Filter has been recently successfully commercialized and is now available on the market.

References

1. S. D. Richardson and T. A. Ternes, *Analytical Chemistry*, 2011, 83 (12), 4614-4648.
2. N. Bolong, A. F. Ismail, M. R. Salim, T. Matsuura, Desalination, 2009, 239(1-3), 229-246.
3. S. Schulze, D. Zahn, R. Montes, R. Rodil, J.B. Quintana, T.P. Knepper, T. Reemtsma, U. Berger, *Water Res.*, 2019, 153, 80-90.
4. https://eur-lex.europa.eu/legal-content/EN/TXT/?uri=CELEX%3A32020L2184.
5. S. Wang, H. Sun, H.M. Ang, M.O. Tadé, *Chem. Eng. J.*, 2013, 226, 336-347.
6. N. Singh, G. Nagpal, S. Agrawal, Rachna, *Environ. Technol. Innov*., 2018, 11, 187-240.
7. C. Backes, A. M. Abdelkader, C. Alonso, A. Andrieux-Ledier, R. Arenal, J. Azpeitia, N. Balakrishnan, L. Banszerus, J. Barjon, R. Bartali, S. Bellani, C. Berger, R. Berger, M. Bernal, C. Bernard, P. Beton, A. Beyer, A. Bianco, P. Bøggild., *2D Materials*, 2020, 7, 2,
8. S. Mantovani, S. Khaliha, L. Favaretto, C. Bettini, A. Bianchi, A. Kovtun, M. Zambianchi, M. Gazzano, B. Casentini, V. Palermo, M. Melucci, Chem. Commun., 2021, 57, 3765-3768.
9. M. Zambianchi, S. Khaliha, A. Bianchi, F. Tunioli, A. M. Kovtun, *J. of Membrane Science, 2022,* 658, 120707.